Chapter 6: Remote Sensing – Validation, spatial and temporal patterns in sea surface temperature and chlorophyll-*a*

Paul Bierman[1,3*], Megan Lewis[1,3], Jason Tanner[1,2,3] and Bertram Ostendorf[1,3]

[1] University of Adelaide, School of Earth and Environmental Sciences, Davies Building DP 614, PMB 1 Glen Osmond, SA 5064
[2] SARDI Aquatic Sciences, PO Box 120, Henley Beach SA 5022
[3] Aquafin CRC

*corresponding author, Phone: +61 8 8303 6571, Fax: +61 8 8303 6717, Email: paul.bierman@adelaide.edu.au

Abstract

This chapter provides the results of an investigation into the seasonal variability of sea surface temperature and chlorophyll-*a* within and adjacent to Spencer Gulf using satellite-based remote sensing imagery. Firstly, MODIS estimated chlorophyll-*a* and sea surface temperature are compared to field-based measurements made in the tuna farming zone (TFZ) to ensure that MODIS methods are valid in the region, and the results from MODIS are representative of the true conditions as measured using traditional techniques. This validation exercise showed that MODIS can accurately determine sea surface temperature measurements within Spencer Gulf, with MODIS estimates explaining 94% of the variation in field temperature measurements. The results for chlorophyll-*a* are less conclusive, with MODIS measurements explaining just 46% of the variation in the field data. Water depth may be a contributing factor to the accuracy of MODIS estimated chlorophyll-*a*, with measurements taken from water depths of more than 20 m displaying a better relationship than those taken from depths of less than or equal to 20 m (77% of variation explained vs 47%). For depths > 20 m, the root mean square (rms) error of 27% falls well within the target error of 35% for MODIS chlorophyll estimations. Validation in areas of Spencer Gulf outside the TFZ is yet to be done.

In the second part of this study, MODIS monthly composite imagery was used to investigate spatial and seasonal variation in both chlorophyll-*a* and sea surface temperature over a period of five years. Both the magnitude of chlorophyll-*a* concentration, and the timing of the seasonal patterns of chlorophyll-*a*, change with distance along a transect running down Spencer Gulf, with highest concentrations in the shallower waters of the north and decreasing concentrations towards the open ocean. There was also an increase in chlorophyll-*a* concentration in close proximity to the TFZ compared to nearby waters of southern Spencer Gulf (by up to 100% in February-July). While bottom reflectance may be causing some interference in shallow northern areas, and thus quantitative measures of chlorophyll-*a* may be incorrect in these areas, the broader spatial and temporal patterns are likely to be correct. Further validation in other areas of the gulf will be undertaken to confirm this. Sea surface temperature measurements showed a clear contrast between gulf and non-gulf waters. Waters within Spencer Gulf showed both the highest summer temperatures and also the lowest winter temperatures, thus undergoing a greater seasonal transition than the waters outside the gulf.

6.1. Introduction

While a significant understanding of the oceanography of Spencer Gulf and the surrounding waters has been developed over the last few decades, we still have little knowledge about how this relates to biological processes in the water column. In particular, we still have a poor understanding of how phytoplankton abundance varies on large spatial scales, how different regions are connected with respect to phytoplankton assemblages, and how temporal variation is related to geographic location.

One possible reason why there is limited information on these topics is the availability of suitable data. Often datasets of chlorophyll-*a* and sea surface temperature (SST) are spatially or temporally restricted and therefore do not cover the large areas and long time periods required to study patterns over an area as large as Spencer Gulf. Satellite remote sensing allows information on chlorophyll-*a* concentrations and sea surface temperature to be collected at moderate resolution, over large areas, over long periods of time, with reasonable accuracy and at low cost. The Moderate Resolution Imaging Spectroradiometer (MODIS) is a passive remote sensing instrument that orbits the earth onboard two satellites, Terra and Aqua. These satellites have sun-synchronous near polar orbits at an altitude of 705 km, which means they orbit the Earth from pole to pole following the sun and therefore pass over the same location at approximately the same local time each day. Each MODIS image spans a distance of 2,330 km with a spatial resolution of 1 km for the bands of interest here. MODIS records the upwelling radiances across 36 spectral bands between 0.4 and 14.4 μm, and these are used to calculate the surface chlorophyll-*a* and temperature of the water, as well as many other properties. Three levels of MODIS imagery are available. Level 1 imagery consists of the raw radiance measurements recorded by the sensor at 250m spatial resolution for bands 1 and 2, 500m for bands 3 – 7 and 1 km for bands 8 – 36 either un-projected (ie without geographic referencing), Level 1A, or projected (with geographic referencing) Level 1B. Level 2 imagery consists of the derived geophysical variables, such as chlorophyll-*a* and SST, at 1 km spatial resolution covering the same area as the original scene. Level 3 imagery is composite imagery produced by averaging multiple Level 2 scenes over a period such as 8 days or a month, with a spatial resolution of 4 km and covering a much larger area than the individual Level 2 scenes. Level 3 monthly climatology imagery is also available, produced by averaging multiple images from the same month over several years.

Many different algorithms exist to derive chlorophyll-*a* measurements from the raw Level 1 MODIS imagery. The standard MODIS chlorophyll-*a* imagery available from the Goddard Space Flight Centre is produced via the OC3M algorithm. The OC3M method is an extension of the empirically derived SeaWiFS OC4v4 algorithm, based upon 2,853 field measurements collected across a range of bio-optical marine provinces (O'Reilly et al., 2000). The OC3M algorithm is in the form of a fourth order polynomial equation and applies the maximum of the ratio of the remote sensing reflectance at 443 nm (blue) to 550 nm (green) or 490 nm (blue) to 550 nm (green). The OC3M algorithm was designed for use in Case II waters, thus it is expected to perform reasonably well in the coastal waters of Spencer Gulf. Case II waters are defined as waters whose optical properties are influenced by a combination of phytoplankton, suspended particles and organic matter, as opposed to Case I waters whose optical properties are dominated by phytoplankton alone (IOCCG, 2000). Other methods also exist for deriving chlorophyll-*a* from MODIS, including a semi-analytical bio-optical model which was designed to take into account absorption by suspended particles, CDOM (coloured dissolved organic matter) and other constituents of Case II waters (Carder et al., 2003).

Despite the complexity of ocean colour algorithms, they exhibit limitations due to influences from other properties of the water column upon the estimation of chlorophyll-*a*. There are a number of water constituents that can influence the chlorophyll-*a* estimation, particularly in Case II waters such as Spencer Gulf. Suspended particulate matter, or coloured dissolved organic matter, for example, can affect the light reflected from the water column and therefore influence the derivation of chlorophyll-*a* concentration. Also there are other properties, such as shallow water depth and proximity to land, that can influence the radiance received by the sensor and therefore affect the chlorophyll-*a* calculation often resulting in an over-estimation. To gain an understanding of how well the MODIS chlorophyll-*a* estimation actually predicts the true chlorophyll-*a* concentration, the satellite derived values need to be compared to field measurements. This validation process is a necessary step to ensure that the satellite derived chlorophyll-*a* measurements are representative of the true concentrations.

While measurements of some surface properties such as chlorophyll-*a* rely upon reflected visible radiation, the calculation of temperature relies upon measuring the infrared radiance emitted from the surface. However, the problem with measuring the temperature of the earth's surface is that the outgoing radiation interacts with the atmosphere. The application of two bands has been shown to reduce the impacts of the atmosphere on the estimation of SST (Anding and Kauth, 1970). MODIS SST algorithms use either bands 22 and 23 at 3.959 and 4.050 μm or bands 31 and 32 at 11 and 12 μm. Bands 31 and 32 in the long-wave infrared part of the spectrum are applied during the day as they are not affected by reflected sunlight; however they are potentially affected by water vapour in the atmosphere. While bands 22 and 23 in the short-wave infrared are less affected by water vapour, they are applied only to night time imagery due to contamination by sunlight (Brown and Minnett, 1999). Daytime SST imagery has been selected for analysis here due to it corresponding with chlorophyll-*a* imagery, and in situ SST measurements.

6.2. Aims

The purpose of this study was initially to investigate the validity of satellite remote sensing to measure chlorophyll-*a* and sea surface temperature in Spencer Gulf. The algorithms, which have been developed and validated for other oceans of the world, need to be proven to be accurate in Spencer Gulf. Once shown to be a valid technique of data collection in the region, the aim was then to apply remotely sensed imagery to better understand the seasonal chlorophyll-*a* and SST variations within and around Spencer Gulf, and how the seasonal variability changes with geographic location. Knowledge of the seasonal variability in chlorophyll-*a* and SST assists in the development of a more comprehensive understanding of the dynamic environment of Spencer Gulf, and thus aids in better understanding the interactions between southern bluefin tuna aquaculture and its immediate environment.

6.3. Methods

6.3.1 Remote Sensing Validation

To investigate the validity of the chlorophyll-*a* and sea surface temperatures derived via MODIS imagery, data extracted from the imagery were compared with measurements taken in the field. In situ measurements of surface chlorophyll-*a* and temperature were collected monthly in the waters offshore from Port Lincoln during the period from August 2005 to September 2006, as described in Chapter 7. Temperature profiles of the water column were recorded using a CTD and the temperature at 1 metre depth used to represent the SST.

Chlorophyll-*a* measurements were determined using HPLC with water samples collected at the surface, as described in Chapter 7.

MODIS Aqua Level 2 daily SST and chlorophyll-*a* imagery at 1 km spatial resolution was obtained from the Goddard Space Flight Centre (oceancolor.gsfc.nasa.gov) for the days corresponding to the collection of field measurements. The daily MODIS images were imported into ENVI (Environment for Visualizing Images ver 4.3, (RSI, 2006)) using the ENVI Plugin for Ocean Color (EPOC), obtained from www.ittvis.com, which converted the HDF (Hierarchical Data Format) files into ENVI image files and reprojected the images. ENVI was then used to extract the geophysical properties from a 3x3 array of pixels centred on the coordinates of the field measurements. Nine pixels were used to allow for potential positional error in the satellite imagery (Bailey and Werdell, 2006). Often one or more of the nine pixels used for validation were affected by cloud, hence could not be used in the calculation of the spatial average, thus only the remaining pixels were used. Only when a minimum of five of the nine pixels were valid was an average value calculated and compared to the field value.

Initially, 128 field chlorophyll-*a* measurements were available; however only measurements collected on a day where a MODIS image was available could be used, and often some or all of the pixels surrounding the collection location were affected by cloud and could not be included. This reduced the dataset to just 35 pairs of measurements. As with chlorophyll-*a*, there were initially 128 SST field measurements recorded. Discarding the measurements where no MODIS SST value was available reduced the dataset to just 20 pairs of measurements. Linear regression was then performed in Microsoft Excel to assess the relationship between the MODIS measurements as the dependent variable and the field measurements as the independent variable. The coefficient of determination, R^2, and the root mean square (rms) error were calculated to show how well the estimated MODIS values resemble the expected field-derived values and the errors associated with the MODIS estimates. To determine whether water depth and bottom reflectance influenced the MODIS measurements, the chlorophyll-*a* dataset was separated into two sets, one for water depths greater than 20 m and another for depths less than or equal to 20 m. Of the 35 chlorophyll-*a* measurements, 15 were from locations where water depth was 20 m or less and the remaining 20 measurements were from locations with water depths greater than 20 metres. If water depth plays a role in the validation then the measurements taken from deeper water would be expected to show a stronger relationship with field measurements.

6.3.2 Spatial and Temporal variability in SST and chlorophyll-*a*

MODIS imagery was used to investigate the annual and inter-annual variations in chlorophyll-*a* and SST within and around Spencer Gulf. Level 3 monthly averaged MODIS Aqua chlorophyll-*a* and SST global composite images at 4 km spatial resolution were downloaded from Goddard Space Flight Centre. Images were obtained for each month for a 5-year period beginning July 2002 and ending June 2007. This provided 60 monthly average images and 12 monthly climatology images for both chlorophyll-*a* and SST. The monthly MODIS images were imported into ENVI and a subset of the South Australian region between 30 ºS and 40 ºS, and 132 ºE and 142 ºE was created from each of the images.

The study area consists of Spencer Gulf and the surrounding coastal waters of South Australia. Within this region, 14 stations were established, inside and outside the gulf, at which the variation in chlorophyll-*a* and SST was observed (Figure 6.1; Table 6.1). Stations A through G lay on a transect that runs down the centre of Spencer Gulf from near the head

to well offshore near the edge of the continental shelf to show how the seasonal patterns vary with position along the gulf. Station H was placed near to the SBT farming zone to show how this region compares to the rest of the gulf, while station I was placed on the opposite side of the gulf, at approximately the same distance from the coast, as a reference for station H. Stations J, K and L were placed on the western side of Eyre Peninsula, and finally, M and N were placed on the southwest corner of Kangaroo Island in order to possibly detect the effects of coastal upwelling.

Table 6.1. The co-ordinates of the stations used to assess spatial variability in chlorophyll-*a* and SST.

Station ID	Latitude (ºS)	Longitude (ºE)
A	33.50	137.53
B	34.00	137.17
C	34.33	136.92
D	34.67	136.67
E	35.00	136.40
F	35.50	136.00
G	36.00	135.55
H	34.67	136.13
I	34.67	137.17
J	34.00	134.83
K	34.33	135.00
L	34.92	135.30
M	35.83	136.30
N	36.25	136.67

At each of the 14 stations, the values of an array of 3x3 pixels were extracted and averaged for each month to enable a temporal profile to be determined for each station. The temporal profiles were compared and the Pearson correlation statistic calculated between stations to show which stations had similar temporal cycles and which did not.

To assess how similar the temporal profiles were at different stations, a hierarchical cluster analysis was applied. Each station was treated as an individual case, with each month considered a variable, and thus similar stations have similar temporal profiles as well as similar absolute values at a given time. Hierarchical cluster analysis was performed in SPSS 15.0 (SPSS, 2006) using Ward's method with squared Euclidean distance to produce a dendrogram visually showing the similarities between stations. To assess broader scale variation in temporal profiles of chlorophyll-*a* and SST, unsupervised classification or non-hierarchical cluster analysis was used over the entire area covered by the MODIS imagery. K-means unsupervised classification was performed in ENVI on the 5 years worth of monthly MODIS imagery with 10 iterations and 6 groups selected for chlorophyll-*a* and 7 groups for SST. Finally, to identify the primary modes of variability within the imagery and identify the characteristics of the dataset responsible for the majority of the variability, principal components analysis (PCA) was used. PCA was performed in ENVI on the 5 years of monthly MODIS imagery. The principal components were calculated using the covariance matrix and the eigenvalues of each extracted component used to calculate the percentage of variance explained by each component.

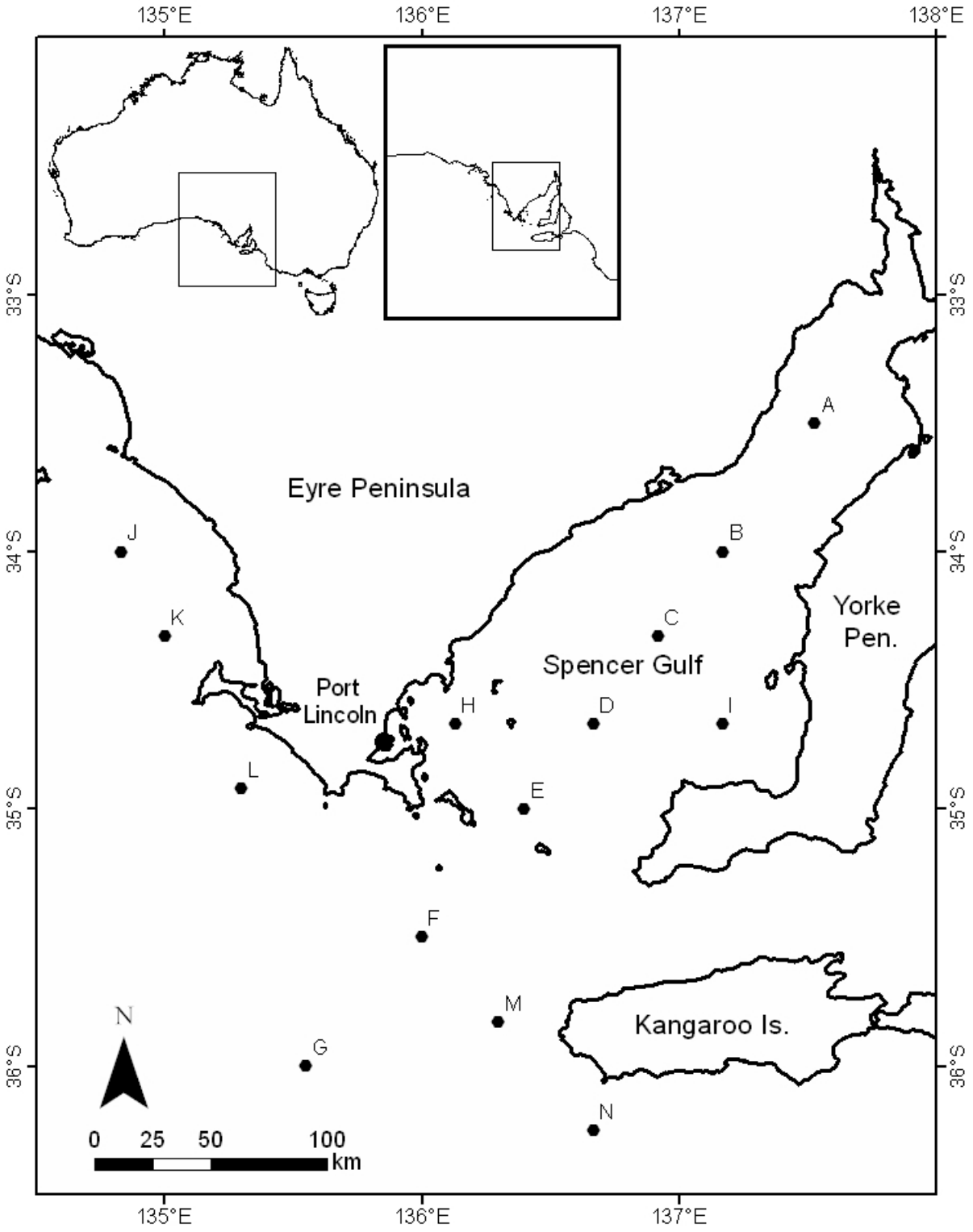

Figure 6.1. The location of stations A to N used to investigate the seasonal chlorophyll-*a* and SST variability within and around Spencer Gulf, South Australia (co-ordinates are given in Table 6.1).

6.4 Results

6.4.1 Remote Sensing Validation

The relationship between the MODIS chlorophyll-*a* measurements and the chlorophyll-*a* measurements obtained from the field was only moderate, with an R^2 value of 0.46 ($p = 8.46 \times 10^{-6}$) and an rms error of 0.37 or 50% (Figure 6.2). MODIS overestimated chlorophyll-*a* in relation to values collected via in situ sampling, particularly when the observed field values were below 0.3 µg L^{-1}. Above 0.3 µg L^{-1} there was a modest relationship between the values obtained using the two methods, although there were several outliers where significant variations between the MODIS estimation and the field value occurred (Figure 6.2). High values measured by MODIS should be treated with particular caution, as they were generally much higher than values measured from in situ sampling. When the chlorophyll-*a* data was separated into two groups based on water depth, a substantial affect upon validation was observed. Using only data for water depths > 20 m produced an improved R^2 value of 0.77 ($p = 3.19 \times 10^{-7}$) and a reduced rms error of 0.18 or 27%, compared to an R^2 of 0.47 ($p = 0.0045$) and an rms error of 0.47 or 55% for measurements where water depth was less than or equal to 20 m. It should be noted that these results only apply to the TFZ, where all the field measurements were made, and validation is yet to be extended to other areas of Spencer Gulf.

The relationship between sea surface temperatures derived from MODIS imagery and temperature measurements taken in the field was very good, with an R^2 value of 0.94 ($p = 8.96 \times 10^{-13}$) and an rms error of just 0.56 or 2.8% (Figure 6.3). The strong relationship indicates that MODIS is able to accurately determine sea surface temperature in Spencer Gulf.

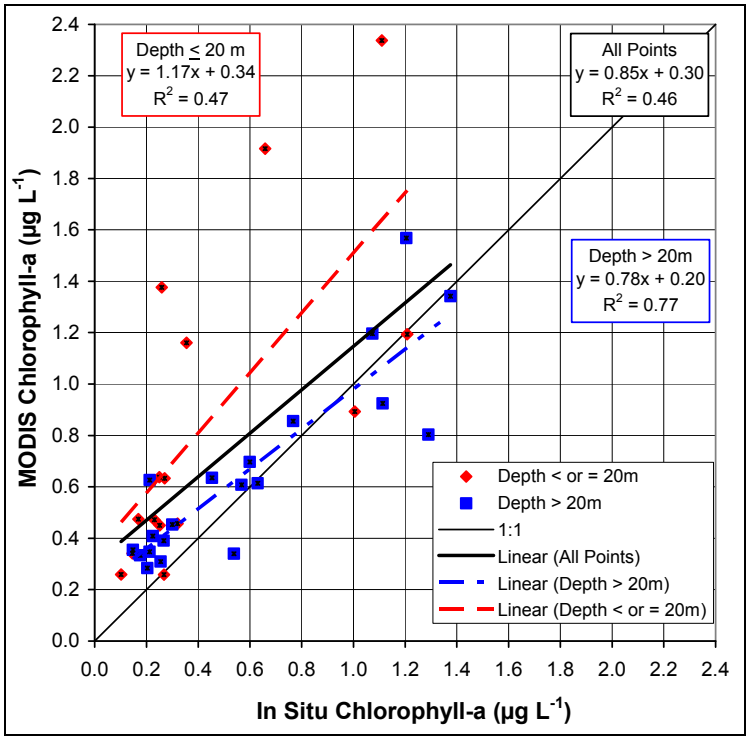

Figure 6.2. Relationship between chlorophyll-*a* determined via MODIS and collected in the field, with measurements shown in red from depths of less than or equal to 20 m and measurements in blue from water depths greater than 20 m.

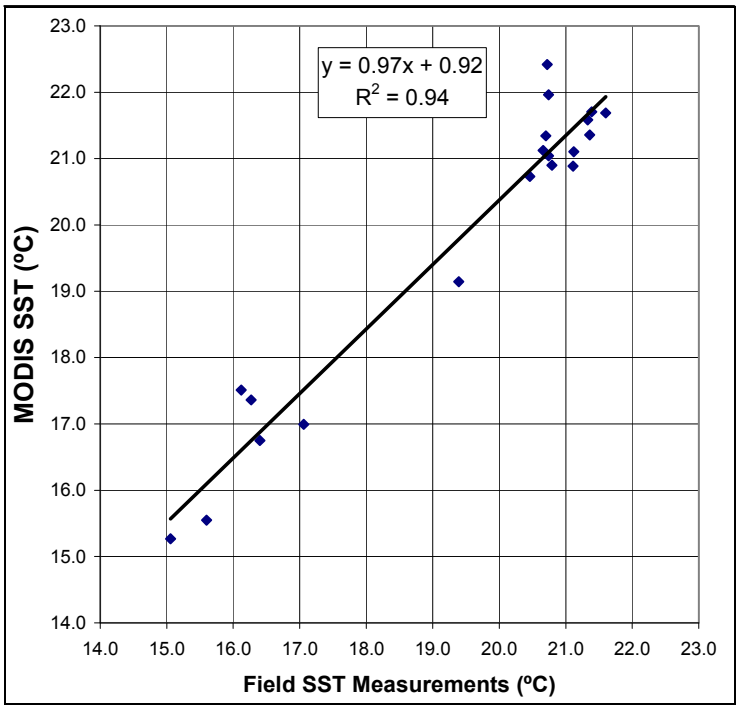

Figure 6.3. Relationship between SST determined via MODIS and measured in the field.

6.5.2 Chlorophyll-*a* Spatial and Temporal Variability

Differences in the magnitude of the chlorophyll-*a* concentrations were observed, and the timing of the seasonal patterns varied between locations in and around Spencer Gulf (Figure 6.4, 6.5). Monthly average chlorophyll-*a* concentrations ranged between a minimum of < 0.1 μg L^{-1} at station G outside the mouth of Spencer Gulf in January 2006 up to a maximum of 2.0 μg L^{-1} at station A in northern Spencer Gulf in March of 2007.

Station A, in northern Spencer Gulf, showed the highest MODIS-derived chlorophyll-*a* concentrations, between 0.5 μg L^{-1} and 2.0 μg L^{-1}, and also the largest seasonal differences. It is yet to be determined if these values are purely due to pelagic chlorophyll-*a*, or if bottom reflectance is causing an overestimate. Maximum chlorophyll-*a* concentrations in the northern gulf occurred between January and May, while minimum concentrations occurred from August to November. The concentration of chlorophyll-*a* decreased further south in the gulf. At station D, in the southern gulf, the chlorophyll-*a* concentrations ranged between 0.2 and 0.9 μg L^{-1}, with maximum concentrations between April and July and minimum concentrations between September and November. Further south, outside of the gulf at station G, concentrations ranged from less than 0.1 μg L^{-1} up to 0.4 μg L^{-1}. At station G the maximum occurred between August and November, with the minimum from December to April. The seasonal patterns at station G outside the gulf were almost the opposite of the seasonal patterns at station A in northern Spencer Gulf as indicated by the negative correlation of -0.58, although the concentrations at station G are much less than at A (Figure 6.5). The differences in chlorophyll-*a* patterns in and around Spencer Gulf throughout the year can be observed in the climatology images of each month (Figure 6.4).

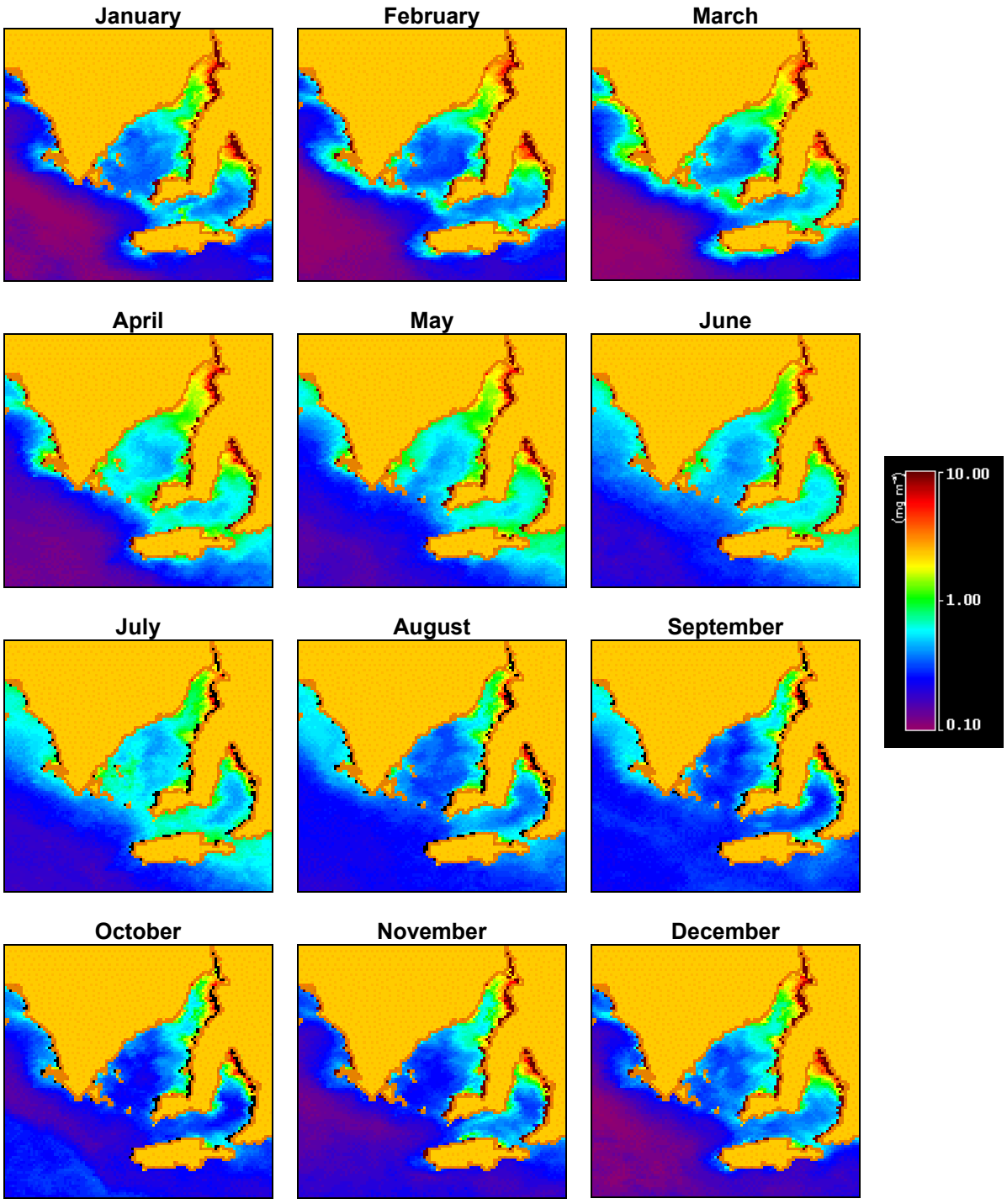

Figure 6.4. South Australian monthly chlorophyll-*a* climatology (μg L^{-1}) from MODIS/Aqua between 2002 and 2007. Note that values along the inshore margins are likely to be overestimated due to bottom reflectance.

Station H is the location of most concern in regards to chlorophyll-*a* concentration as it is located near the TFZ. The chlorophyll-*a* at station H ranges from 0.3 μg L^{-1} up to 1.4 μg L^{-1}, with maximum concentrations between March and July and minimum concentrations between September and January (Figure 6.6). The chlorophyll-*a* characteristics at station H were similar to station D, which lies directly east of H in the centre of the gulf. However, the concentrations at H were consistently higher than at D (Figure 6.6). On average the chlorophyll-*a* at station H was 0.18 μg L^{-1} greater than nearby station D, but was consistently

0.4 µg L^{-1} greater than D during the period from March to July. Station I is placed on the opposite side of the gulf to H, at a similar distance offshore. Station I also showed slightly greater concentrations than D during some periods of the year, however not as high as station H. This suggests that proximity to land influences the chlorophyll-*a* concentrations, but does not account for all of the increase at H.

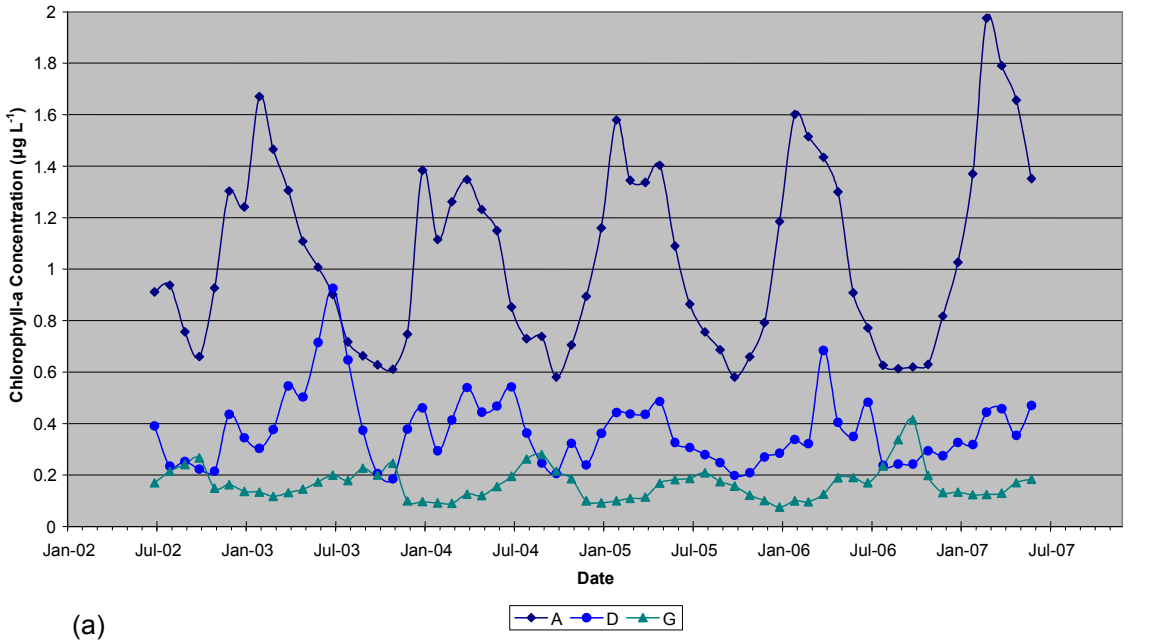

(a)

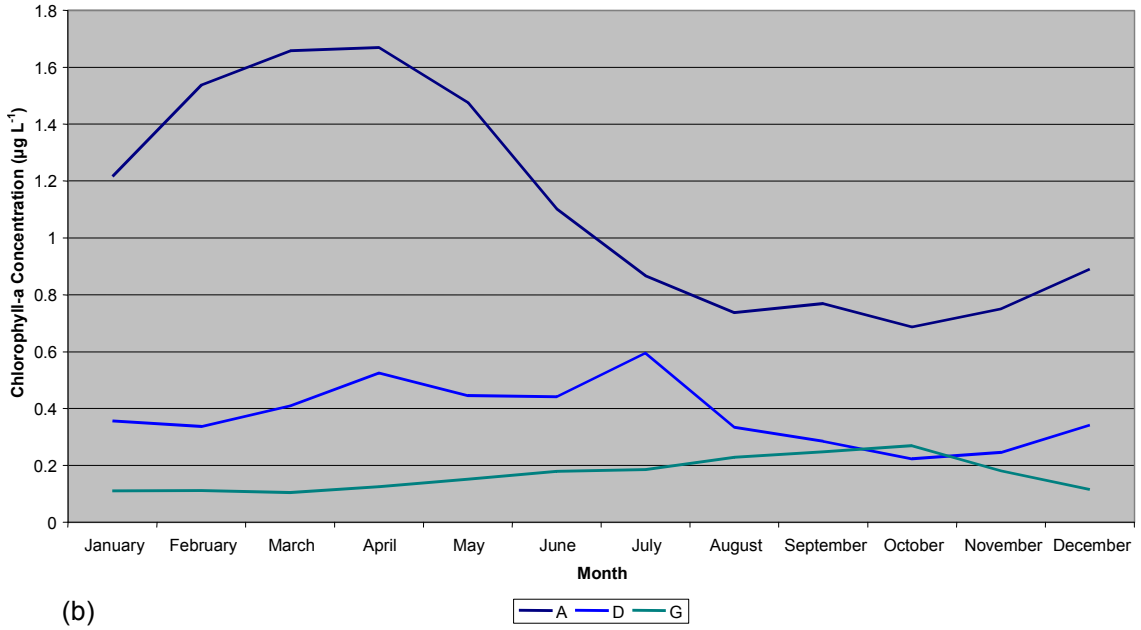

(b)

Figure 6.5. The monthly chlorophyll-*a* concentrations at stations A, D and G from July 2002 to June 2007 (a) and the monthly climatology averaged over the 5 year period (b).

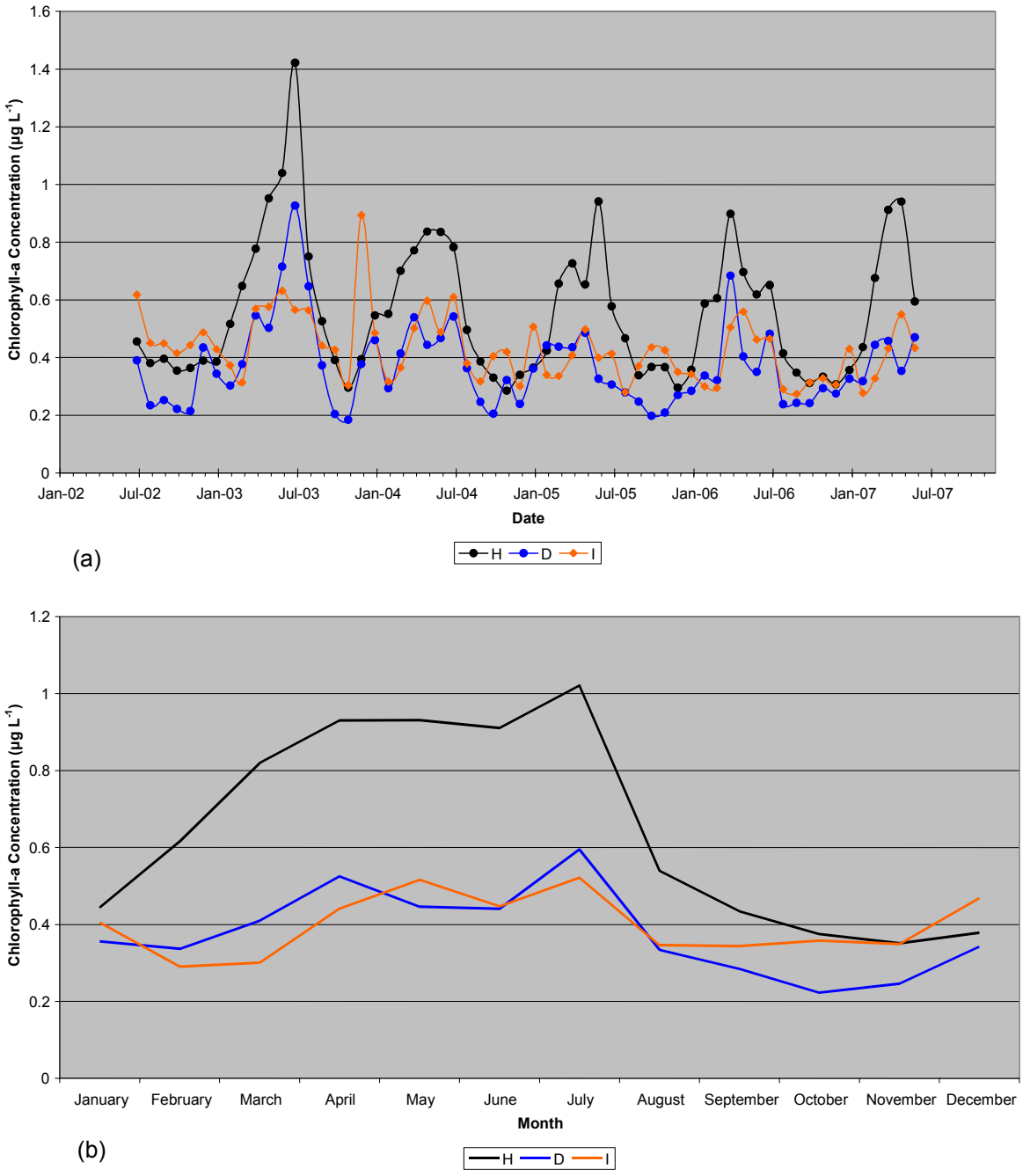

Figure 6.6. The monthly chlorophyll-*a* concentrations at stations H, D and I from July 2002 to June 2007 (a) and the monthly climatology averaged over the 5 year period (b).

As mentioned, the magnitude of the chlorophyll-*a* concentrations varied with distance from the head of the gulf, therefore the monthly climatology images of the chlorophyll-*a* concentrations were used to show how they change along the transect that runs along the centre of the gulf in each month of the year (Figure 6.7). In all months, station A had the highest chlorophyll-*a*, and there was a clear decrease from the head towards the mouth. The high chlorophyll-*a* measurements at station A are most likely due to the combined influence of shallow water depth, proximity to land, and suspended matter in the water column, and not solely to increased phytoplankton. In all months except October and November the lowest concentration was at G, in October and November the lowest concentration was at the nearby

station F. The decrease in chlorophyll-*a* concentration from A to F or G was not linear however. The concentration decreased rapidly from A to C in all months, but in April, June, July, and August there was a slight increase in chlorophyll-*a* at station E before the concentration decreased further at stations F and G.

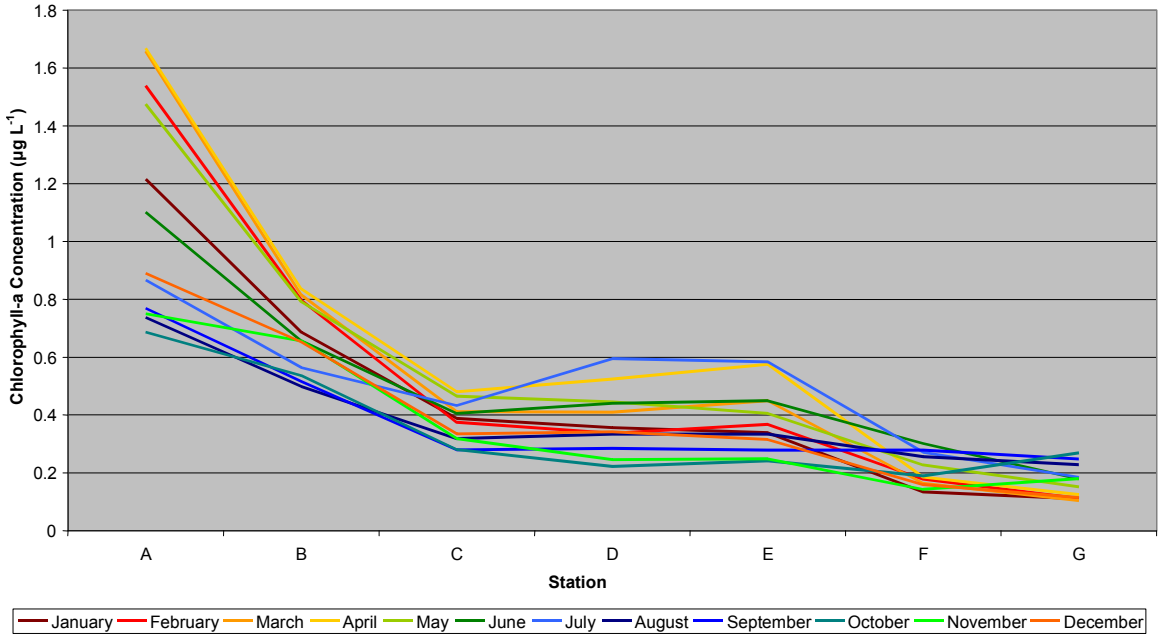

Figure 6.7. The chlorophyll-*a* climatology in each month of the year at stations along the transect from A in northern Spencer Gulf to G outside the mouth of the gulf.

Hierarchical cluster analysis of chlorophyll-*a* showed that stations F, N, M and G outside the mouth of Spencer Gulf are similar as are C, D, E and I in the southern Spencer Gulf. Stations J, K and L on the western side of Eyre Peninsula are more similar, in terms of their chlorophyll-*a* characteristics, to the stations in the southern part of the gulf than they are to the other stations outside the gulf. Station H, in the SBT aquaculture zone is more similar to station B, further north in the gulf, than it is to any of its nearby stations and stations A, B and H are all very dissimilar to all the other stations in the study area (Figure 6.8).

An unsupervised classification was performed upon the monthly chlorophyll-*a* images of South Australia, enabling grouping of all the pixels of the imagery. Each pixel of the imagery was grouped into one of six classes. Two of the classes represented land and unclassifiable pixels (pixels for which one or more bands had no value) accounting for 46.7 % and 32.3 % of the scene respectively. The remainder of the region was classified into one of 4 groups covering the marine region, which were interpreted to represent oceanic, shelf, coastal and shallow water. The area of the scene covered by each class is approximately 143,539 km^2 (13.7%) for oceanic waters, 47,111 km^2 (4.5%) for shelf waters, 26,123 km^2 (2.5%) for coastal waters and just 3,807 km^2 (0.4%) for the shallow waters.

It can be seen that the classification of the 14 stations is mostly consistent with the hierarchical cluster analysis. Stations F, G, M and N all belong to the open ocean region, stations J, L, C, D, E and I belong to the shelf region, while stations A, B, H and K are in the coastal water region (Figure 6.9).

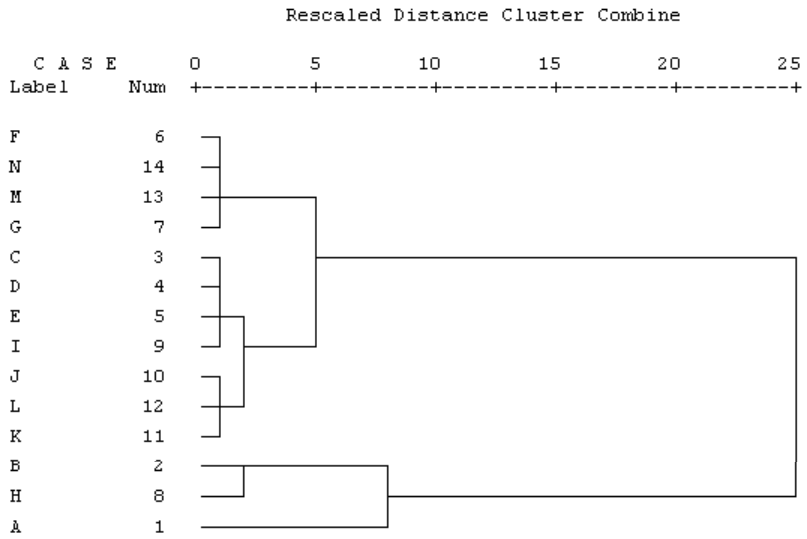

Figure 6.8. Dendrogram from hierarchical cluster analysis using Ward's method showing the similarities between stations based on chlorophyll-*a*.

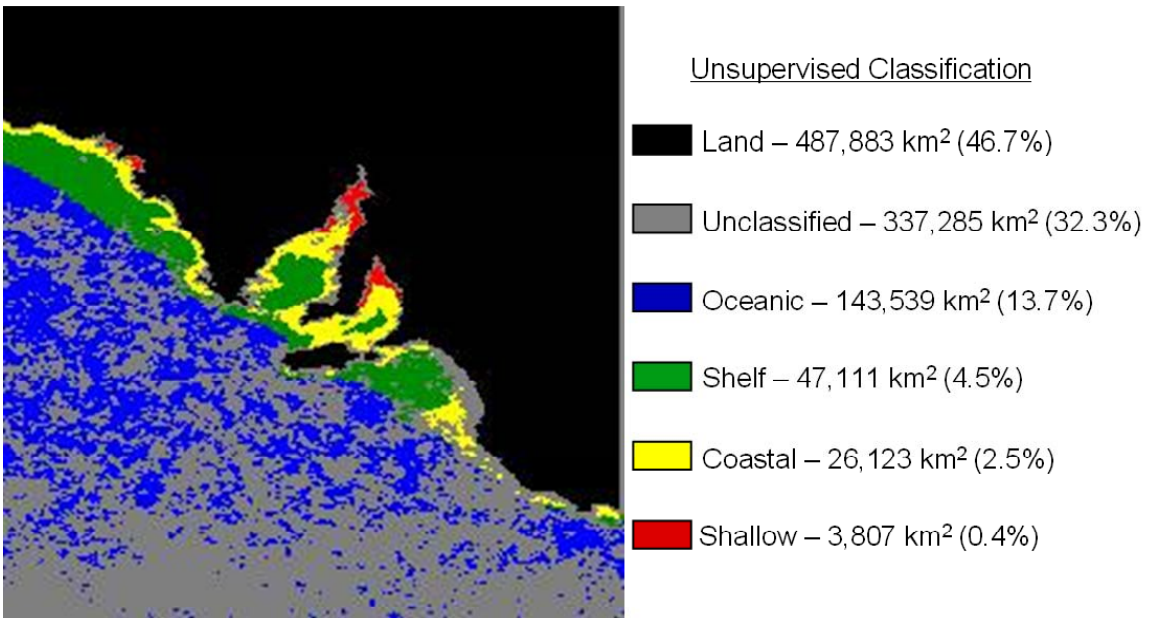

Figure 6.9. Results of an unsupervised classification upon 60 MODIS monthly chlorophyll-*a* images between July 2002 and June 2007.

The principal components analysis identified one component that accounted for a significant amount of the total variance. The first component, representing 82.7% of the variance, is a representation of the overall high and low chlorophyll-*a* areas of the region. It identifies the areas where chlorophyll-*a* concentrations are relatively high in all months, within the gulfs and along the coastline, and the offshore waters with relatively low chlorophyll-*a* in all months. The following components represented significantly less of the total variability. Principal component 2 accounts for just 4.0% of the variance, showing negative values throughout the Great Australian Bight (GAB) and the gulfs and positive values offshore and in the far north of the gulfs. This pattern is consistent with a seasonal contrast identifying the areas with a peak in chlorophyll-*a* in summer with areas with peak chlorophyll-*a* in winter.

6.5.3 Sea Surface Temperature Spatial and Temporal Variability

The monthly average SST ranged from a minimum of just under 13 ºC at station A in August 2003 up to a maximum of over 24 ºC, also at station A in February 2007 (Figure 6.10, 6.11). The range of temperatures experienced at Station A is larger than at any other station, 11.3 ºC compared with the smallest range of just 4.4 ºC at station L. Stations inside Spencer Gulf showed a greater average annual range in temperature than stations outside the gulf (7.6 ºC inside compared to just 3.8 ºC outside). As a result, the waters of Spencer Gulf are warmer than nearby ocean water during summer, but cooler during winter, resulting in a temperature gradient that reverses in direction between summer and winter (Figure 6.12).

The monthly climatology SST images were used to observe the changes in temperature along the Spencer Gulf transect in each month of the year (Figure 6.12). From October through to April there was a decrease in temperature with distance from the northern gulf, when gulf waters were warmer than ocean water. During June, July and August there was an increase in temperature towards the south, when the ocean waters were warmer than the gulf. During September and May there was very little difference along the transect. Station A was over 4 ºC warmer than G from December to February while station G was just over 2 ºC warmer than A in July.

A hierarchical cluster analysis of SST showed that the stations within Spencer Gulf (A, B, C, D, H and I) and those outside formed two distinct groups (Figure 6.13). Station E, at the mouth of Spencer Gulf, was grouped with the outside stations and was most similar to stations J and K off western Eyre Peninsula. An unsupervised classification of SST images classified pixels into 7 groups. The waters of Spencer Gulf and Gulf St Vincent formed one group, distinct from the rest of the region, but only accounted for 3.1% of the area of the image. The remaining 4 water groups formed bands moving from the coastline towards the open ocean accounting for 8.9%, 10.1%, 15.3% and 14.6% of the area respectively (Figure 6.14). The land and unclassifiable pixels accounted for 46.7% and 1.4% of the area. The fact that the classification places gulf waters into their own group further emphasises that the waters inside Spencer Gulf are different from waters outside the gulf. The classification also showed waters of the upwelling regions as belonging to a class found further offshore than would normally be the case without the affects of upwelling on the water temperature (Figure 6.14).

Three principal components were identified representing the majority of the variability in SST. Principal component 1, which represented 78.7% of the variability, appears to be a contrast between inshore and offshore waters. Principal component 2, which represented 11.0% of the variance, is a seasonal cycle. PC 2 clearly shows a contrast between Spencer Gulf waters and the water outside of the mouth in response to the large seasonal SST range within the gulf and the small annual range immediately outside the mouth. PC 3, which accounted for just 3.2%, appears to be related to upwelling, showing a clear contrast between the areas where upwelling is known to occur, in the south east of SA and on the western side of Eyre Peninsula, with the rest of the region.

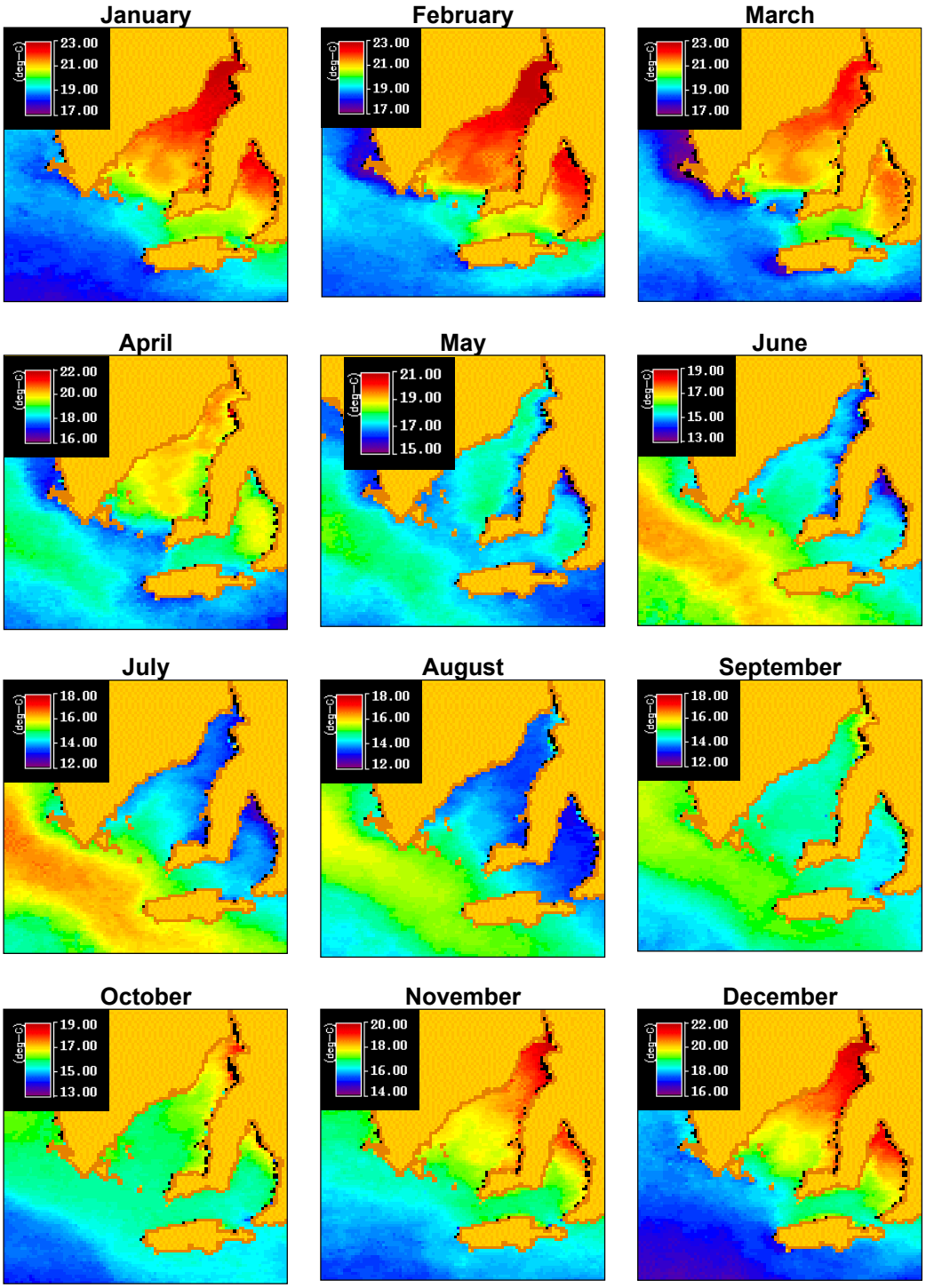

Figure 6.10. South Australian monthly SST climatology (°C) from MODIS/Aqua between 2002 and 2007.

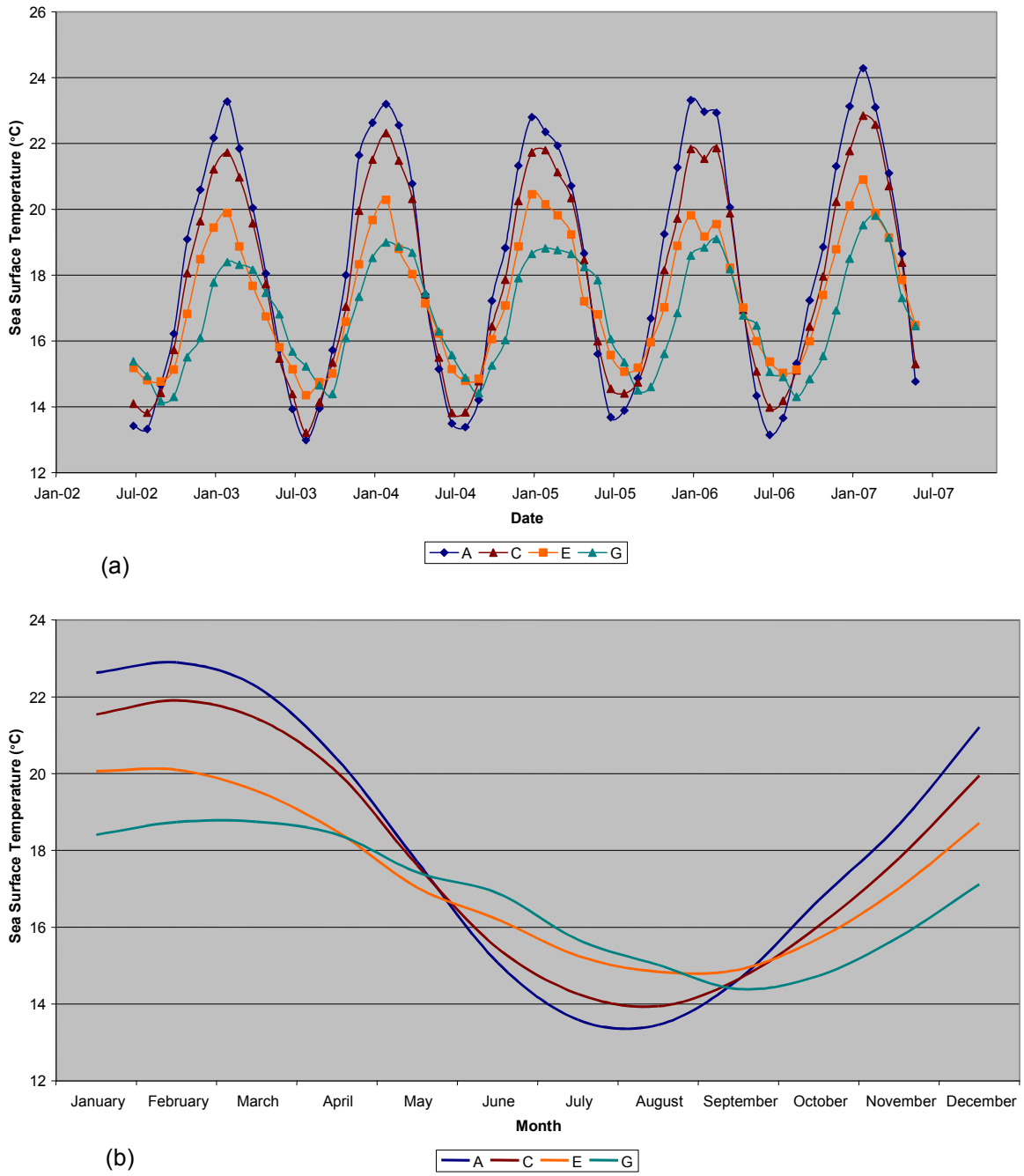

Figure 6.11. Monthly average SST (a) and monthly SST climatology (b) at stations A, C, E and G highlighting the decrease in range of temperatures experienced with distance from northern Spencer Gulf.

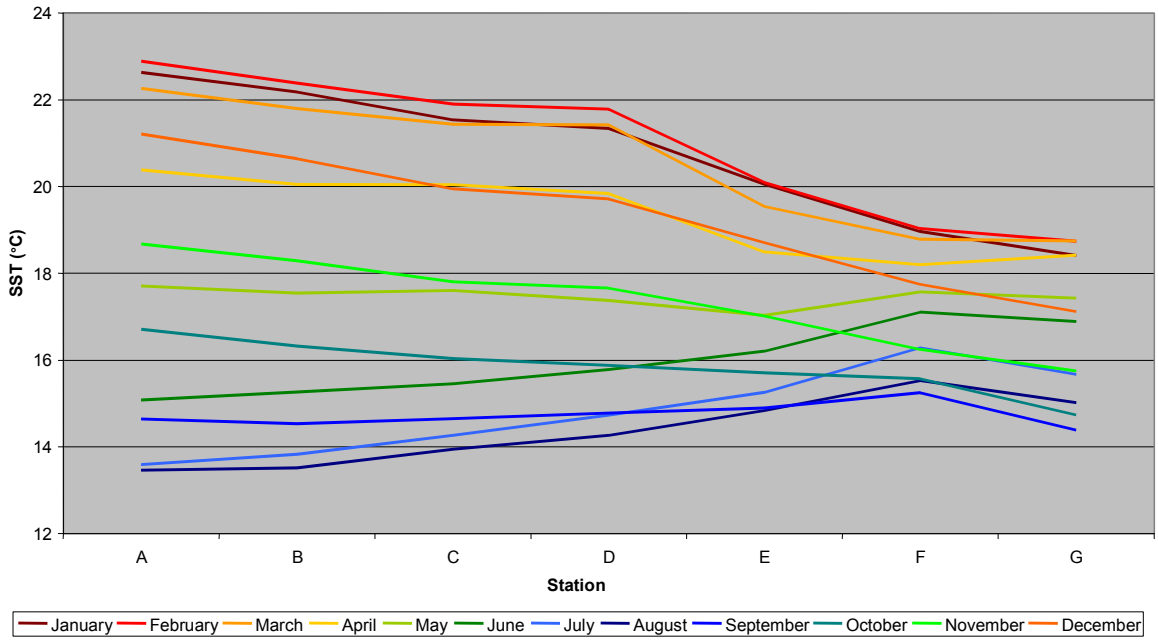

Figure 6.12. The SST climatology at stations along the transect from station A in northern Spencer Gulf and G outside the mouth of the gulf.

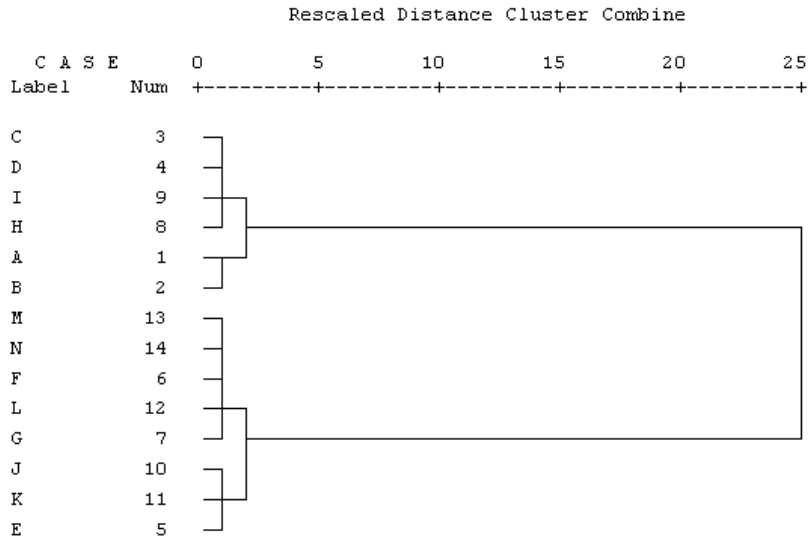

Figure 6.13. Dendrogram from hierarchical cluster analysis using Ward's method showing the similarities between stations based on SST.

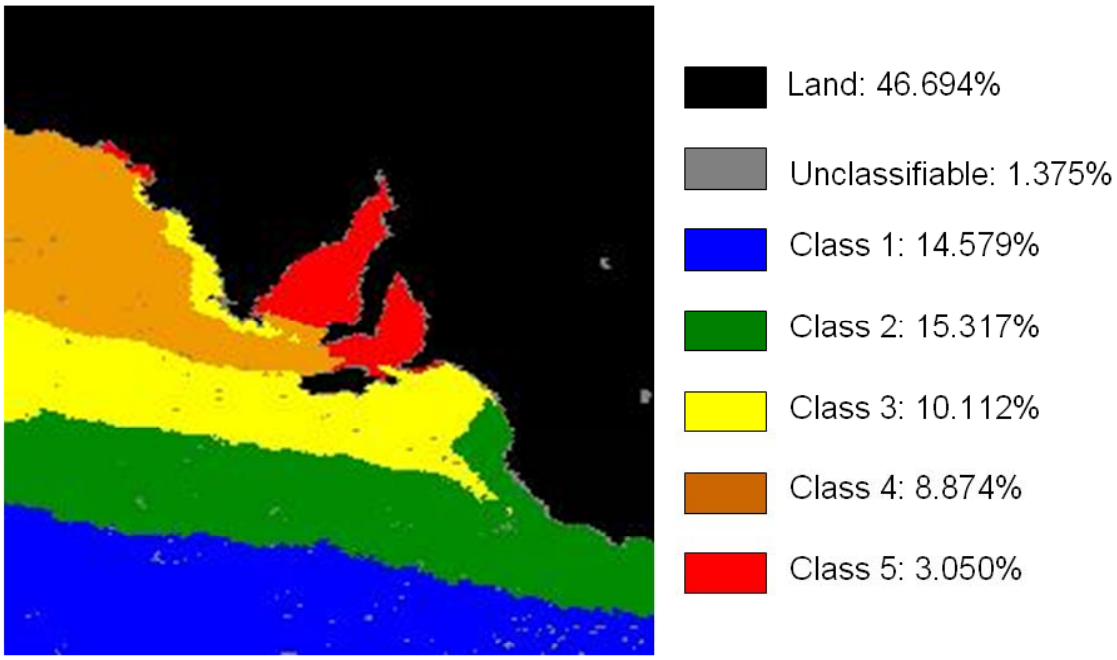

Figure 6.14. Results of an unsupervised classification upon 60 MODIS monthly SST images between July 2002 and June 2007.

6.6 Discussion

In order to have confidence in the data collected via satellite remote sensing, it must first be validated. Many different algorithms exist to estimate chlorophyll-*a* from MODIS imagery and several studies have been undertaken throughout the world's oceans and seas in an effort to validate the MODIS chlorophyll-*a* products. The chlorophyll-*a* validation presented here shows only a moderate relationship between MODIS estimated chlorophyll-*a* and in situ measurements. There are numerous factors that could influence the validation results. One of these factors is the difference between the regions for which the algorithms are developed and those in which they are applied.

Carder et al. (2004) assessed the performance of the MODIS empirical OC3M algorithm and a semi-analytical algorithm against chlorophyll-*a* data collected in the field across a range of marine provinces. Chlorophyll-*a* concentrations derived via each algorithm for MODIS Terra imagery were compared to field chlorophyll-*a* data collected for the SeaWiFS SeaBASS data archive from the Antarctic, Equatorial Pacific, California Current and West Florida Shelf. It was found that the OC3M algorithm produced an rms error of 21%, while the semi-analytical algorithm performed only slightly better with an rms error of 20%. The OC3M method resulted in slight overestimation of chlorophyll-*a* at low concentrations, consistent with the results shown here, and underestimation at higher concentrations. However the results suggested that for both methods the errors were within the 35% goal set for MODIS chlorophyll-*a* accuracies. The rms error of 27% found here for areas > 20 m deep also falls well within the 35% goal, whereas the 50% error for all depths combined, and the 55% error for depths ≤ 20 m, do not.

Carder et al. (2004) obtained good results for chlorophyll-*a* retrievals using the OC3M algorithm in the open ocean. However, Spencer Gulf is a coastal body of water where other factors such as organic matter and shallow water depth may impact on recorded chlorophyll-*a* values. Darecki and Stramski (2004) evaluated the performance of the OC3M algorithm and

two other MODIS and one SeaWiFS chlorophyll-*a* algorithms in the Baltic Sea. The OC3M algorithm performed the best compared to the field chlorophyll-*a* data as a result of the algorithm being designed for retrieval from Case II waters. However, the OC3M algorithm still performed poorly, and overestimated chlorophyll-*a* as a result of the influence of CDOM.

Limited field-based SST and chlorophyll-*a* data has been obtained from Spencer Gulf to compare to MODIS imagery to provide comprehensive validation of the image outputs. The data obtained show a good relationship between field and satellite derived SST, as expected. However, results for chlorophyll-*a* were less than ideal. MODIS overestimated chlorophyll-*a* when the values were low, and often produced outliers where the MODIS chlorophyll-*a* was more than double the concentration measured in the field. This poor predictive ability may be firstly attributed to the empirical algorithm developed for other oceans rather than the waters of Spencer Gulf. Other reasons could be due to differences in the scale and timing of measurements. Each MODIS pixel provides an average surface chlorophyll-*a* value for an area of 1 km^2. Furthermore, 9 pixels were averaged to account for possible positional errors. Field-based chlorophyll-*a* measurements, however, were determined from 1 litre water samples collected at the surface from a single location within this large area; thus, where there is high spatial variability of chlorophyll-*a* within this 9 km^2 area large variations between MODIS and field measurements could occur. Chlorophyll-*a* may also vary throughout the water column, meaning that a sample from a single depth does not sufficiently represent what MODIS is detecting, although CTD data indicate that this is not occurring in the TFZ (unpublished data). The timing of measurements can also affect the validation. High temporal variability at the point of measurement could lead to large differences between the two methods when measurements are not collected at corresponding times of the day. Bailey and Werdell (2006) suggest a window of ± 3 hours between field collection and satellite overpass to reduce the affects of temporal variability, a criterion that was not taken into account in this study. Another source of error may be the water depth, as reflectance from the seafloor can influence the estimation of chlorophyll-a in optically shallow waters. In Spencer Gulf, for measurements taken from a depth of greater than 20 m, there was a much stronger relationship between MODIS and field measurements than for depths of less than or equal to 20 m, indicating that water depths of 20 m or less are probably producing bottom reflectance that influences the MODIS estimates.

In the present study the seasonal characteristics of sea surface temperature and chlorophyll-*a* were investigated using MODIS satellite imagery. Throughout the study area there was a large range of chlorophyll-*a* and SST values observed. Chlorophyll-*a* values differed greatly with location. The chlorophyll-*a* values observed in far northern Spencer Gulf were considerably higher than at any other location, likely as a result of shallow water depth and the interference of bottom reflectance and suspended particles upon the measured reflectance. The average depth around station A is 20.45 m, but ranges between 9 and 31 m. Results of the MODIS chlorophyll-*a* validation showed that the relationship between MODIS chlorophyll-*a* and in situ chlorophyll-*a* measurements was much stronger when the water depth is greater than 20 m.

Another interesting feature observed in the MODIS chlorophyll-*a* measurements is an apparent increase in chlorophyll-*a* in the waters east of Port Lincoln in the TFZ compared to the centre of the gulf. As shown in Figure 6.6, the monthly chlorophyll-*a* measurements at station H, near the SBT aquaculture, were considerably higher than at station D, located in the centre of the gulf at the same latitude, with the greatest discrepancies occurring during the

period from March through to July. The first consideration is whether the measured chlorophyll-*a* is affected by water depth. Water depth at station H is approximately 21.8 metres, with the majority of the region deeper than 20 m, suggesting bottom reflectance is not a major issue. It is also likely that the waters around station H are influenced by suspended particles and organic matter, which may cause overestimation of chlorophyll-*a*. Another possibility is that the waters are actually higher in chlorophyll-*a*, perhaps as a result of increased nutrients available from aquaculture activities and other coastal industries, or from naturally occurring factors or processes. Sea cage aquaculture is known to release nutrients into the water column as a result of waste products, uneaten feed and faecal material (Gowen and Bradbury, 1987). Fernandes et al. (2007) modelled the nitrogen release from southern bluefin tuna aquaculture and suggested that more than 85% of the nitrogen in the baitfish fed to the tuna is expected to be lost to the environment. However the regional affects of this excess nitrogen upon the environment of the TFZ are still under investigation (Fernandes et al., 2007). The period of greatest increase in chlorophyll-*a* occurs from March through to July, which corresponds to the SBT farming season.

Hierarchical cluster analysis and unsupervised classification of chlorophyll-*a* measurements showed that station H was actually more similar to stations A and B in the northern gulf, than to the closer stations C, D and E. This finding is most likely a result of coastal influences, which A and B are also exposed to. The principal components analysis highlighted that most of the variability, ~82.7%, was associated with the high chlorophyll-*a* coastal areas differing from the lower chlorophyll-*a* offshore waters. From PCA and unsupervised classification it can be seen that station H is within the coastal classification. Since the remaining principal components were small compared to the spatial pattern, the affect of seasonal changes upon differences between station H and other stations is small. Thus, the differences between H and other stations are as a result of its location near to the coast, and not a characteristic of its temporal chlorophyll-*a* variability.

SST imagery identified a temperature gradient throughout Spencer Gulf that reverses in direction during winter (Figure 6.12) not only as a result of the decrease in SST within the gulf, but also as a result of a plume of relatively warm water extending from the GAB which spans the mouth of the gulf during the winter months (Figure 6.15 b). Although the wintertime GAB SST plume is of cooler water than is present during summer, it is significantly warmer than surrounding waters at the same time of the year. It is this GAB plume that is responsible for the higher SST observed at stations F and G throughout winter. This plume has previously been described by Herzfeld (1997) who investigated the annual cycle of SST in the Great Australian Bight using satellite SST imagery. The warm waters form in the shallow coastal waters of the GAB during summer and autumn and spread eastwards to form a tongue of warm water extending eastwards of 136ºE (Herzfeld, 1997), past the mouth of Spencer Gulf. During late autumn the warm GAB surface waters join up with the warm Leeuwin Current, which flows into the GAB from the Western Australian coastline, to produce a continuous band of warm water along the southern Australian coastline during winter (Herzfeld, 1997). Thus, the increase in SST from stations E through to G (Figure 6.12) observed during June, July and August is a result of the warm GAB surface waters extending across the mouth of Spencer Gulf (Figure 6.15 b).

Another oceanographic feature of Spencer Gulf, identified in the MODIS imagery, which plays an important role in circulation of the gulf during summer, is the sea surface temperature front (Figure 6.15 a). The front marks the boundary between the shallow, warm waters of Spencer Gulf and the deeper, cooler oceanic waters. Previous work using daily

AVHRR SST imagery by Petrusevics (1993) has shown that the front begins to develop in November, as summertime solar heating intensifies, and persists until May, with the greatest temperature difference of 4°C occurring in April. CTD surveys by Petrusevics (1993) showed that the SST front is also a density minimum, where currents from Spencer Gulf and the shelf converge, generating upwelling that isolates gulf and shelf waters. SST in Spencer Gulf can be seen to decrease between stations D and E from December through to April (Figure 6.12) as a result of the SST front. The front appears to be a key factor accounting for the pattern seen in the unsupervised classification of the SST. The classification image separated the gulf waters from nearby ocean waters at a location where the SST front is known to occur (Figure 6.14; 6.15 a).

Another feature of the region observable from satellite SST imagery is coastal upwelling. Upwelling is known to occur at three locations along the South Australian coastline: the Bonney coast in the southeast of the state; the southwestern coast of Kangaroo Island; and the western coast of Eyre Peninsula. Approximately 2 or 3 upwelling events occur simultaneously at these 3 locations each summer, each lasting approximately 1 week and resulting in decreases of SST of 2 – 3 ºC and increases in chlorophyll-*a* up to 4 µg L^{-1} (Kaempf et al., 2004). Although the short time span of each event, ~ 1 week, is masked within monthly composite imagery, evidence of the occurrence of upwelling is available within the monthly SST imagery, particularly during months when multiple upwelling events have occurred. March 2003 is one month where the effects of coastal upwelling are visible in the monthly SST imagery (Figure 6.16). Cooler surface waters are evident along the Bonney Coast, Kangaroo Island and Eyre Peninsula where upwelled water is 2 – 3 ºC cooler. Upwelling in these regions is a common occurrence and is detected by the unsupervised classification, which shows the water in these regions as belonging to a class that is cooler (Figure 6.14).

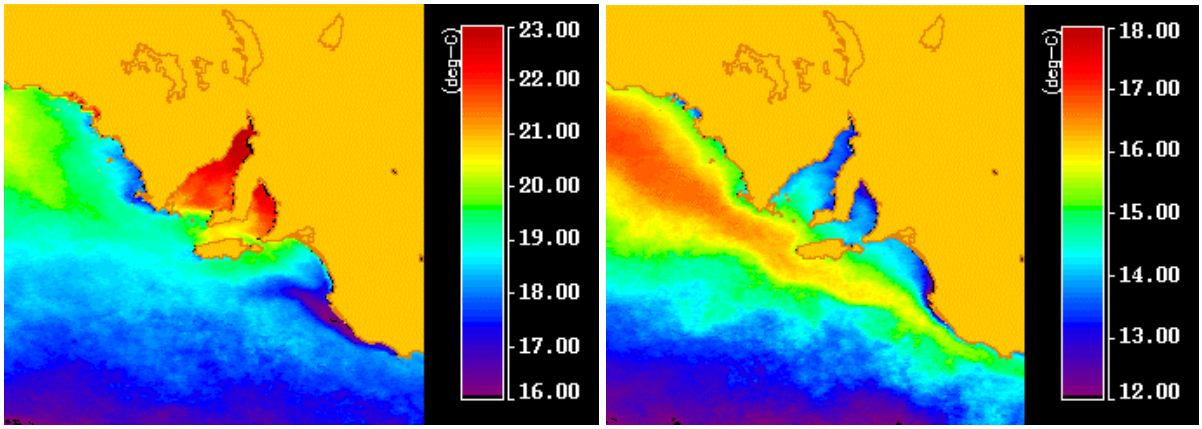

(a) Summer SST front (b) Winter warm GAB plume

Figure 6.15. (a) Monthly SST climatology during February, showing the warm gulf waters isolated from the adjacent shelf waters by the SST front during summer and (b) Monthly SST climatology during July, showing the tongue of warm GAB water extending past the mouth of Spencer Gulf during winter. Note the different scales on the colour bars.

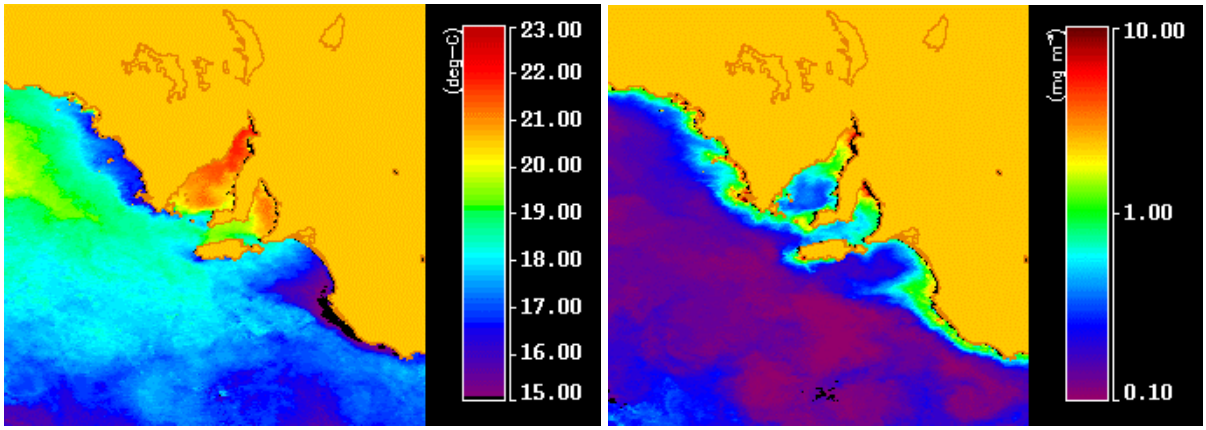

(a) (b)

Figure 6.16. Monthly SST (a) and monthly chlorophyll-*a* (b) of March 2003 showing upwelling in the southeast of SA, on southwestern Kangaroo Island and on western Eyre Peninsula as indicated by cooler surface temperatures and increased chlorophyll-*a*.

6.7 Conclusions

MODIS Aqua chlorophyll-*a* and sea surface temperature imagery was compared to chlorophyll-*a* concentrations and temperature measurements obtained from Spencer Gulf in an attempt to show that MODIS algorithms are valid in this study area. Limited amounts of field data were available for comparison, resulting in a limited validation. MODIS SST performed well compared to field measurements obtained 1 m below the sea surface with an R^2 value of 0.94. MODIS chlorophyll-*a* concentrations did not perform as well. MODIS often overestimated chlorophyll-*a* measurements when concentrations were low, and produced frequent outliers that were several times greater than measured concentrations. Despite this, MODIS measurements of chlorophyll-*a* followed the general trend of field-based measurements, with an R^2 value of 0.46. The relationship for chlorophyll-*a* improved when only measurements from a water depth of > 20 m were used ($R^2 = 0.77$), with the rms error of 27% falling well within the target error of 35% that MODIS was designed to achieve.

Monthly composite imagery allowed the seasonal variations in SST and chlorophyll-*a* to be described. Seasonal chlorophyll-*a* variations differed greatly at different locations in and around Spencer Gulf. Chlorophyll-*a* concentrations were highest in northern Spencer Gulf, with the peak occurring from January to May and minimum concentrations from August to November. The satellite chlorophyll-*a* measurements in the northern gulf are possibly influenced by the adjacent land as a result of the shallow water depth, reflectance from the land, and suspended matter, resulting in an overestimation of chlorophyll-*a*. In the southern part of the gulf, concentrations were much lower than in the northern part, and the periods of maximum and minimum chlorophyll-*a* occurred from April to July and September to November respectively. Further south, outside the mouth of Spencer Gulf, the concentrations were lower again and the periods of maximum and minimum occurred from August to November and December to April, almost the opposite seasonal cycle to the northern part of the gulf. The region around the TFZ showed higher chlorophyll-*a* concentrations than nearby gulf waters, likely as a result of shallower water depth and coastal influences, but possibly also as a result of farming practices. A hierarchical cluster analysis and unsupervised classification of the imagery have shown that the TFZ is more similar to the northern part of the gulf and other coastal areas than to waters in the centre of Spencer Gulf, closer to the TFZ.

Sea surface temperature varied greatly between Spencer Gulf and nearby ocean waters. Waters within the gulf showed a greater seasonal range than waters outside the gulf. As a result the gulf waters are warmer than nearby ocean waters in summer, but cooler during winter. There was also a noticeable gradient in the seasonal temperature range through the gulf, with warmest summer temperatures and coolest winter temperatures in the northern part of the gulf. Moving south through the gulf the summertime maximum temperature decreased and the wintertime minimum increased resulting in an annual temperature change of only a few degrees in the waters outside of the gulf. This result is consistent with previous studies that have described the seasonal temperature characteristics of Spencer Gulf. Results from hierarchical cluster analysis, unsupervised classification and principal components analysis have all confirmed that based on SST Spencer Gulf, and Gulf St Vincent, are different from the other waters of the region, as a result of the large seasonal changes in temperature.

6.8 References

Anding, D. and R. Kauth (1970). "Estimation of Sea Surface Temperature from Space." Remote Sensing of Environment 1: 217-220.

Bailey, S. W. and P. J. Werdell (2006). "A multi-sensor approach for the on-orbit validation of ocean color satellite data products." Remote Sensing of Environment 102: 12-23.

Brown, O. B. and P. J. Minnett (1999). MODIS Infrared Sea Surface Temperature Algorithm Version 2.0. Algorithm Theoretical Basis Document, University of Miami.

Carder, K. L., F. R. Chen, J. P. Cannizzaro, J. W. Campbell and B. G. Mitchell (2004). "Performance of the MODIS semi-analytical ocean color algorithm for chlorophyll-a." Advances in Space Research 33: 1152-1159.

Carder, K. L., F. R. Chen, Z. Lee, S. K. Hawes and J. P. Cannizzaro (2003). Case 2 Chlorophyll a Version 7. Algorithm Theoretical Basis Document, University of South Florida.

Darecki, M. and D. Stramski (2004). "An evaluation of MODIS and SeaWiFS bio-optical algorithms in the Baltic Sea." Remote Sensing of Environment 89: 326-350.

Fernandes, M., P. R. Lauer, A. Cheshire and M. Angove (2007). "Preliminary model of nitrogen loads from southern bluefin tuna aquaculture." Marine Pollution Bulletin. 54: 1321-1322.

Gowen, R. J. and N. B. Bradbury (1987). "The ecological impact of salmonid farming in coastal waters: a review." Oceanography and Marine Biology Annual Review 25: 563-575.

Herzfeld, M. (1997). "The annual cycle of sea surface temperature in the Great Australian Bight." Progress in Oceanography 39: 1-27.

IOCCG (2000). Remote Sensing of Ocean Colour in Coastal, and other Optically-Complex, Waters. Reports of the International Ocean-Colour Coordinating Group, No. 3. S. Sathyendranath. Dartmouth, Canada, IOCCG.

Kaempf, J., M. Doubell, D. Griffin, R. L. Matthews and T. M. Ward (2004). "Evidence of a Large Seasonal Coastal Upwelling Sysem along the Southern Shelf of Australia." Geophysical Research Letters 31.

O'Reilly, J. E., S. Maritorena, D. Seigel, M. O'Brien, D. Toole, B. G. Mitchell, M. Kahru, F. P. Chavez, P. Strutton, G. F. Cota, S. B. Hooker, C. R. McClain, K. L. Carder, F. E. Muller-Karger, L. Harding, A. Magnuson, D. Phinney, G. F. Moore, J. Aiken, K. R. Arrigo, R. M. Letelier and M. E. Culver (2000). Ocean Color Chlorophyll a Algorithms for SeaWiFS, OC2 and OC4: Version 4. SeaWiFS Postlaunch Technical Report Series Volume 11. SeaWiFS Postlaunch Calibration and Validation Analyses, Part 3. S. B. Hooker and E. R. Firestone.

Petrusevics, P. (1993). "SST Fronts in Inverse Estuaries, South Australia - Indicators of Reduced Gulf-Shelf Exchange." Australian Journal of Marine and Freshwater Research 44: 305-323.
RSI (2006). "ENVI: Environment for Visualizing Images". Version 4.3. Research Systems Inc., Boulder, CO, USA
SPSS (2006). "SPSS 15.0 for Windows."

Chapter 7: Temporal and spatial variability in phytoplankton abundance and community composition, and pelagic biogeochemistry in the tuna farming zone

Paul Van Ruth[1,3*], Peter Thompson[2,3], Susan Blackburn[2,3], Pru Bonham[2,3]

[1]South Australian Research and Development Institute, Aquatic Sciences
[2]CSIRO Division of Marine and Atmospheric Research
[3]Aquafin CRC

*corresponding author: SARDI Aquatic Sciences, PO Box 120, Henley Beach, SA, 5022
Phone: +61 (8) 8207 5421, Email: vanruth.paul@saugov.sa.gov.au

Abstract

Spatial and temporal variation in phytoplankton biomass, abundance, and community composition, were examined in the tuna farming zone (TFZ). Data from samples collected monthly during 2005-2006 were compared with long-term datasets to assess whether any patterns identified in abundance and composition are consistent annual features of the region. Particular emphasis was placed on the presence of harmful microalgae, and their potential to cause toxic blooms. Results indicate a peak in phytoplankton abundance in May 2006, which is driven by a diatom peak. Analysis of long term datasets suggest that predominately diatom peaks have been consistent phenomena in the TFZ during late autumn or early winter. The May peak in diatoms appears to be made possible, in part, by a February peak in silica concentrations (>3.5 μmol L^{-1}). A range of Harmful Algal Bloom (HAB) species were detected in the TFZ, but there is little evidence of a HAB having occurred in the region. However, abundances of known ichthyotoxic phytoplankton species are sufficiently dense to warrant monitoring and caution. There is evidence that ichthytoxic species are more prevalent in some locations than others (e.g.: Bickers Island and Boston Bay), which suggests that local populations of harmful microalgae may be developing in the vicinity of the TFZ. A risk assessment of the potential for HABs in the TFZ is presented, with possible future scenarios that could increase the risk of HABs forming in the TFZ.

7.1. Introduction

The coastal waters of southern Spencer Gulf, South Australia, are of high economic importance to the state, and support important pelagic fisheries, including the South Australian sardine (*Sardinops sagax*) fishery, the largest marine scale-fish fishery in Australia. The area around Port Lincoln in south-west Spencer Gulf, supports an intensive aquaculture industry, with southern bluefin tuna (*Thunnus maccoyii*) farmed in the tuna farming zone (TFZ). The marine ecosystem in this economically important area requires careful management to ensure the sustainable continuation of the fishing and aquaculture industries in the region. It is also important to ensure that the practices of the fisheries and aquaculture industries are conducted in a sustainable way, minimising the impact of these industries both on the local and also the regional ecosystems.

Phytoplankton underpin the autotrophic food chain in marine ecosystems, and an understanding of phytoplankton dynamics is essential for ecosystem management. To understand phytoplankton dynamics one must consider the factors that are likely to influence phytoplankton growth and productivity, which primarily are the availability of nutrients and light. Nutrient regime shifts in a given region could lead to changes in phytoplankton abundance and community structure. These changes may be beneficial to the ecosystem (i.e. drive an increase in phytoplankton biomass with a resultant increase in food web productivity including commercially important fish species), but they can also be detrimental (e.g. an increase in abundance of harmful algal blooms (HABs) that can cause widespread problems for the aquaculture industry). HABs may be stimulated through increased eutrophication from nutrient inputs from domestic and industrial wastewater, as well as from wastes from aquaculture operations (Hallegraeff 1993). Previous studies in and around the TFZ have documented the presence of HAB speicies in the phytoplankton community in the region (Clarke, 1996; Paxinos et al., 1996). Knowledge of spatial and temporal variations in nutrient concentrations is important in explaining phytoplankton dynamics and assessing the risk of HABs to the aquaculture industry and the ecosystem of the TFZ.

The aim of this study was to examine temporal and spatial variability in nutrient concentrations and phytoplankton abundance and community structure in the TFZ ecosystem in order to identify and explain any patterns that may occur in these features. Long-term phytoplankton datasets were used to assess whether any patterns identified in field data from this study are consistent annual features of the region. Particular emphasis was placed on the presence of harmful algae, and their potential to cause toxic blooms. Knowledge gained from this study is used to evaluate possible risks posed by harmful algae to the ecosystem and the aquaculture industry in TFZ, and will help to formulate possible responses to minimise the impact of any risks on the ecosystem and industry in the area.

7.2. Methods

Phytoplankton samples were collected monthly between September 2005 and September 2006 aboard the RV Breakwater Bay. Sampling sites were located in Boston Bay and surrounding waters, in south-west Spencer Gulf, South Australia (Figure 7.1). Surface samples and deepwater samples (~1m from the bottom) were collected via Niskin bottle at all sampling sites and were processed as follows.

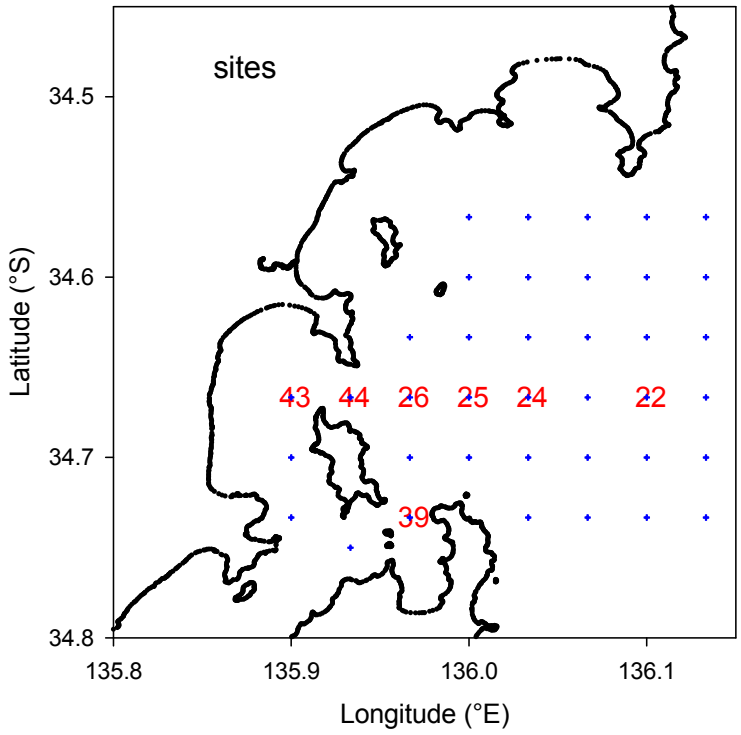

Figure 7.1. Map of sites (43, 44, 39, 26, 25, 24, 22) sampled from August 2005 to September 2006 in the TFZ.

7.2.1. Phytoplankton biomass and abundance

The concentrations of various pigments and the abundance of individual taxa were determined to estimate phytoplankton biomass. For pigments, two size fractions were collected as 1 or 2 litre samples filtered through mesh (to retain cells >5 µm), then glass fibre filters (to retain cells <5 µm), and the filters or mesh stored in cryo-vials in liquid nitrogen prior to their return to the laboratory. In the laboratory, filter or mesh samples were immersed in 100% acetone (3 mL) in a 10 mL centrifuge tube. The samples were vortexed for about 30 seconds and then sonicated in an ice-water bath for 15 minutes in the dark. The samples were then kept in the dark at 4 °C for approximately 15 hours. After this time, 300 µL water was added to the acetone such that the final extract mixture was 90:10 acetone:water (vol:vol) and sonicated once more in an ice-water bath for 15 minutes. The extracts were quantitatively transferred to a clean centrifuge tube and centrifuged to remove debris. The final extract was filtered through a 0.2 µm membrane filter (Whatman, anatope) prior to analysis by HPLC using a Waters-Alliance high performance liquid chromatography system, comprising a 2695XE separations module with column heater, a refrigerated autosampler and a 2996 photo-diode array detector. Immediately prior to injection the sample extract was mixed with a buffer solution (90:10 v/v of 28 mM tetrabutyl ammonium acetate at pH 6.5: methanol) within the sample loop. After injection, pigments were separated using a Zorbax Eclipse XDB-C8 stainless steel 150 mm x 4.6 mm ID column with 3.5 µm particle size (Agilent Technologies) and the gradient elution procedure of Van Heukelem and Thomas (2001) with minor modifications. The flow rate was 1.1 mL min^{-1} and the column temperature was 55°C. The separated pigments were detected at 436 nm and identified against standard spectra using Waters Empower software. Concentrations of chlorophyll-*a*, chlorophyll-*b* and β,β-carotene in sample chromatograms were determined from Sigma standards (USA) while all other pigment concentrations were determined from DHI standards (Denmark).

One litre samples from the surface and deep water were fixed with acidified Lugol's iodine solution for phytoplankton enumeration and identification. Identification and enumeration to genera or species level was carried out using light microscopy by Microalgal Services, Victoria, Australia. Abundance data were pooled by depth, and temporal variation in abundance and community structure was examined via indicator species analysis using PC-Ord 5 (McCune and Mefford 1999). Indicator values were calculated using the method of Dufrene & Legendre (1997).

7.2.2. Long term datasets

Remote sensed data

To assess whether the seasonal trend in phytoplankton biomass observed in 2005-2006 was a regular feature of this region, satellite data were compiled and analysed. For this analysis the 'region' was defined as a 120 x 120 nautical mile box around southern Eyre Peninsula. Satellite fluorescence data for the period 1997-2006 was used in this analysis. See section 5.3.4. for further details.

South Australian Environmental Protection Authority data

The South Australian Environmental Protection Authority (SA EPA) data on chlorophyll-*a* concentrations for 6 locations (North Shields, Point Boston, Boston Island, Town Jetty, Billy Lights Point and Proper Bay) in Boston Bay (http://www.epa.sa.gov.au/boston.html) were examined to expand the spatial and temporal information on chlorophyll-*a* in the region. EPA sampling was ~ bimonthly from 1997. Sites further afield were also sampled by the EPA with those from Coffin Bay and Port Hughes providing a useful comparison. The temporal periods for which data were available varied from 4 years (Coffin Bay, Venus Bay) to 11 years (Port Hughes, Boston Bay), and the total number of observations varied (see section 5.3.3.).

Tuna Boat Owners Association of South Australia data

Another long-term dataset of phytoplankton taxa and their abundance that was made available to the project was the Tuna Boat Owners Association of South Australia (TBOASA – now ASBTIA) phytoplankton database. The database contains abundance and composition data from fresh, unfixed samples collected within the TFZ between 1999 and 2006. Samples were collected by divers at various locations within the zone, at various depths, with no continuity in sampling locations or the number of samples collected between months within years, or between years. To enable comparisons with our 2005-2006 abundance data, the mean abundance of all samples collected at all depths within the TFZ in a given month of a given year was calculated and taken to represent phytoplankton abundance within the TFZ in that month.

South Australian Shellfish Quality Assurance Program data

The South Australian Shellfish Quality Assurance Program (SASQAP) is a joint initiative between the Department of Primary Industries and Resources South Australia (PIRSA) and the shellfish industries of South Australia, and is the principal organisation charged with monitoring and maintaining shellfish safety in South Australia. SASQAP routinely monitor a large number of sites throughout South Australia for the presence of toxic microalgae that are harmful to the shellfish industry. These data were kindly made available for comparative analyses in this study. This analysis of the SASQAP data is restricted to observations from 5 sites in or near the TFZ (Table 7.1).

Table 7.1. List of sites from the SASQAP database used in the analysis of spatial and temporal variations in Harmful Algal Bloom species in the TFZ.

Site	Number of observations [1]	Start date	End date
Bickers Island	2798	11/5/1999	3/7/2006
Lincoln	16	10/4/2001	3/7/2006
Proper Bay	2766	7/1/1999	3/7/2006
Loth Bay	2061	10/8/1999	3/7/2006
Boston Bay	2487	22/1/2000	3/7/2006

[1]every previously encountered toxic taxa counts as an observation in each sample regardless of presence, e.g. 15 taxa found in one sample = 15 observations, or the absence of the same 15 taxa in one sample = 15 observations.

7.2.3. Nutrient analysis

Fifty millilitre water samples for nutrient analysis were filtered through Whatman 0.45µm polypropylene filters, and frozen until analysed. Dissolved inorganic nutrient concentrations (silica (Si), nitrite (NO_2^-), nitrate (NO_3^-), ammonia (NH_3 + NH_4^+), and filterable reactive phosphorus (FRP)) were analysed by the water studies centre at Monash University, Victoria, Australia. Detection limits were 0.17 µM for Si, 0.022 µM for NO_2^-, 0.016 µM for NO_3^-, 0.059 µM for NH_3, and 0.011 µM for FRP. Concentrations of NO_2^- in this study were generally at or below detection limits. When detected, NO_2^- concentrations were added to NO_3^- concentrations to get total oxidised nitrogen, and the total referred to as NO_3^- for simplicity. Analytical methods are detailed in section 5.2.2.

7.2.4. Community connectivity with the wider region

To examine the potential connectivity of the phytoplankton community in the TFZ with the wider region, a comparison of phytoplankton community data collected for this project (as outlined in Figure 7.1) was made with data collected in the eastern Great Australian Bight (EGAB) in February 2005 (Van Ruth, PhD thesis in prep). EGAB community data were collected in seven regions between Kangaroo Island and the head of the bight, four near-shore and three at the shelf edge. Three replicate samples were collected from each region. Data collected in February 2006 from three near-shore sites in the TFZ (sites 25, 39 and 44) were included as replicates within an eighth region in the analysis (Figure 7.2). Data were analysed via non-metric multidimensional scaling (nMDS) and indicator species analysis using PC-Ord 5 (McCune and Mefford 1999).

Data from the South Australian Shellfish Quality Assurance Program (SASQAP) provide a unique opportunity to assess whether toxic microalgae from other sites are the same or different from those in the TFZ. Data on the abundance and type of toxic species identified during May 2006, which were collected at 19 sites in coastal waters throughout the Eyre Peninsula region, were analysed for similarity with the TFZ data from this study using PATN™ software (Belbin et al. 1992).

As part of this project, some sampling of the phytoplankton community composition was made at sites outside the TFZ near the southern boundary of Spencer Gulf (Figure 7.3). In order to make statistical comparisons between sites it was necessary to make the observations as consistent as possible. This necessitated reducing the number of taxa to those most commonly observed. For each location (inside TFZ, and outside TFZ within southern Spencer Gulf) the 10 'indicator' species found consistently at all sites were used after log transformation followed by analyses for significant differences by Student's t-tests. The degree of similarity in phytoplankton community composition across the sites in the TFZ and southern Spencer Gulf was further compared by PATN™ software (Belbin et al. 1992) using

a Bray and Curtis association matrix based upon the samples collected during February 2006. In this analysis, only those species found at more than three sites were included, reducing the data set to 20 more common species.

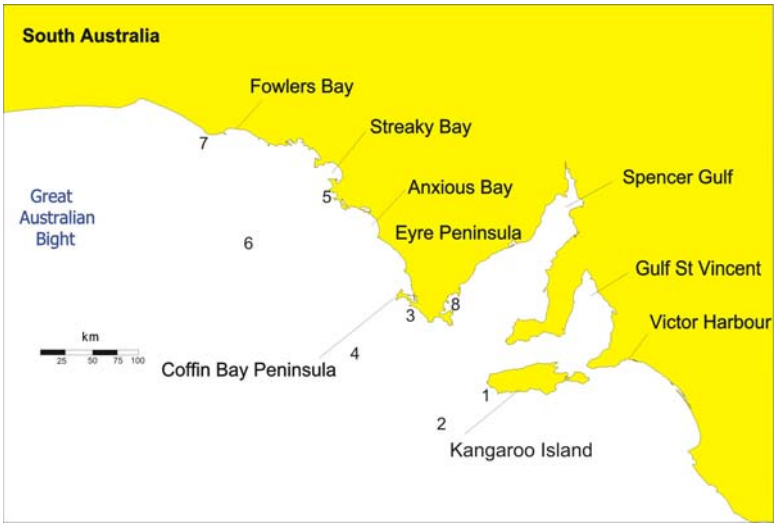

Figure 7.2. Regions used in the non-metric Multidimensional Scaling (nMDS) analysis of community composition in the TFZ and the eastern Great Australian Bight.

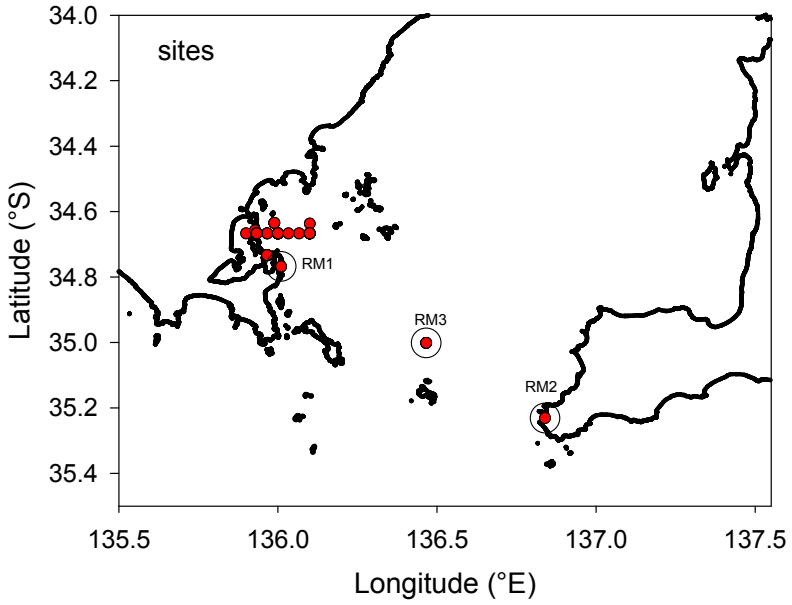

Figure 7.3. Sites outside Boston Bay (circled) used in a comparison of phytoplankton community composition between the TFZ and other regions of southern Spencer Gulf.

7.3. Results

7.3.1. Monthly biomass and abundance data

Phytoplankton biomass measured as chlorophyll-*a* showed a high degree of spatial variation, with no clear pattern evident between depths or with distance from shore. More than half of the total chlorophyll-*a* occurred in the small size fraction (<5 µm, Figure 7.4). Mean chlorophyll-*a* concentrations in this fraction peaked in May 2006 (Figure 7.4). Mean

concentrations in the large size fraction (>5 μm) peaked in May 2006 in surface samples, and in April 2006 in deepwater samples (Figure 7.4).

The summed density of all phytoplankton cells across all taxa varied, but there were no clear spatial patterns in total cell abundance evident between sites or depths (Figure 7.5). Total cell abundances mirrored the chlorophyll-*a* biomass with a maximum in May 2006, with means (± standard error) of 2.6 ± 0.90 x 10^5 cells L^{-1} in surface waters and 3.8 ± 0.85 x 10^5 cells L^{-1} in deepwater samples. An examination of the different phytoplankton groups revealed that diatoms dominated the total abundances, with mean diatom cell densities peaking in May 2006 at 2.2 ± 0.88 x 10^5 cells L^{-1} in surface samples and 3.3 ± 0.81 x 10^5 cells L^{-1} in deepwater samples. Dinoflagellates were present in all months of the study at abundances <60,000 cells L^{-1}, and do not appear to be contributing significantly to the temporal variation evident in total abundances. Other phytoplankton included chlorophytes, chrysophytes, cryptophytes, dictyochophytes, euglenophytes, haptophytes, prasinophytes, and rhaphidophytes. These 'other' phytoplankton had a similar temporal pattern to the dinoflagellates, with abundances <60,000 cells L^{-1} for most of the year, apart from a peak in April 2006 when mean abundances reached 0.96 ±0.25 x 10^5 cells L^{-1} in surface waters, and 0.70 ± 0.11 x 10^5 cells L^{-1} in deepwater samples (Figure 7.5).

Indicator species analysis to examine the species/genera contributing significantly to differences in community composition between months (Table 7.2) confirmed the patterns observed in the abundance data (Figure 7.5). The spike in abundance of 'other' phytoplankton (Figure 7.5) was primarily an increase in the abundance of *Hemiselmis* sp., *Plagioselmis prolonga*, *Pyramimonas* spp., *Chrysoshromulina* spp., and *Tetraselmis* spp. (Table 7.2). The diatom *Guinardia striata* was also present in considerably higher numbers in April 2006. There were significant increases in diatom abundance in May 2006 and June 2006, with these peaks (Figure 7.5) driven by *Leptocylindrus minimus* and *Leptocylindrus danicus* in May 2006, and *Chaetoceros* spp. in June 2006 (Table 7.2).

Marker pigments give a picture of the phytoplankton community that can be more powerful than light microscopic identification for certain groups e.g. small species generally <10 μm. An examination of selected marker pigments normalized to chlorophyll-*a* suggests strong seasonality in the taxa found in the study area (Figure 7.6), and supports the trends outlined in the abundance data. In the < 5 μm size fraction, fucoxanthin, an indicator of the presence of diatoms, was the dominant marker pigment with a peak in May 2006. Chlorophyll-*b* in the small size fraction peaked in January 2006, and again in July 2006, and in the absence of lutein and prasinoxanthin suggests an increased presence of certain prasinophytes (Jeffrey and Wright 2006) during these periods. 19'-hexanoyloxyfucoxanthin was most prevalent in February 2006 indicating an increased presence of haptophytes, while a peak in zeaxanthin in January 2006 suggests an increase in the cyanobacteria in the summer months. In the large size fraction (Figure 7.7), a peak in fucoxanthin (diatoms) was detected ~ April/May 2006, and there was a small spike in peridinin (dinoflagellates) in July 2006.

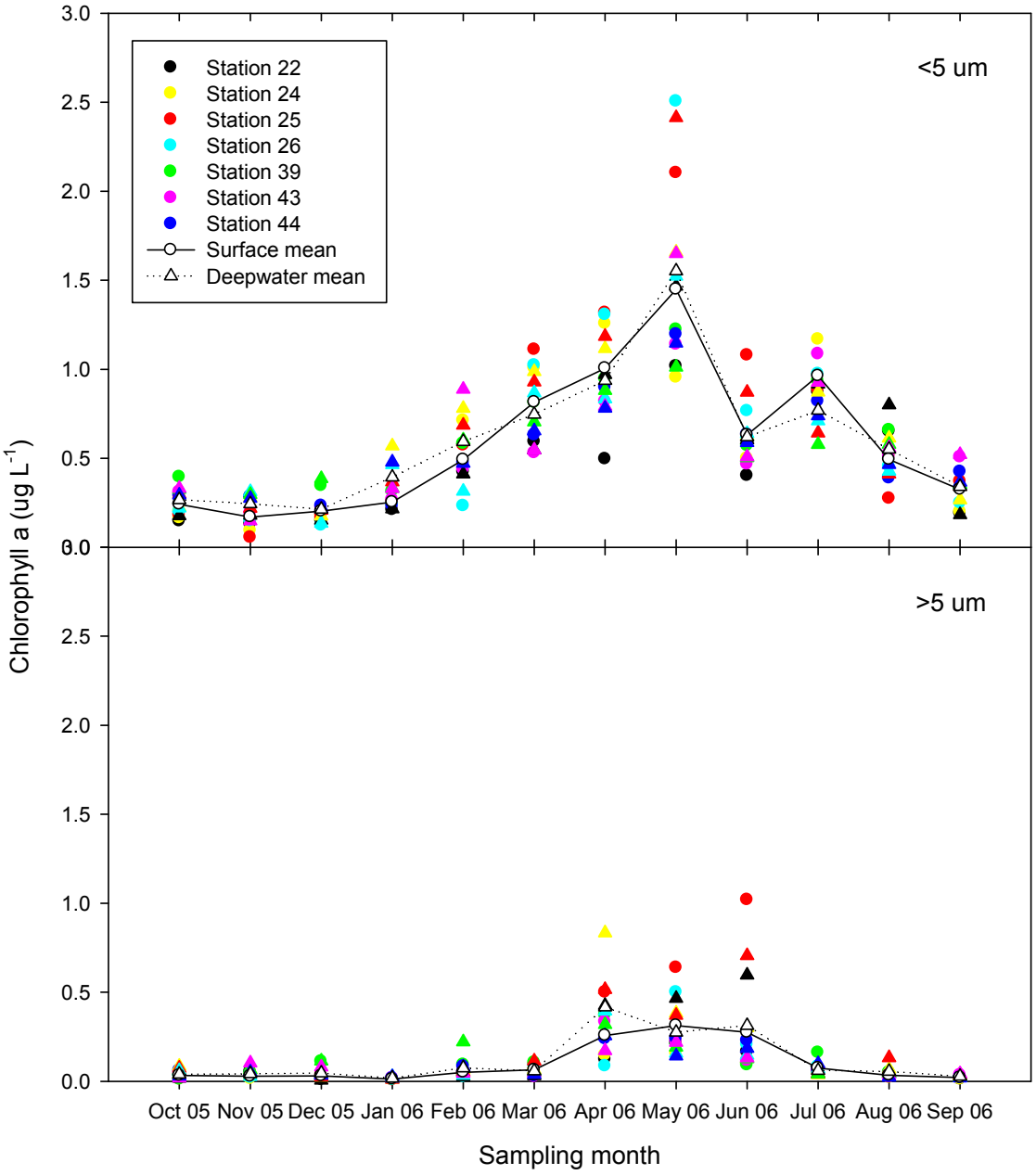

Figure 7.4. Size fractionated chlorophyll-*a* concentrations at 7 sites in the TFZ (see Figure 7.1) during part of 2005 and 2006. Circles indicate surface samples. Triangles indicate deepwater samples. Means are regional means (ie: the mean for all sites in the figure).

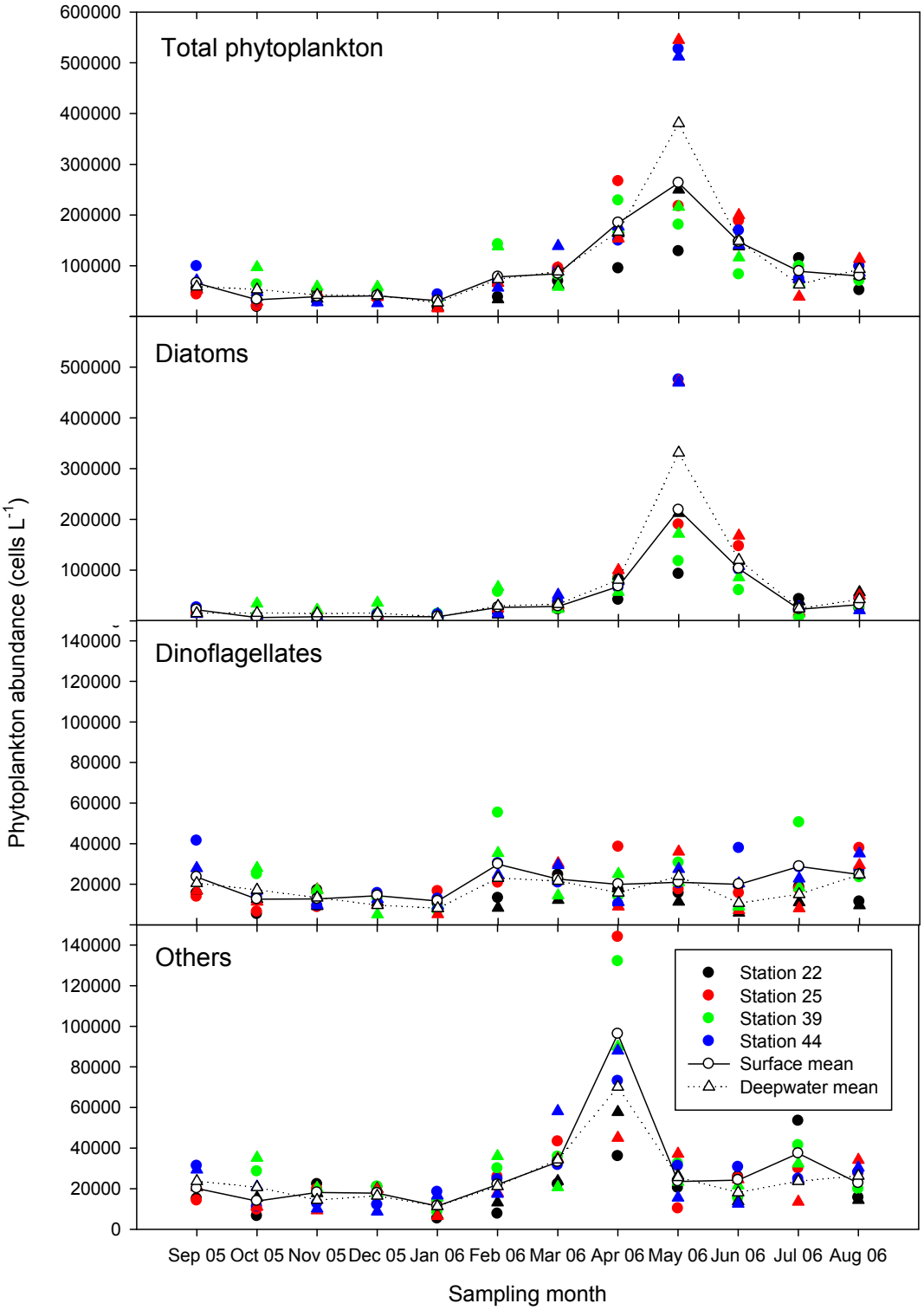

Figure 7.5. Monthly variations in phytoplankton abundance in the TFZ. Site locations shown in Figure 7.1. Circles indicate surface samples. Triangles indicate deepwater samples. Note the change in scale on the y axis for dinoflagellates and other phytoplankton. Means are regional means (ie: the mean for all sites in the figure).

Table 7.2. Indicator species analysis to determine the taxa of phytoplankton contributing significantly to differences in community structure between months (probabilities (p) less than 0.05 are considered statistically significant). Mean abundance in cells L^{-1} ± standard error; n = 4, except in September 05 when n = 3. Rel. freq. = relative frequency (%), i.e. the % of samples in a given month where a given species is present.

Type	Species	Month	p	Mean abundance	Rel. freq.
Cryptophyte	*Leucocryptos marina*	Sep-05	0.003	3133 (± 1964)	100
Chrysophyte	*Ochromonas* spp.	Sep-05	0.005	2833 (± 536)	100
Chrysophyte	*Calycomonas* sp.	Sep-05	0.039	1400 (± 529)	100
Cryptophyte	*Rhodomonas salina*	Sep-05	0.046	567 (± 348)	67
Cryptophyte	*Teleaulax acuta*	Dec-05	0.046	2713 (± 951)	100
Dinoflagellate	*Ceratium lineatum*	Mar-06	0.004	4225 (± 1490)	100
Diatom	*Entomoneis* spp.	Mar-06	0.018	6300 (± 2372)	100
Diatom	*Coscinodiscus* spp.	Mar-06	0.005	1425 (± 284)	100
Dinoflagellate	*Amphidinium* sp.	Mar-06	0.037	1575 (± 333)	100
Diatom	*Guinardia striata*	Apr-06	0.0002	74500 (± 8849)	100
Prymnesiophyte	*Chrysochromulina* spp.	Apr-06	0.0002	19788 (± 6027)	100
Cryptophyte	*Hemiselmis* sp.	Apr-06	0.0002	71938 (± 14401)	100
Dinoflagellate	*Prorocentrum gracile*	Apr-06	0.002	1500 (± 300)	100
Cryptophyte	*Plagioselmis prolonga*	Apr-06	0.003	34275 (± 7285)	100
Dinoflagellate	*Dinophysis caudata*	Apr-06	0.003	712.5 (± 384)	75
Prasinophyte	*Tetraselmis* spp.	Apr-06	0.005	13925 (± 2457)	100
Diatom	*Cocconeis* spp.	Apr-06	0.018	6625 (± 433)	100
Prasinophyte	*Pyramimonas* spp.	Apr-06	0.038	21450 (± 3063)	100
Diatom	*Dactyliosolen fragilissimus*	May-06	0.0002	46750 (± 8892)	100
Diatom	*Dactyliosolen phuketensis*	May-06	0.0002	34650 (± 7429)	100
Diatom	*Leptocylindrus minimus*	May-06	0.0002	271500 (± 118849)	100
Diatom	*Skeletonema spp.*	May-06	0.0002	23050 (± 4662)	100
Diatom	*Asterionellopsis glacialis*	May-06	0.0004	14150 (± 5335)	100
Diatom	*Asteromphalus sarcophagus*	May-06	0.0004	3000 (± 812)	100
Diatom	*Leptocylindrus danicus*	May-06	0.002	76250 (± 19345)	100
Diatom	*Thalassiosira* cf. *mala*	May-06	0.014	18850 (± 2869)	100
Diatom	*Eucampia zodiacus*	Jun-06	0.0002	3200 (± 787)	100
Diatom	*Cerataulina pelagica*	Jun-06	0.003	5500 (± 1308)	100
Diatom	*Chaetoceros* spp.	Jun-06	0.003	44500 (± 11478)	100
Diatom	*Pseudonitzschia fraudulenta*	Jun-06	0.003	14150 (± 6304)	75
Diatom	*Pseudonitzschia delicatissima* complex	Jun-06	0.004	21100 (± 7664)	100
Diatom	*Guinardia flaccida*	Jun-06	0.006	2250 (± 665)	100
Diatom	*Thalassiosira* sp.	Jun-06	0.015	4100 (± 1308)	100
Dinoflagellate	*Protoperidinium* spp.	Jun-06	0.018	2900 (± 1063)	100
Diatom	*Bacteriastrum elegans*	Jun-06	0.025	7200 (± 4705)	75
Diatom	*Rhizosolenia* spp.	Aug-06	0.002	4975 (± 1795)	100

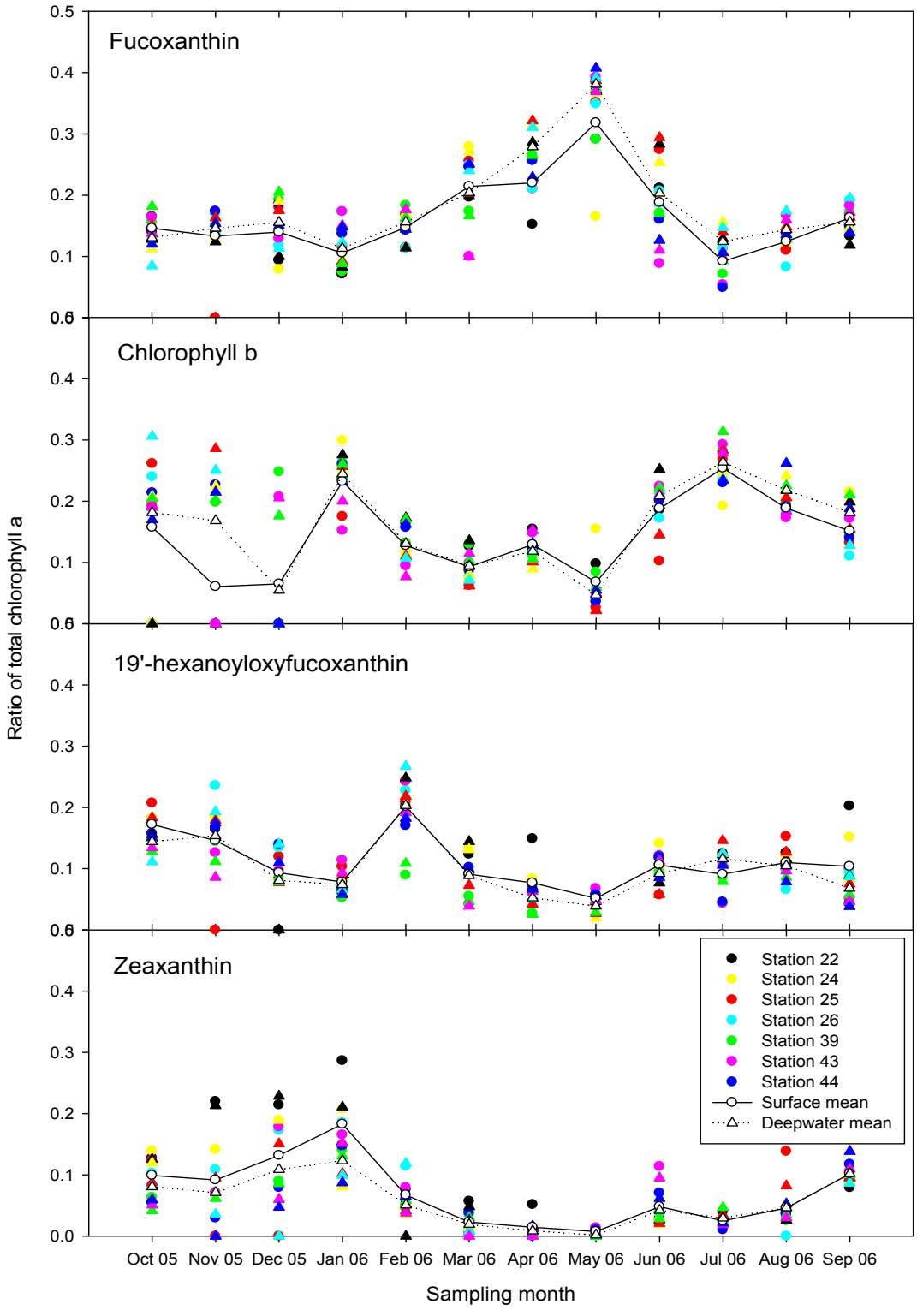

Figure 7.6. Temporal variation in the concentration of selected marker pigments as a ratio of total chlorophyll-*a* (weight:weight) in the small size fraction (<5 µm) from samples collected in the TFZ during 2005 and 2006. Generally fucoxanthin is considered a marker for diatoms, chorophyll *b* in the absence of lutein and prasinoxanthin suggests an increased presence of certain prasinophytes, 19'-hexanoyloxyfucoxanthin of haptophytes and zeaxanthin suggests an increase in the cyanobacteria (see text for more details). Means are regional means (ie: the mean for all sites in the figure).

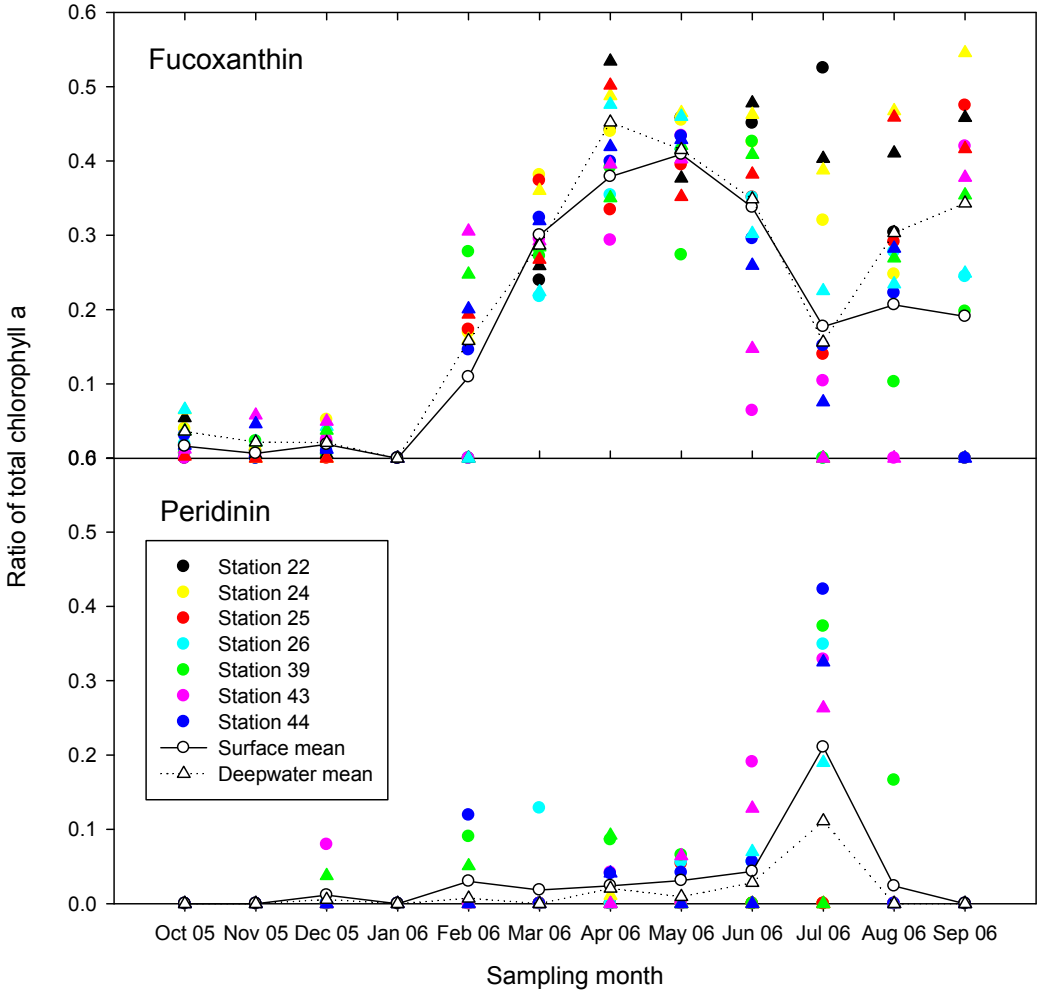

Figure 7.7. Temporal variation in the concentration of selected marker pigments as a ratio of total chlorophyll-*a* (weight:weight) in the large size fraction (>5 µm) from samples collected in the TFZ during part of 2005 and 2006. Generally fucoxanthin is considered a marker for diatoms and peridinin a marker for dinoflagellates (see text for more details). Means are regional means (ie: the mean for all sites in the figure).

7.3.2. Long term trends in biomass and abundance

Examination of the remotely sensed data indicates that the mean chlorophyll-*a* concentrations in the region over the time period from 1997 to 2006 showed a typical pattern of decline in concentration with distance from shore (Figure 7.8). The eight day composite SeaWiFs chlorophyll-*a* data for this region show a strong seasonal cycle with a peak of chlorophyll-*a* in ~ May of each year (Figure 7.9). Considerable interannual variability is evident in the average chlorophyll-*a* biomass and the peak biomass during the predominantly single annual peak. Further analysis shows that 2003 was a year of greater than normal chlorophyll-*a* while 2002 had the lowest average amount of chlorophyll-*a* (Figure 7.9). Pooling the SeaWiFs data and modelling as a Gaussian curve to examine seasonal trends shows the annual peak in chlorophyll-*a* normally occurs about day 137 (~ May 17th) with some intriguing interannual variability (Figure 5.7).

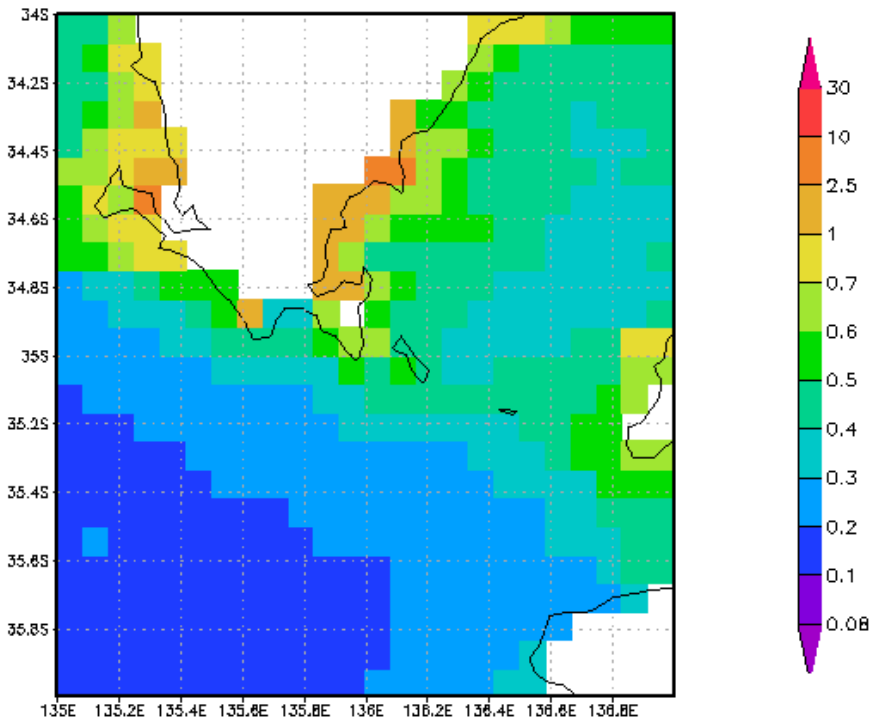

Figure 7.8. The region of southern Spencer Gulf and Eyre Peninsula used to assess the temporal pattern of phytoplankton biomass using SeaWiFs chlorophyll-*a* data from 29 Aug 1997 to 13 Sept 2006. Average chlorophyll-*a* for the entire period is given in µg L^{-1} chlorophyll-*a*.

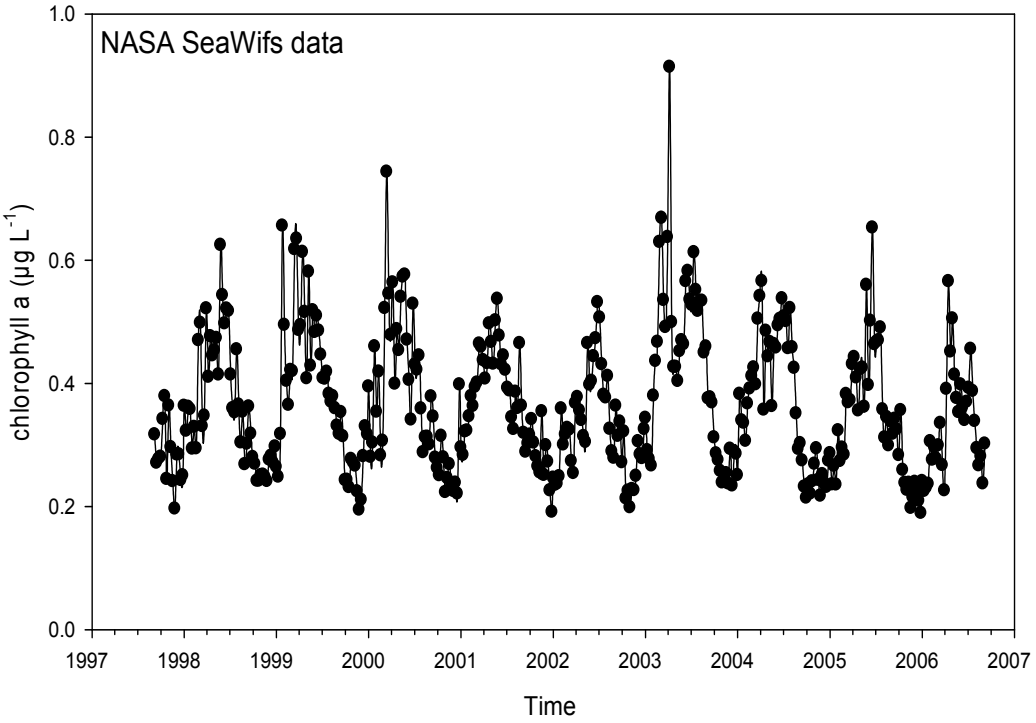

Figure 7.9. Eight day average SeaWiFs chlorophyll-*a* data for the region from 34°S to 36°S and 135°E to 137°E (see Figure 7.8).

A plot of chlorophyll-*a* concentration versus time from the SA EPA data shows a relatively consistent temporal pattern with higher concentrations during late autumn and early winter (Figure 7.10). The mean concentrations at these 6 EPA sites were generally greater than the range of chlorophyll-*a* concentrations observed during 2005-2006 at the 7 sites sampled by the R&R project (Figure 7.11). A simple nonparametric statistical analysis using paired by time observations showed that the mean chlorophyll-*a* concentration at North Shields (EPA1) was significantly lower than at any of the other EPA sites (Table 5.4). Locations on the western side of the Eyre Peninsula had ~ 2 times more chlorophyll-*a* than Boston Bay. Boston Bay and Port Hughes varied only slightly in median chlorophyll-*a* concentration.

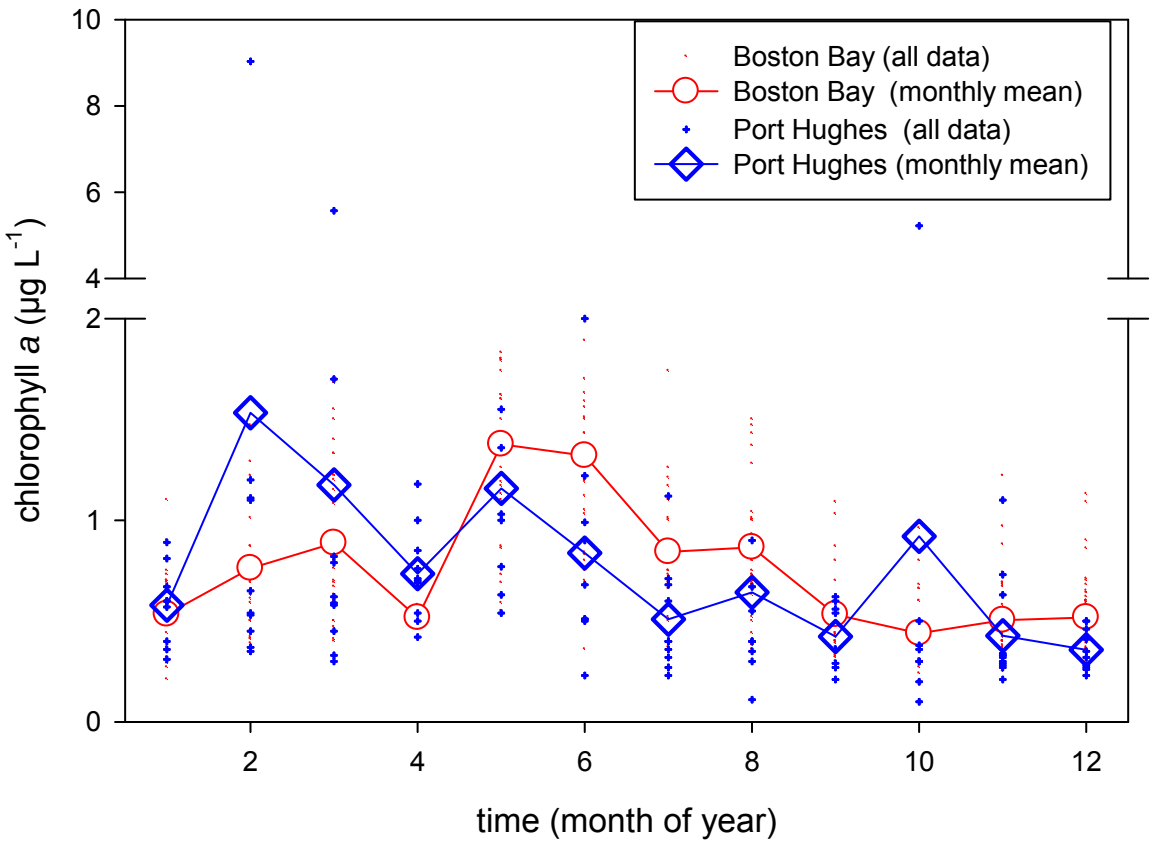

Figure 7.10. A comparison of chlorophyll-*a* data from 6 EPA sites in Boston Bay with a single site at Port Hughes, Yorke Peninsula.

An examination of temporal variation in mean phytoplankton abundance data from the TBOASA database reveals high inter-annual variability, with peaks in total abundance generally occurring between February and June (Figure 7.12). Diatoms dominated with cell abundance patterns mirroring the total abundance, whereas abundance of dinoflagellates and other phytoplankton were relatively constant and low throughout any given year. The latter two groups therefore do not contribute significantly to patterns in total abundances. In all samples examined between 1999 and 2006, dinoflagellates were present in abundances of <15,000 cells L^{-1} and other phytoplankton were present in abundances <60,000 cells L^{-1}.

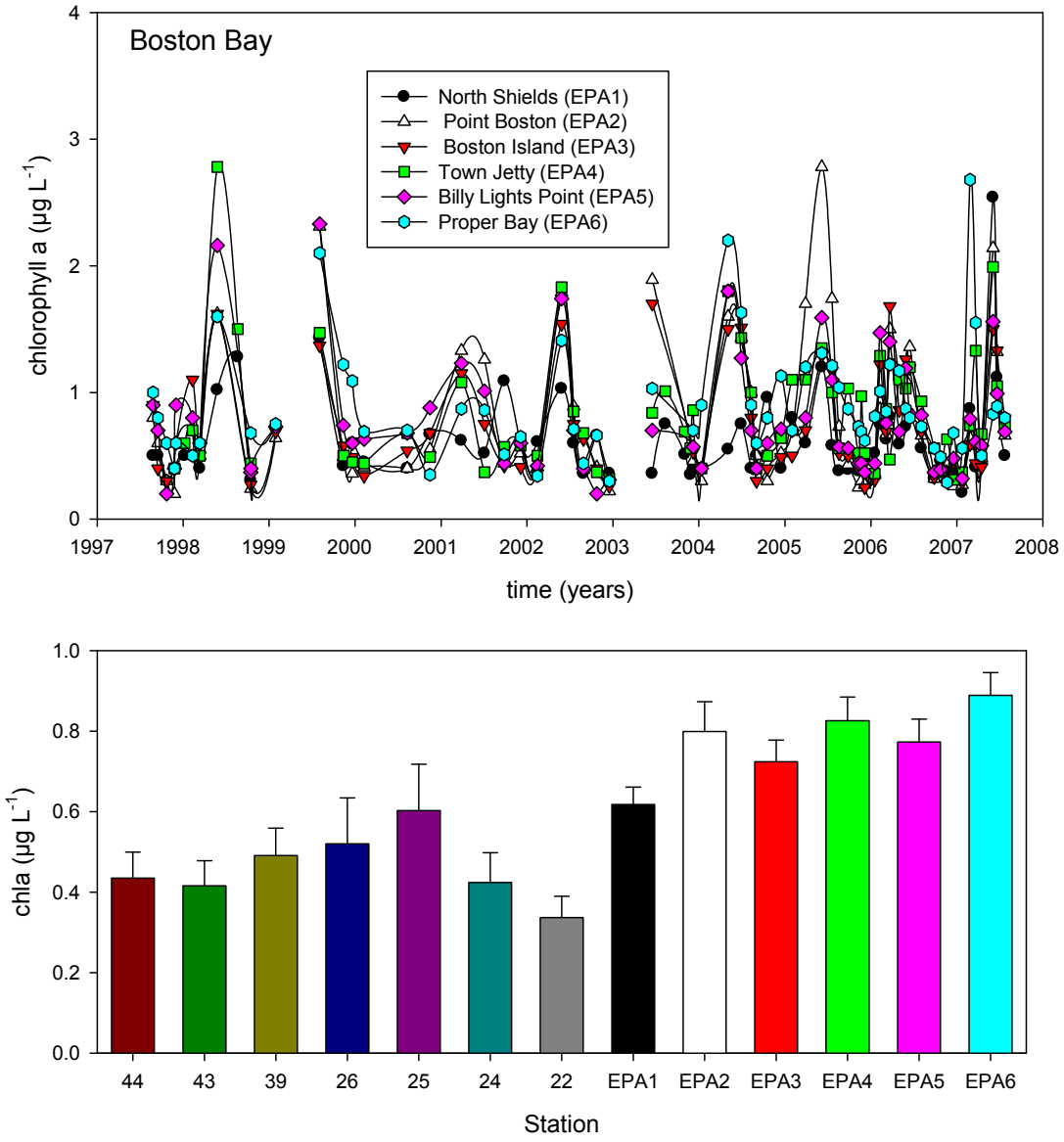

Figure 7.11. Top panel, time series of chlorophyll-*a* data from EPA sites in Boston Bay. Bottom panel, mean chlorophyll-*a* concentrations for Risk and Response sampling sites (2005-2006 data only) and EPA sites (1998-2007). Error bars are standard error of the mean. Analysis of EPA chlorophyll-*a* data shows that EPA1 (North Shields) is significantly different from all other EPA sites (statistics by nonparametric, paired (by time) comparisons).

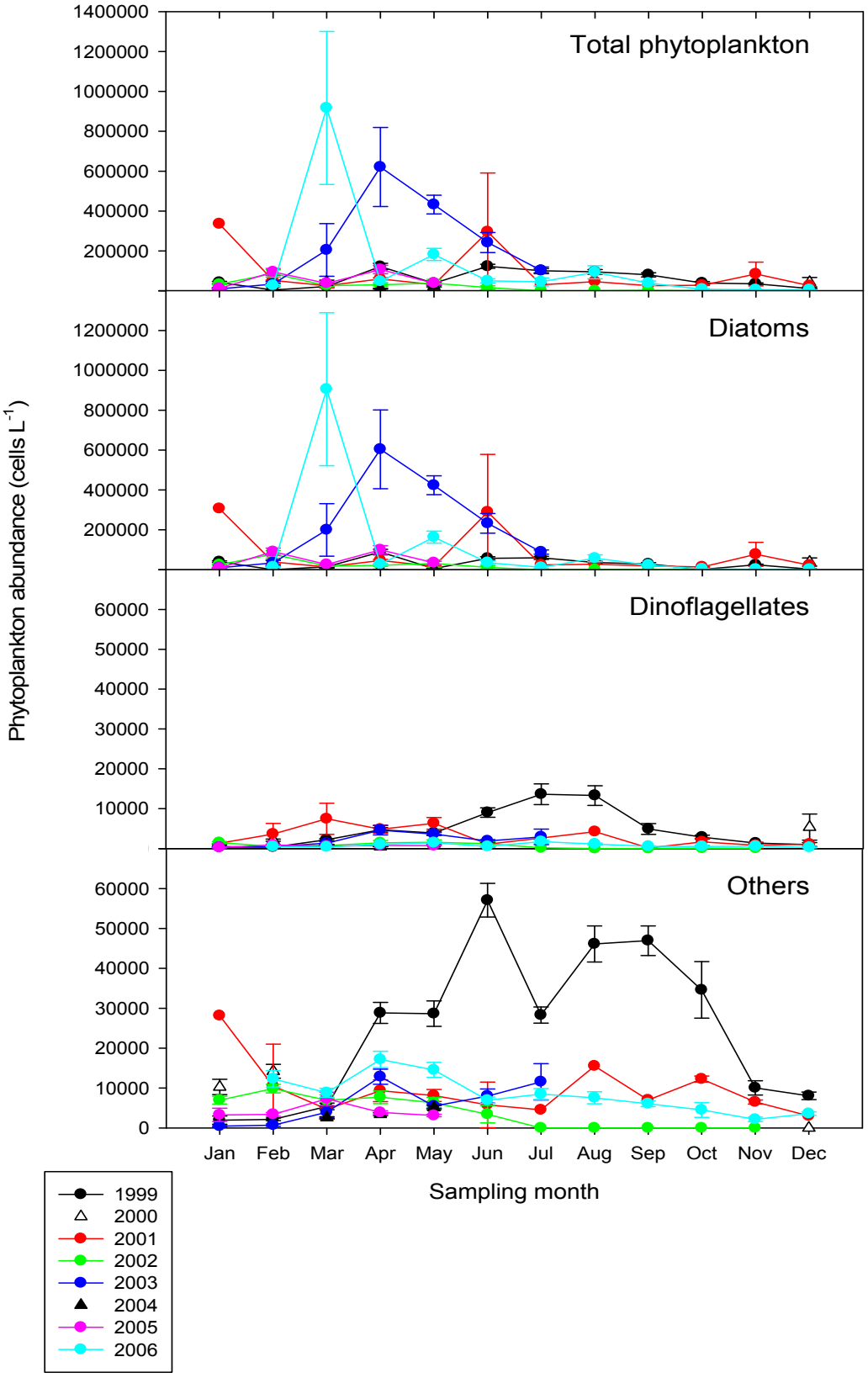

Figure 7.12. Temporal variation in phytoplankton abundance in the TFZ from the TBOASA data. Note the change in scale on the y axis for dinoflagellates and other phytoplankton.

7.3.3. Monthly nutrient data

There was a high degree of spatial and temporal variation in nutrient concentrations, with no clear spatial patterns evident between sites or depths (Figure 7.13). Silica concentrations peaked in February 2006 with mean concentrations of 3.07 ± 0.23 μmol L^{-1} (mean ± SE) in surface samples and 3.00 ± 0.30 μmol L^{-1} in deepwater samples. A second, smaller peak in silica was observed in July 2006, with mean concentrations of 1.36 ± 0.16 μmol L^{-1} in surface samples and 1.30 ± 0.22 μmol L^{-1} in deepwater samples. Mean nitrate concentrations were between 0.7 and 1.0 μmol L^{-1} in both surface and deepwater samples from September to November 2005, before dropping to <0.1 μmol L^{-1} in December 2005. A rise in nitrate concentrations was observed in March 2006, with mean concentrations reaching 0.38 ± 0.03 μmol L^{-1} in surface samples and 0.42 ± 0.05 μmol L^{-1} in deepwater samples, before falling to <0.1 μmol L^{-1} by May 2006. The highest nitrate concentrations occurred toward the end of the study, and rose from mean concentrations of <0.1 in August 2006 in both surface and deepwater samples, to a surface mean of 2.23 ± 0.08 μmol L^{-1}, and a deepwater mean of 2.12 ± 0.11 μmol L^{-1} in September 2006. Mean ammonia concentrations remained ≤0.5 μmol L^{-1} throughout the study. Mean FRP concentration remained below 0.3 μmol L^{-1} throughout the study period, and peaked in surface waters at 0.16 ± 0.03 μmol L^{-1} in March 2006. The peak in mean FRP concentration in deepwater samples was 0.21 ± 0.06 μmol L^{-1}, which occurred in June 2006. A more detailed analysis of nutrient dynamics is made in chapter 5.

7.3.4. Community connectivity with the wider region

Non-metric Multidimensional Scaling (nMDS) ordination showed a clear difference between the community in the EGAB and the community in the TFZ (Figure 7.14). An analysis of phytoplankton indicator species showed several species that were contributing significantly to the difference in the TFZ community relative to the community of the EGAB (Table 7.3). Of these, species belonging to the diatom genera, *Amphora*, *Cocconeis*, *Entomoneis*, *Minidiscus*, *Nitzschia*, and the dinoflagellate genera *Gyrodinium*, and *Heterocapsa* were only present in the TFZ community. The remaining genera were present in the TFZ community in numbers an order of magnitude higher than in the EGAB community, with flagellates present in the TFZ community in numbers two orders of magnitude higher than in the EGAB community. The taxa used in the nMDS ordination (Table 7.2) were present at the TFZ sites (25, 39, 44), but were sparsely distributed in the EGAB community.

The primary (and potentially toxic) taxa in the SASQAP data were *Dinophysis acuminata*, *Dinophysis caudata*, *Dinophysis fortii* and *Pseudo-nitzschia* spp. The PATN analysis shows that local sites in the TFZ are more similar to each other in terms of the abundance of these 5 taxa and are significantly separated from those sites further away (Figure 7.15).

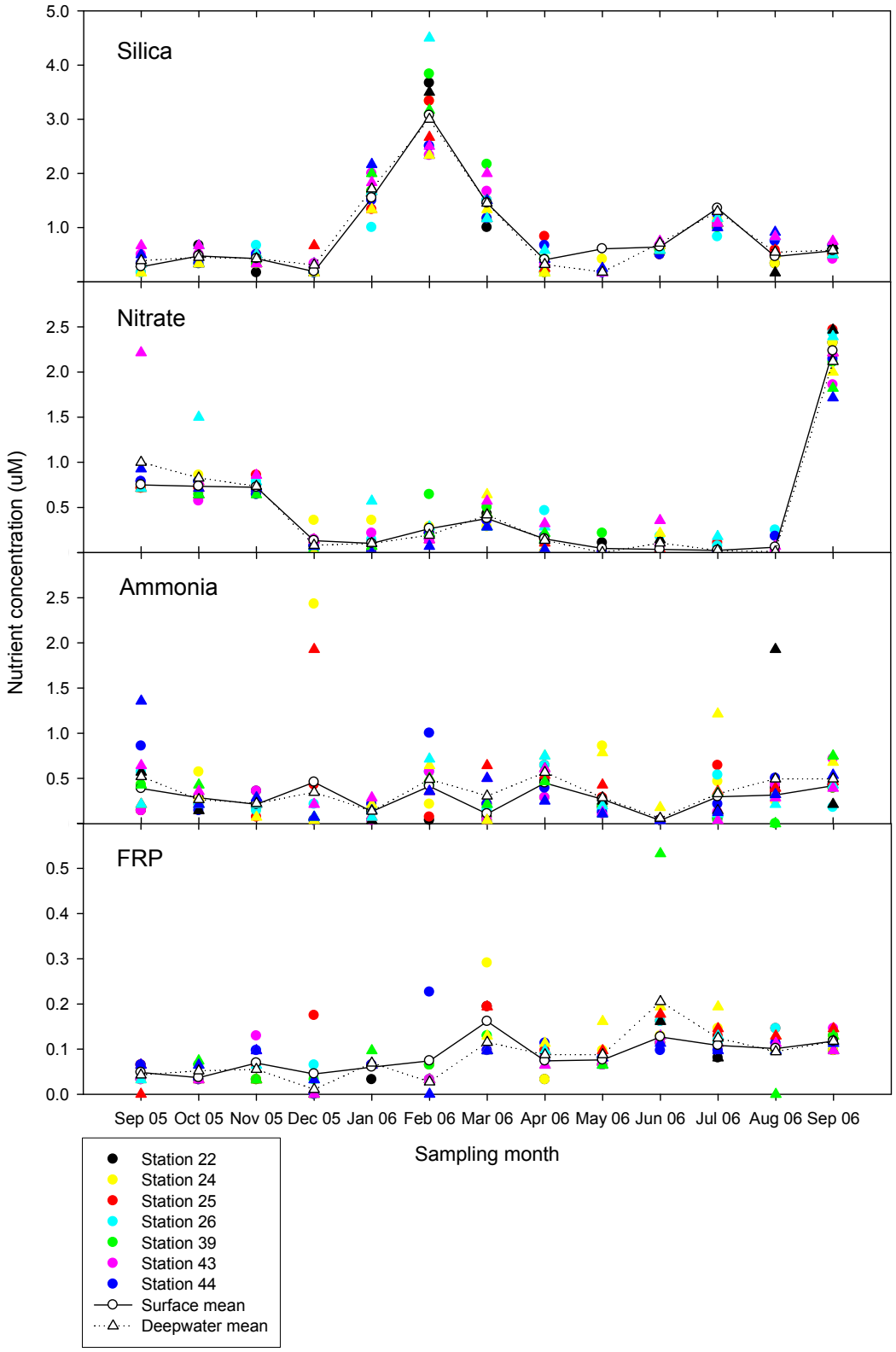

Figure 7.13. Temporal variation in nutrient concentrations in the TFZ. Circles represent surface concentrations, triangles represent deepwater samples. Means are regional means (ie: the mean for all sites in the figure).

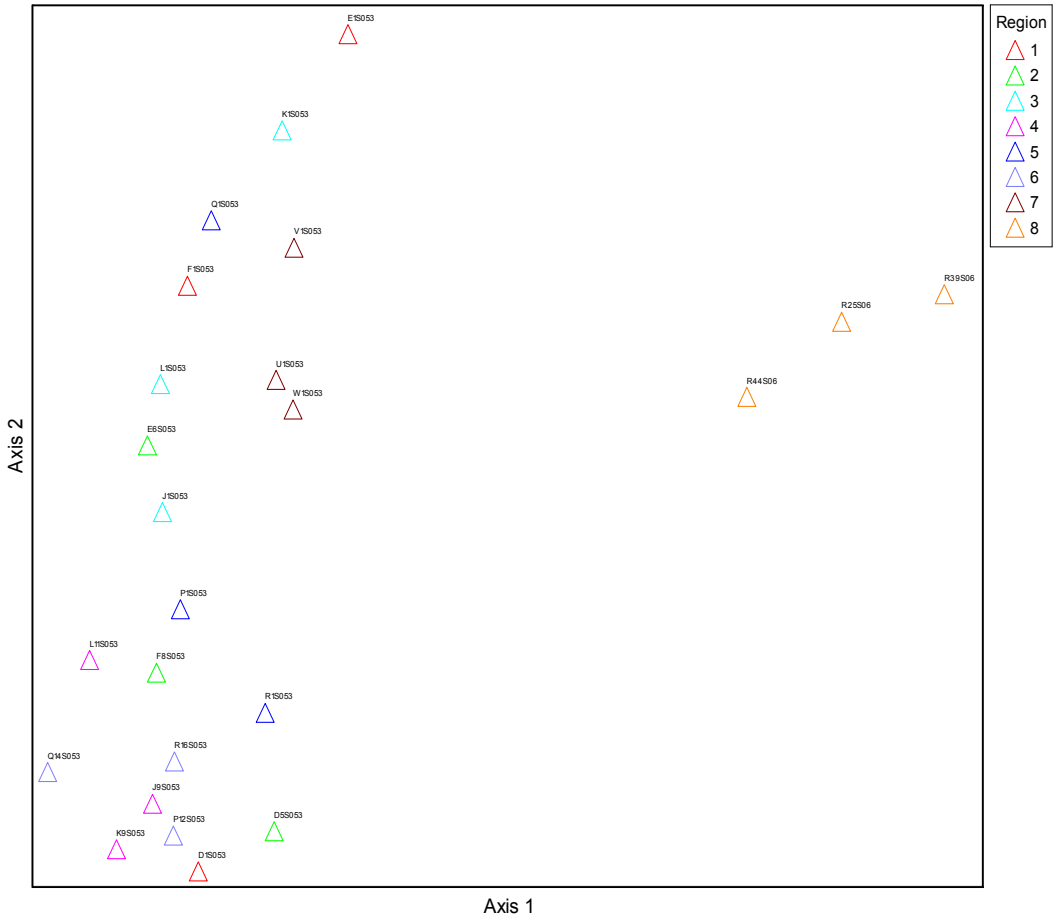

Figure 7.14. Non-metric Multidimensional Scaling (nMDS) ordination plot showing spatial variation in phytoplankton community composition in the eastern Great Australian Bight and south western Spencer Gulf. Regions are outlined in Figure 7.2.

Table 7.3. Indicator species analysis: Phytoplankton genera with significantly greater presence in the TFZ compared with the wider eastern Great Australian Bight region (probabilities (p) less than 0.05 are considered statistically significant).

Genus / Type	**p**
Flagellates	0.002
Amphora	0.0026
Chaetoceros	0.0026
Cocconeis	0.0026
Entomoneis	0.0026
Minidiscus	0.0026
Nitzschia	0.0026
Ceratium	0.0026
Gymnodinium	0.0026
Gyrodinium	0.0026
Heterocapsa	0.0026
Navicula	0.007
Thalassiosira	0.0276
Dactyliosolen	0.0326

Phytoplankton community composition inside the TFZ and in southern Spencer Gulf was broadly similar when sampled in September 2005 and again in February 2006. Student's t-tests indicated no significant difference in abundance for 9 of the 10 commonly found species, albeit the statistical power was low (Table 7.4). Only the dinoflagellate *Heterocapsa rotundata* was found to be less abundant at RM3 (Figure 7.3) relative to the TFZ. Further comparisons using PATN™ software indicated significant differences between groups of sites (Figure 7.16) with RM1 and RM3 clustered with the most offshore site from the TFZ (R22). The most distant site, RM2, clustered closely with R44, an inshore site located in the TFZ. The association of sites based on Bray and Curtis analysis indicated 3 significantly different groups. These groups were defined by the abundances of the 20 most common phytoplankton species. *Nitzschia* spp., *Hemiselmis* sp., *Pyramimonas* spp., *Plagioselmis prolonga*, and *Gyrodinium* spp. all tended to be low in abundance at sites R22, RM1 and RM3 (Figure 7.17). Site R39 was separated because of greater abundances of most of the common species.

Table 7.4. Comparison of phytoplankton abundance between the TFZ (RM5) and mid southern Spencer Gulf (RM3). Probabilities less than 0.05 are considered statistically significant. Statistical power < 0.80 indicates a high degree of variability in the data and that negative findings (e.g. no difference between sites) should be interpreted cautiously.

Species	normality	equal variance	Difference between sites	power
Cylindrotheca closterium	>0.2	0.081	0.491	0.05
Naviculoid spp.	>0.2	0.423	0.561	0.05
Nitzschia spp.	>0.2	0.097	0.652	0.05
Thalassionema sp.	>0.2	0.673	0.556	0.05
Gymnodinioid spp.	>0.2	0.485	0.167	0.18
Gyrodinium spp.	>0.2	0.802	0.51	0.05
Heterocapsa rotundata	>0.2	0.586	0.039	0.581
Chrysochromulina spp.	>0.2	0.615	0.206	0.139
Plagioselmis prolonga	>0.2	1	0.376	0.05
Pyramimonas spp.	>0.2	0.902	0.742	0.050

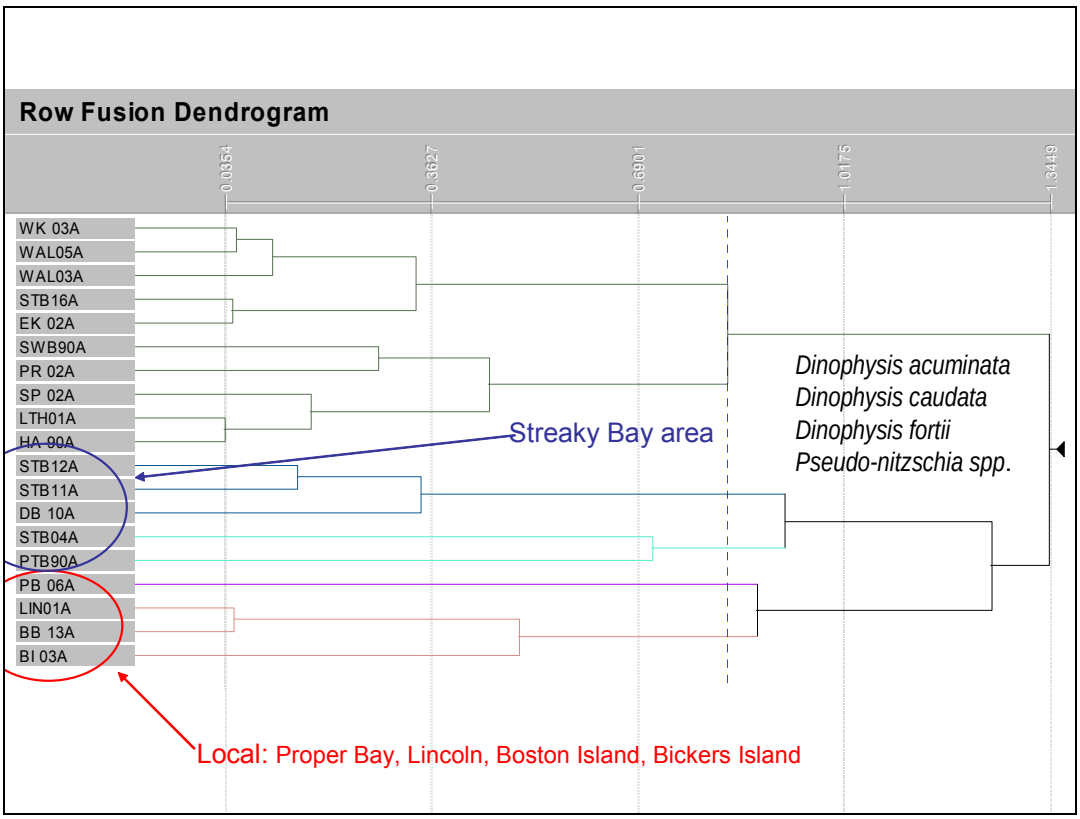

Figure 7.15. Statistical analysis of the degree of similarity in toxic phytoplankton species found across 19 sites across the Spencer Gulf and Eyre Peninsula during May 2006. Site identifiers are consistent with SASQAP database. Sites that cluster together (colour groups) are similar. Sites that link with short lines are most similar.

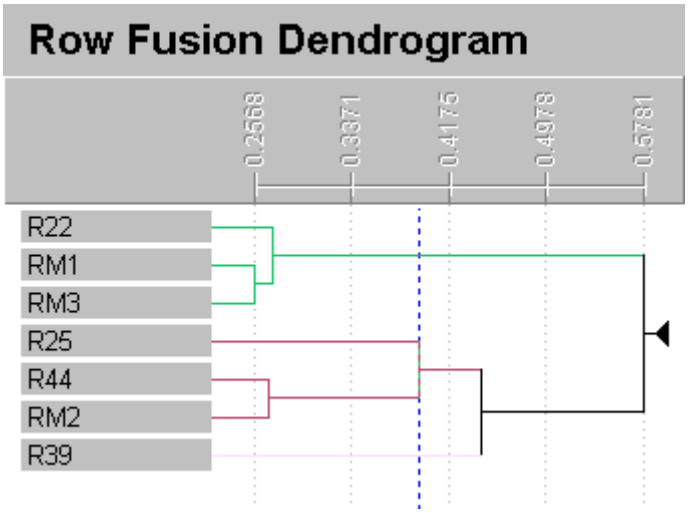

Figure 7.16. A dendogram of the Bray & Curtis association matrix for phytoplankton community composition at 7 different sites in the TFZ and lower Spencer Gulf. Sites that cluster together (colour groups) are similar. Sites that link with short lines are most similar.

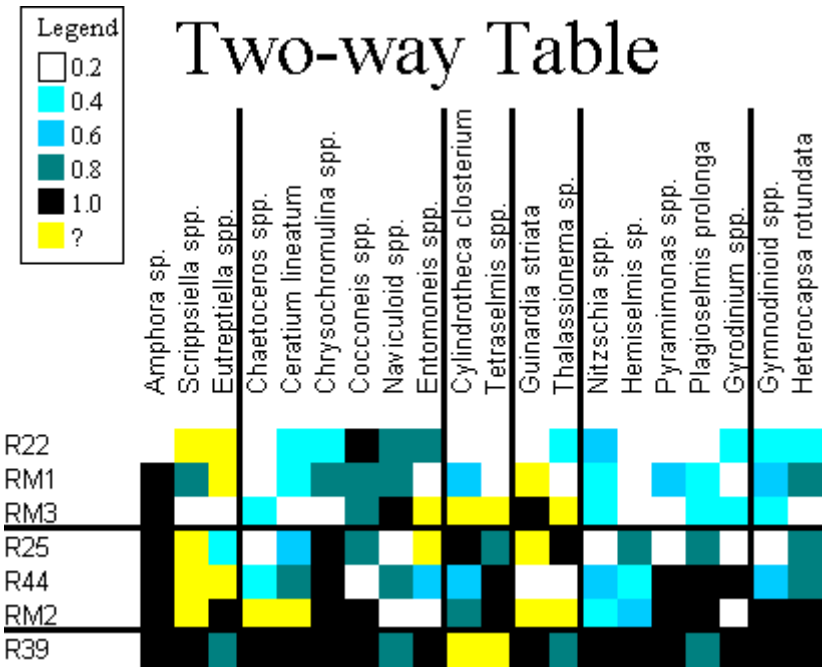

Figure 7.17. Statistical analysis of the phytoplankton species discriminating the 7 sites in the TFZ and lower Spencer Gulf. Colour indicates the degree of similarity between sites (see legend). Black indicates a high degree of similarity in species abundance while white indicates a low degree of similarity. For example the taxa *Amphora* sp. was often found at similar abundances at sites RM1, RM3, R25, R44, RM2, R39 but not R22. Site R22 was most different from site R39 in terms of species composition and abundance.

7.3.5. Harmful algal bloom species

A range of known and potentially harmful algal bloom (HAB) species are part of the phytoplankton community in the TFZ. These include both toxic and non-toxic species. The non-toxic but harmful species include diatoms such as *Chaetoceros* spp. that can cause harm even at low cell densities because of physical damage caused by the setae of the siliceous exoskeleton. Potentially toxic are members of the diatom genus *Pseudo-nitzschia*, considered the most likely cause of Amnesic Shellfish Poisoning. Fish-killing (ichthytoxic) HAB species such as the dinoflagellates *Karenia* spp. and other gymnodinoid species such as *Gymnodinium pulchellum*, raphidophytes species *Akashiwo* and *Chattonella* spp. and haptophytes *Chrysochromulina* spp. also occur in the TFZ phytoplankton. Of less direct influence on fish but still significant both ecologically and for the shellfish industry are the Diarrhetic Shellfish Poisoning (DSP)-producing *Dinophysis* and *Prorocentrum* species and some gymnodinoid species.

In the Risk and Response and TBOASA data sets, however, bloom occurrences of these HAB species are rare. From October 2005 to September 2006, HAB species formed part of the dinoflagellate and 'other' phytoplankton community at relatively low, non-bloom cell densities. *Karenia* spp. were present in very low numbers (hundreds of cells per litre, Figure 7.18a) most of the year, while mixed gymnodinoid species (not necessarily harmful) averaged higher densities (between 5,000 and 10,000 cells L^{-1} in surface waters, Figure 7.18b). There was a similar pattern between sites although there is evidence of a deep water maxima compared with surface waters in April and May 2006, consistent for both months, only at the inshore site 44. The pattern for other months was for surface waters to show equal or higher abundance compared to deep waters. Other potentially toxic dinoflagellates, *Prorocentrum* spp. were only detected in abundances over 500 cells L^{-1} in April to June 2006 (Figure 7.19),

with deep water maxima detected at Site 39. DSP-producing *Dinophysis caudata* was found only during April 2006 at abundances <1,000 cells L^{-1} (most samples <500 cells L^{-1}) at sites 39 and 44 and only at depth at site 22.

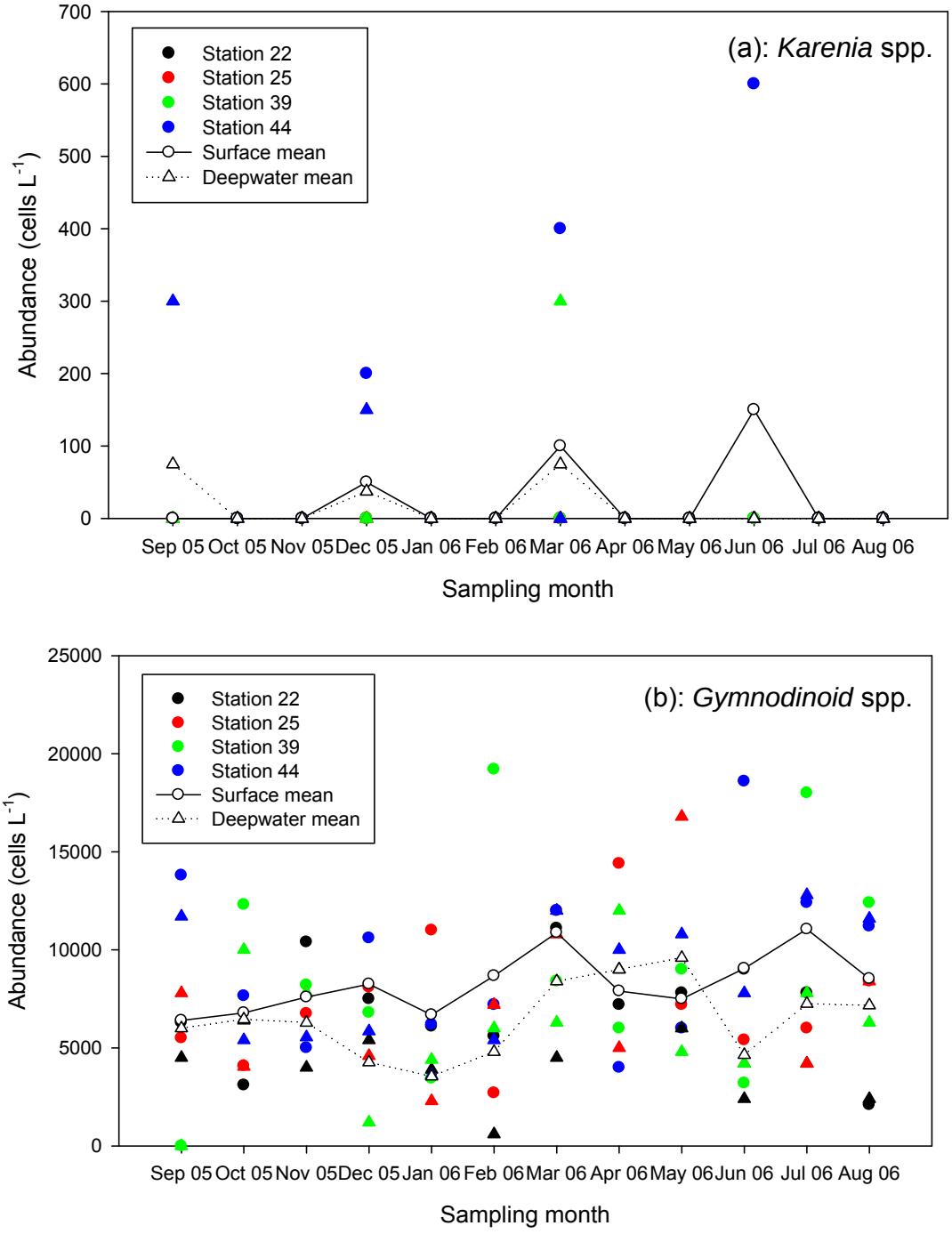

Figure 7.18. TFZ Harmful Algal Bloom (HAB) species, 2005-06. Temporal variation in abundance of (a) *Karenia* spp. and (b) *Gymnodinoid* spp. Circles represent surface samples, triangles represent deepwater samples. Means are regional means (ie: the mean for all sites in the figure).

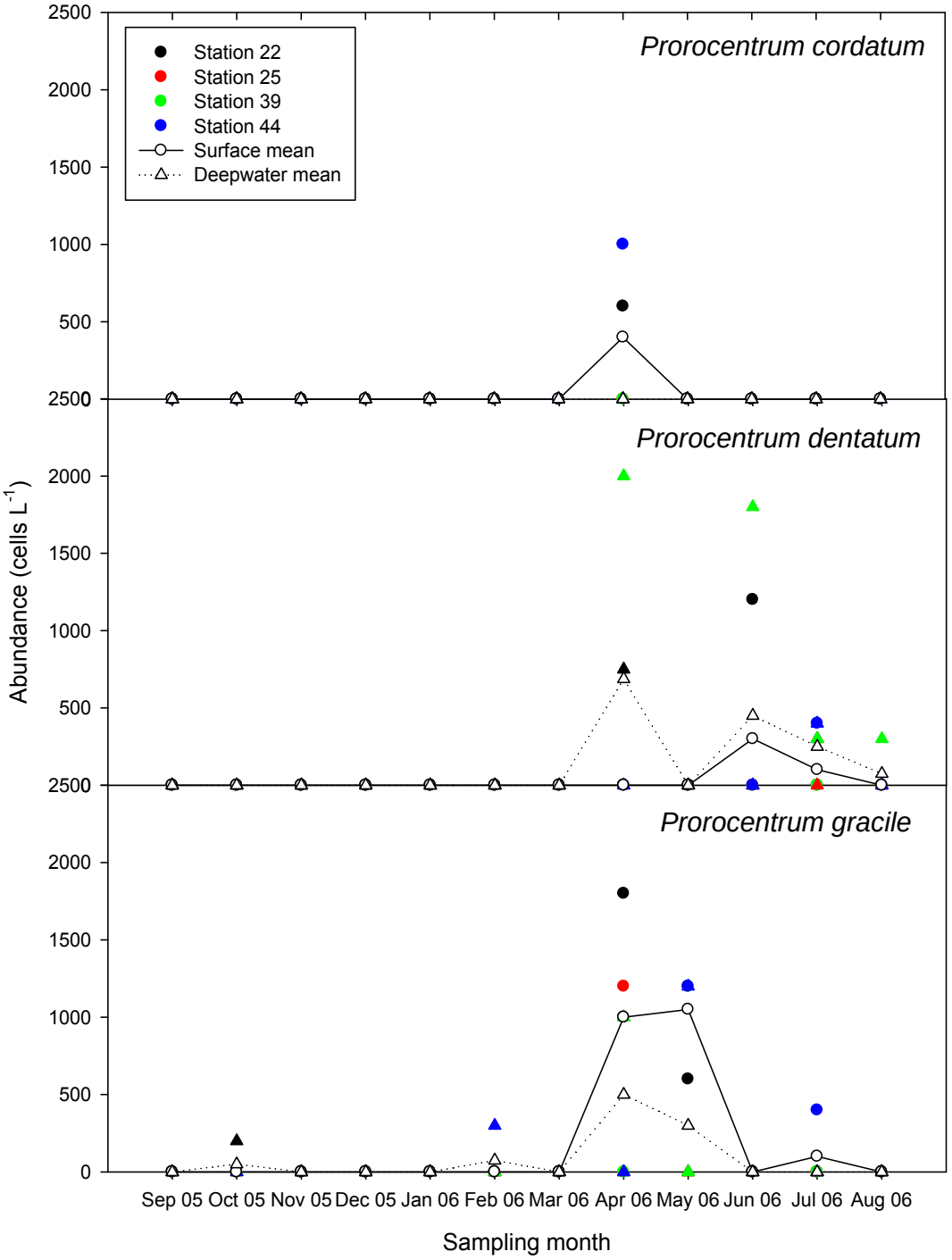

Figure 7.19. TFZ Harmful Algal Bloom (HAB) species, 2005-06: temporal variation in abundance of *Prorocentrum* spp. Circles represent surface samples, triangles represent deepwater samples. Means are regional means (ie: the mean for all sites in the figure).

The potentially ichthytoxic haptophytes *Chrysochromulina* spp. peaked in April 2006 at all sites with a surface mean of approximately 14,000 cells L^{-1} (Figure 7.20). The icthytoxic raphidophytes *Akashiwo sanguineum* and *Chattonella* spp. were detected at hundreds of cells per litre with deep water maxima for both genera at site 39 and for *Chattonella* spp. at site 25 in December 2005 (Figure 7.21), and sites 25 and 44 in February and March 2006, respectively.

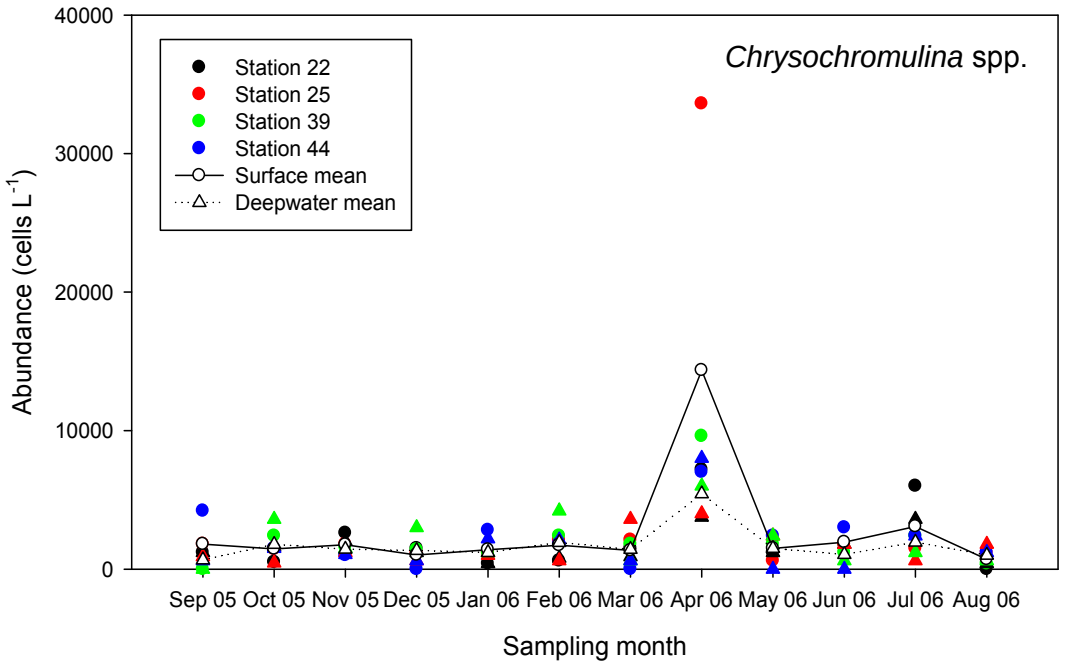

Figure 7.20. TFZ Harmful Algal Bloom (HAB) species, 2005-06: Temporal variation in abundance of *Chrysochromulina* spp. Circles represent surface samples, triangles represent deepwater samples. Means are regional means (ie: the mean for all sites in the figure).

Of the dominant diatoms in the TFZ only *Pseudo-nitzschia* spp. are a potential risk for toxic HABs. Cell numbers peaked in March and June 2006 (Figure 7.22) but the small cell size and the fact that the dominant *Pseudo-nitzschia* species present, *P. pseudo-delicatissima*, is not toxic (Hallegraeff 2002), suggests that the risks are low. While *Chaetoceros* spp. were dominant diatoms (Table 7.1), there were no records of the harmful species *Chaetoceros convolutus* and *C. concavicornis*.

Interannual variation in HAB species is evident in the TBOASA data. In general, however, HAB species are low in abundance with no consistent interannual patterns (Figures 7.23-7.26). In August – September 1999 there were significant numbers (>10,000 cells L^{-1}) of the ichthytoxic *Karenia mikimotoi* with lower densities of *Chattonella globosa* (1100 cells L^{-1}) and *C. marina* (400 cells L^{-1}), while *K. brevis* and other *Chattonella* species peaked in March – April in 2001 (Figures 7.23, 7.25). *Gymnodinium* spp. were also present between May and November 1999 at abundances between 200 and 1000 cells L^{-1} (Figure 7.24a), but these did not include the ichthytoxic *Gymnodinium* aff. *puchellum* which was near or below detection limits except in January 2002 when it was present at 100 cells L^{-1} (Figure 7.24b). The haptophyte *Chrysochromulina* spp. peaked at 1700 cells L^{-1} in 1999. Also known for avoidance by fish and fish deaths in the North Atlantic is the haptophyte *Phaeocystis pouchetii* found at densities up to 15,000 cells L^{-1} in the TFZ in 2003. The bloom forming cyanobacterium *Trichodesmium erythraeum* was detected at 20,000 cells L^{-1} in January 2001 with lower abundances detected from February onwards (Figure 7.26). It is interesting that in January 2000 *Trichodesmium* spp. were present only at depth at 1500 cells L^{-1} (Figure 7.26b).

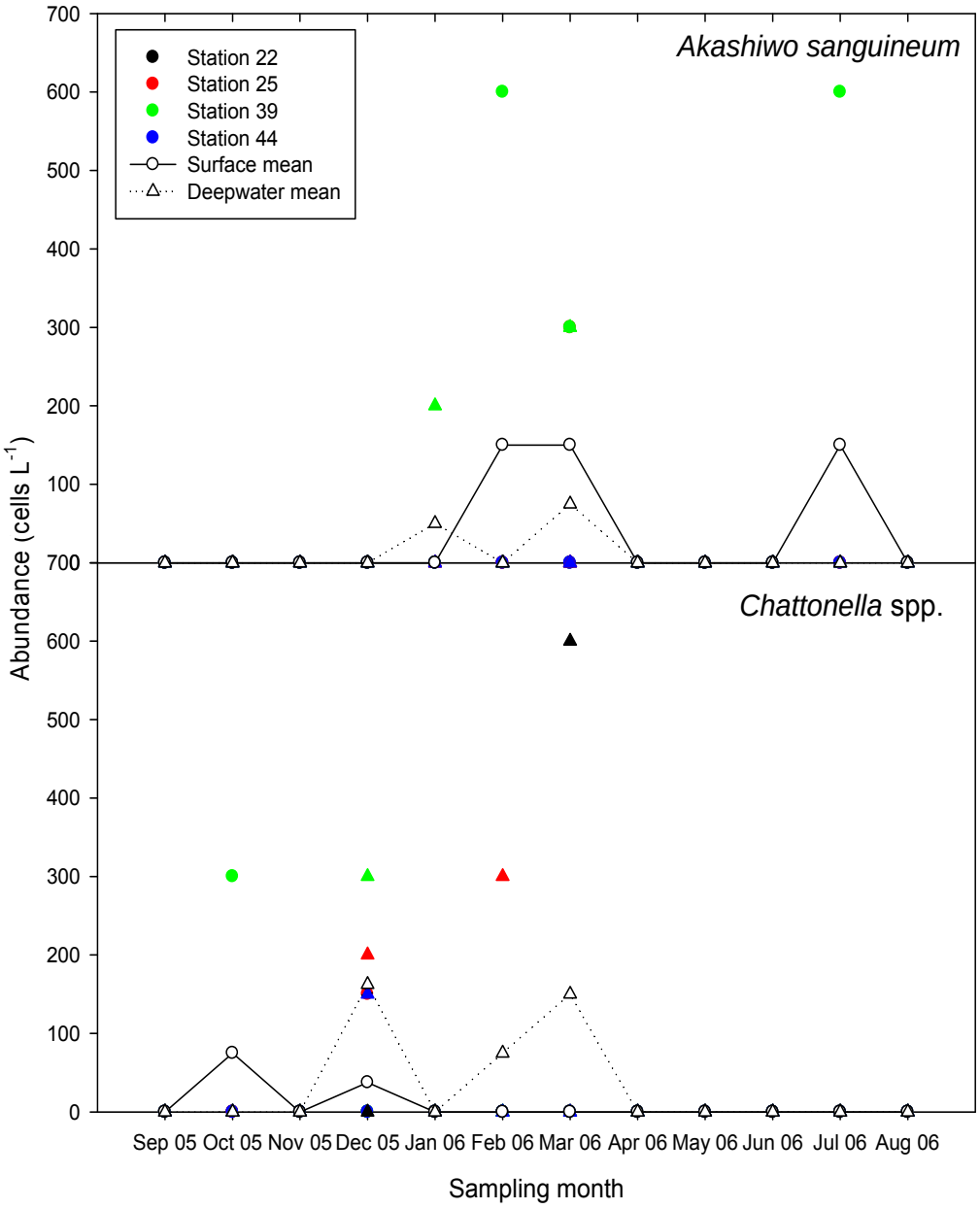

Figure 7.21. TFZ Harmful Algal Bloom (HAB) species, 2005-06: Temporal variation in abundance of *Akashiwo sanguineum* and *Chattonella* spp. Circles represent surface samples, triangles represent deepwater samples. Means are regional means (ie: the mean for all sites in the figure).

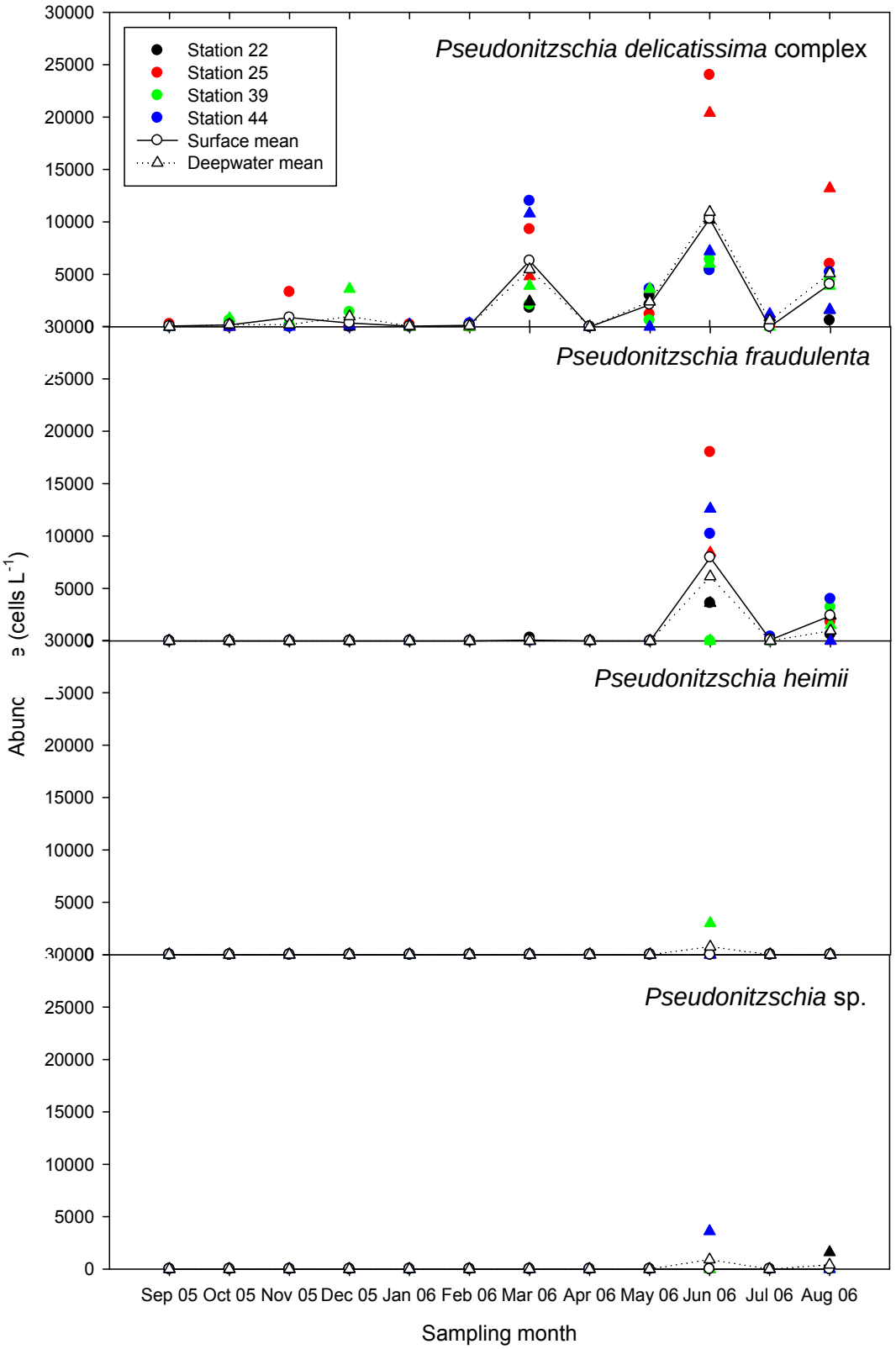

Figure 7.22. TFZ Harmful Algal Bloom (HAB) species, 2005-06: Temporal variation in abundance of *Pseudonitzschia* spp. Circles represent surface samples, triangles represent deepwater samples. Means are regional means (ie: the mean for all sites in the figure).

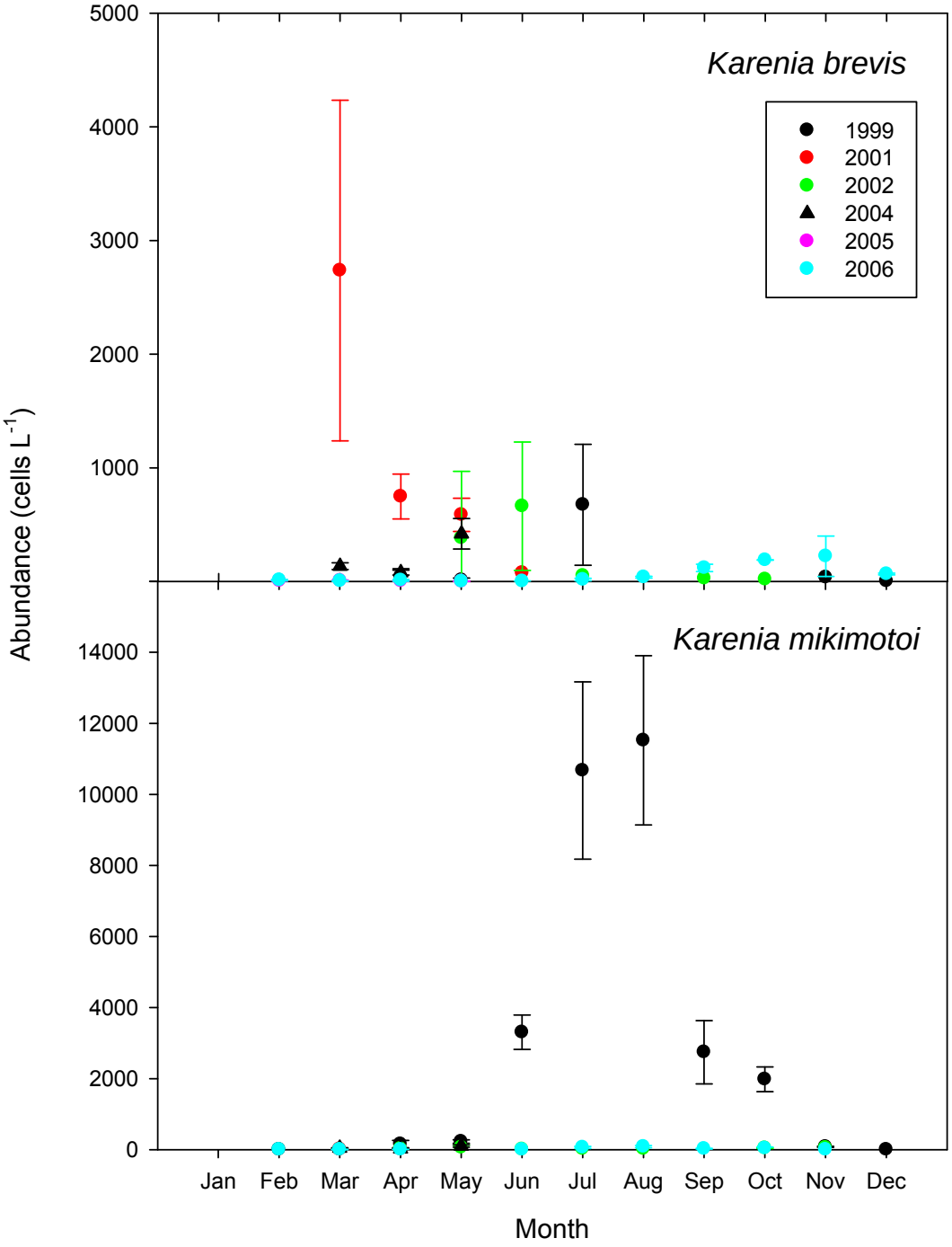

Figure 7.23. TBOASA database Harmful Algal Bloom (HAB) species: Temporal variation in abundance of *Karenia* spp. Note different scales on y axis.

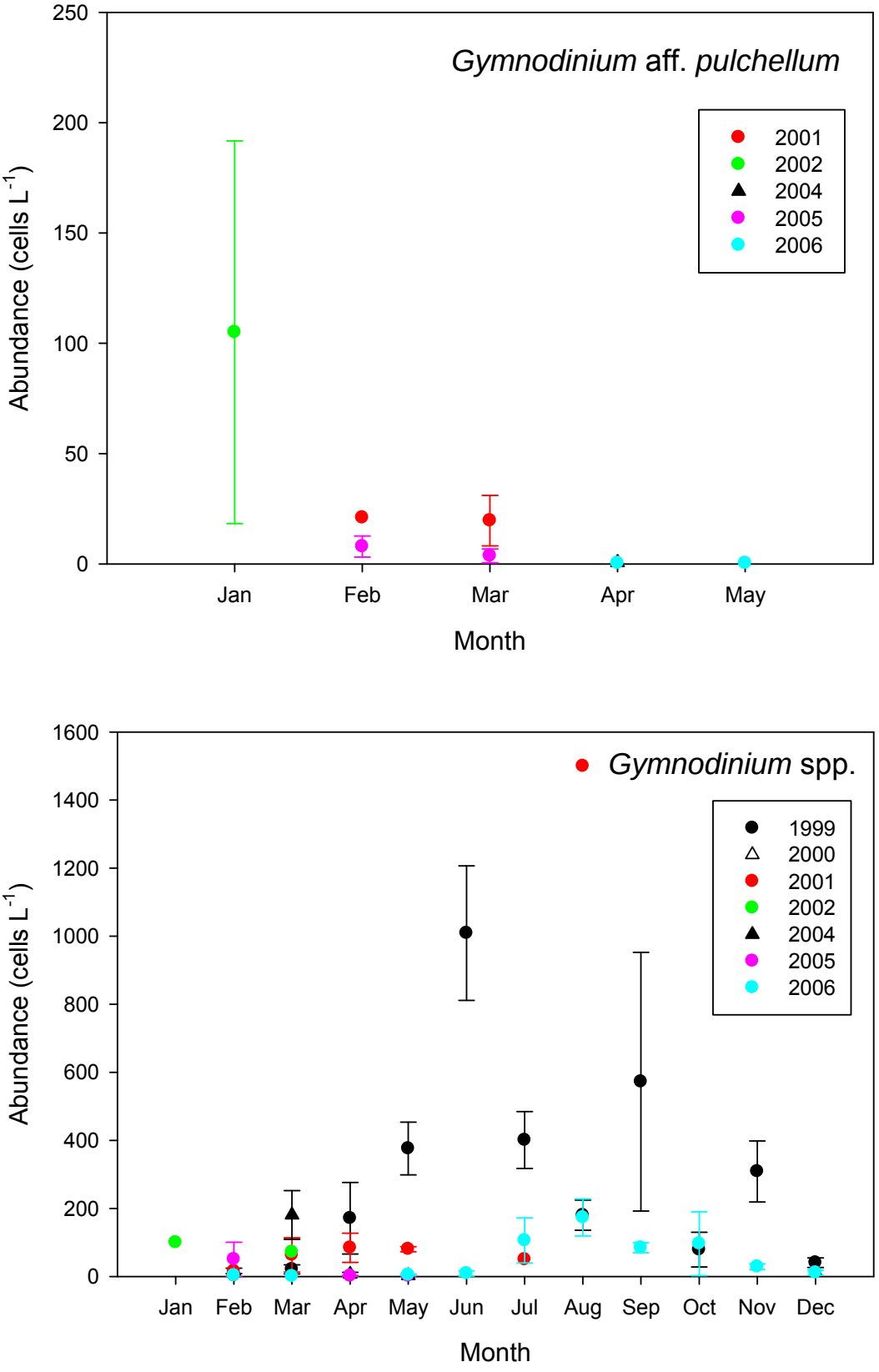

Figure 7.24. TBOASA database Harmful Algal Bloom (HAB) species: Temporal variation in abundance of *Gymnodinium* spp.

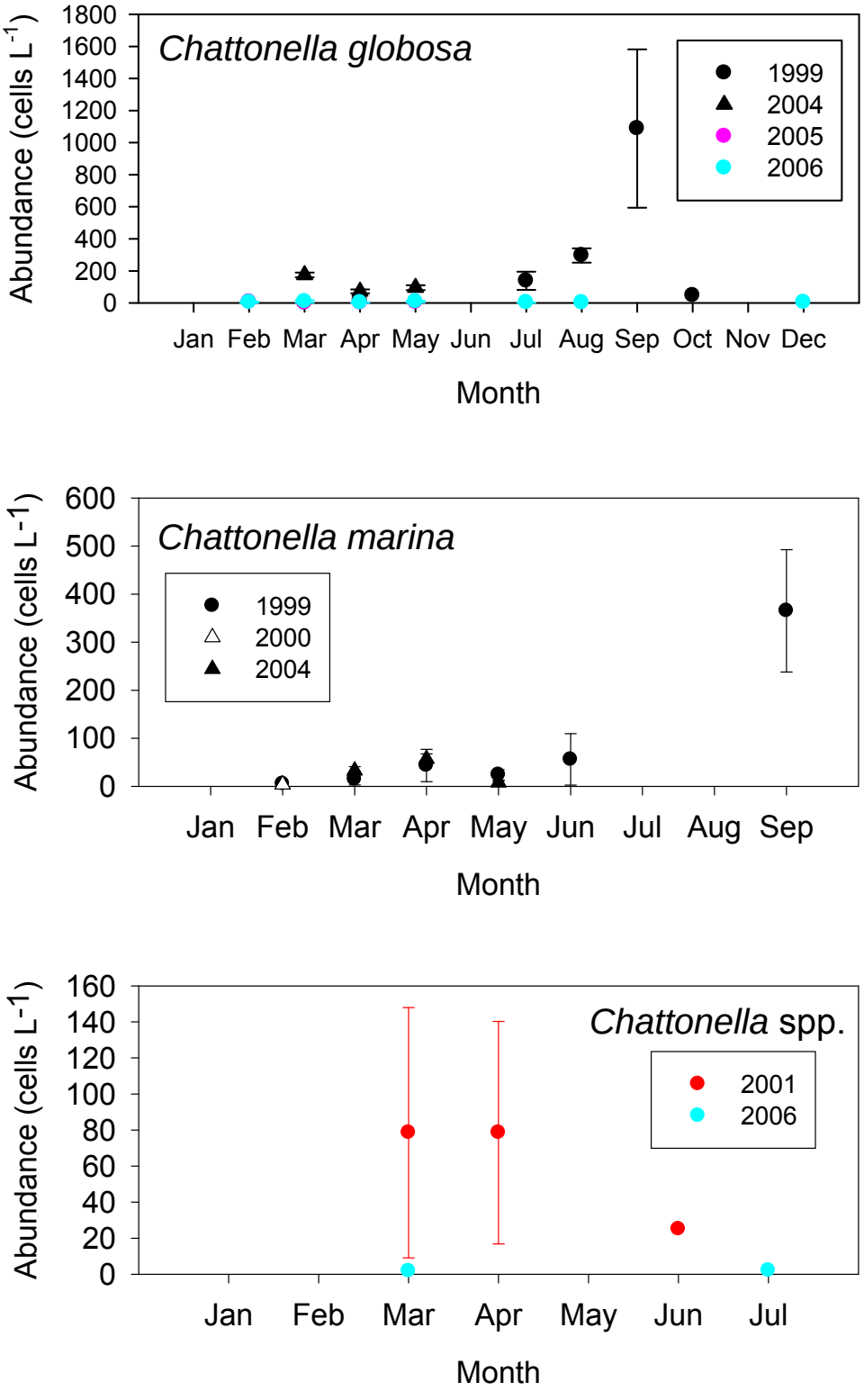

Figure 7.25. TBOASA database Harmful Algal Bloom (HAB) species: Temporal variation in abundance of *Chattonella* spp.

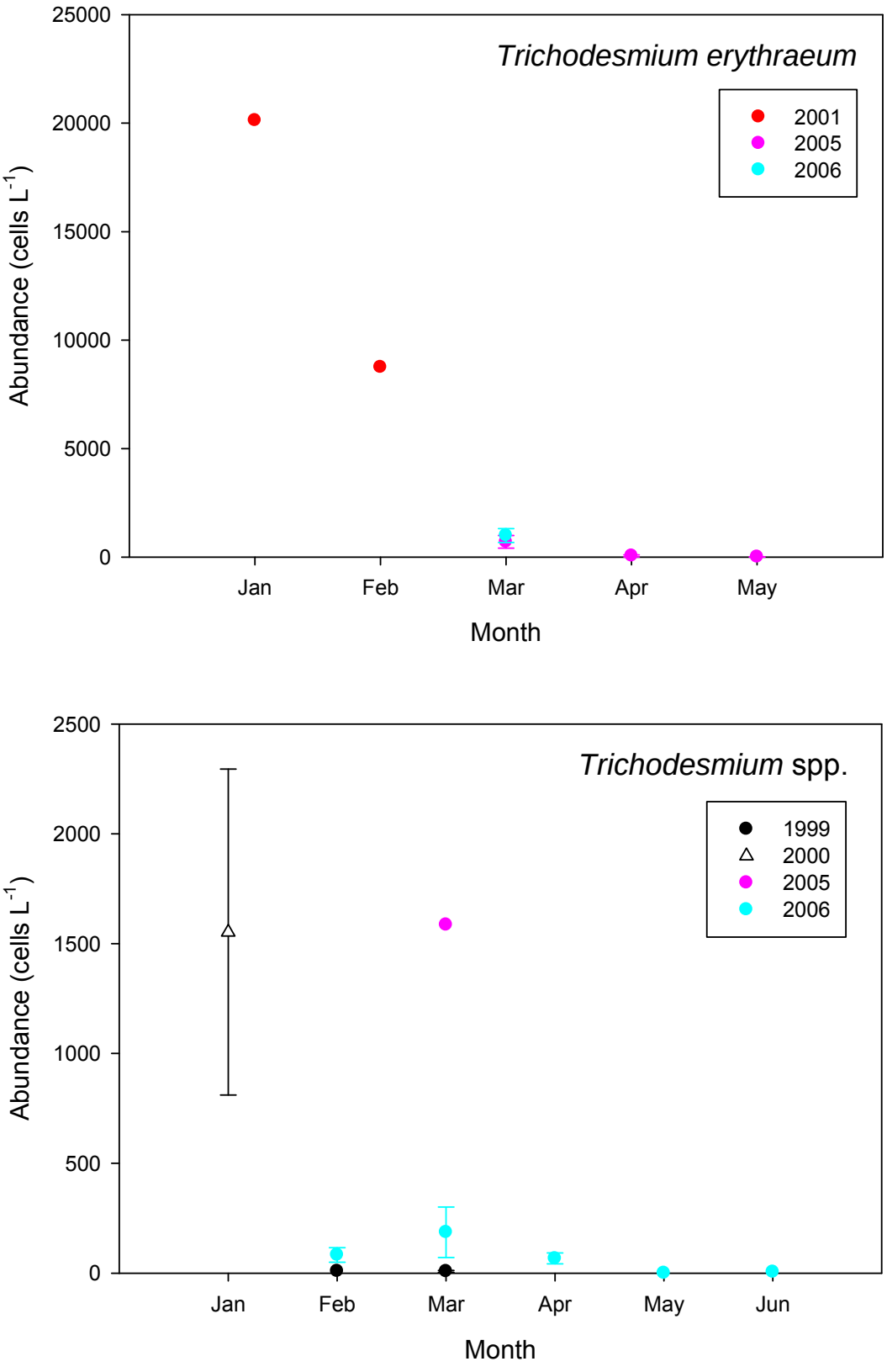

Figure 7.26. TBOASA database Harmful Algal Bloom (HAB) species: Temporal variation in abundance of *Trichodesmium* spp.

Data from the South Australian Shellfish Quality Assurance Program (SASQAP) focuses upon harmful or potentially harmful species. Data for the most toxic genera: *Alexandrium*, *Chattonella*, *Dinophysis*, *Gymnodinium*, *Karenia*, *Prorocentrum* and *Pseudonitzchia* were extracted at the five sites listed in Table 7.5. The maximum observed densities for these toxic genera occurred at Boston Bay (*Karenia*), Bickers Island (*Alexandrium*, *Prorocentrum*, and *Pseudonitzschia*) and Proper Bay (*Chattonella*, *Dinophysis* and *Gymnodinium*). All of the peak abundances occurred between March and June. The average and peak abundances of *Alexandrium* species were very low at 1 and 625 cells L^{-1} respectively. Although *Gymnodinium* has been reported to be ichthyotoxic, the species responsible was the affinity *pulchellum* which has only occurred 9 times in the SASQAP data base at these 5 sites, reaching a peak of 1000 cells L^{-1} on 10/05/2001 at Bickers Island. The toxic genera assessed to have the greatest potential risk to tuna in the TFZ, based on observed abundances in one or more data sets and reported toxicity, were *Karenia* and *Chattonella*. The three taxa selected to investigate further in terms of variation in time and space were: *Chattonella* (all species), *Karenia brevis* and *Karenia mikimotoi*. The data from all five sites indicates that the abundance of *Chattonella* spp. has declined dramatically from a peak in 2000 to no observations at any site from 2002 to 2006 (Figure 7.27). The abundances of both *Karenia* spp. appear to have peaked in 2003 and 2004 with lower abundances observed since. Of these three species, *Karenia brevis* tended to reach the greatest abundances with a peak density of 36,000 L^{-1} at Boston Bay on May 26, 2003. Most of the peak densities of these ichthyotoxic species were observed in ~ May-June. The spatial distribution of these 3 main ichthyotoxic species was examined by calculating the mean abundance at each of the 5 sites (although the relatively small number of samples from Port Lincoln had no observation of these species) across all available observations. The data (Figure 7.28) show that *Chattonella* spp. and *K. mikimotoi* were relatively evenly distributed across the 4 main sites. In contrast *K. brevis* tended to be more abundant at Bickers Island and Boston Island.

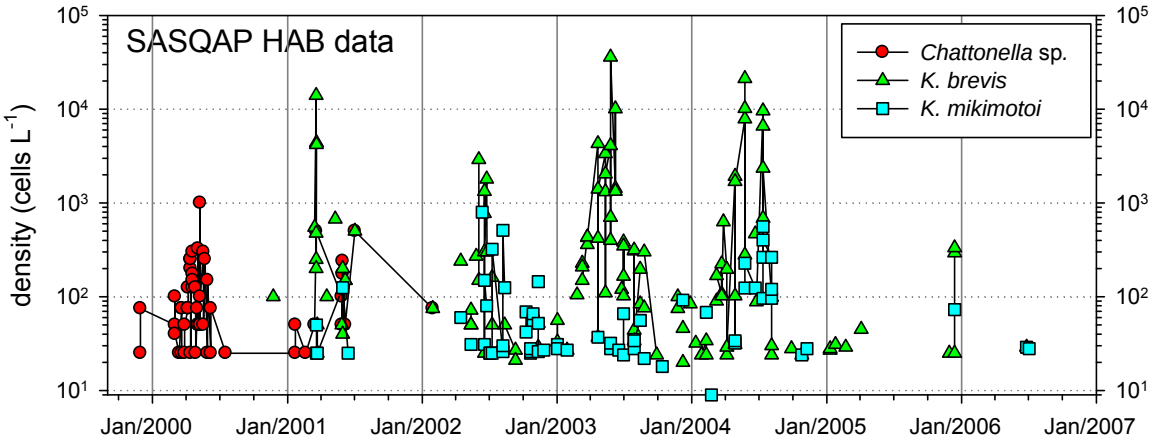

Figure 7.27. A time series of the SASQAP data for densities of *Chattonella* (all species), *Karenia brevis* and *Karenia mikimotoi* at the 5 sites (Bickers Island, Boston Bay, Proper Bay, Louth Bay, Lincoln) in or near the TFZ.

Table 7.5. Observations of the maximum cell densities of 6 toxic genera of phytoplankton as recorded in the SASQAP database for 5 sites: Bickers Island (BI), Boston Bay (BB), Proper Bay (PB), Louth Bay (LB), Lincoln (L) in, or near, the TFZ. A discussion of their toxicity can be found in the text.

Genera	**Possible species**	**Cells L^{-1}**		**Where & when**	**Specific type**	**Known toxic to:**
		Ave	**Max**			
Alexandrium	*catenella, cysts, margalefi, minutum, ostenfeldi, tamarense,* spp.	1	**625**	BI 2/03/2000	spp.	humans fish
Chattonella	spp.	133	**1000**	PB 9/05/2000	spp.	fish
Dinophysis	*acuminate, acuta, caudate, fortii, hastata, mitra, rotundata,* spp.	39	**4800**	PB 7/06/2000	*D. caudata*	humans
Gymnodinium	*catenatum,* affinity *pulchellum*	92	**18000**	PB 30/05/2001	spp.	fish (*pulchellum* only) humans
Karenia	*brevis, mikimotoi, umbella,*	201	**36000**	BB 26/05/2003	*K. brevis*	fish humans
Prorocentrum	*gracile, lima, triestinum,*	152	**32000**	BI 1/05/2000	*P. triestinum*	humans
Pseudonitzchia	*pseudo delicatissima, australis* spp.	15176	**856800**	BI 30/05/2005	spp.	humans

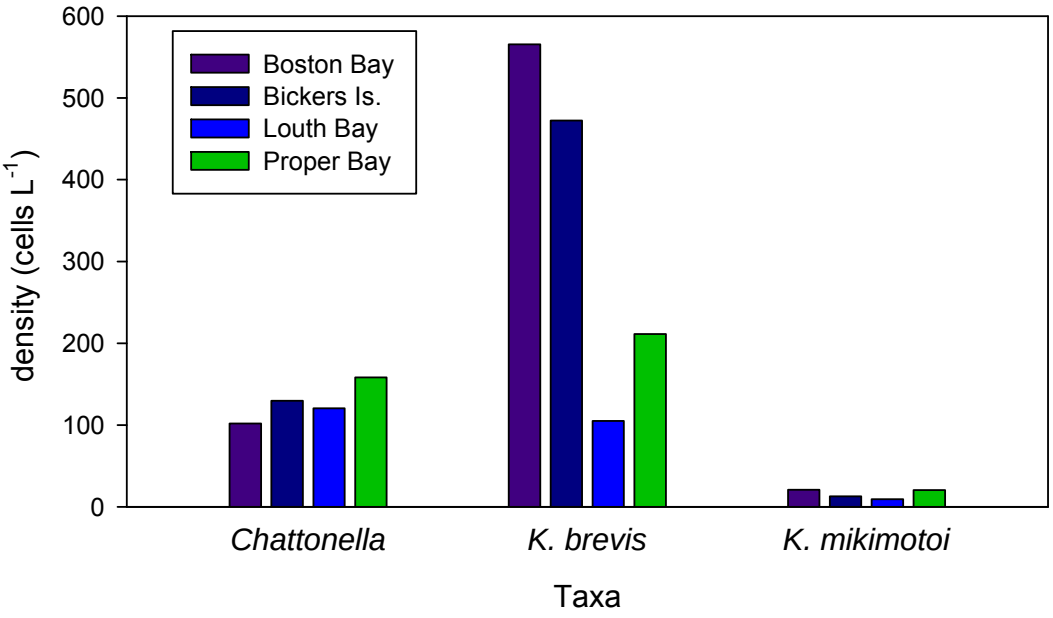

Figure 7.28. The spatial distribution of the 3 main ichthyotoxic species *Chattonella* (all species), *Karenia brevis* and *Karenia mikimotoi* showing the mean density at 5 SASQAP sites: Bickers Island, Boston Bay, Proper Bay, Louth Bay & Port Lincoln, in or near the TFZ. (Note the relatively small number of samples from Lincoln had no observations of these species).

7.4. Discussion

Monthly biomass and abundance data indicate a peak in phytoplankton abundance in May 2006, which is driven by a diatom peak. These patterns are reflected in longer term datasets including remotely sensed pigment data and TBOASA abundance data, although there is considerable inter-annual variability in the size and the timing of the peaks. From the comparison of field data collected in 2005 – 2006 with the longer term remotely sensed chlorophyll-*a*, we can conclude that the peak observed in the TFZ during May 2006 is a consistent feature of the annual cycle of biological oceanography in this region. This conclusion is further supported by the TBOASA abundance data, although these data indicate that mean annual peaks in total phytoplankton abundance may occur between February and June. The relatively high concentrations of fucoxanthin present in May 2006, together with the 2005-2006 taxa abundance data indicate that this peak consists of predominantly diatoms. The close link between patterns in total phytoplankton abundances and patterns in diatom abundances in the TBOASA data (Figure 7.8), in agreement with 2005-2006 abundance data from the transect through the TFZ, indicate that predominately diatom peaks have been a consistent phenomena in the TFZ during late autumn or early winter.

The May peak in diatoms observed in the 2005-2006 transect data appears to be made possible, in part, by a February peak in silica concentrations, a nutrient that is implicitly required by diatoms for survival (Egge and Aksnes 1992). The origin of this February peak in silica concentrations is still unclear. Silica generally enters the marine environment via river inflows or groundwater intrusions (Treguer et al. 1995). There are no major river inflows in the study area, and there is no evidence of groundwater inflow in temperature and salinity profiles (chapter 1). Another major source of silica in the marine environment may be upwelled water (Treguer et al. 1995). Similar silica concentrations, comparable to those measured in this study (>3.5 μmol L^{-1}), were measured in the eastern Great Australian Bight

(EGAB) upwelling off southern Eyre Peninsula in February 2006 (Van Ruth PhD thesis, in prep). Recent hydrological data provided evidence of this upwelled water in the study area (chapter 1), suggesting that water from the EGAB upwelling may be responsible for the February silica peak. The upwelling season in the EGAB generally runs from ~November to May (Kampf et al. 2004; McClatchie et al. 2006; Ward et al. 2006; Middleton and Bye 2007). The annual peaks in diatom abundance in the TBOASA data occurred between February and June, which is mid to late upwelling season in the EGAB. The oceanographic conditions associated with upwelling, such as a deepening of the surface mixed layer and elevated nutrient concentrations, are known to favour diatoms over other phytoplankton (Litchman et al. 2006). Inter annual variation in the timing of the end of the upwelling season may be responsible for inter annual variability in the timing of the phytoplankton peak identified in the chlorophyll-*a* data cell abundance data, SeaWIFS data and TBOASA phytoplankton data. However, as suggested in chapter 5, upwelled water seems unlikely to be the source of the rise in silicate in the TFZ since there was little or no increase in nitrate. It is possible that the silica is derived from a more localized source: silicate recycling of the annual diatom peak that has sedimented out to the bottom and been remineralised.

There are several other questions that arise when examining the abundance data together with nutrient concentrations. For example, why is there a lag between the February peak in silica and the May peak in diatom abundances? Studies have shown that a non-limiting supply of silica alone is insufficient to ensure the dominance of diatoms. In order to compete for silica, diatoms need enough nitrogen for the formation of the proteins in the silicon transport chain (Sullivan 1976; Brzezinski et al. 1990). Si:N ratios in our study suggest potential N limitation of phytoplankton growth between December 2005 and January 2006, and from May-August 2006. This N limitation may prevent diatoms from utilising the silica as soon as it becomes available. Nitrate concentrations increased through February 2006 to a small peak in March 2005, corresponding to a decline in Si concentrations as Si was used up as N ceased to be limiting. By May 2006, the peak in diatom abundance, Si concentrations were low having been incorporated into diatom biomass. A second, smaller peak in silica occurred in July 2006, and may signify the end of the phytoplankton peak, and the remineralisation of biogenic Si. However, there was no increase in diatom biomass associated with this July silica peak. Diatom growth was probably limited by the availability of nitrate during this time, with Si:N ratios suggesting potential N limitation between May and August 2006.

Si:N ratios also suggest potential silica limitation of diatom growth from September to December 2005, which poses another interesting question: Why don't dinoflagellates or other phytoplankton dominate the community when silica is potentially limiting diatom productivity? The answer may lie in an examination of N:P ratios, which indicate potential P limitation of phytoplankton growth between September and December 2005, possibly preventing dinoflagellates and other phytoplankton from dominating the community. Variations in zooplankton grazing pressure and phytoplankton growth rates may also play an important role in the regulation of phytoplankton abundances in the TFZ, a possibility that is examined in further detail in chapter 9.

Comparisons between the phytoplankton community of the TFZ during February 2006 with that of the EGAB during February 2005 showed little similarity, suggesting different factors are determining community composition in these two areas during the same time of the year. At a finer spatial scale, analysis of the SASQAP data indicates little physical connection between the phytoplankton community in the TFZ and other coastal areas of the western Eyre Peninsula. It is worth noting that the *Dinophysis* species that are differentially present in both

areas are relatively slow growing and should not form unique communities quickly. That these two areas maintain divergent phytoplankton communities, even during May when the physical exchange of water is likely to be maximal, suggests that phytoplankton communities are isolated for sufficient time to develop some unique populations.

In southern Spencer Gulf, there were similarities between phytoplankton communities in near-shore and offshore regions. The most distant site, RM2, clustered closely with R44, an inshore site located in Boston Bay, while the most offshore site in the TFZ (R22) clustered with sites RM1 and RM3, in the offshore regions of the southern Spencer Gulf. Thus, shallow sites some distance away may share a similar phytoplankton community, and other factors are likely to be important in determining the presence/absence or abundance of certain species. Further analysis may reveal which environmental factors may be responsible for determining the distribution of these more common species.

A range of HAB species is present in the TFZ. The ichthytoxic species pose a potentially serious threat to the southern bluefin tuna farms. Both in the data presented in this report covering 1999 – 2007, and also in the study of Boston Bay and upper and lower Spencer Gulf from September 1997 to March 1999 by Paxinos (2007), ichthytoxic species such as *Karenia brevis* and *K. mikimotoi* did not reach fish-killing levels (10,000 cells L^{-1} compared with more than 1 million cells L^{-1} for blooms in Japan (Ishimara et al. 1989; Okaichi 1997)). The gymnodinoid species are not necessarily harmful. The harmful paralytic shellfish poisoning (PSP) species *Gymnodinium catenatum* was not observed – this is a morphologically distinct chain-forming species that would be easily recognised in phytoplankton samples. The ichthytoxic *Gymnodinium* aff. *puchellum*, while present, was near or below detection over the study period.

In April 1996 a mass mortality of farmed tuna co-occurred with storm conditions and with the presence of the ichthytoxic raphidophyte *Chattonella marina* at densities of 66,000 cells L^{-1} (Hallegraeff et al. 1998; Munday and Hallegraeff 1998). Fish killing events due to *Chattonella* species in other parts of the world have occurred at much greater cell densities (e.g. 500,000 cells L^{-1} caused a mass mortality of yellowtail fish *Seriola quinqueradiata* in the Seto Inland Sea (Okaichi et al. 1989)). *C. marina* from Port Lincoln grows across a broad range of temperatures, salinities and irradiances, factors which influence its free fatty acid and reactive oxygen production and may be linked to ichthytoxcy (Marshall and Hallegraeff 1999; Marshall et al.2003). Maximum observed densities of *Chattonella marina* and other *Chattonella* species in the TFZ area from 1999 to 2007 were only 100s L^{-1}. Another ichthytoxic raphidophyte, *Heterosigma*, caused mortality of cage-reared chinook salmon in Big Glory Bay, New Zealand in 1989. In this case the blooms were very dense at 2 $x10^6$ cells L^{-1} and appeared to be promoted by high nutrient levels and higher than usual temperatures and a stratified water column (Chang et al. 1990). In all the data evaluated from the TFZ during 1999 to 2007, *Heterosigma* species was detected only at densities of 100s L^{-1}, which is not considered harmful. To date, no SBT deaths can be attributed to the HAB species observed in the waters of the TFZ.

Some of the harmful or potentially harmful phytoplankton species may have a benthic resting stage as part of their life cycle. Storm events can cause resuspension of resting cells, potentially changing the phytoplankton community. Bolch (1997) found that cysts of the toxic dinoflagellate *Gymnodinium catenatum* were widespread around Port Lincoln, Boston Bay and the nearby coastal area. There are, however, no records of *G. catenatum* blooming in these areas, suggesting that conditions are not conducive to growth of this species, which is known to thrive in the stratified water column of the Huon Estuary in south east Tasmania

(CSIRO 2000). *Chattonella marina* is known to form dormant cells in Japanese waters (Imai and Itoh 1987), however, Bolch (1997) did not confirm the presence of *Chattonella* cysts in the TFZ so that there is no evidence to date that *Chattonella* in the phytoplankton is seeded from cysts.

There is little evidence of a HAB having occurred in the TFZ. Paxinos (2007) concluded that growth limiting factors probably reduce phytoplankton biomass, including harmful species, in Boston Bay and surrounds. In the current study, it appears that nutrient concentrations are frequently low, possibly preventing dinoflagellates and other flagellates from dominating the phytoplankton community. Given the wide diversity of potentially problematic HAB species present, this could be an important ecosystem feature in preventing HABs from occurring. Also the well-mixed water column with low stratification (chapter 1) is not conducive to HABs. Nonetheless, lack of complete definition of the factors promoting toxicity in some species e.g. *Chattonella* spp. suggests a precautionary approach to HAB risk should be used.

The bloom forming cyanobacterium *Trichodesmium erythraeum* and other *Trichodesmium* spp. have been documented in Spencer Gulf commonly in January when conditions are warm and calm, with blooms stretching for 20 km recorded (Paxinos 2007). However, the data sets examined in the current study do not demonstrate regular *Trichodesmium* blooms in the TFZ. As these blooms may originate in the eastern Great Australian Bight, it suggests the lack of connection between the phytoplankton communities in these regions (see above).

7.4.1. Risk Assessment for HAB species in the TFZ.

A qualitative assessment of the risk posed to tuna farming in the TFZ from harmful phytoplankton was undertaken by the project team. The team considered the data on the abundance of known ichthyotoxic species previously observed in the TFZ. Several data sets were examined as part of this risk assessment including 1 year of sampling as part of the current project, the data available from the TBOASA and data made available by the South Australian Shellfish Quality Assurance Program. Other analyses of these data are presented elsewhere in this chapter. These data sets were collected for a range of different purposes and their various limitations mean they are not well suited to being combined or subject to any rigorous statistical tests. These sorts of weakness in the available data reduce the value of the risk assessment in terms of being robust and predictive.

For the purpose of this risk assessment we considered the potential for HAB species to contribute risk (= likelihood x consequence, after Fletcher et al. 2004). For the purpose of this report we have considered that the more abundant, the more widespread, and the more persistent an ichthytoxic species is the greater the consequences. We applied the risk assessment framework (Table 7.6, after Fletcher et al. (2004)) to identify any known HAB that would constitute a high level of risk (> 12) to tuna farming. In Table 7.6, consequence ratings (Table 7.7b) are multiplied by likelihood ratings (Table 7.7a) to give risk categories (Table 7.7c) with values of 1 – 6 considered low; 7 – 12 ( ) moderate, > 12 ( ) high (adapted from Fletcher et al. 2004).

Table 7.6. Risk matrix – numbers in cells are the product of the consequence and the likelihood ratings = the risk (adapted from Fletcher et al. 2004).

Likelihood rating		Consequence rating				
		Insignificant	Minor	Moderate	Major	Catastrophic
		1	**2**	**3**	**4**	**5**
Rare	**1**	1	2	3	4	5
Unlikely	**2**	2	4	6	8	10
Moderate	**3**	3	6	9	12	15
Likely	**4**	4	8	12	16	20
Almost certain	**5**	5	10	15	20	25

Table 7.7. (a) Likelihood ratings adopted for this risk assessment

Description	Score & Likelihood of occurrence
Rare	1 - the event may occur only in exceptional circumstances
Unlikely	2 - the event may occur at some time (once in 10 years)
Moderate	3 - the event should occur at some time (once in 3 years)
Likely	4 - the event will probably occur in most circumstances (once a year)
Almost certain	5 - the event is expected to occur in most circumstances (many times a month)

Table 7.7. (b) Consequence ratings. The consequences of the identified risks with specific reference to SBT.

Description	Score & Impact
Catastrophic	5 - serious long-term or widespread harm to the industry
Major	4 - significant harm with long-term recovery (major losses in 1 year or moderate losses over several years)
Moderate	3 - moderate harm with mid-term recovery (moderate stock losses in a single year)
Minor	2 - transient harm (Decreased fish growth/condition, minimal losses)
Insignificant	1 - brief impact and tuna are known to be robust

Table 7.7. (c) Risk ratings.

Risk Ranking	Score (multiply scores from (a) and (b)) & Assessment
Low	1-6, minimal risk, no specific management actions needed
Moderate	7-12, possibly acceptable, managed by current procedures, report
High	>12, action is required, additional management needed, full performance report

The best data set available to assess likelihood (SASQAP) indicates populations of ichthyotoxic species have varied over time but that there have been seasonal peaks, most commonly during May-June. Population peaks were evident in 5 of 7 years, making significant increases in phytoplankton abundances "likely". These increases in abundance have not been reported to exceed 36,000 cells L^{-1} over the period from 1999 to 2006 (although the 1996 event did have one occurrence of 66,000 L^{-1}) and such densities are a long way below those reported in association with ichythotoxic events internationally. In addition a comparison of the SASQAP and the TBOASA data sets suggests that densities are lower further offshore. Unfortunately, precise estimates of the toxicity of these phytoplankton

species to SBT are not available. There is very limited evidence of toxicity at densities below 100,000 cells L^{-1} although some increasing mortality has been reported in damsel fish exposed to densities < 100,000 cells L^{-1} (Marshall et al. 2003). At the lower densities that have been observed in the TFZ, while the likelihood is high (5 or 6) the consequences of these low density events are anticipated to be minor (1) due to the low probability of causing significant mortality to fish. Therefore the overall risk rating is ~ 6.

The densities of known ichthyotoxic phytoplankton species in the region have been reported to range above 10,000 cells L^{-1}. While these densities have not been reported in association with a known ichthyotoxic event, they are sufficiently dense to warrant monitoring and caution. There is evidence that ichthyotoxic species are more prevalent in some locations than others (e.g.: Bickers Island and Boston Bay). Consequently any local inputs of nutrients that might support HABs should be identified and regulated.

A number of possible future scenarios could increase the risk to tuna farmers from HABs. Some of the more probable include:

a. Persistent stratification through May-June. At the moment stratification weakens during autumn and diatoms dominate the phytoplankton biomass. Climate change may result in stratification persisting into autumn and dinoflagellates are likely to become increasingly dominant. Most HAB species are dinoflagellates.

b. Local circulation is relatively weak and any increase in nutrient load is likely to increase the local phytoplankton biomass.

c. If more nutrients are input during summer or early autumn when the water column is more stratified there is a greater chance of dinoflagellate blooms. These have an increased probability of being toxic.

d. A loss of benthic flora is likely to increase phytoplankton.

e. Arrival of a new or different ichthyotoxic species (potentially via ballast water). The available data suggest there has been significant inter annual variation in the dominant ichthyotoxic species, a new HAB species entering the region may be more toxic or better adapted to the local conditions.

Acknowledgements
We thank the South Australian Shellfish Quality Assurance Program and the Tuna Boat Owners Association of South Australia for making their data available for this analysis. We thank Sonja Venema, Kate Rodda, Emlyn Jones, Brenton Ebert, and Neil Evans (SARDI Aquatic Sciences) for assistance with field sampling, and Lesley Clementson (CSIRO) for assistance with interpretation of marker pigment data. We thank Tina Hines from the Water Studies Centre at Monash University for nutrient analyses. John Volkman, Jenny Skerratt, Lesley Clementsen, and Milena Fernandes provided valuable feedback on the HAB risk assessment.

7.5. References

Belbin, L., Faith, D. P., Milligan, G. M. (1992) A comparison of two approaches to beta flexible clustering. Multivariate Behavioural Research 27: 417-433.

Bolch, C. J. S. (1997) Dinoflagellate cysts in sediments from Port Lincoln, Boston Bay and surrounds. Appendix. In Clarke, S., Cartwright, C., Smith, B., Madigan, S., Haskard, K. (Ed.), Southern Bluefin Tuna (*Thunnus maccoyii*) Aquaculture Environmental

Monitoring Report 1996-1998. South Australian Research and Development Institue, Aquatic Sciences, 101 pp.
Brzezinski, M. A., Olson, R. J., Chisholm, S. W. (1990) Silicon availability and cell cycle progression in marine diatoms. Marine Ecology Progress Series 67: 83-96.
Chang, F. H., Anderson, C., Boustead, N. C. (1990) First record of a *Heterosigma* (Raphidophyceae) bloom with associated mortality of cage reared salmon in Big Glory Bay, New Zealand. New Zealand Journal of Marine and Freshwater Research 24: 461-469.
Clarke, S.M. 1996. Tuna mortalities: April-May 1996. South Australian Research and Development Institute, Adelaide, 20pp.
Dufrene, M., Legendre, P. (1997) Species assemblages and indicator species: the need for a flexible asymmetrical approach. Ecological Monographs 67: 345-366.
Egge, J. K., Aksnes, D. L. (1992) Silicate as a regulating nutrient in phytoplankton competition. Marine Ecology Progress Series 83: 281-289.
Fletcher, W. J., Chesson, J., Fisher, M., Sainsbury, K. J., Hundloe, T. J. (2004) National ESD Reporting Framework: The 'How To' Guide for Aquaculture. Version 1.1. FRDC, Canberra, Australia 88 pp.
Hallegraeff, G. M. (1993) A review of harmful algal blooms and their apparent global increase. Phycologia 32: 79-99.
Hallegraeff, G. M. (2002) Aquaculturalists' Guide to Harmful Australian Microalgae. School of Plant Science, University of Tasmania, Hobart
Hallegraeff, G. M., Munday, B. L., Baden, D. G., Whitney, P. L. (1998) *Chattonella marina* rhaphidophyte bloom associated with mortality of cultured bluefin tuna (*Thunnus maccoyii*) in South Australia. In Reguera, B., Blanco, J. L., Fernandez, M. L., Wyatt, T. (Ed.), Harmful Algae. Xunta de Galacia and IOC of UNESCO, Spain, 93-96.
Imai, I., Itoh, K. (1987) Annual life cycle of *Chattonella* spp., causative flagellates of noxious red tides in the inland Sea of Japan. Marine Biology 94: 287-292.
Ishimara, T., Takeuchi, T., Fukuyo, Y., Kodama, M. (1989) The selenium requirement of *Gymnodinium nagasakiense*. In Okaichi, T., Anderson, D. M. (Ed.), Red Tides: Biology, Environmental Science and Toxicology. Elsevier.,
Jeffrey, S. W., Wright, S. W. (2006) Photosynthetic pigments in marine microalgae: insights from cultures and the sea. In Subba Rao, D. V. (Ed.), Algal Cultures, Analogues of Blooms and Applications. Science Publishers, 33 - 90.
Kampf, J., Doubel, M., Griffin, D. A., Matthews, R., Ward, T. M. (2004) Evidence of a large seasonal coastal upwelling system along the southern shelf of Australia. Geophysical Research Letters 31(L09310): doi:10.1029/2003GL019221.
Litchman, E., Klausmeier, C. A., Miller, J. R., Schofield, O. M., Falkowski, P. G. (2006) Multi-nutrient, multi-group model of present and future oceanic phytoplankton communities. Biogeosciences Discussion 3: 607-663.
Marshall, J. A., Nichols, P. D., Hamilton, B., Lewis, R. J., Hallegraeff, G. M. (2003) Ichthiotoxicity of *Chatonella marina* (Raphidophyceae) to damselfish (*Acanthochromis polycanthus*): the synergistic role of reactive oxygen species and free fatty acids. Harmful Algae 2: 273-281.
McClatchie, S., Middleton, J. F., Ward, T. M. (2006) Water mass analysis and alongshore variation in upwelling intensity in the eastern Great Australian Bight. Journal of Geophysical Research 111(C08007): doi:10.1029/2004JC002699.
McCune, B., Mefford, M. J. (1999). PC-ORD. Multivariate Analysis of Ecological Data, Version 5., MjM Software Design, Gleneden Beach, Oregon, USA.
Middleton, J. F., Bye, J. A. T. (2007) A review of the shelf slope circulation along Australia's southern shelves: Cape Leeuwin to Portland. Progress in Oceanography 75: 1-41.

Munday, B. L., Hallegraeff, G. M. (1998) Mass mortality of captive Southern Bluefin Tuna (*Thunnus maccoyii*) in April/May 1996 in Boston Bay, South Australia: A complex diagnostic problem. Fish Pathology 33: 93-96.

Okaichi, T. (1997) Red tides in the Seto Inland Sea. In Okaichi, T., Yanagi, T. (Ed.), Sustainable Development in the Seto Inland Sea. Terra Scientific Publishing, Tokyo,

Okaichi, T., Ochi, T., Nishio, S., Takano, H., Marsuna, K., Morimoto, T., Murakami, T., Shimada, M. (1989) The cause of fish kills associated with red tides of *Chattonella antiqua* (Hada) Ono. In Miyachi, S., Karube, I., Ishida, Y. (Ed.), Current Topics in Marine Biotechnology. Japanese Society for Marine Biotechnology, Tokyo, 185-188.

Paxinos, R., Clarke, S. M., and Matsumoto, G. I. 1996. Phytoplankton dynamics of Boston Bay, South Australia. South Australian Research and Development Institute, Aquatic Sciences, 23 pp.

Paxinos, R. (2007). Dynamics of phytoplankton in relation to tuna fish farms in Boston Bay and near-shore Spencer Gulf, South Australia., PhD thesis, Flinders University: 172p.

Sullivan, C. W. (1976) Diatom mineralization of silicic acid. 1. Si(OH)4 transport characteristics in *Navicula pelliculosa*. Journal of Phycology 12: 390-396.

Treguer, P., Nelson, D. M., Van Bennekom, A. J., De Master, D. J., Leynaert, A., Queguiner, B. (1995) The silica balance in the World Ocean: A re-estimate. Science 268: 375-379.

Van Heukelem, L., Thomas, C. S. (2001) Computer-assisted high-performance liquid chromatography method development with applications to the isolation and analysis of phytoplankton pigments. Journal of Chromatography 910(1): 31-49.

Ward, T. M., McLeay, L. J., Dimmlich, W. F., Rogers, P. J., McClatchie, S., Matthews, R., Kampf, J., Van Ruth, P. D. (2006) Pelagic ecology of a northern boundary current system: effects of upwelling on the production and distribution of sardine (*Sardinops sagax*), anchovy (*Engraulis australis*) and southern bluefin tuna (*Thunnus maccoyii*) in the Great Australian Bight. Fisheries Oceanography 15(3): 191-207.

Chapter 8: Temporal and spatial variability in microphytobenthos, biogeochemistry and light in southern Spencer Gulf

Lesley Clementson [1,4]*, Susan Blackburn [1,4], Milena Fernandes [2,4], Emlyn Jones [3,4]

[1]CSIRO Marine and Atmospheric Research, PO Box 1538, Hobart, Tasmania 7001
[2]SARDI Aquatic Sciences, PO Box 120, Henley Beach SA 5022
[3]Flinders University of South Australia, GPO Box 2100, Adelaide SA 5001
[4]Aquafin CRC

*corresponding author. Phone:+61 (3) 6232 5337, Email: Lesley.Clementson@csiro.au

Abstract

Microphytobenthos (MPB) biomass and community composition were determined for the subtidal environment in the tuna farming zone (TFZ) in lower Spencer Gulf, South Australia, during 16 field trips over a two year period (2005-2007). A significant difference between MPB biomass at the offshore sites and the inshore sites was found, while the community composition at all sites at all times of the year was dominated by benthic diatoms. This dominance of diatoms suggests silica availability from porewaters was not limiting. Photosynthetically active radiation measurements showed light not to be limiting either, with between 4-28% of incident irradiance calculated at the sediment surface. High concentrations of chlorophyll degradation products and the pigment astaxanthin in the MPB samples suggest grazing of the MPB by benthic copepods.

8.1. Introduction

Microphytobenthos (MPB) are the photosynthetic microalgae, including both attached (epipsammon) and free-living (epipelon) forms, that inhabit the very top layer of the sediment in environments ranging from permanently exposed mud flats to intertidal and subtidal estuarine and coastal regions. In the past, most MPB studies have been devoted to intertidal and very shallow sites, where it has been shown that MPB can significantly contribute (up to 50%) to the total benthic and pelagic productivity of an ecosystem (Varela and Penas, 1985; MacIntyre and Cullen, 1995; Montani et al., 2003). Similar results have been found in subtidal environments (Cahoon et al., 1993; Nelson et al., 1999). MPB in subtidal environments often have to adapt to large changes in light, temperature, nutrient availability and grazing pressure. Of these parameters, light is thought to be the most important in relation to the development of the MPB community (Miles and Sundbäck, 2000; Cibic et al., 2007a) and therefore MPB communities are often composed of low-light adapted species – frequently benthic diatoms (Cahoon et al., 1993; Nelson et al., 1999; Cibic et al., 2007a,b).

Provided there is sufficient light at the sediment surface, changes in nutrient availability, temperature and the grazing community composition will cause changes in the MPB community composition, either by change in species of the same algal group or in seasonal succession of algal groups. Light availability at the sediment surface is determined by the optical properties of the overlying water column. The extent to which the pelagic phytoplankton, non-algal suspended matter and the chromophoric dissolved organic matter (CDOM) absorb the light will determine what percentage of incident irradiance reaches the sediment surface. Increases in any one of these parameters, due to storm events, terrestrial runoff, algal blooms, or other factors, will decrease the light reaching the sediment surface and affect the MPB biomass and composition.

The biomass and productivity of MPB in shallow water systems worldwide has been reviewed by MacIntyre et al. (1996), while Table 8.1 summarises biomass as chlorophyll-*a* values from several recent subtidal studies. The results collated in Table 8.1 illustrate some of the problems encountered in comparing data from different sites and studies. The first problem is the depth of sample collected; MPB can migrate vertically within the sediment and are often found several centimetres below the surface, but it is considered that due to light limitation, only the MPB within the top 2 mm are able to photosynthesize. The measurement of chlorophyll-*a* within the top 1 cm could therefore include "non-functional" chlorophyll-*a* and overestimate the MPB biomass. Alternatively, if the sample is collected while the benthic algae are migrating into the sediment, then the measurement of chlorophyll-*a* within the top 2 mm could miss the "functional" chlorophyll-*a* and underestimate the MPB biomass (Longphuirt et al. 2006). The second problem is the range of units that are used to measure the chlorophyll-*a* biomass, making comparisons difficult; conversion of mg per g or cm^3 to an areal measurement must include the determination of the density of the sample. These and other issues connected to the accurate estimation of MPB biomass have been discussed in Grinham et al. (2007).

Table 8.1. Reported values of MPB biomass, measured as chlorophyll-*a* in subtidal environments.

Location	Water depth (m)	Sediment depth (mm)	Chlorophyll-*a* concentration	Units	Reference
Stellwagen Bank, Massachusetts Bay, USA	20 - 28	300	39.8	mg m^{-2}	Cahoon et al. (1993)
Georgia Shelf, South Atlantic Bight, USA	14 - 40	5	0.6 - 3.77	μg cm^{-2}	Nelson et al. (1999)
Florida Shelf, South Atlantic Bight, USA	20 - 40	5	1.06 – 4.09	μg cm^{-2}	Nelson et al. (1999)
Northern Adriatic Sea	13 - 66	10	11.2 – 278.8	mg m^{-2}	Totti (2003)
Targus Estuary, Portugal	1 -4	2	18.3 – 60.7	mg m^{-2}	Cartaxana et al. (2006)
Bay of Brest, France	<5 - 8	2	0.3 -16.9	mg m^{-2}	Longphuirt et al. (2006)
Dogger Bank, North Sea	< 30	< 5	1.25 – 2.16	μg cm^{-3}	Reiss et al. (2007)
	> 30	< 5	1.84 – 2.55	μg cm^{-3}	
Gulf of Trieste, Northern Adriatic Sea	17	< 10	0.16 – 29.14	μg cm^{-3}	Cibic et al. (2007a)
Trondheimsfjord, Norway	8	5	2.19 – 2.87 45.11 – 59.12	μg g^{-1} dry wt. mg m^{-2}	Cibic et al. (2007b)
Seto Inland Sea, Japan	5 - 15	10	1.9 – 46.5	mg m^{-2}	Yamaguchi et al. (2007)
Marmion Lagoon, WA, Australia	8 - 9	20	0.7 – 2.2	μg g^{-1} dry wt.	Kendrick et al. (1998)
Cockburn Sound, WA, Australia	1.5 - 14	5	42.3 – 89.1	mg m^{-2}	Forehead (2006)
Bunbury, WA, Australia	10 - 12	2	0.45 – 7.85 2.25 – 29.18	μg g^{-1} wet wt. mg m^{-2}	Clementson and Lourey, (unpublished results)
Southern Spencer Gulf, SA, Australia	17 - 20	2	0.60-11.1 1.05 – 19.46	μg g^{-1} wet wt. mg m^{-2}	this study

The region offshore of Boston Island in the southern end of Spencer Gulf, South Australia, is a coastal zone with extensive seacage tuna farming. Previous environmental monitoring studies within the area have reported the phytoplankton distribution (Paxinos et al. 1996) and the water column parameters and macroinfauna composition of the sediments (Clarke et al. 1999, 2000), but the MPB biomass and composition has not been considered. In this study we have determined the MPB biomass along the same east-west transect through the tuna farming zone (TFZ) and into Spencer Gulf that was sampled in chapter 7 for phytoplankton, and report on the spatial and temporal distribution of the MPB biomass and community composition over a two year period from October 2005 to October 2007. The MPB could potentially form an important sink for nutrients, may harbour potentially harmful species, and if resuspended could cause problems for the tuna aquaculture industry. Given that almost nothing is known about this component of the benthos in the TFZ, it is thus important to assess their spatial and temporal dynamics to determine if they play an important role in the ecosystem or not.

8.2. Methods

8.2.1. Sample sites and collection

Replicate samples for the analysis of pigment composition and concentration of the MPB were collected in the southern region of Spencer Gulf from 4 sites: 22, 25, 44 and 39 (Figure 8.1); monthly, between October 2005 and September 2006, and quarterly (March, May, July and October) in 2007. Due to bad weather in July 2006, there were no samples collected from sites 22, 25 and 44. Water depth above the benthos ranged from 17 m (sites 39 and 44) to 21 m (sites 22 and 25) and there was a distance of 18 km between the most inshore site (44) and the offshore site (22). Site 25 was in the centre of the TFZ.

Samples were collected with 67 mm (internal diameter - i.d.) stainless steel tubes in a HAPS Corer (KC Denmark) deployed by a crane from the back of the research vessel RV Breakwater Bay, while it was anchored. Two replicate core samples were obtained at each site for the analysis of MPB, and two replicate core samples for the analysis of porewaters. Depending on water depth and weather conditions, replicate samples could be a maximum of 30 m from each other.

Upon retrieval, the overlying water in the tube was carefully discarded to minimise surface disturbance. MPB samples were scraped from across the surface of the core (approximately 2 mm deep), transferred to cryo-vials and stored in liquid nitrogen until analysis. Porewater samples were obtained by slicing the top 0-2 cm layer of each core, which was transferred into a centrifuge tube and stored on ice before transfer to the laboratory for analysis of nutrient concentration.

Profilies of photosynthetically active radiation (PAR) were collected with a Biospherical Instruments QSP2300 PAR sensor attached to a conductivity, temperature and depth sensor (CTD).

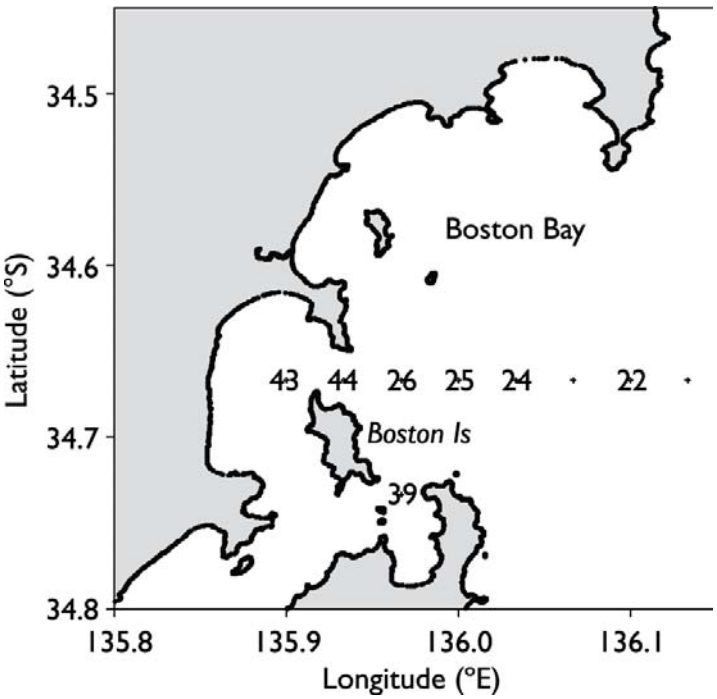

Figure 8.1. Map of southern Spencer Gulf with site locations sampled from October 2005 – October 2007 for microphytobenthos (sites 22, 25, 39, 44) and water column phytoplankton (all sites, refer chapter 7).

8.2.2. Sample analysis

The MPB samples were weighed and quantitatively transferred to 50 mL centrifuge tubes. 100% acetone (8-10 mL) was added to each tube; the tubes were vortexed for about 30 seconds and then sonicated in an ice-water bath for 15 minutes in the dark. The samples were then kept in the dark at 4 °C for approximately 15 hours. After this time the tubes were centrifuged and the supernatant from each tube decanted into separate 25 mL volumetric flasks which were stored in the dark at 4 °C. A second extraction was performed on each MPB sample with a resting time of only 3 hours. The samples were again centrifuged and the supernatant of the second extraction was added to the first. A pre-determined volume of water was added to each flask such that the final extract mixture was 90:10 acetone:water (vol:vol). Each flask was made up to the 25 mL mark with 100% acetone and then filtered through a 0.2 µm membrane filter (Advantec MFS). Samples were then analysed using a Waters - Alliance high performance liquid chromatography (HPLC) system, comprising a 2695XE separations module with column heater, refrigerated autosampler and a 2996 photo-diode array detector. Immediately prior to injection the sample extract was mixed with a buffer solution (90:10 28 µM tetrabutyl ammonium acetate, pH 6.5 : methanol) within the sample loop. After injection, pigments were separated using a Zorbax Eclipse XDB-C8 stainless steel 150 mm x 4.6 mm i.d. column with 3.5 µm particle size (Agilent Technologies) and the gradient elution procedure of Van Heukelem and Thomas (2001) with minor modifications. The flow rate was 1.1 mL min^{-1} and the column temperature was 55°C. The separated pigments were detected at 436 nm and identified against standard spectra using Waters Empower software. Concentrations of mono-vinyl chlorophyll-*a* (MV chlorophyll-*a*), chlorophyll-*b* and β,β-carotene in sample chromatograms were determined from Sigma™ standards (USA) while all other pigment concentrations were determined from DHI™ standards (Denmark).

Samples collected for the determination of the porewater nutrient concentration were centrifuged at 3,000 rpm (1,400 g) for 10 min, filtered (0.45 µm) and stored frozen (-20 ºC) until analysis. Ammonium (APHA-AWWA-WPCF, 1998a) and phosphate (APHA-AWWA-WPCF, 1998b) were determined by flow injection analysis with a QuickChem 8000 Automated Ion Analyser (see detailed methods in section 5.2.2).

Statistical analysis was performed using R software (version R-2.6.2).

8.3. Results and Discussion

8.3.1. Spatial and temporal variability

Accurate estimates of MPB biomass can often be difficult to obtain due to the pelagic/benthic interface where microalgae from the water column can settle in the benthos and benthic microalgae can be resuspended into the water column. This is especially the case in subtidal environments where sampling may have to be done by remote means, as in this study.

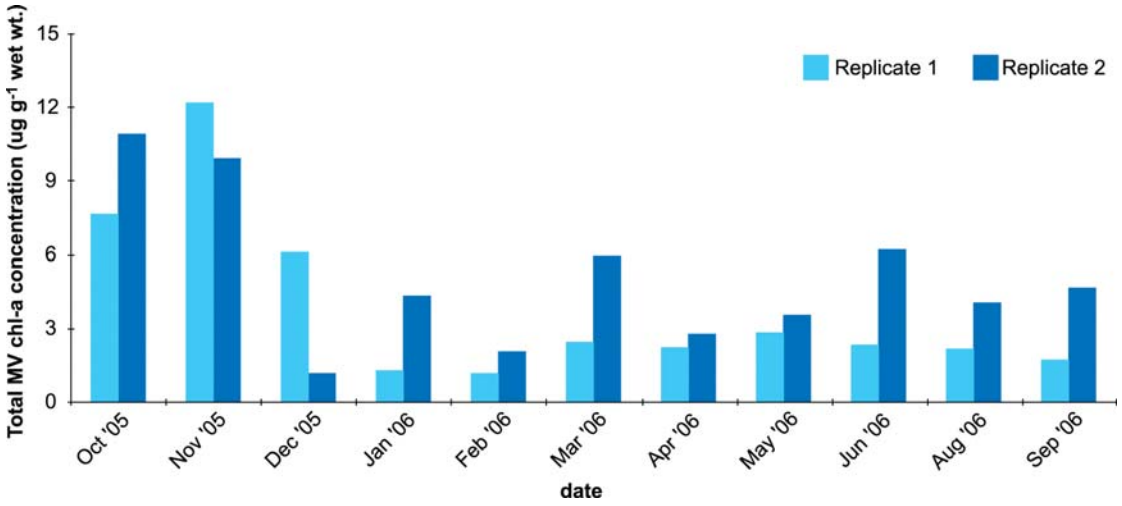

Figure 8.2. The total MV chlorophyll-*a* concentration in replicate samples collected monthly during 2005/06 from site 22.

High variability was often observed between the replicate samples from each site (Figure 8.2). The results for one site are shown in Figure 8.2, but the pattern of variability is representative of the results for all sites. In this study, core samples were collected using a crane from the back deck of the research vessel and due to weather conditions and time between replicate sample collection, the distance between the replicate samples could be as much as 30 m. The variability could be the result of the sample collection technique, but other studies have also noted high variability over relatively small spatial scales. In a study on the Georgia Shelf of the South Atlantic Bight, Nelson et al. (1999) observed variability in MPB biomass over scales of meters to tens of meters, measured as chlorophyll-*a* concentration in replicate cores, to account for 52% of the total variability and over scales of a few centimetres (replicate samples from each core) to account for 17% of the total variability. Varela and Penas (1985) observed a three fold variation in the chlorophyll-*a* concentration of 25 MPB samples collected from a 50 x 50 cm area of sediment on an intertidal sand flat. Conversely, Moreno and Niell (2004) concluded from their study in the Palmones River estuary, Spain that the most important variation occurred at the broad scale of sites while the spatial variation between replicate samples (small scale) was less important.

Due to the, often, high variability between replicates in this study, the results reported are the mean values of the two replicates.

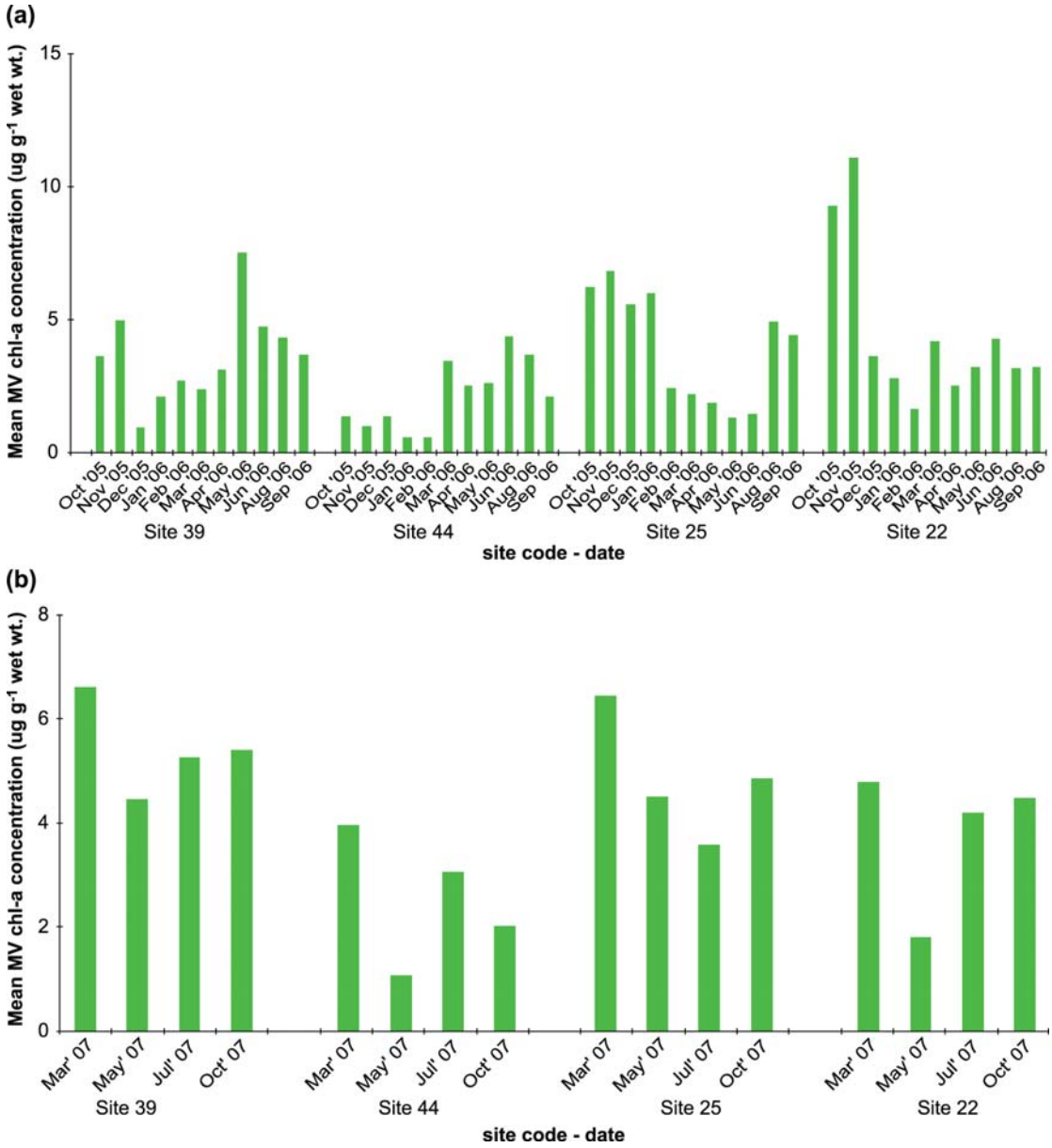

Figure 8.3. The mean MV chlorophyll-*a* concentration in samples collected (a) monthly during 2005/06 and (b) quarterly during 2007 from sites 22, 25, 39 and 44.

8.3.2. MPB biomass

MPB biomass, as indicated by the chlorophyll-*a* concentration for the four sites sampled, is shown in Figure 8.3. The highest MPB biomass was observed at the offshore site, 22, during October and November 2005 (9.3 and 11.1 mg g^{-1} wet wt. respectively), while the lowest biomass was observed at the inshore site, 44, during January and February 2006 (0.60 mg g^{-1} wet wt.). The range of values for MPB offshore of Boston Island (sites 22 and 25) are similar to those found at two coastal sites in Western Australia (Kendrick et al., 1998; Clementson and Lourey, unpublished data) and also in some northern hemisphere studies (Longphuirt et al., 2006; Yamaguchi et al., 2007) (Table 8.1).

Due to the high variability between replicates, statistical differences in biomass between sites were not able to be determined. A generalised linear model showed a significant site by season interaction for all sites, however the relationship with season was not the same at all sites (Figure 8.4). Except for site 25, all sites showed the lowest MPB biomass to be in the summer months, while the highest MPB biomass was during spring for sites 22 and 25 and during autumn/winter for the more inshore sites, 39 and 44.

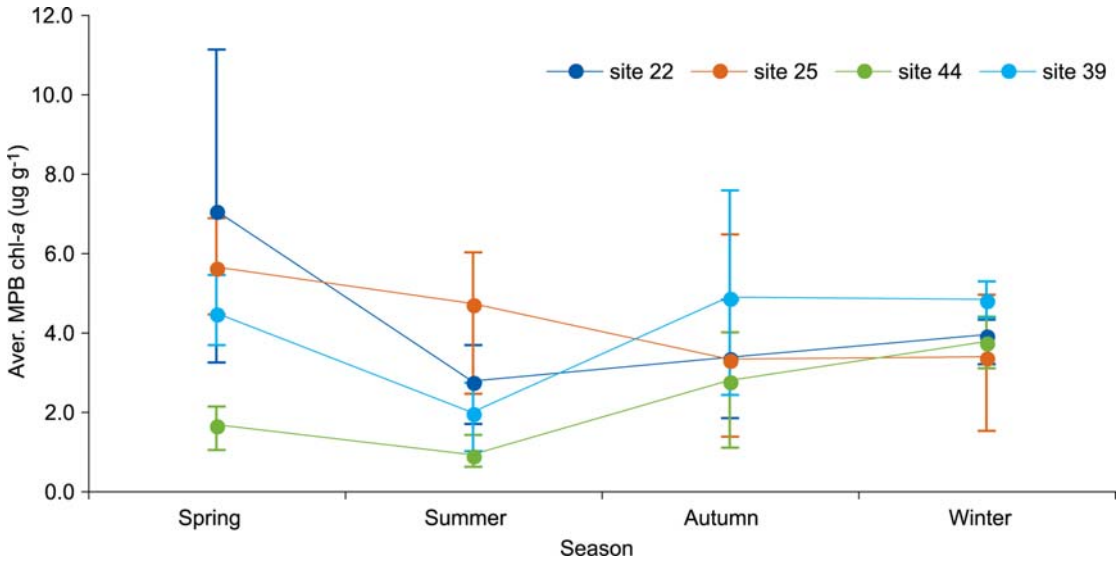

Figure 8.4. The average seasonal MPB chlorophyll-*a* concentration for samples collected from October 2005 to October 2007 from sites 22, 25, 39 and 44.

Biomass results for the water column samples from the four sites showed no difference between sites (refer chapter 7). Similar results were observed during an environmental monitoring survey, which included the area where sites 39 and 44 from this study are located, made between July 1996 and December 1998 (Clarke et al. 1999). In that work, analysis of the environmental and phytoplankton data, in the water column, indicated that the locations within Boston Bay and just to the east of Boston Island were similar. The seasonal pattern for the water column biomass, unlike the MPB biomass, was the same at each site with maximum biomass being observed during May 2006 suggesting minimal interaction between the pelagic and benthic environments.

In this study, site 25 was the only site where a strong negative correlation (R^2 = 0.75) between MPB chlorophyll-*a* and depth integrated chlorophyll-*a* (determined using trapezoidal integration) was observed and this relationship can be seen for all seasons for both parameters (Figure 8.5a; site 22 shows a similar pattern).

This suggests that the biomass in the MPB and that in the overlying water column, at these sites, are not related, in that the MPB biomass does not primarily originate from the water column, although settling phytoplankton would make a small contribution to the MPB biomass. At the more inshore site 39 (similar results observed at site 44) the relationship between biomass in the water column and the MPB is different (Figure 8.5b). At these two sites the seasonal cycle of the biomass in the water column and the MPB appear to increase and decrease similarly.

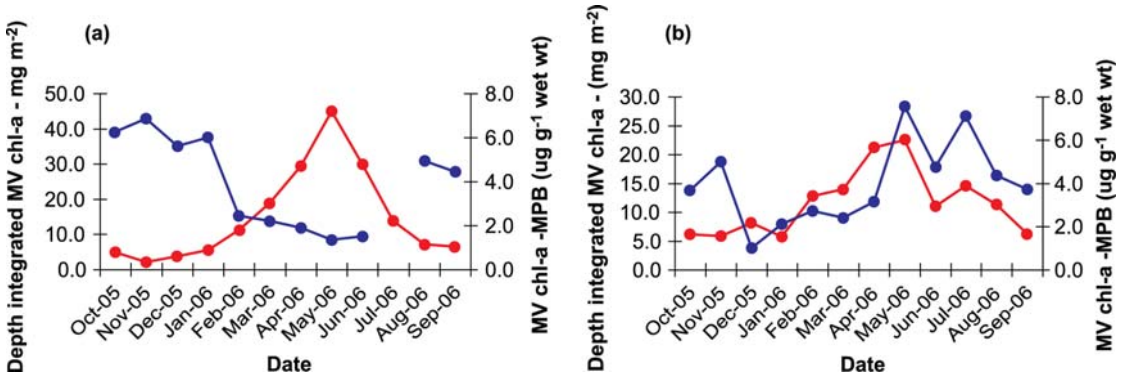

Figure 8.5. The mean MV chlorophyll-*a* concentration in surface water (red line) and MPB (blue line) samples collected monthly during 2005/06 from (a) offshore site - 25 and (b) inshore site - 39.

The location of site 25 during 2005/06 was in the centre of the TFZ (see Figure 5.1) which contained between 130 and 150 sea-cages of southern bluefin tuna. Cages are approximately 40 m in diameter with a net wall depth of 10 m and are typically stocked at densities of 2-3 kg m^{-3} generally between late summer (February) and late winter (August) of each year (Fernandes et al., 2007). The position of these cages almost certainly impacts on the MPB biomass, even when the cage is tens of meters from the site location. Due to a low sun angle during the winter months, significant shading of the benthos may occur from the cages, especially if fouling organisms are allowed to build up on them. Higher pelagic phytoplankton biomass, as observed during late autumn (May) in this study, and solid wastes (mostly faeces) near the cages will also contribute to shading of the benthos. Lowest MPB biomass at site 25 is observed during the autumn and winter months, when the cages are present. The proximity of this site to the tuna cages may also explain the strong negative correlation observed between MPB chlorophyll-*a* and depth integrated chlorophyll-*a* at this site. Site 22 was just on the edge of the TFZ in 2005/06 and the benthos at this site is unlikely to have been affected by the cages as much as site 25. Sites 39 and 44 were outside the TFZ.

8.3.3. MPB pigment composition

Pigment analysis is used to estimate microalgal community composition and concentration. Pigments which relate specifically to an algal class are termed marker or diagnostic pigments (Jeffrey and Vesk, 1997; Jeffrey and Wright, 2006). Some of these diagnostic pigments are found exclusively in one microalgal class (e.g. prasinoxanthin in prasinophytes), while others are the principal pigments of one class but are also found in other classes (e.g. fucoxanthin in diatoms and some haptophytes; 19'-*b*utanoyloxyfucoxanthin in chrysophytes and some haptophytes). The presence or absence of these diagnostic pigments can provide a simple guide to the composition of an algal community, including identifying small phytoplankton, nanoplankton (< 5 μm) and picoplankton (< 2 μm) that cannot be determined by normal light microscopy techniques.

The MPB community composition, as indicated by the pigment composition, was quite stable over the period of both surveys at all sites. The dominance of the carotenoid fucoxanthin (45% of the concentration of chlorophyll-*a*) in all samples at all sites (Figure 8.6a, b) generally indicates a dominance of benthic diatoms (Bacillariophyta) which is commonly observed in MPB communities (Cahoon et al., 1993; Nelson et al., 1999; Cibic et al., 2007a,b). Of particular interest is the presence of chlorophyll *c3* (chl-*c3*) in all MPB samples. This pigment is considered an accessory pigment associated with haptophyte species (Haptophyta), of which 19'-hexanoyloxyfucoxanthin (hex-fuco) is generally the marker

pigment, but it has also been shown to be present in some pennate diatom species (Stauber and Jeffrey, 1988). Hex-fuco was present in only 15 of 120 MPB samples analysed, thus it is unlikely that the chl-*c3* is from haptophytes, but more likely to be associated with benthic pennate diatoms. Microscopic analysis of the benthos was not done during this study, however other studies have reported large numbers of diatom species present in the benthos; 83 species in the Gulf of Trieste (Cibic et al. 2007a) and 94 species in Trondheimsfjord (Cibic et al. 2007b). Low concentrations of the photoprotective pigments, diadino-xanthin (5% of the concentration of chlorophyll-*a*) and diatoxanthin (<1%), suggest benthic diatoms adapted to low light.

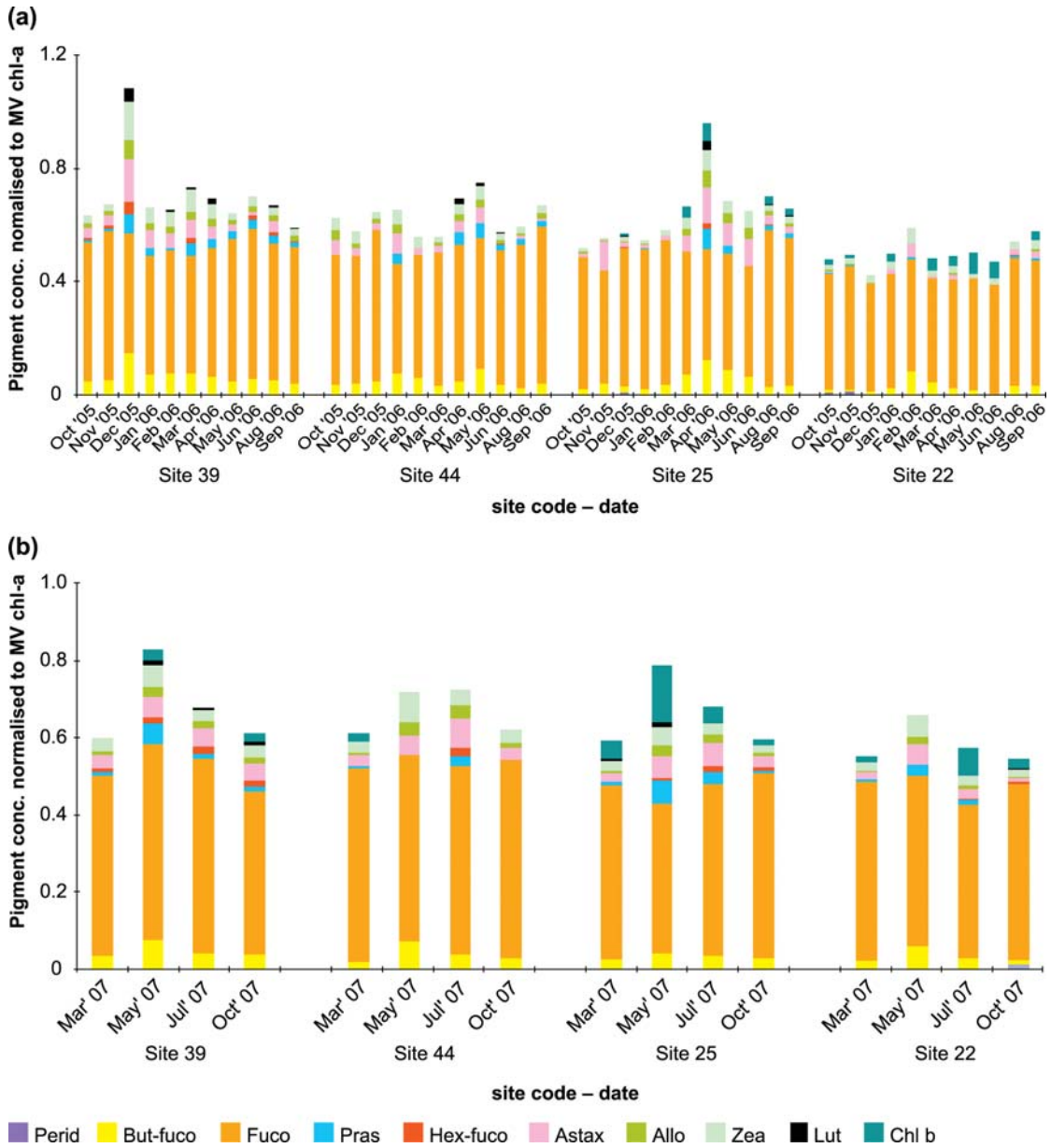

Figure 8.6. The composition of marker pigments for MPB samples collected (a) monthly during 2005/06 and (b) quarterly during 2007 from sites 22, 25, 39 and 44. Pigments are Perid (peridinin); But-fuco (19'-*b*utanoyloxyfucoxanthin); Fuco (fucoxanthin); Pras (prasinoxanthin); Hex-fuco (19'-hexanoyloxyfucoxanthin); Astax (astaxanthin); Allo (alloxanthin); Zea (zeaxanthin); Lut (lutein); Chl *b* (chlorophyll-*b*).

Small amounts of cyanobacteria (indicated by zeaxanthin, 3.5% of the concentration of chlorophyll-*a*), chlorophytes (lutein, <1% and chlorophyll-*b*, 1%), prasinophytes (prasinoxanthin, <2%), cryptophytes (alloxanthin, <2%) and chrysophytes (But-fuco, 4%) are also present.

Chlorophyll-*b* (chl-*b*), an indicator of the green algal lineage, was commonly observed at the more offshore sites (22, 25), but lutein, an indicator of the class of green algae, chlorophytes, was observed primarily at the inshore site (44). These observations suggest that there are spatially different types of green algae along the transect; the most likely scenario being that Type 1 chlorophytes which contain lutein (Jeffrey and Wright, 2006) are present in the MPB at sites closest to the shore, while other green algae, possibly euglenophytes or Type 2 prasinophytes which contain no lutein, (Jeffrey and Wright, 2006) are present in the MPB at the more offshore sites.

The pigment astaxanthin was found in all samples from sites 25, 44 and 39 and only in four samples from the offshore site 22. Astaxanthin is found in a few green algae, but is also associated with the distinct pink colouration of most copepod species (Lotocka and Styczynska-Jurewicz, 2001). The astaxanthin is most likely from the carapaces of dead copepods or due to small benthic copepods that live and feed amongst the MPB in the surface sediments (Buffan-Dubau et al., 1996) rather than from green algae. Astaxanthin is a very minor pigment in the few green algae where it is found so that if green algae were the source of the astaxanthin then there would have to be large concentrations of chl-*b* in the samples, which isn't observed.

8.3.4. MPB phaeopigment composition

Phaeopigments are the degradation products of chlorophyll-*a*, and are produced through predation or natural senescence of living microalgal cells (and also of macroalgae). The five common degradation pigments of MV chlorophyll-*a* are chlorophyllide-*a* (chlide-*a*), phaeophorbide-*a* (phide-*a*), pyrophaeophorbide-*a* (pphide-*a*), phaeophytin-*a* (phytin-*a*) and pyrophaeophytin-*a* (pphytin-*a*). It is generally considered that the presence of chlide-*a* represents senescence and the presence of the other phaeopigments represents predation, however this is probably a simplistic view, with the real situation being far more complex (Louda et al., 1998).

Several studies have shown a relationship between heterotrophic grazing and the presence of phaeopigments (Barranguet et al., 1997; Louda et al., 1998, 2002; Cartaxana et al., 2003), suggesting that one or more of the phaeopigments can be used as an indicator of grazing pressure. During an experiment where the copepod *Calanus* spp. grazed on diatoms, Head and Harris (1992) observed that only pphide-*a* and pphytin-*a* and a pyrolised derivative of phaeoporphyrin-c were produced, except when the degree of chlorophyll-*a* degradation was high, then there were additional unidentified degradation products. In all but one experiment, these pyrophaeopigments accounted for more than 70% of the total identifiable pigments in the faecal pellets, with pphide-*a* ranging from 44 to 71%.

The biomass of phaeopigments in the MPB in this study was often equal to or, in a few samples, greater than the biomass of MPB chlorophyll-*a* (Figure 8.7a, b; Table 8.2), indicating a high proportion of dead algal cells from either natural senescence or heavy grazing. Only four of the previously named phaeopigments were detected in MPB samples with pphide-*a*, on average, clearly the most dominant phaeopigment in all samples from all sites (Figure 8.8a, b; Table 8.2).

Of the other phaeopigments, phytin-*a* was only detected in seven samples of which five of the samples were from site 39 and there was between 6 - 38 times more chlide-*a* at site 22 than the other sites, indicating that there was a combination of predation and senescence processes at this offshore site compared to the other sites.

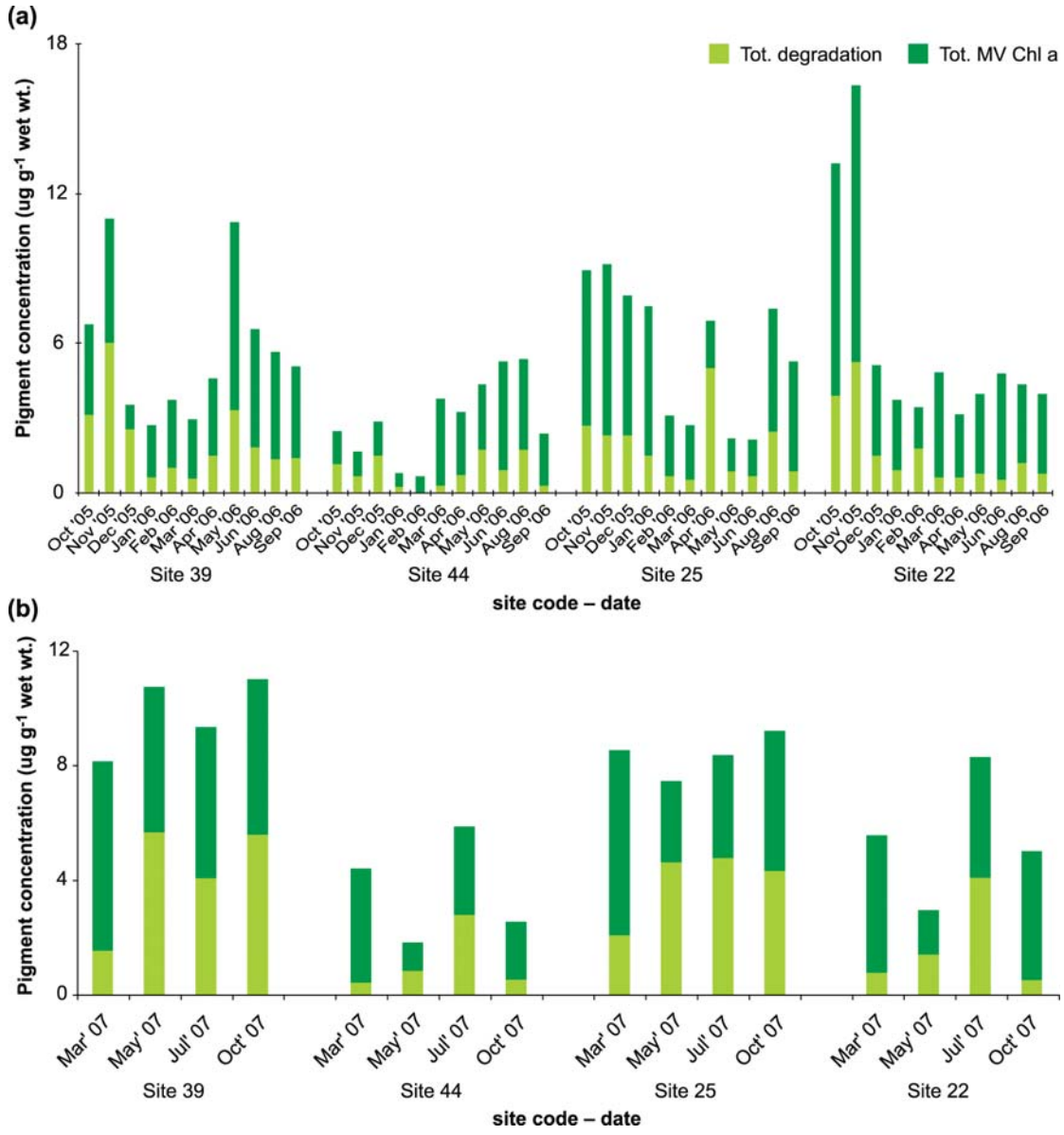

Figure 8.7. The proportion of "living" biomass (as indicated by total MV chlorophyll-*a*) and "non-living" biomass (as indicated by the total of degradation pigments) for MPB samples collected (a) monthly during 2005/06 and (b) quarterly during 2007, from sites 22, 25, 39 and 44.

Phaeopigments were not detected in any of the 796 water column samples collected during the first year (2005/06) of the study (refer chapter 7), suggesting that there wasn't heavy grazing of the pelagic microalgae and the dominance of the pphide-*a* in the MPB samples is primarily a result of grazing on the benthic diatoms. The routine observance of astaxanthin in all MPB samples from sites 25, 39 and 44 also suggests that the grazers were likely to be benthic copepods (Buffan-Dubau et al., 1996), although the carapaces of dead copepods and faecal matter settling from the water column would also contribute to the phaeopigment

concentration in the MPB samples. Astaxanthin was only rarely observed in the samples from the offshore site, 22, confirming that there were different degradation processes occurring at this site.

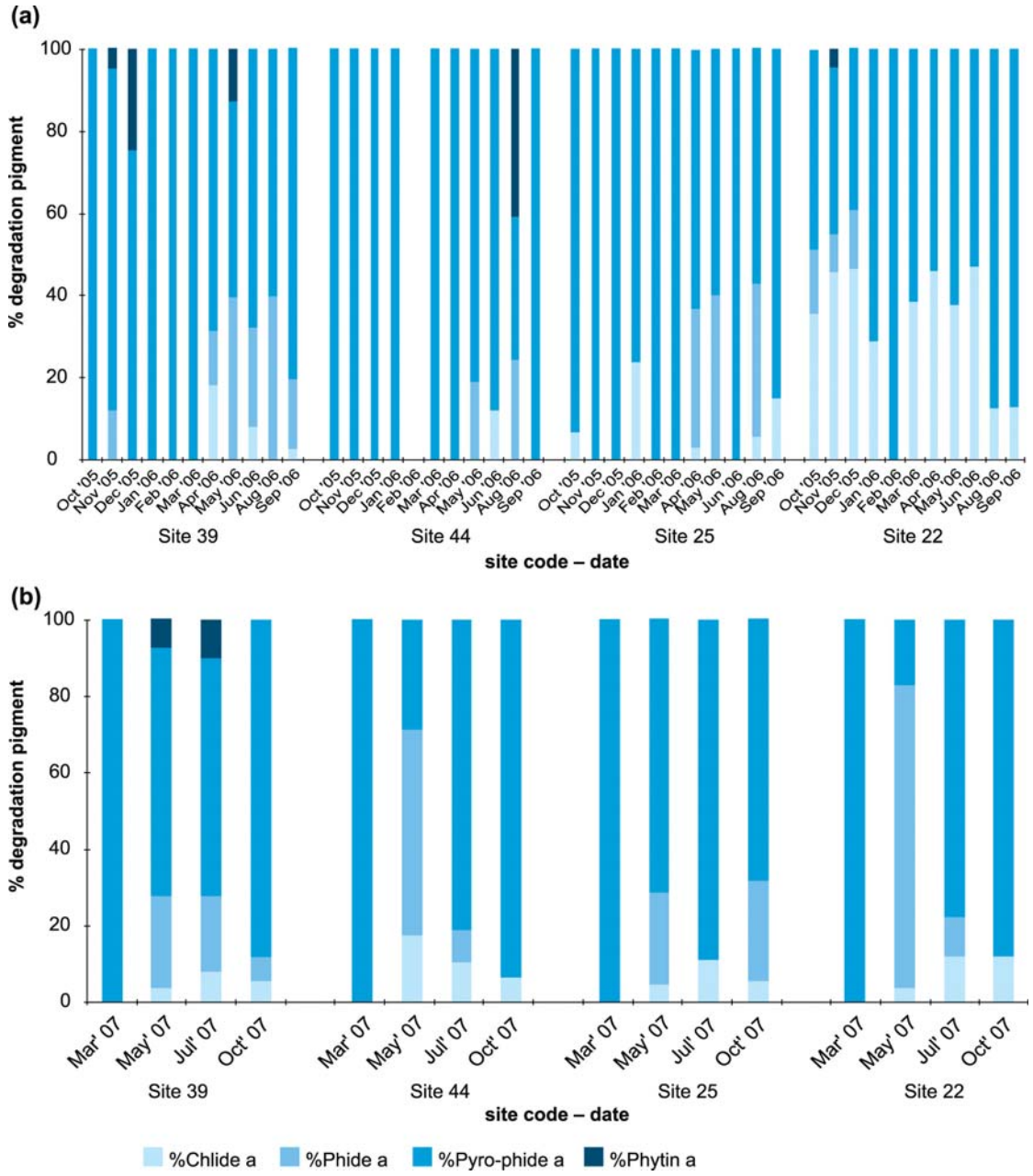

Figure 8.8. The proportion of different degradation pigments for MPB samples collected (a) monthly during 2005/06 and (b) quarterly during 2007 from sites 22, 25, 39 and 44.

8.3.5. Benthic algal resting stages in harmful algal blooms

Some phytoplankton form resting stages as part of their life cycle and as non-motile, dormant cells they are found in the benthos. Resting stages, particularly the robust resting cysts formed as part of a sexual life cycle in some dinoflagellates and other microalgae, can remain viable for many years, even under anoxic conditions, acting as a reservoir for seeding the phytoplankton population (Blackburn and Parker, 2005). Resting stages either germinate when an endogenous dormancy period has passed, when environmental conditions are

conducive to growth, or when a catastrophic event such as a storm stirs up sediments bringing the resting cells to the sediment surface or resuspends them in the water column.

Bolch (1997) surveyed the Boston Bay area and surrounds for resting cysts and found extensive cyst beds, primarily inshore around Boston Bay along with one site close to the northern side of Boston Island (near to Site 44 in the present study). The toxic harmful algal bloom (HAB) forming dinoflagellate *Gymnodinium catenatum* as well as another similar but, smaller *Gymnodinium* sp. made up more than 15% of the cyst population in the sediments at the latter site. Sediments identified with moderate to high cyst populations tended to be coarse to medium sandy sediments, sometimes including fine clay on top. Fernandes et al. (2006) found coarse to medium grained sediments widespread in south-west Spencer Gulf including outer areas not surveyed by Bolch (1997). However, the tendency for the cyst 'hot spots' to be close to the shore indicates wave protected areas are potentially better for cyst accumulation.

From the pigment composition reported in this study for the top 2 mm of sediment, the diagnostic pigment for dinoflagellates – peridinin, was not observed in any samples, however this does not preclude the presence of dinoflagellate resting stages or cysts in the benthos at the sites sampled. The resting stages of dinoflagellates and other phytoplankton generally have thicker cell walls than those of living cells. Extraction of cysts for pigment analysis would therefore require vigorous disruption, such as grinding of the sample to fully extract the pigments and this was not done in this study. However, *G. catenatum* has been below detection in the water column in south-west Spencer Gulf between 1999 and 2007 (TBOASA data and the present study), and along with other potential HAB forming species, the cyst beds within the study area appear not to translate to HAB development, or even significant presence in the phytoplankton community (refer chapter 7).

In April 1996 a mass mortality of farmed tuna co-occurred with storm conditions and with the presence of the ichthytoxic raphidophyte *Chattonella marina* at densities of 66,000 cells L^{-1} (Clarke 1996; Hallegraeff et al. 1998; Munday and Hallegraeff 1998), although it is not known if they played a role in the mortality event, which has been attributed to suspended sediment. Bolch (1997) was unable to confirm the presence of *Chattonella* cysts in south-west Spencer Gulf so that there is no evidence to date that *Chattonella* in the phytoplankton is seeded from cysts.

Other than the survey reported by Bolch (1997) there is a lack of information on the resting stages of phytoplankton commonly found in south-west Spencer Gulf. With the limited data available it seems that there is no direct relationship between the presence of cysts and the development of HABs. Nonetheless the presence of cysts as a seed source for blooms under unusual circumstances should not be discounted and if HABs do occur it would be advisable to check sediments for cysts.

8.3.6. Nutrient concentrations, water temperature and PAR

Concentrations of ammonia and phosphate in porewaters generally increased from the inshore site 44 to the offshore site 22 along the transect to the north of Boston Island, but were also relatively high at the inshore site 39 (Figure 8.9; refer chapter 4). Concentrations of ammonia were typically higher between January and June, peaking in February (Figure 8.9). This trend was more marked with distance from shore and at site 39. In contrast, there was little temporal variability for phosphate, except for one sample with a very high concentration collected in April at site 22. The replicate of this sample was lost and therefore we have no

means to ascertain the validity of this result. However, the same sample also showed a peak in ammonia, suggesting real values.

Since nutrient concentrations in porewaters were high, these will only be limiting for MPB growth if uptake is greater than diffusion to the surface. The availability of nitrogen was considered higher than phosphorus when N:P molar ratios were > 16, the ideal value for the growth of marine plankton (Redfield et al., 1963). For the inshore sites (39, 44), nitrogen matched or was in excess of phytoplankton requirements between December and May, while at the offshore sites (22, 25), N:P ratios were comparatively lower (Figure 8.10). Site 25, located centrally in the TFZ, had low ratios throughout the year, with the exception of a peak in February.

Site 22 showed a similar peak in February, with ratios remaining high until June. Overall, nitrogen concentrations in the sediment porewater were potentially limiting towards the end of the year between July and October, and abundant in the warmer months of the year and during the tuna farming season.

Nutrient concentrations in the water column were, as would be expected, much lower than the porewater concentrations (refer to chapter 7) with ammonia never exceeding 1 μM and phosphate always less than 0.5 μM. Silica concentrations were generally less than 1 μM except during January to March 2006 when concentrations peaked at around 2.5 - 4 μM at all sites. Water column silica concentrations showed no correlation with MPB biomass which suggests that silica in the porewaters was unlimited and therefore met the requirements of the benthic diatoms, allowing them to outcompete other algal groups and dominate the benthic community.

Water temperature at the bottom of the water column ranged from 13º C (July) to 21º C (January – March), which is similar to the range of 12 – 23º C found in a previous study in the area (Paxinos et al., 1996). Cibic et al. (2007a) observed during a study in the Gulf of Trieste, that, although diatoms dominated the benthos throughout the seasons, the species composition changed with changes in temperature, with the abundance of smaller cell size species increasing with decreasing temperature, over a range 6.4 to 25.5 ºC. Microscopic analysis of the benthos was not done during this study, however there was no correlation between bottom temperature and MPB biomass, nor was there any change in the fucoxanthin to chlorophyll-*a* ratio during the first year of the study. Changes in either of these parameters could suggest a change in species composition. The range of 13 – 21º C is probably therefore within the temperature tolerance of the dominant benthic diatom species within the study region, allowing them to persist year-round.

Light is considered by many studies to be the limiting factor in MPB community development and sustainability, especially in subtidal environments (Miles and Sundbäck, 2000; Cibic et al., 2007a). In this study, from PAR profiles collected during seven field trips (January – September 2006), the percent incident irradiance calculated at the sediment surface ranged from 4 – 28% at all sites, suggesting that the MPB was not light limited in the TFZ area. Other studies where light has been considered to be limiting have reported a strong positive correlation between PAR and MPB biomass (Cibic et al., 2007a). Such a relationship was not observed at any site in this study, confirming that light was not a limiting factor in MPB development. However, light may become limiting for short periods of time during storm events when resuspension of the sediment and the benthic microalgae into the water column can occur.

Table 8.2a. Percentages of chlorophyll-*a* and individual phaeopigments in samples from sites 22 and 25 (note pphytin-*a* is not in the table as it wasn't detected in any sample)

Site	Date	Total Chl-*a*	Total phaeo-pigments	% Chl-*a*	% Chlide-*a*	% Phide-*a*	% Pyrophide-*a*	% Phytin-*a*
22	Oct ' 05	9.325	3.853	70.76	10.34	4.65	14.25	0.00
	Nov' 05	11.107	5.196	68.13	14.47	2.95	12.98	1.47
	Dec' 05	3.669	1.452	71.65	13.09	4.08	11.18	0.00
	Jan' 06	2.845	0.870	76.58	6.73	0.00	16.69	0.00
	Feb' 06	1.677	1.722	49.33	0.00	0.00	50.67	0.00
	Mar' 06	4.233	0.571	88.12	4.53	0.00	7.35	0.00
	Apr' 06	2.545	0.565	81.84	8.32	0.00	9.84	0.00
	May' 06	3.228	0.735	81.44	6.95	0.00	11.61	0.00
	Jun' 06	4.304	0.496	89.67	4.83	0.00	5.50	0.00
	Aug' 06	3.179	1.164	73.20	3.32	0.00	23.48	0.00
	Sep' 06	3.219	0.705	82.03	2.27	0.00	15.70	0.00
	Mar' 07	4.801	0.779	86.04	0.00	0.00	13.96	0.00
	May' 07	1.562	1.411	52.53	1.54	37.75	8.18	0.00
	Jul' 07	4.212	4.090	50.73	5.75	5.14	38.37	0.00
	Oct' 07	4.496	0.528	89.49	1.23	0.00	9.27	0.00
25	Oct ' 05	6.263	2.656	70.23	1.90	0.00	27.87	0.00
	Nov' 05	6.859	2.279	75.06	0.00	0.00	24.94	0.00
	Dec' 05	5.619	2.240	71.50	0.00	0.00	28.50	0.00
	Jan' 06	5.998	1.431	80.74	4.51	0.00	14.75	0.00
	Feb' 06	2.440	0.607	80.09	0.00	0.00	19.91	0.00
	Mar' 06	2.208	0.468	82.53	0.00	0.00	17.47	0.00
	Apr' 06	1.907	4.970	27.73	1.98	24.63	45.65	0.00
	May' 06	1.359	0.821	62.35	0.00	14.96	22.69	0.00
	Jun' 06	1.504	0.636	70.29	0.00	0.00	29.71	0.00
	Aug' 06	4.937	2.386	67.41	1.73	12.17	18.69	0.00
	Sep' 06	4.431	0.841	84.04	2.34	0.00	13.62	0.00
	Mar' 07	6.455	2.096	75.49	0.00	0.00	24.51	0.00
	May' 07	2.828	4.641	37.86	2.60	15.01	44.53	0.00
	Jul' 07	3.604	4.778	43.00	6.09	0.00	50.91	0.00
	Oct' 07	4.879	4.332	52.97	2.39	12.33	32.30	0.00

Table 8.2b. Percentages of chlorophyll-*a* and individual phaeopigments in samples from sites 44 and 39 (note pphytin-*a* is not in the table as it wasn't detected in any sample)

Site	Date	Total Chl-*a*	Total phaeo-pigments	% Chl-*a*	% Chlide-*a*	% Phide-*a*	% Pyrophide-*a*	% Phytin-*a*
44	Oct ' 05	1.371	1.092	55.66	0.00	0.00	44.34	0.00
	Nov' 05	1.023	0.618	62.33	0.00	0.00	37.67	0.00
	Dec' 05	1.402	1.452	49.13	0.00	0.00	50.87	0.00
	Jan' 06	0.598	0.195	75.40	0.00	0.00	24.60	0.00
	Feb' 06	0.621	0.00	100.00	0.00	0.00	0.00	0.00
	Mar' 06	3.490	0.231	93.79	0.00	0.00	6.21	0.00
	Apr' 06	2.532	0.680	78.82	0.00	0.00	21.18	0.00
	May' 06	2.633	1.665	61.26	0.00	7.25	31.48	0.00
	Jun' 06	4.385	0.869	83.46	1.95	0.00	14.58	0.00
	Aug' 06	3.681	1.662	68.90	0.00	7.47	10.93	12.71
	Sep' 06	2.110	0.238	89.88	0.00	0.00	10.12	0.00
	Mar' 07	3.981	0.431	90.23	0.00	0.00	9.77	0.00
	May' 07	1.008	0.837	54.65	7.72	24.50	13.12	0.00
	Jul' 07	3.080	2.795	52.43	4.84	4.10	38.63	0.00
	Oct' 07	2.036	0.533	79.27	1.27	0.00	19.47	0.00
39	Oct ' 05	3.664	3.087	54.28	0.00	0.00	45.72	0.00
	Nov' 05	4.985	5.982	45.46	0.00	6.36	45.48	2.71
	Dec' 05	0.994	2.503	28.43	0.00	0.00	53.82	17.75
	Jan' 06	2.108	0.567	78.82	0.00	0.00	21.18	0.00
	Feb' 06	2.721	0.972	73.67	0.00	0.00	26.33	0.00
	Mar' 06	2.403	0.537	81.75	0.00	0.00	18.25	0.00
	Apr' 06	3.144	1.465	68.21	5.68	4.23	21.87	0.00
	May' 06	7.564	3.254	68.92	0.00	11.85	14.36	3.87
	Jun' 06	4.751	1.788	72.66	2.14	6.63	18.57	0.00
	Aug' 06	4.345	1.276	77.30	0.00	8.98	13.72	0.00
	Sep' 06	3.716	1.325	73.71	0.61	4.47	21.20	0.00
	Mar' 07	6.620	1.544	81.09	0.00	0.00	18.91	0.00
	May' 07	5.080	5.672	47.25	1.75	12.70	34.25	4.05
	Jul' 07	5.277	4.082	56.39	3.33	8.70	27.22	4.37
	Oct' 07	5.429	5.602	49.22	2.67	3.21	44.90	0.00

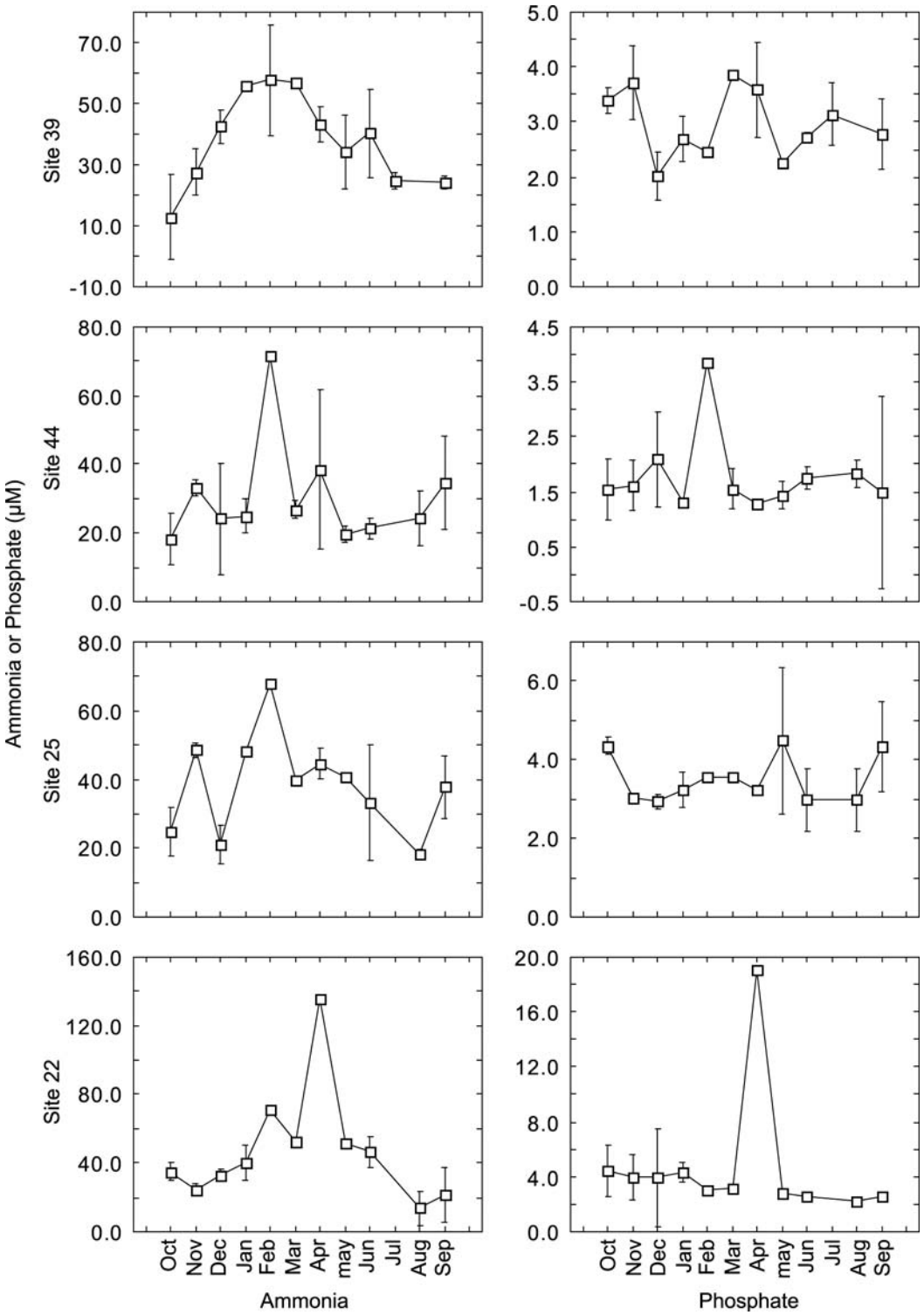

Figure 8.9. Mean monthly concentrations of ammonia (left column) and phosphate (right column) in porewaters collected monthly during 2005/06 from sites 22, 25, 39 and 44. Error bars indicate standard deviation.

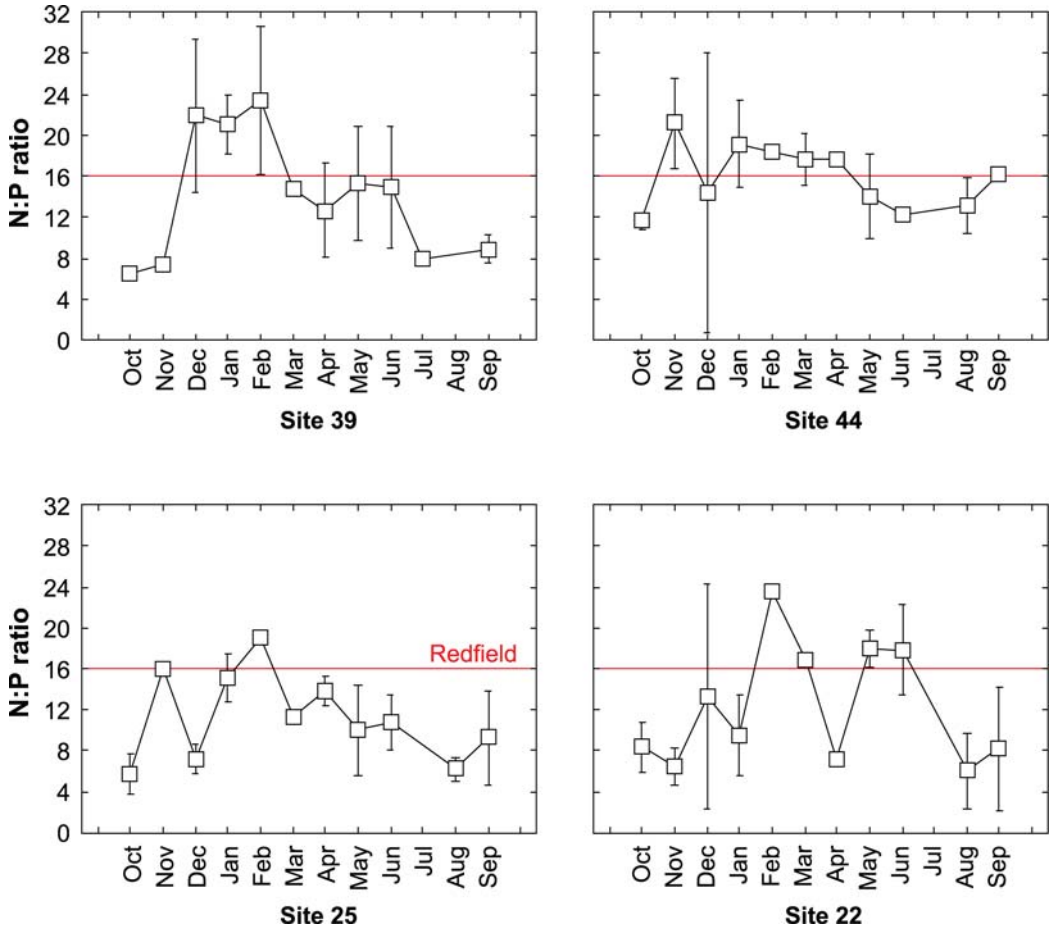

Figure 8.10. The N:P ratio in porewaters collected monthly during 2005/06 from sites 22, 25, 39 and 44. Error bars indicate standard deviation.

8.3.7. Sediment and wave characteristics

The continental shelf on which Spencer Gulf and the offshore TFZ are situated forms part of one of the largest cool-water carbonate facies in the world (Fuller et al., 1994). The sediment characteristics of the TFZ region have been previously discussed in Fernandes et al. (2006) and were further analysed during this study. All sites where MPB samples were collected, with the exception of site 25, formed part of a sediment survey grid, sampled in August 2005 (refer chapter 3). Sediment samples from all sites showed similar percentages of carbonate, N and P concentrations, however site 39 and 25 had elevated levels of organic carbon and porewater nutrients (Figures 3.18 – 3.25). These sites are located in a nutrient rich band of sediments (refer chapter 3) and the elevated organic carbon and porewater levels at site 39 are likely to be a result of the site's proximity to seagrass beds immediately west of Cape Donnington and to aquaculture activities located immediately south of Boston Island. Sediments in the area are typically a mix of very fine to fine sands with the grain size decreasing along the east-west transect from inshore to offshore (Figure 3.5). Average grain size at site 44 ranged between 170 – 250 μm due to the high tidal currents inherent to this area (Grzechnik, 2000), while at site 22 the range was 50 – 90 μm.

As the grain size decreases the sediment particles provide a greater surface area for adsorption of the MPB and the porewater nutrients, which may explain, in part, the significant difference for MPB biomass between the offshore and inshore sites.

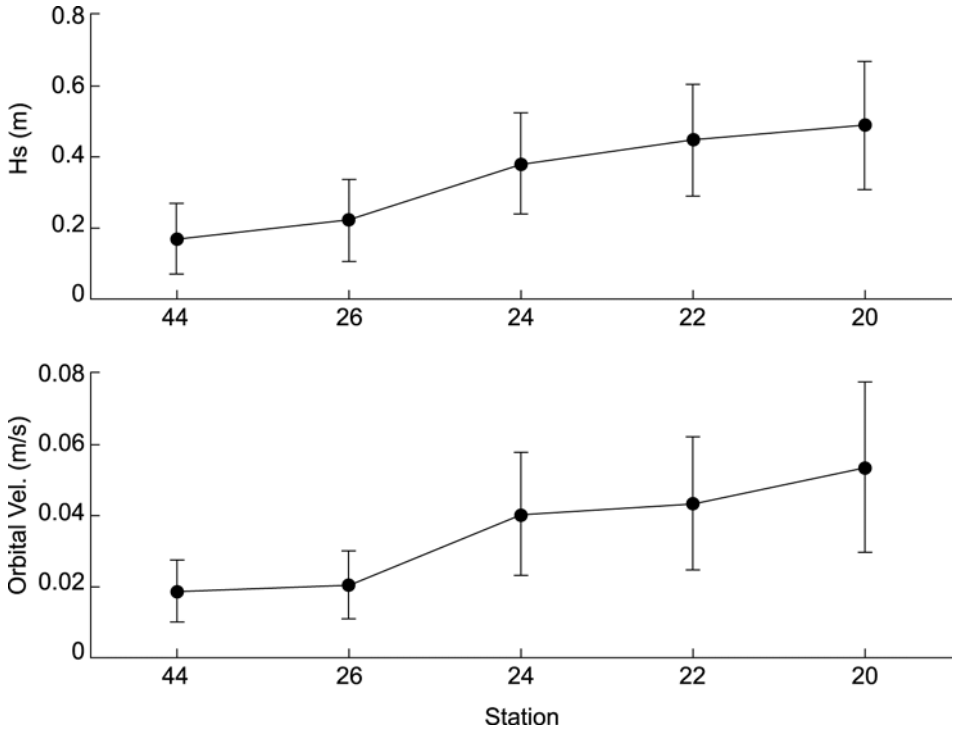

Figure 8.11. The variation of wave characteristics collected monthly during 2005/06 along the E-W transect. (a) the mean wave height (H_s) and (b) the orbital velocity at each site with ± standard deviation error bars.

Using the wave model described in chapter 2, model outputs were recorded at sites on the east-west transect (Figure 8.11). The mean wave height, along with other wave characteristics, varies along the transect by a factor of two (Figure 8.11). The inshore site (44) experiences significantly lower orbital velocities than the offshore site (22). Wave induced orbital velocities generate a thin bottom boundary layer where particles of sediment or benthic microalgae can be resuspended when a critical threshold shear stress is exceeded (refer chapter 3). Typical orbital velocities required to resuspend non-cohesive material in a bottom benthic layer are in the order of 0.08 – 0.12 m s^{-1}. The inshore sites rarely exceed this threshold, however the offshore sites could exceed this threshold during a particularly energetic weather event. During a storm event in mid-September 2005, the observed mean wave height near site 25 peaked at 1.0 m (refer chapter 2), however the effects of this event on the MPB community are unknown as it occurred a month prior to MPB sample collection.

8.4. Conclusion

MPB biomass and composition was measured for the first time in the TFZ and was found not to be limited by light as, on average, light penetration at the sediment surface generally exceeded 10% of incident irradiance. Areal values of MPB biomass were generally less than the depth integrated water column biomass, the exception being at the more offshore sites, 22 and 25, during October 2005 to January 2006. Given that MPB biomass can sometimes exceed that in the overlying water column, this group may play an important role in nutrient cycling. This importance can be assessed further using the biogeochmical model developed in chapter 10. A significant difference in the MPB biomass between inshore and offshore sites exits and is likely to be due to inshore/offshore differences in porewater nutrient concentrations (possibly related to tuna farming), sediment grain size and exposure to winds and waves. Pigment analysis indicated that the MPB community composition was consistently dominated by diatoms at all sites and throughout all seasons, suggesting that the

nutrient requirements of the diatoms were never limited, allowing this algal group to outcompete other algal groups in the benthic environment. The constant presence of the pigment astaxanthin together with high concentrations of the phaeopigment pyro-phaeophorbide-*a* suggests that at all sites except the offshore site (22), benthic diatoms were heavily grazed by copepods. At the offshore site the highest concentrations of chlorphyllide-*a* were observed indicating that grazing occurred in combination with other degradation processes.

Acknowledgements

The authors would like to thank Sonja Venema, Brenton Ebert, Bruce Miller-Smith, Yvette Eglington, Mandee Theil and Jeremy Barnett for sample collection; Gen Mount for sample preparation and database entry (SARDI Aquatic Sciences); Kate Berry and Pru Bonham (CMAR) for MPB analysis; Tina Hines for porewater nutrient analyses (Water Studies Centre, Monash University); Scott Foster (CMIS, Hobart) for statistical advice; Lea Crosswell (CMAR) for preparation of figures.

8.5. References

APHA-AWWA-WPCF 1998a. Method 4500-NH3-I. *In* Standard methods for the examination of water and wastewater, 20th edition, (L.S. Clesceri, AE. Greenberg and A.D. Eaton), Washington: American Public Health Association. pp 4 – 11.

APHA-AWWA-WPCF 1998b. Method 4500-PG. *In* Standard methods for the examination of water and wastewater, 20th edition, (L.S. Clesceri, AE. Greenberg and A.D. Eaton), Washington: American Public Health Association. pp 4 – 149.

Barranguet, C., Herman, P. M. J., and Sinke, J. J. 1997. Microphytobenthos biomass and community composition studied by pigment biomarkers: importance and fate in the carbon cycle of a tidal flat. *Journal of Sea Research*, 38, 59-70.

Blackburn, S. and Parker, N. 2005. Microalgal life cycles: Encystment and excystment. *In*: Algal Culturing Techniques, Andersen, R.A., (Ed.), Elsevier Academic Press, 399-417.

Bolch, C. 1997. Dinoflagellate cysts in sediments from Port Lincoln, Boston Bay and surrounds. *Appendix in*: Southern Bluefin Tuna (*Thunnus maccoyii*) Aquaculture Environmental Monitoring report 1996 - 1998. Clarke, S., Cartwright, C., Smith, B., Madigan, S., and Haskard, K. 1999. South Australian Research and Development Institute, Aquatic Sciences, 101 pp.

Buffan-Dubau, E., de Wit, R., and Castel, J. 1996. Feeding selectivity of the harpacticoid copepod *Canuella perplexa* in benthic muddy environments demonstrated by HPLC analyses of chlorine and carotenoid pigments. *Marine Ecology Progress Series*, 137**,** 71-82.

Cahoon, L. B., Beretich Jr., G. R., Thomas, C. J., and McDonald, A. M. 1993. Benthic microalgal production at stellwagen bank, Massachusetts Bay, USA. *Marine Ecology Progress Series*, 102**,** 179-185.

Cartaxana, P., Jesus, B., and Brotas, V. 2003. Pheophorbide and pheophytin *a*-like pigments as useful markers for intertidal microphytobenthos grazing by *Hydrobia ulvae*. *Estuarine Coastal and Shelf Science*, 58**,** 293-297.

Cartaxana, P., Mendes, C. R., van Leeuwe, M. A., and Brotas, V. 2006. Comparative study on microphytobenthic pigments of muddy and sandy intertidal sediments of the Tagus estuary. *Estuarine, Coastal and Shelf Science*, 66, 225-230.

Cibic, T., Blasutto, O., Falconi, C., and Umani, S. F. 2007a. Microphytobenthic biomass, species composition and nutrient avalability in sublittoral sediments of the Gulf of Trieste (northern Adriatic Sea). *Estuarine, Coastal and Shelf Science*, 75, 50-62.

Cibic, T., Blasutto, O., Hancke, K., and Johnsen, G. 2007b. Microphytobenthic species composition, pigment concentration, and primary production in sublittoral sediments of the trondheimsfjord (Norway). *Journal of Phycology*, 43, 1126-1137.

Clarke, S.M. 1996. Tuna mortalities: April-May 1996. South Australian Research and Development Institute, Adelaide, 20pp.

Clarke, S., Cartwright, C., Smith, B., Madigan, S., and Haskard, K. 1999. Southern Bluefin Tuna (*Thunnus maccoyii*) Aquaculture Environmental Monitoring report 1996 - 1998. South Australian Research and Development Institute, Aquatic Sciences, 101 pp.

Clarke, S., Madigan, S., Edwards, J., Mathews, C., Preece, P., and Haskard, K. 2000. Southern Bluefin Tuna (*Thunnus maccoyii*) Aquaculture Environmental Monitoring report 1999 - 2000. South Australian Research and Development Institute, Aquatic Sciences.

Fernandes, M., Cheshire, A., and Doonan, A. 2006. Sediment geochemistry in lower Spencer Gulf, South Australia: implications for southern bluefin tuna farming. *Australian Journal of Earth Sciences*, 53, 421-432.

Fernandes, M., Lauer, P., Cheshire, A. and Angove, M. 2007. Preliminary model of nitrogen loads from southern bluefin tuna aquaculture. *Marine Pollution Bulletin*, 54, 1321-1332.

Forehead, H.I. 2006. The ecology and biogeochemistry of sandy sediments in the warm temperate coastal waters of Western Australia. Ph.D thesis, University of Western Australia, School of Plant Biology, pp. 133.

Fuller, M.K., Bone, Y., Gostin, V.A., and von der Borch, C.C. 1994. Holocene cool-water carbonate and terrigenous sediments from southern Spencer Gulf, South Australia. *Australian Journal of Earth Sciences*, 41, 353-363.

Grinham, A. R., Carruthers, T. J. B., Fisher, P. L., Udy, J. W., and Dennison, W. C. 2007. Accurately measuring the abundance of benthic microalgae in spatially variable habitats. *Limnology and Oceanography: Methods*, 51, 19-125.

Grzechnik, M. P. 2000. Three dimensional tide and surge modelling and layered particle tracking techniques applied to southern Australian coastal seas., The University of Adelaide**:** 207.

Hallegraeff, G.M., Munday, B.L., Baden, D.G. and Whitney, P.L. 1998. *Chattonella marina* Raphidophyte bloom associated with mortality of cultured bluefin tuna (*Thunnus maccoyii*) in South Australia. *In*: Harmful Algae, reguera, B., Blanco, J., Fernandez, M.L. and Wyatt, T., (Eds.), Xunta de Galicia and IOC of UNESCO, Spain, 93-96.

Head, E. J. H. and Harris, L. R. 1992. Chlorophyll and carotenoid transformation and destruction by *Calanus* spp. grazing on diatoms. *Marine Ecology Progress Series*, 86, 229-238.

Herzfeld, M., Middleton, J.F., Andrewartha, J.R., Luick, J. and Wu, L. (2008) Numerical Hydrodynamic Modelling of the tuna farming zone, Spencer Gulf. Technical report, Aquafin CRC Project 4.6, FRDC Project 2005/059. Aquafin CRC, Fisheries Research & Development Corporation and South Australian Research & Development Institute (Aquatic Sciences), Adelaide. SARDI Publication No F2008/000745-1, SARDI Research Report Series No 342, 100 pp.

Jeffrey, S.W., and Vesk, M. 1997. Introduction to marine phytoplankton and their pigment signatures. *In*: Phytoplankton Pigments in Oceanography: guidelines to modern methods, Jeffrey, S.W., Mantoura, R.F.C., Wright, S.W., (Eds.), UNESCO Publishing, 37-84.

Jeffrey, S.W., and Wright, S.W. 2006. Photosynthetic pigments in marine microalgae: insights from cultures and the sea. *In:* Algal Cultures, Analogues of Blooms and Applications, Subba Rao, D.V., (Ed.), Science Publishers, 33 - 90.

Kendrick, G. A., Langtry, S., Fitzpatrick, J., Griffiths, R., and Jacoby, C. A. 1998. Benthic microalgae and nutrient dynamics in wave-disturbed environments in Marmion Lagoon, Western Australia, compared with less disturbed mesocosms. *Journal of Experimental Marine Biology and Ecology*, 22, 883-105.

Longphuirt, S. N., Leynaert, A., Guarini, J.-M., Chauvaud, L., Claquin, P., Herlory, O., Amice, E., Huonnic, P., and Ragueneau, O. 2006. Discovery off microphytobenthos migration in the subtidal zone. *Marine Ecology Progress Series*, 32, 8143-154.

Lotocka, M. and Styczynska-Jurewicz, E. 2001. Astaxanthin, canthaxanthin and astaxanthin esters in the copepod *Acartia bifilosa* (Copepoda, Calanoida) during ontogenetic development. *Oceanologia*, 43, 487-497.

Louda, J. W., Li, J.; Liu, L., Winfree, M. N., and Baker, E. W. 1998. Chlorophyll-*a* degradation during cellular senescence and death. *Organic Geochemistry*, 29, 1233-1251.

Louda, J. W., Liu, L., and Baker, E. W. 2002. Senescence- and death-related ateration of chlorophylls and carotenoids in marine phytoplankton. *Organic Geochemistry*, 33, 1635-1653.

MacIntyre, H. L. and Cullen, J. J. 1995. Fine-scale vertical resolution of chlorophyll and photosynthetic parameters in shallow-water benthos. *Marine Ecology Progress Series*, 122, 227-237.

MacIntyre, H. L., Geider, R. J., and Miller, D. C. 1996. Microphytobenthos: The ecological role of the "secret garden" of unvegetated, shallow-water marine habitats. I. Distribution, abundance and primary production. *Estuaries*, 19, 186-201.

Miles, A. and Sundbäck, K. 2000. Diel variation in microphytobenthic productivity in areas of different tidal amplitude. *Marine Ecology Progress Series*, 205, 11-22.

Montani, S., Magni, P., and Abe, N. 2003. Seasonal and interannual patterns of intertidal microphytobenthos in combination with laboratory and areal production estimates. *Marine Ecology Progress Series*, 249, 79-91.

Moreno, S. and Niell, F. X. 2004. Scales of variability in the sediment chlorophyll content of the shallow Palmones River Estuary, Spain. *Estuarine, Coastal and Shelf Science*, 60, 49-57.

Munday, B.L. and Hallegraeff, G.M. 1998. Mass mortality of captive southern Bluefin tuna (*Thunnus maccoyii*) in April/May 1996 in Boston Bay, South Australia: A complex diagnostic problem. *Fish Pathology*, 33, 93-96.

Nelson, J. R., Eckman, J. E., Robertson, C. Y., Marinelli, R. L., and Jahnke, R. A. 1999. Benthic microalgal biomass and irradiance at the sea floor on the continental shelf of the South Atlantic bight: spatial and temporal variability and storm effects. *Continental Shelf Research*, 19, 477-505.

Paxinos, R., Clarke, S. M., and Matsumoto, G. I. 1996. Phytoplankton dynamics of Boston Bay, South Australia. South Australian Research and Development Institute, Aquatic Sciences, 23 pp.

Redfield, A.C., Ketchum, B.H. and Richards, F.A. 1963. The influence of organisms on the composition of seawater. In M.N. Hill, The Sea, Vol. 2., pp. 26-77. New York: Interscience.

Reiss, H., Wieking, G., and Kröncke, I. 2007. Microphytobenthos of the Dogger Bank: a comparison between shallow and deep areas using phytopigment composition of the sediment. *Marine Biology*, 150, 1061-1071.

Stauber, J. L. and Jeffrey, S. W. 1988. Photosynthetic pigments in fifty-one species of marine diatoms. *Journal of Phycology*, 24, 158-172.

Totti, C. 2003. Influence of the plume of the River Po on the distribution of subtidal microphytobenthos in the Northern Adriatic Sea. *Botanica Marina*, 46, 161-178.

Van Heukelem, L. and Thomas, C. 2001. Computer assisted high-performance liquid chromatography method development with applications to the isolation and analysis of phytoplankton pigments. J. Chromatogr. A., 910, 31-49.

Varela, M. and Penas, E. 1985. Primary production of benthic microalgae in an intertidal sand flat of the Ria de Arosa, NW Spain. *Marine Ecology Progress Series,* 25, 111-119.

Yamaguchi, H., Montani, S., Tsutsumi, H., Hamada, K.-I, Ueda, N., and Tada, K. 2007. Dynamics of microphytobenthic biomass in a coastal area of western Seto Inland Sea, Japan. Estuarine, *Coastal and Shelf Science*, 75, 423-432.

Chapter 9: Plankton Ecology: Primary Production, Zooplankton Community Composition and Grazing

Paul van Ruth[1,4*], Pru Bonham[2,4], Emlyn Jones[3,4], Peter Thompson[2,4]

[1]SARDI Aquatic Sciences, PO Box 120, Henley Beach SA 5022
[2]CSIRO Division of Marine and Atmospheric Research
[3]Flinders University of South Australia, GPO Box 2100, Adelaide SA 5001
[4]Aquafin CRC

*corresponding author, Phone: +61 (8) 8207 5421, Email: vanruth.paul@saugov.sa.gov.au

Abstract

Seasonal variation in primary productivity, and zooplankton abundance and grazing were examined in the tuna farming zone (TFZ) in 2007. The highest rates of primary production in the TFZ occurred in March (~1200 mg C m^{-2} day^{-1}), in the lead up to the autumn phytoplankton peak that has been identified as a regular occurrence in the region. Highest phytoplankton growth rates occurred during May, at the height of the autumn phytoplankton peak. Peak micro-zooplankton abundance and biomass also occurred during May, with micro-zooplankton grazing ~70% of phytoplankton standing stock d^{-1} during this period. Peak meso-zooplankton abundance and biomass occurred during March, with ~300% of phytoplankton standing stock grazed by meso-zooplankton d^{-1} at this time. Meso-zooplankton grazing impact fell to ~30% of standing stock d^{-1} in May.

9.1. Introduction

Primary productivity and zooplankton grazing are important processes governing the flux of carbon and other nutrients through marine ecosystems. An understanding of these processes can provide important information for the management and conservation of ecologically and economically important species.

Primary production is the rate at which phytoplankton photosynthesise (i.e. take up carbon and convert it into organic matter). Along with carbon, the phytoplankton are expected to take up nitrogen (in a range of potential forms such as NO_3^-, NO_2, NH_4^+, N_2, organic N); phosphorus and other nutrients required for growth. In pelagic ecosystems these processes dominate biogeochemical transformations and are typically high when phytoplankton growth is high. Primary productivity is primarily affected by the availability of nutrients and light (Olivieri and Hutchings 1987; Daneri et al. 2000). Photosynthetic rates are generally measured across a range of irradiances and the rates modelled as a function of irradiance to give two photosynthetic parameters: 1) the maximum photosynthetic rate per unit phytoplankton, P^B_{max}; and 2) the initial slope of the irradiance versus carbon fixation curve, alpha (α). These two parameters can be used to integrate primary production across depths and times and to compare across ecosystems.

Understanding the distribution and community dynamics of the zooplankton is also important when examining the fate of marine primary production and the flux of carbon through marine ecosystems. As primary consumers, zooplankton form an important link between primary producers and higher trophic levels, effectively repackaging autotrophic carbon into larger particles which are more readily available to secondary consumers and beyond (Swadling et al. 1997; Clarke et al. 2001). In the last few decades numerous studies have demonstrated that microzooplankton (<200μm body length) consisting of heterotrophic protists including flagellates, ciliates, heterotrophic dinoflagellates, microcrustaceans, sarcodines and small metazoans (Capriulo et al. 1991) play a significant role in the consumption of phytoplankton. The proportion of the phytoplankton grazed varies in relation to the density and composition of both the phytoplankton and microzooplankton population (Martin 1970; Lampert and Taylor 1985; Turner and Graneli 1992), with a worldwide average of ~ 60% of new production grazed by microzooplankton on a daily basis (Calbet and Landry 2004), although sometimes grazers consume ≥100% of the daily primary production (e.g. Burkill et al. 1987; Froneman et al. 1996; James and Hall 1998). It has also been suggested that microzooplankton not only control the biomass of the phytoplankton community but may also control the growth of certain algal populations by selective grazing (Burkill et al. 1987; Strom and Welschmeyer 1991) and the regeneration of nutrients (Probyn 1987). Selective grazing and short generation times are thought to allow microzooplankton to play a significant role in structuring plankton communities and determining the fate of phytoplankton production (Michaels and Silver 1988; Strom and Strom 1996; Wassmann 1998).

Mezo-zooplankton (200-20,000μm body length) grazing of phytoplankton may also play a significant role in controlling the flux of carbon through marine ecosystems, possibly preventing blooms. Meso-zooplankton grazing impact has been estimated to be 5-55% of primary productivity in highly productive, upwelling-influenced waters (Verheye et al. 1992; Landry 1994; Gonzalez et al. 2000). In less productive oligotrophic waters, with food webs driven by pico-phytoplankton which are too small to be effectively grazed by meso-zooplankton (Hewes et al. 1985; Hansen et al. 1994; Roman and Gauzens 1997; Sautour et al.

2000), meso-zooplankton grazing impact may be reduced. In these waters, micro-zooplankton may become an important source of food for the meso-zooplankton in the absence of other suitably sized food particles (Calbet and Landry 1999; Roman et al. 2000; Nejstgaard et al. 2001).

A study of spatial and temporal variation in primary productivity and zooplankton ecology was made in the tuna farming zone (TFZ, Figure 9.1). To our knowledge, this study represents the first ever estimates of zooplankton grazing anywhere in Spencer Gulf. Based upon studies elsewhere, we can be confident that the growth of phytoplankton and their consumption by grazers are the most important fluxes of nutrients (nitrogen and phosphorus) in this ecosystem. As such, they have an important role in the nutrient balance for the region including the transformation and fate of any nutrients added to the environment through activities such as aquaculture.

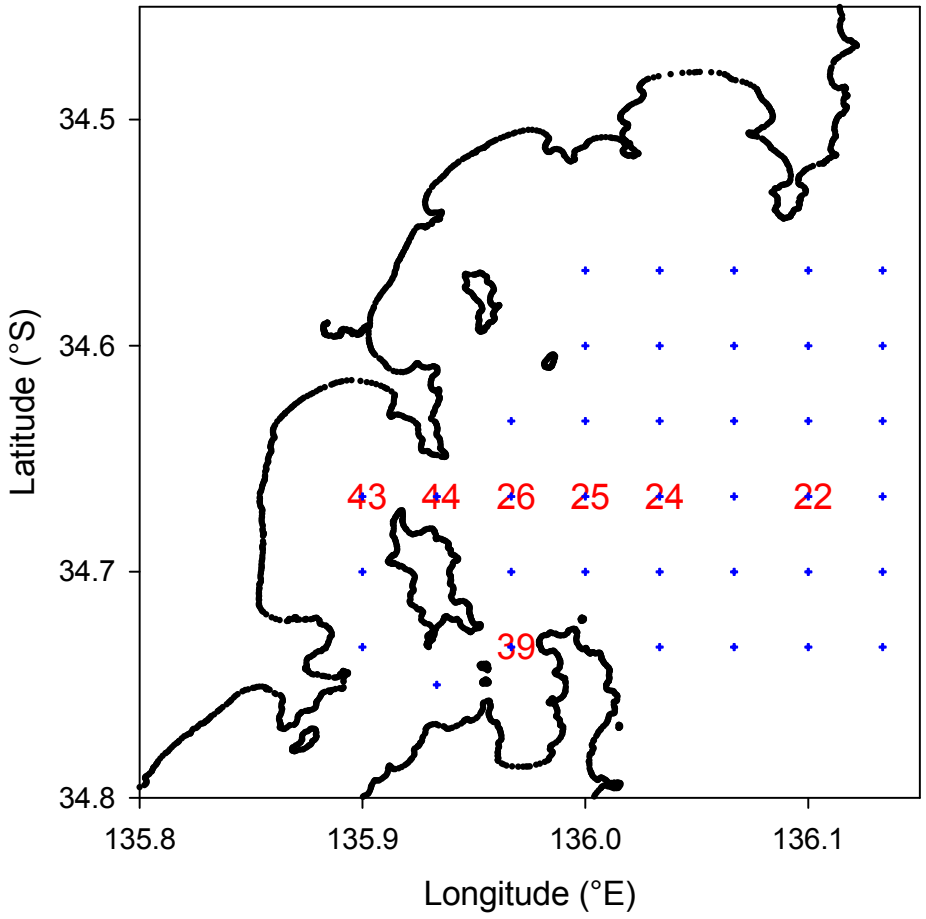

Figure 9.1. Map of sampling sites for plankton ecology. The ADCP was moored at site 24 in July 2007.

9.2. Methods

Experiments on phytoplankton primary production in the TFZ were conducted during March, May, July, and October 2007 using surface water collected from sites 22, 25, and 44 (Figure 9.1.) with a Niskin bottle. Full methods are described in Van Ruth et al 2008. The procedure used methods outlined by Parsons et al. (1984), Lohrenz et al. (1992), and Mackey et al. (1995), with 7 irradiance levels including: 0% (dark), 0.4%, 1.2%, 1.5%, 6.5%, 50%, and 100% of natural sunlight. Three replicate 250 ml bottles were prepared for each irradiance.

$NaH^{14}CO_3$ (20 μCi) was added and bottles were then incubated for 24 hours at *in-situ* water temperatures. After filtering through *Whatman* GF/F filters at low vacuum pressure, 200μl of 5N HCl was used to drive off any unfixed inorganic carbon. Four mL of scintillation fluid (Ultima Gold high flashpoint LSC cocktail) was then added to each vial and, after 24 hours, radioactivity was determined as disintegrations per minute using a scintillation counter (Packard Tricarb 2100TR). Total CO_2 concentration in each sample was estimated from salinity using the method of Parsons et al. (1984). Measured photosynthetic rates were fit to the hyperbolic tangent equation of Jassby and Platt (1976) to provide estimates of photosynthetic efficiency (α), maximum biomass specific photosynthetic rates (P^B_{max}), and irradiances corresponding to the onset of light saturation of photosynthesis (I_k). These data were used to examine spatial and temporal variation in daily integral productivities in the TFZ, which were modelled using Talling's model (Talling 1957).

Water samples for microzooplankton grazing experiments were collected on March 5 and 7, and July 9-10, 2007 from both sites 25 and 44, and on May 9 and October 19 from site 25 alone (Figure 9.1). Samples were incubated for ~ 24 hours to determine grazing as per Van Ruth et al. (2008). Silicate, nitrate, nitrite and phosphate samples were also analysed, as were pigment concentrations and phytoplankton and micro-zooplankton abundances (Van Ruth et al. 2008).

Meso-zooplankton samples were collected at site 26 (Figure 9.1). Zooplankton samples were collected at six hour intervals (0600, 1200, 1800, 2400 hours) on one day in each sampling month (March, May, July, December 2007). Two size fractions were measured (> 500 μm and > 150 μm). PERMANOVAs (two-way factorial model, Sorensen distance measure, 4999 permutations) were performed on data for both size fractions, using methods outlined in Anderson (2001) to examine the effect of month and sampling time on community structure in south-west Spencer Gulf, with a significance value of 0.05. An Acoustic Doppler Current Profiler (ADCP) was also used to investigate patterns in zooplankton abundance during July 2007. Mesozooplankton grazing pressure was estimated from biomass using equations in Huntley and Boyd (1984) and Conover (1978).

9.3. Results

9.3.1. Primary Production

A single example of the photosynthetic rates as determined in July 2007 is shown (Figure 9.2). The data show a typical response to irradiance rising rapidly to a plateau. In July the offshore site (22) had less primary production than the sites closer to shore (25, 44). The model output agrees well with the observations. Data from other sampling times were very similar.

The photosynthetic parameters (P^B_{max} and α) showed a high degree of spatial and temporal variation. Generally P^B_{max} and α were greatest in March 2007, decreasing steadily to be lowest in October 2007 (Figure 9.3). A pattern of increasing P^B_{max} and α with distance from shore was evident in March 2007 but it had reversed by October. Over all observations, the mean ± standard deviation for alpha was 0.16 ± 0.19 mg C (mg Chl*a*)$^{-1}$ h^{-1} (μmol photons m^{-2} s^{-1})$^{-1}$, while the mean value for P^B_{max} was 2.6 ± 2.2 mg C (mg Chl*a*$^{-1}$) h^{-1}.

Daily integrated (from surface to bottom) productivity was greatest in March 2007 (Figure 9.4). By May productivity was already falling and by July 2007 it had decreased substantially to ~ 30-40% of March rates (Figure 9.4). Productivity further declined into October 2007 to

be ~ 20% of the productivity observed during March 2007. Spatial patterns in daily integral productivity indicated lower levels near shore at site 44 and substantially greater levels at site 25. The turnover time for phytoplankton was estimated to be longest during the autumn phytoplankton peak, requiring 3 days for gross primary production to replace the standing stock of phytoplankton during May (Figure 9.4). At all other times turnover times were faster. The converse was true for estimated gross phytoplankton growth rates, which were greatest in March, falling throughout winter and rising again in October (Figure 9.4).

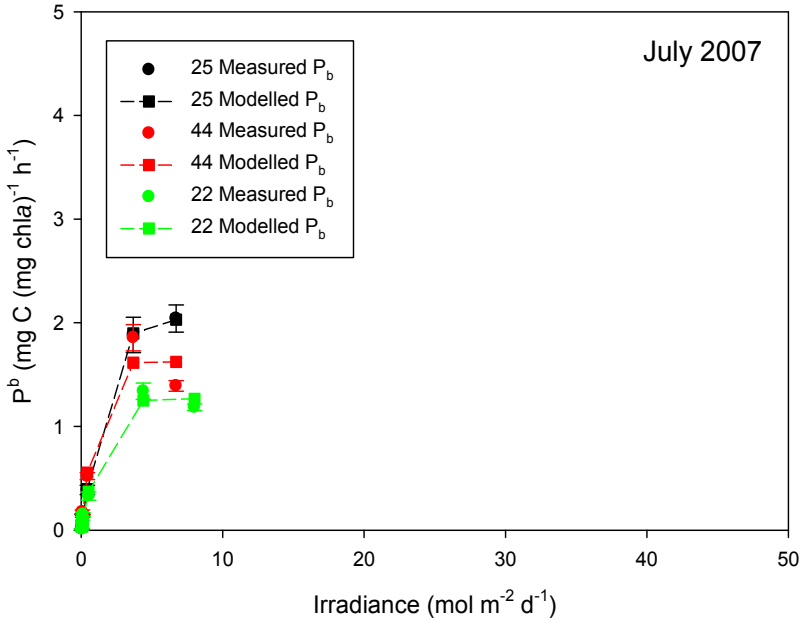

Figure 9.2. Spatial variation in phytoplankton photosynthesis-irradiance characteristics in the TFZ in July 2007 (see Figure 9.1 for site locations). Circles indicate mean measured values ± standard error, n = 3.

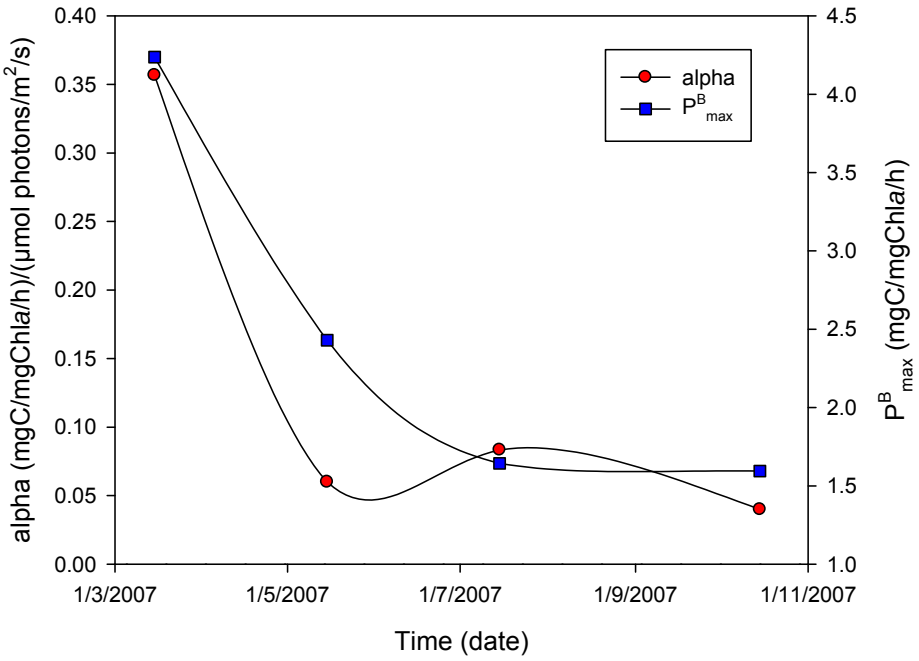

Figure 9.3. Photosynthetic parameters alpha (α) the initial slope of the photosynthesis versus irradiance relationship, and P^B_{max} the maximum photosynthetic rate.

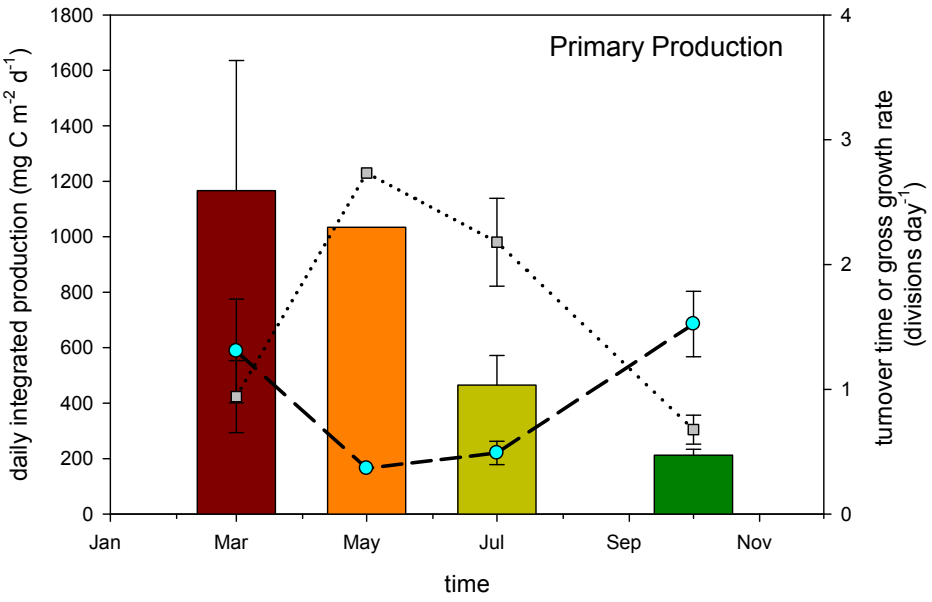

Figure 9.4. Daily integrated primary production (bars) for multiple sites in the TFZ from March 2007 to October 2007. Turnover times (TT) calculated as standing stock of chlorophyll-*a* /maximum photosynthetic rate (squares), the inverse (1/TT) as the gross phytoplankton growth rate (circles).

9.3.2. Microzooplankton Grazing

A single example of the results for chlorophyll-*a* from microzooplankton grazing experiments shows the estimated apparent growth rates for the 12 incubated bottles plotted against the fraction of unfiltered seawater (Figure 9.5). The grazing rate is the slope of this line (-0.8005 d^{-1}) and the gross phytoplankton growth rate is estimated from the intercept of this line with the y-axis (~ 1.2 d^{-1}).

The gross phytoplankton growth rates were always > 0.5 d^{-1} (Figure 9.6) except for site 44 in March. The highest gross rates in this study were observed in March and May and declined in June and October. A high degree of spatial variability was evident in the results with gross growth rates at the two sites (25, 44) being considerably different from each other in March and July.

The grazing rate of microzooplankton upon phytoplankton (*g)* at site 25 peaked in May and declined steadily until October (Figure 9.7). The inshore site (44) had very low grazing rates in July. Again considerable spatial variability was evident in the data as grazing rates at the two sites (25, 44) were considerably different from each other in March and July.

In summary, the net phytoplankton growth rates μ_n ($\mu_g - g$) were about ~0.4 d^{-1} in March at both sites, with greater grazing rates at site 44 leading to lower net phytoplankton growth at site 44 in March (Figure 9.8). In May and July, there were very low or zero net phytoplankton growth rates at both sites despite high initial chlorophyll-*a.* These results indicate ~ 100% of the new primary production by phytoplankton was being grazed by microzooplankton during May and July, and the autumn-winter peak was likely to subside as grazing was approximately equal to growth. In spring (October) the net growth had risen from that observed in mid winter, but was still only half that of the previous March. There was no evidence of a spring bloom from the net growth rates or the standing stock of phytoplankton biomass.

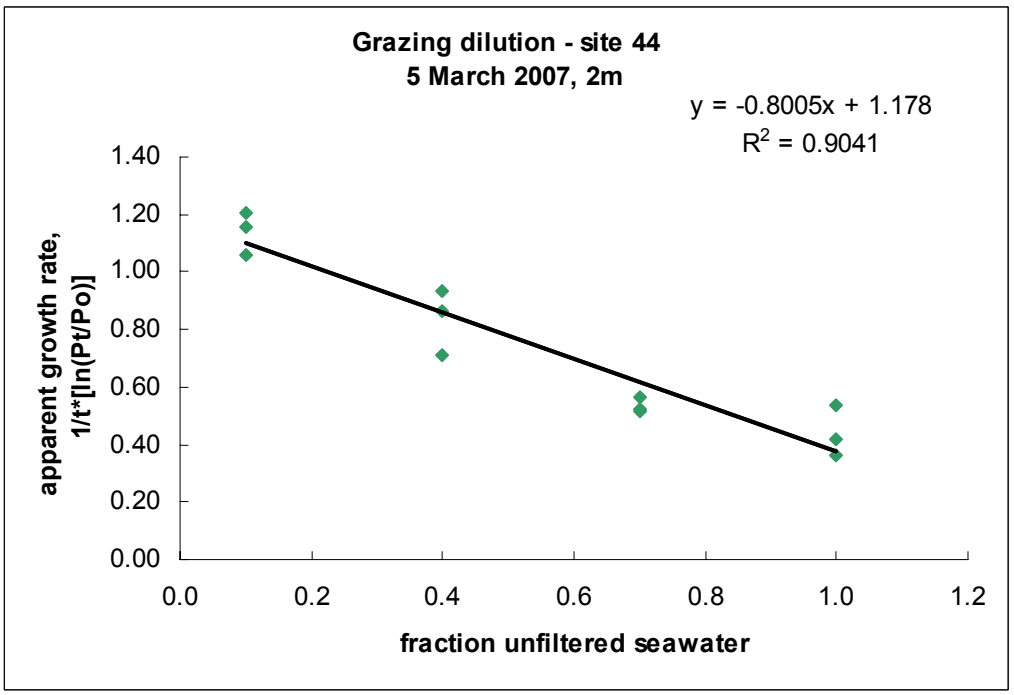

Figure 9.5. A single example of the experimental results showing the apparent growth rates of phytoplankton for the 12 incubated bottles plotted against the fraction of unfiltered seawater.

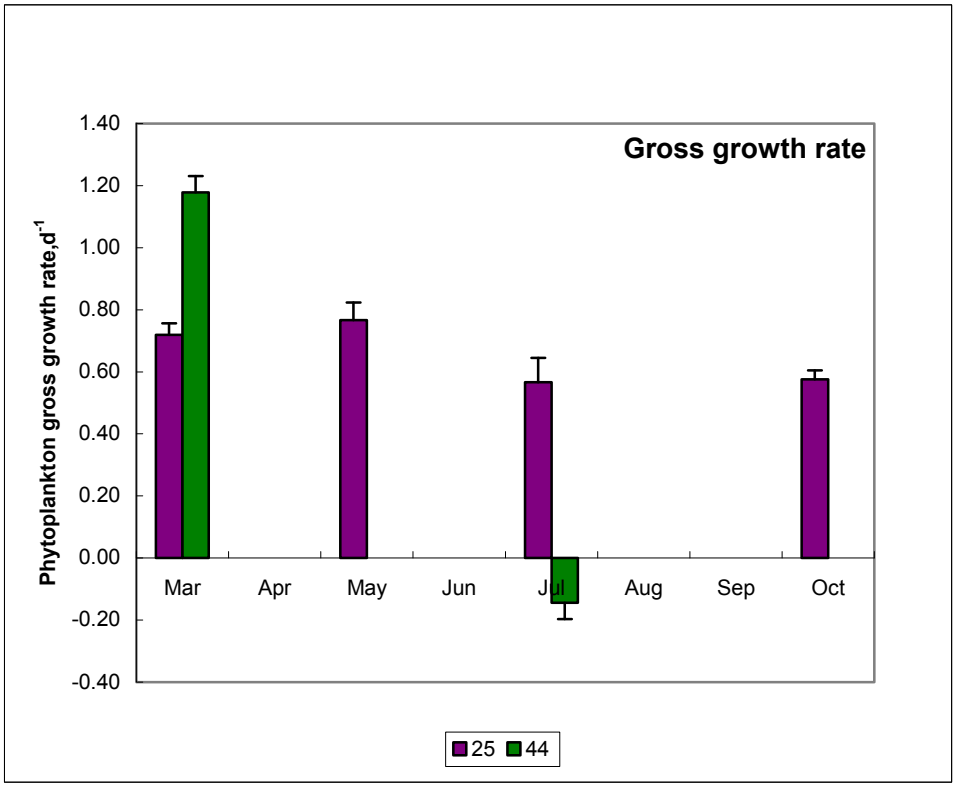

Figure 9.6. Summary of phytoplankton gross growth rates (μ_g) at sites 25 and 44 during 2007. Error bars indicate standard error.

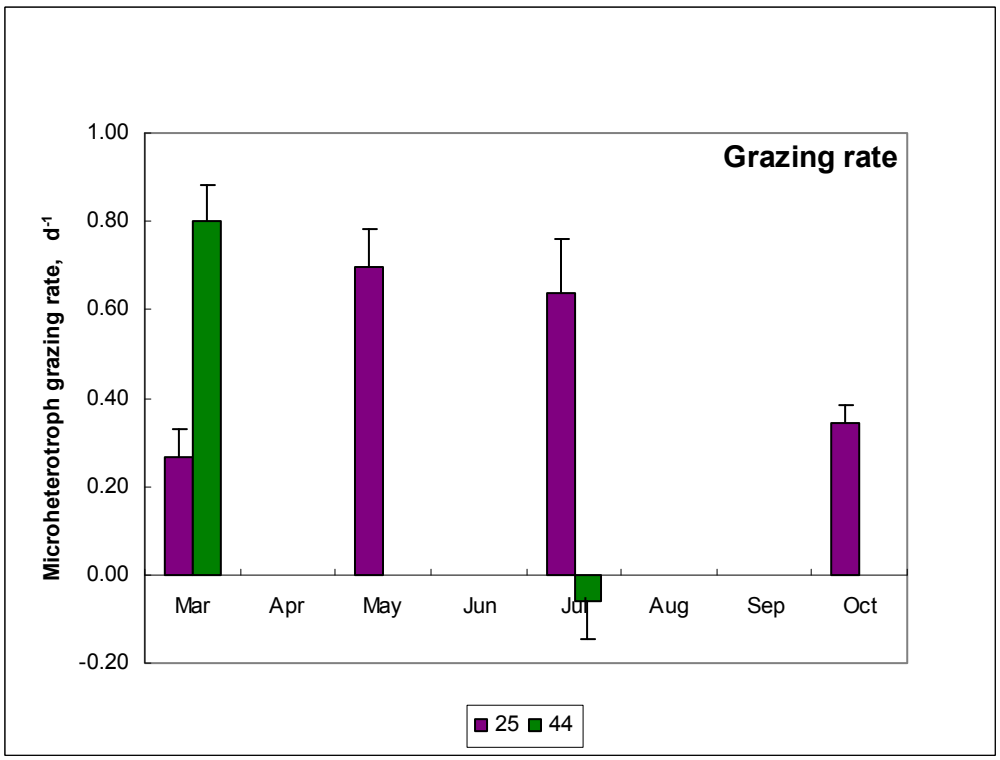

Figure 9.7. Summary of grazing rate (g) of microhetertrophs on phytoplankton at sites 25 and 44 during 2007. Error bars indicate standard error.

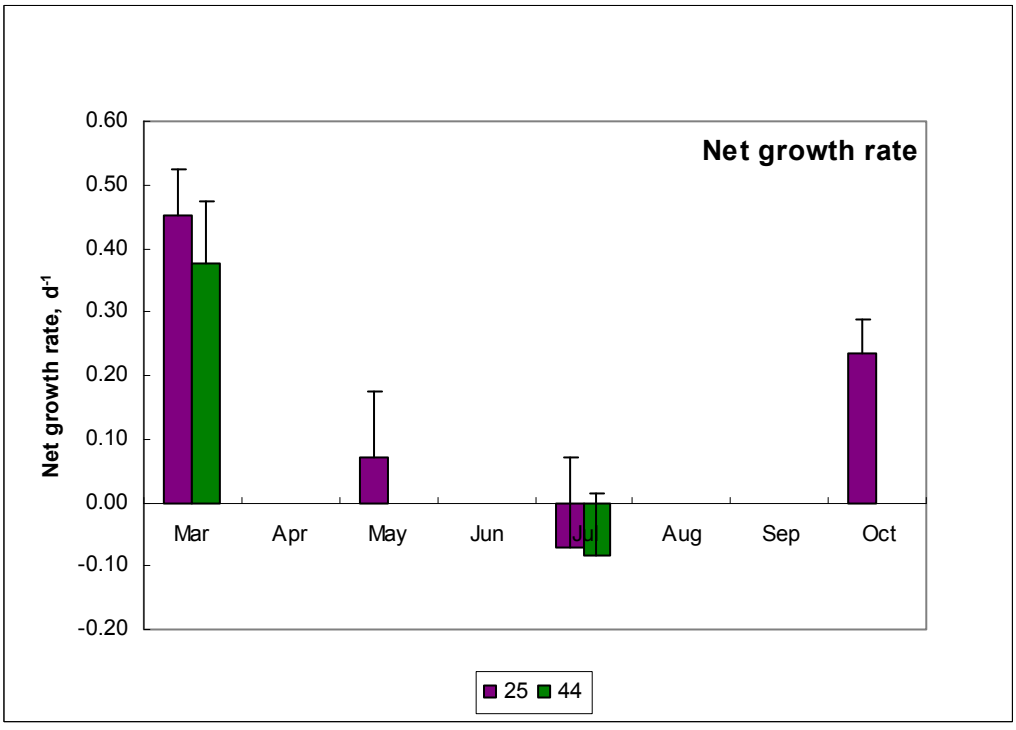

Figure 9.8. Net growth rates of phytoplankton (μ_n) at sites 25 and 44 during 2007. Error bars indicate standard error.

Net fucoxanthin-specific growth rates of phytoplankton tended to be greater than net prasinoxanthin-specific growth rates, suggesting diatoms were generally growing faster than prasinophytes (Figure 9.9a versus 9.9b).

Total microzooplankton densities were generally below about 1,500 cells L^{-1} except for higher ciliate counts in March and May (Figure 9.10). In May the microzooplankton counts were 2 to 3 times those of March. Generally aloricate, these ciliates dominated throughout the year, with tintinnids, heterotrophic dinoflagellates, and copepods present in medium to high densities. In addition there were low numbers of Appendicularia, bivalve larvae, Cnidaria (medusae), and polychaetes. (Figure 9.10.)

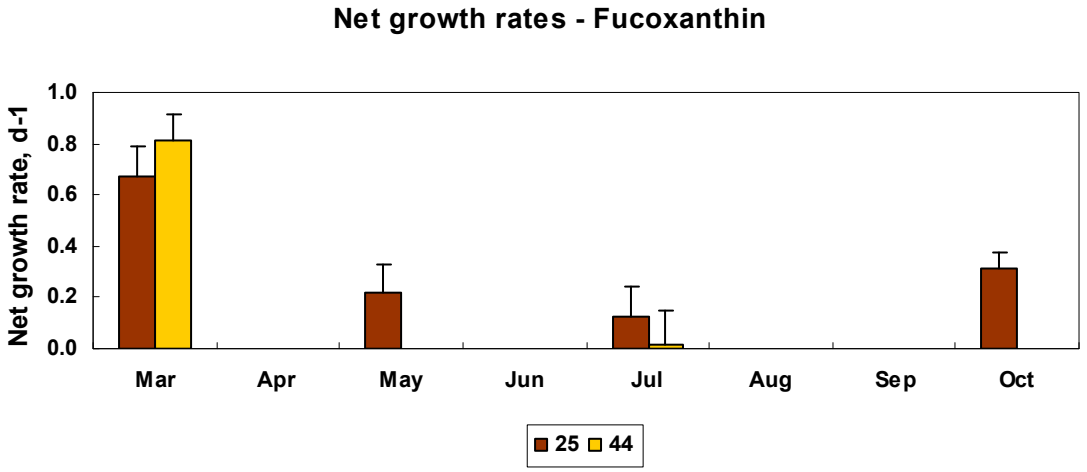

(a)

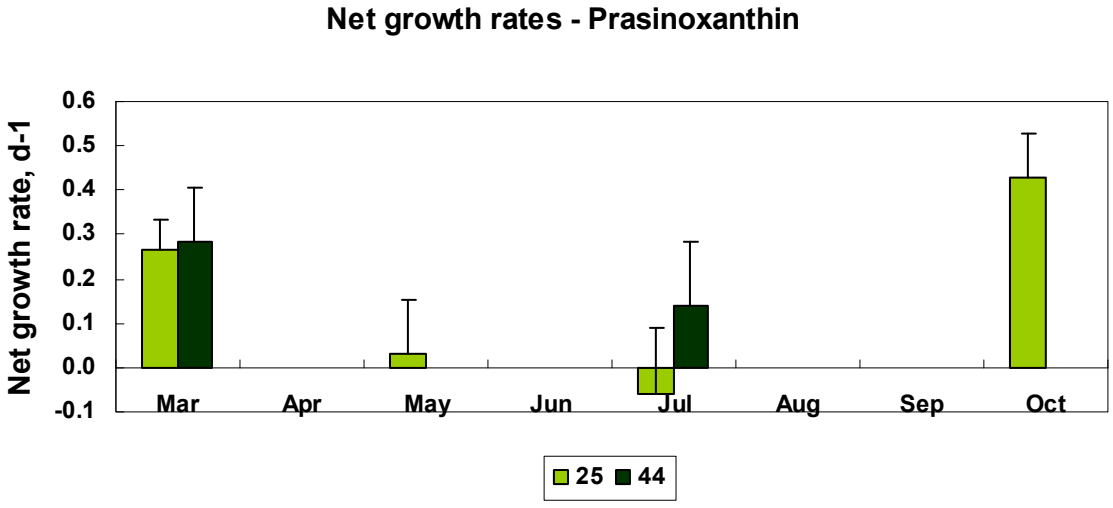

(b)

Figure 9.9. (a) Net growth rates for fucoxanthin in microzooplankton grazing experiments during 2007. **(b)** Net growth rates for prasinoxanthin in microzooplankton grazing experiments during 2007. Error bars indicate standard error.

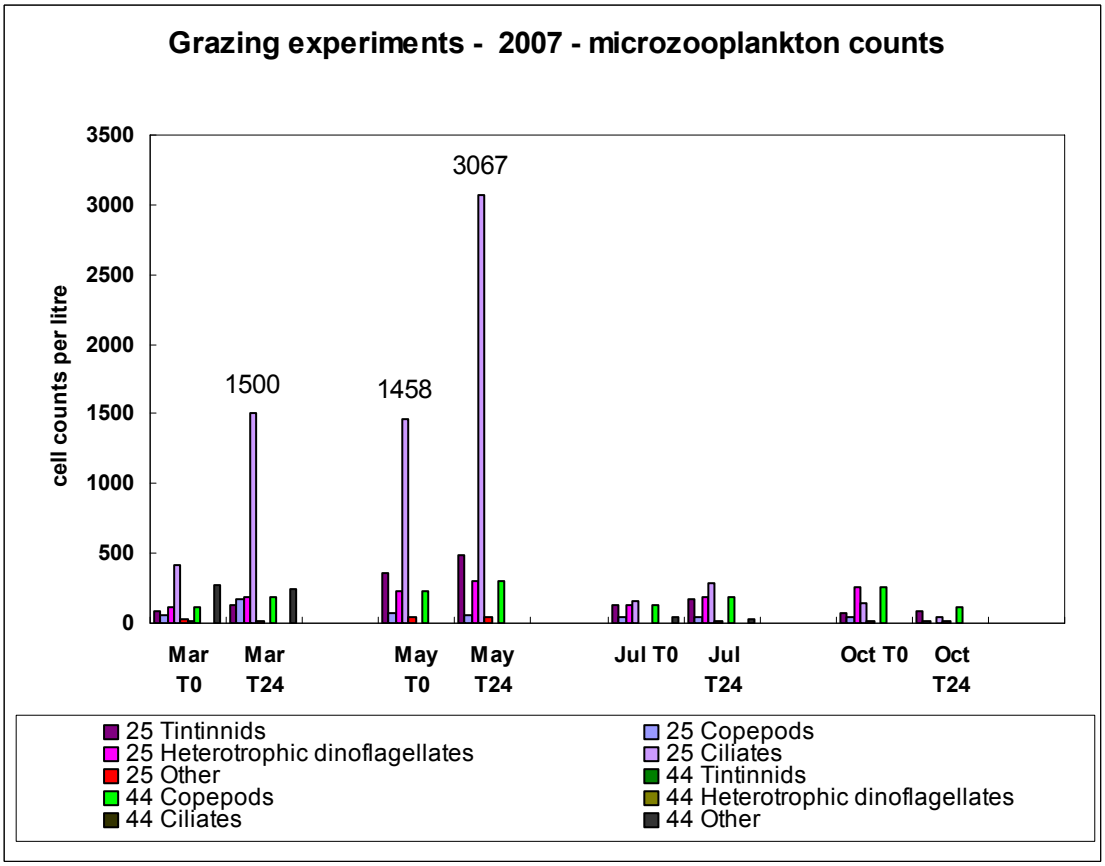

Figure 9.10. Microzooplankton densities from the grazing dilution experiments in the TFZ, March to October 2007, sites 25 and 44. T0 = time zero, the beginning of the experiment. T24 = time 24 hours, the end of the experiment.

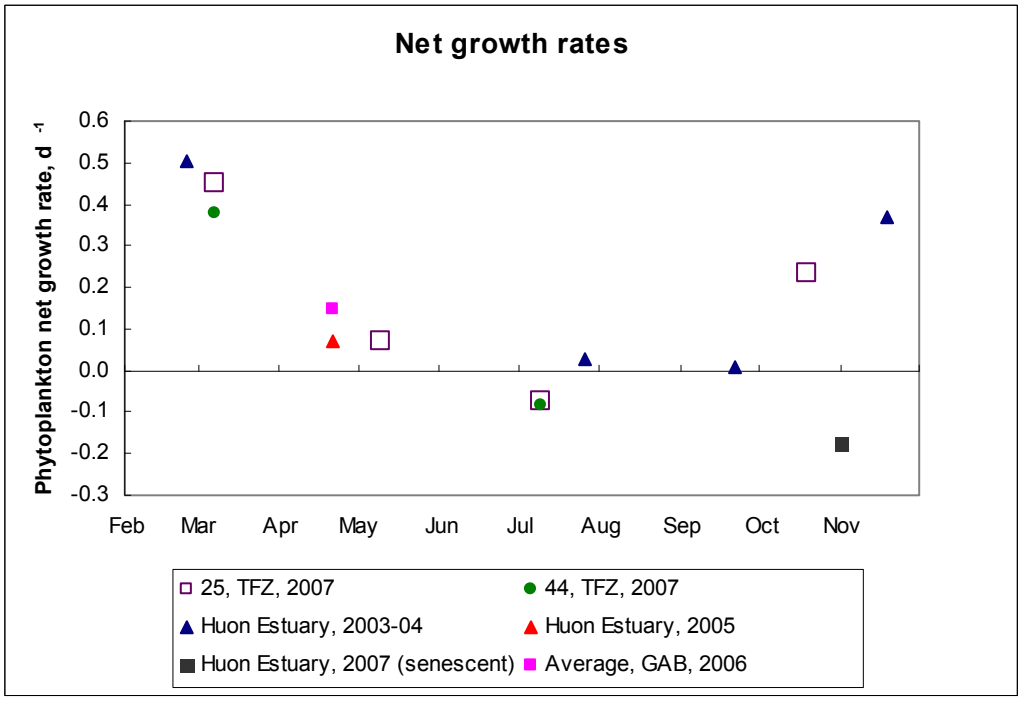

Figure 9.11. Net growth rates (μ_n) for sites in the TFZ (SA) in 2007, Huon Estuary (Tasmania) in 2003-04, 2005 & 2007, and the Great Australian Bight (GAB), 2006.

9.3.3. Meso-zooplankton Grazing

Based on meso-zooplankton settled volume (ml m^{-3}), the average amount of biomass in the large size fraction was 5.2 ± 0.72 ml m^{-3} or about 14 times greater than the 0.38 ± 0.26ml m^{-3} in the small size fraction. In general, copepods dominated the meso-zooplankton community (Figure 9.12), being more than 50% of all individuals in the large and small size categories across all times of day and all months (Figure 9.12). In the large size fraction, cladocerans were the second most dominant taxa, while bivalve larvae and gastropods were second and third, respectively, in the small size fraction (Figure 9.12).

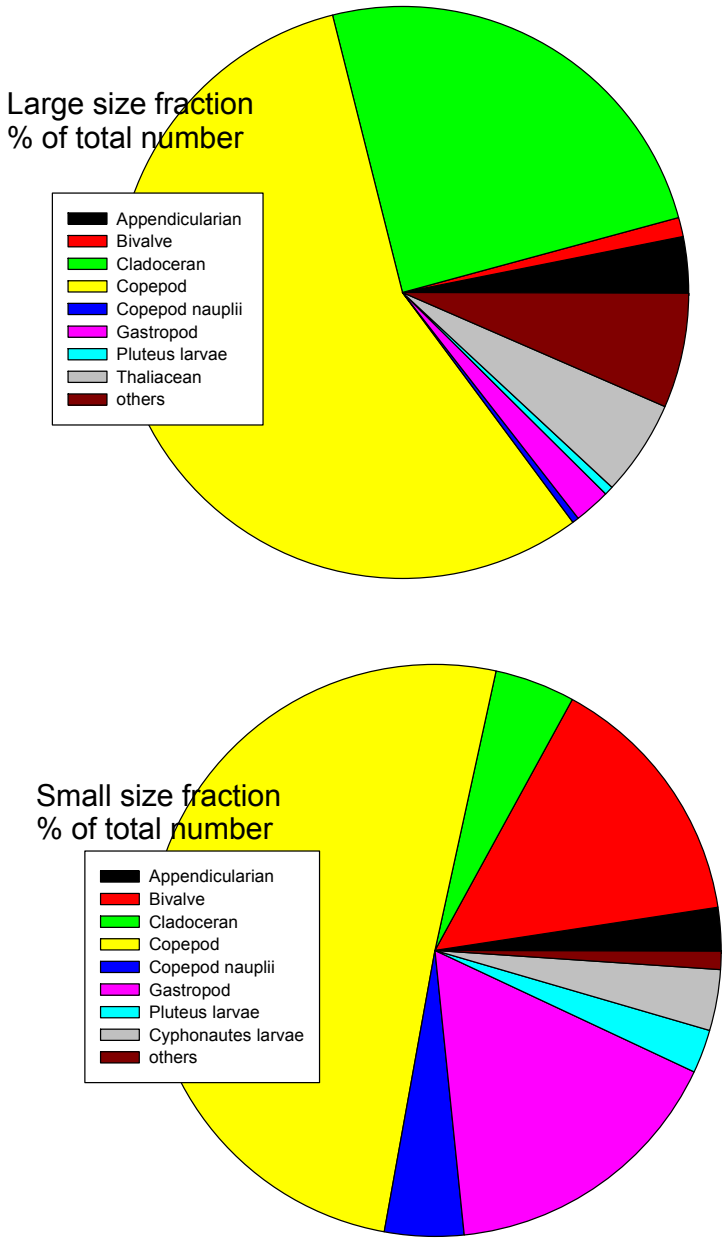

Figure 9.12. Composition of the large and small zooplankton community averaged over all times and all dates.

The ADCP mounted on the mooring at site 24 during July 2007 revealed a very clear signal during the first 4 days of the deployment (Figure 9.13). At approximately 1800 hours on the 13/07/07, the echo intensity (EI) increased at 18 m and over the next 4 hours the EI progressively increased throughout the water column. At ~0400 hours on the 14/7/07 the EI signal throughout the water column decreased until ~0600 hours, when it remained at a minimum until 1800 hours. This pattern repeated until the 17/7/07, when the signal became messy at the surface and throughout the water column. This break in the pattern coincides with poor weather when the significant wave height reached >1.0 m during a storm event. The EI pattern resumed at 1800 hours on the 18/7/07.

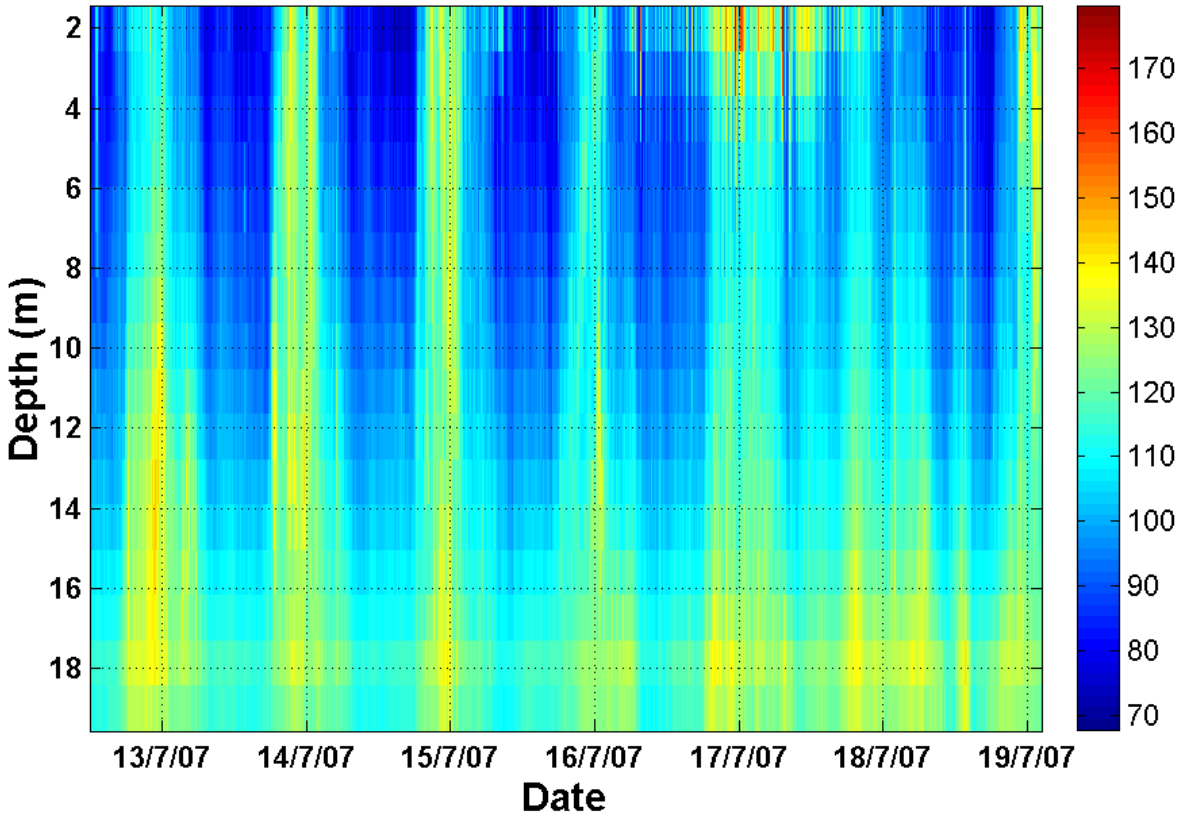

Figure 9.13. The echo intensity from an ADCP mounted on a mooring at site 24 (see Figure 9.1) deployed from 12/7/07 to the 19/7/07.

As mentioned above, the large size fraction of the zooplankton was dominated by copepods or cladocera. Copepods made up 32% of the community in March 2007, 77% of the community in May 2007, and 79% and 85% of the community in July and December 2007 respectively. Cladocera dominated in March 2007 (46%) with a decreasing presence in the community in the following months (16% in May 07, 7% in July 2007, and 7% in December 2007). In March and May 2007, the dominant Cladocera were *Penilia spp.*, while during July and December 2007 dominant Cladocera were *Evadne spp.* and *Podon spp*. PERMANOVA results indicate that both month and sampling time had a significant effect on community structure in the large size fraction ($p = 0.0002$, see Van Ruth et al. 2008). The zooplankton community in the large size fraction at 2400 hours was significantly different to the community present at all other sampling times. Total abundances in the small size fraction showed similar patterns to those identified in the large size fraction. Copepods also

dominated the small fraction of the zooplankton community in all sampling months, constituting 44%, 59%, 40%, and 66% of the community in March, May, July, and December 2007 respectively. Major variations in community structure were in the proportions of bivalves and gastropods in the community. Bivalves were 9% of the community in March, 19% in May, 32% in July, and 11% in December 2007. Gastropods made up 27%, 10%, 5%, and 5% of the community in March, May, July and December 2007 respectively. PERMANOVA results for the small size fraction indicate that community structure was significantly different between months and sampling times (Van Ruth et al. 2008).

The greatest meso-zooplankton biomass occurred in March 2007, with a gradual decrease through to December 2007. Estimates of potential meso-zooplankton growth rates were highest in March 2007, and decreased toward July 2007, before increasing again in December 2007 (Figure 9.14). Mean potential grazing rates peaked in March 2007 at 2400 hours (111.2 ±21.2 mg C m^{-3} d^{-1}), with lowest potential grazing rate in December 2007 at 0600 hours (1.7 ±0.4 mg C m^{-3} d^{-1}).

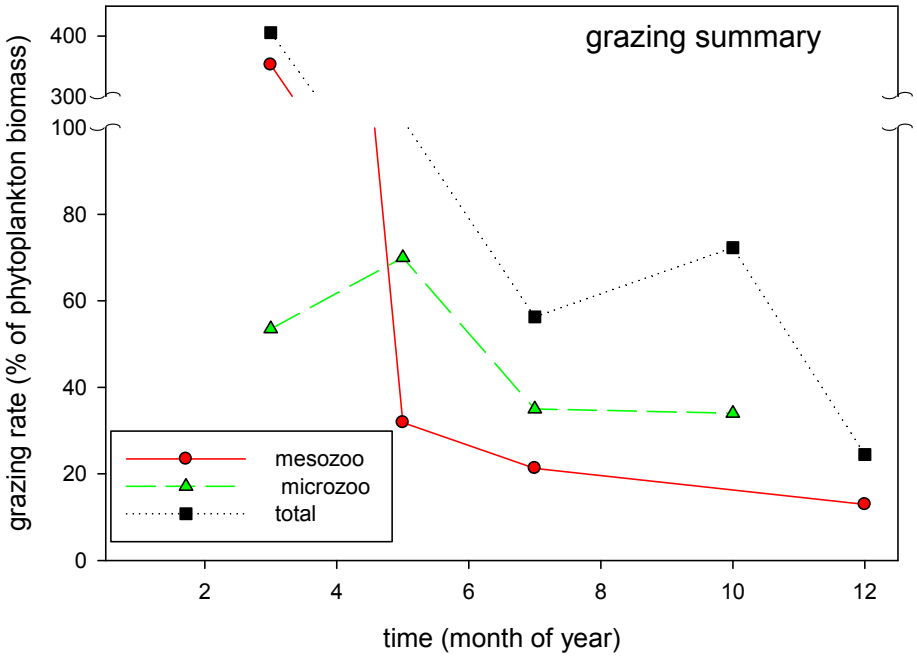

Figure 9.14. Estimated grazing rates by meso and microzooplankton as a percentage of phytoplankton standing stock per day.

9.4. Discussion

The greatest primary production rates in the TFZ observed between March and November 2007 occurred in the lead up to the autumn phytoplankton peak that has been identified as a regular occurrence in the region, after a late summer rise in silica and nitrate concentrations (chapter 7). Gross growth rates, α, and P^{B}_{max}, were high as diatoms thrived in the silica rich conditions. Low biomass and very high gross growth rates occurred in March 2007 as the phytoplankton biomass was rapidly growing to its May-June peak. Productivity decreased slightly and gross growth rates fell substantially during the May phytoplankton peak,

signalling the end of the peak. α was substantially lower in May, possibly due to the onset of nutrient limitation as Si and NO_x became limiting in late autumn. Despite a fall in α and P^B_{max}, the high biomass from the phytoplankton peak results in relatively high daily depth-integrated primary production. In July 2007, productivity was in decline, presumably as decreasing nutrient availability reduced α, P^b_{max}, and the gross growth rates, while grazing reduced biomass in the wake of the phytoplankton peak. Shorter daylengths were also a factor contributing to reduced daily integrated productivity in July. The lowest primary production occurred in October 2007. The low values for α and P^B_{max} suggest that by October the phytoplankton had experienced a protracted period of low nutrient availability despite the apparent rise in NO_x that may occur at this time of year (chapter 5). Low α and P^b_{max} may be due to Si limitation of diatom productivity, and FRP limitation of productivity of other phytoplankton, as has been suggested to occur in the area in spring (chapter 5).

During the formation of the autumn phytoplankton peak (March 2007 to May 2007), rates of primary production in the TFZ fell within ranges reported for the productive eastern boundary current upwelling systems off southern Africa (1000-3500 mg C m^{-2} d^{-1}, Brown et al. 1991), South America (800-5100 mg C m^{-2} d^{-1}, Daneri et al. 2000), and south western USA (500-2600 mg C m^{-2} d^{-1}, Pilskaln et al. 1996), and the upwelling influenced areas of the eastern Great Australian Bight (540-5030 mg C m^{-2} d^{-1}, Van Ruth PhD thesis in prep). Primary production rates measured after the phytoplankton peak (July and October) were generally comparable to those reported for the oligotrophic waters off the west coast of Australia (110-530 mg C m^{-2} d^{-1}, Hanson et al. 2005).

Comparison of grazing and growth rates obtained from diatom-dominated samples in the Huon Estuary, Tasmania in 2003-2004 (Thompson and Bonham, 2005), with the 2007 rates for the TFZ shows that rates in February - March in the Huon were similar to those at site 44, in the northern entrance to Boston Bay, and higher than the rates for site 25, in the middle of the TFZ (Figure 9.11). Winter (July) rates tended to be lower in both locations, with net growth rates showing a lot of spatial variability during spring.

A comparison of mean microzooplankton abundances in the TFZ with those in the Huon Estuary during 2003-04 showed that generally abundances in the Huon Estuary were at least two to four times those in the TFZ (Thompson and Bonham, 2005).

Peak total meso-zooplankton abundance and biomass occurred during the onset of the phytoplankton peak that has been identified as an annual feature in the region (chapter 7). The gradual decrease in meso-zooplankton abundance from March 2007 to December 2007 probably reflects a decrease in food availability as phytoplankton abundance also decreased from the May peak (chapter 7). Meso-zooplankton abundances and biomass measured in March 2007 were ~4-5 times higher than those measured in coastal waters of the eastern Great Australian Bight (van Ruth PhD thesis in prep), and an order of magnitude higher than measured in the Huon Estuary in February 2005 (6,800 individuals m^{-3}, Thompson et al. 2008). Greatest zooplankton abundances were found at 2400 hours probably reflecting the diel vertical migration of zooplankton from the sediments to the surface in the hours of darkness (Haney 1988).

The dominance of copepods and cladocerans in the meso-zooplankton community is consistent with patterns reported from other studies conducted in Australian waters and elsewhere in the ocean. More than 90% of zooplankton abundance and biomass observed during the Joint Global Ocean Flux Study (JGOFS) of the equatorial Pacific consisted of

copepods (Roman et al. 1995). Copepods made up >70% of zooplankton abundance in a study of the northeast Atlantic (Clark et al. 2001), and >95% of the total zooplankton assemblage in a study of waters off central Chile (Grunewald et al. 2002). Copepods also dominate zooplankton assemblages in the Arabian Sea (Roman et al. 2000), and off south-western Africa (Verheye et al. 1992).

Estimated meso-zooplankton grazing rates were greatest in March 2007, when meso-zooplankton biomass was at its greatest, most likely in response to an increase in phytoplankton biomass in the onset of the regional autumn phytoplankton peak (chapter 7). Peak meso-zooplankton growth rates and grazing rates were considerably greater than both those reported for coastal waters off south western Eyre Peninsula in February/March 2004 and 2005 (Van Ruth, PhD thesis in prep) and for the Huon Estuary in February 2005 (Thompson et al. 2008).

Acknowledgments
For field sampling and carrying out the microzooplankton grazing experiments in May-October we thank Sonja Venema, Kate Rodda and the crew of the RV Breakwater Bay (Brenton Ebert and Neil Evans) (SARDI Aquatic Sciences) for assisting with field sampling throughout the year. Tina Hines (Water Studies Centre-Monash University) performed the nutrient analysis. Funding was provided by the Aquafin CRC, FRDC, and CSIRO. Some data was obtained through research cooperation with the University of Western Australia and Murdoch University.

9.5. References

Anderson, M. J. (2001) A new method for non-parametric multivariate analysis of variance. Austral Ecology 26: 32-46.

Brown, P. C., Painting, S. J., Cochraine, K. L. (1991) Estimates of phytoplankton and bacterial biomass and production in the northern and southern Benguela ecosystems. South African Journal of Marine Science 11: 537-564.

Burkill, P. H., Mantoura, R. F. C., Llewellyn, C. A., Owens, N. J. P. (1987) Microzooplankton grazing and selectivity of phytoplankton in coastal waters. Marine Biology 93: 581-590.

Calbet, A., Landry, M. R. (2004) Phytoplankton growth, microzooplankton grazing, and carbon cycling in marine systems. Limnology and Oceanography 49: 51-57.

Capriulo, G. M., Sherr, E. B., Sherr, B. F. (1991) Trophic behaviour and related community feeding activities of heterotrophic marine protists. Protozoa and their role in marine processes, edited by Reid, PC, Turley, C., and Burkill, PH, Springer-Verlag, Berlin: 219–279.

Clark, D. R., Aazem, K. V., Hays, G. C. (2001) Zooplankton abundance and community structure over a 4000 km transect in the north-east Atlantic. Journal of Plankton Research 23: 365- 372.

Conover, R. J. (1978) Transformations of organic matter. In O. Kinne, Marine Ecology V. 4. Dynamics. John Wiley, Chichester, 221-456.

Daneri, G., Dellarossa, V., Quinones, R., Jacob, B., Montero, P., Ulloa, O. (2000) Primary production and community respiration in the Humboldt Current System off Chile and associated oceanic areas. Marine Ecology Progress Series 197: 41-49.

Froneman, P. W., Perissinotto, R., McQuaid, C. D. (1996) Seasonal variations in microzooplankton grazing in the region of the Subtropical Convergence. Marine Biology 126: 433-442.

Grunewald, A. C., Morales, C. E., Gonzalez, H. E., Sylvester, C., Castro, L. R. (2002) Grazing impact of copepod assemblages and gravitational flux in coastal and oceanic

waters off central Chile during two contrasting seasons. Journal of Plankton Research 24: 55-67.
Haney, J. F. (1988) Diel patterns of zooplankton behaviour. Bulletin of Marine Science 43: 583-603.
Hanson, C. E., Pattiaratchi, C. B., Waite, A. M. (2005) Sporadic upwelling on a downwelling coast: Phytoplankton responses to spatially variable nutrient dynamics off the Gascoyne region of Western Australia. Continental Shelf Research 25: 1561-1582.
Huntley, M., Boyd, C. M. (1984) Food-limited growth of marine zooplankton. The American Naturalist 124: 455-478.
James, M. R., Hall, J. A. (1998) Microzooplankton grazing in different water masses associated with the Subtropical Convergence round the South Island. New Zealand 45: 1689-1707.
Jassby, A. D., Platt, T. (1976) Mathematical formulation of the relationship between photosynthesis and light for phytoplankton. Limnology and Oceanography 21: 540-547.
Lampert, W., Taylor, B. E. (1985) Zooplankton Grazing in a Eutrophic Lake: Implications of Diel Vertical Migration. Ecology 66: 68-82.
Lohrenz, S. E., Wiesenberg, D. A., Rein, C. R., Arnone, R. A., Taylor, C. D., Knauer, G. A., Knap, A. H. (1992) A comparison of in-situ and simulated in-situ methods for estimating oceanic primary production. Journal of Plankton Research 14: 201-221.
Mackey, D. J., Parslow, J., Higgins, H. W., Griffiths, F. B., O'Sullivan, J. E. (1995) Plankton productivity and biomass in the western equatorial pacific: Biological and physical controls. Deep Sea Research Part 2 42: 499-533.
Martin, J. H. (1970) Phytoplankton-zooplankton relationships in Narragansett Bay. 4. The seasonnal importance of grazing. Limnology and Oceanography 15: 413-418.
Michaels, A. F., Silver, M. W. (1988) Primary production, sinking fluxes and the Microbial food web. Deep-sea research. Part A. Oceanographic research papers 35: 473-490.
Olivieri, E. T., Hutchings, L. (1987). Volumetric estimates of phytoplankton production in newly upwelled waters of the southern Benguela Current. Limnology and Oceanography 32: 1099-1111.
Parsons, T. R., Maita, Y., Lalli, C. M. (1984) "A Manual of Chemical and Biological Methods for Seawater Analysis" (Pergamon Press Ltd., Oxford)
Pilskaln, C. H., Paduan, J. B., Chavez, F. P., Anderson, R. Y., Berelson, W. M. (1996) Carbon export and regeneration in the coastal upwelling system of Monterey Bay, central California. Journal of Marine Research 54: 1149-1178.
Probyn, T. A. (1987) Ammonium regeneration by microplankton in an upwelling environment. Mar. Ecol. Prog. Ser 37: 53-64.
Roman, M. R., Dam, H. G., Gauzens, A. L., Urban-Rich, J., Foley, D. G., Dickey, T. D. (1995) Zooplankton variability on the equator at 140 deg W during the JGOFS EqPac study. Deep Sea Research 2 42, 673-693.
Roman, M., Smith, S., Wishner, K., Zhang, X., Gowing, M. (2000) Mesozooplankton production and grazing in the Arabian sea. Deep Sea Research 2 47, 1423-1450.
Strom, S. L., Strom, M. W. (1996) Microzooplankton growth, grazing, and community strucure in the nothern Gulf of Mexico. Mar. Ecol. Prog. Ser. 130: 229-240.
Strom, S. L., Welschmeyer, N. A. (1991) Pigment-specific rates of phytoplankton growth and microzooplankton grazing in the open subarctic Pacific Ocean. Limnology and Oceanography 36: 50-63.
Talling, J. F. (1957) The phytoplankton population as a compound photosynthetic system. The New Phytologist 56: 133-149.
Thompson, P. A., Bonham, P. (2005). Effects of grazing by microzooplankton on phytoplankton in the Huon Estuary. In: System-wide environmental issues for

sustainable salmonid aquaculture: interim report, J. K. Volkman, J. S. Parslow, P. A. Thompson, M. Herzfeld, K. Wild-Allen, S. I. Blackburn, C. Crawford, P. Bonham, D. G. Holdsworth, P. V. Sakov, J. R. Andrewartha, and A. T. Revill. Hobart, Tas.: CSIRO Marine and Atmospheric Research. (Aquafin CRC technical report).

Thompson, P.A., Bonham, P.I., Swadling, K.M. (2008) Phytoplankton blooms in the Huon Estuary, Tasmania: top down or bottom up control? Journal of Plankton Research doi:10.1093/plankt/fbn044

Turner, J. T., Graneli, E. (1992) Zooplankton Feeding Ecology: Grazing During Enclosure Studies of Phytoplankton Blooms from the West Coast of Sweden. Journal of Experimental Marine Biology and Ecology 157: 19-31.

van Ruth, P., Thompson, P., Bonham, P., Jones, E. (2008) Primary productivity and zooplankton ecology in the tuna farming zone. Technical report, Aquafin CRC Project 4.6, FRDC Project 2005/059. Aquafin CRC, Fisheries Research & Development Corporation and South Australian Research & Development Institute (Aquatic Sciences), Adelaide. SARDI Publication No F2008/000789-1, SARDI Research Report Series No 343, 58 pp.

Verheye, H. M., Hutchings, L., Huggett, J. A., Painting, S. J. (1992) Mesozooplanktonm dynamics in the Benguela ecosystem, with emphasis on the herbivorous copepods. South African Journal of Marine Science 12: 561-584.

Wassmann, P. (1998) Retention versus export food chains: processes controlling sinking loss from marine pelagic systems. Hydrobiologia 363: 29-57.

Chapter 10: Biogeochemical Modelling in the Southern Bluefin Tuna Farming Zone

Karen Wild-Allen*, Jennifer Skerratt

CSIRO Marine and Atmospheric Research, PO Box 1538, Hobart, Tasmania 7001

and Aquafin CRC

*corresponding author. Phone: +61 (3) 6232 5010, Fax +61 (3) 6232 5000, E-mail: karen.wild-allen@csiro.au

Abstract

The biogeochemical model used for the Tuna Farming Zone (TFZ) was initialised in September 2005 with spatially uniform pelagic and sediment concentrations of dissolved nutrients, plankton biomass, macrophytes and detritus. Where possible, tracer concentrations were derived from observations made throughout the region or historical data. Model results are only presented from January 2006 onwards due to the inherent uncertainty in the initial fields and to let the biogeochemistry in the model 'spin up' or forget the initial conditions. Finfish farm inputs for 2006 were derived from monthly feed data in the region. Feed data were converted to environmental dissolved and particulate nutrient loads. The model was able to reproduce the major features of the observed seasonal cycles of chlorophyll and dissolved inorganic phosphorus (DIP) when compared with observations. It successfully represented the timing and the nature of the autumn diatom peak. Preliminary model results suggest that phytoplankton productivity is seasonally limited by phosphorus during the summer months. However, uncertainty remains in the observed nutrient biogeochemistry of the region. At inshore sites the model underestimated the observed concentration of DIP, possibly due in part to the omission of coastal sewerage loads. The impacts of farm discharge on the regional biogeochemistry were investigated by comparing scenario simulations with and without farm loads. Nutrient levels increased near the tuna leases, and these form observable nutrient hotspots in the model results. Fish farm inputs may also lead to environmental effects distant from the farming zone. Modification to the seasonal timing of feed inputs (e.g. changing the stocking period or moving to long-term holding), or changing to manufactured feeds, may have an effect on the regions biogeochemistry and could be included in future modelling studies. More observations in the embayments and near-shore areas would help model calibration as the model is not yet well constrained and these results must be viewed as preliminary.

10.1. Introduction

The marine biogeochemistry and phytoplankton dynamics of Boston Bay and the Tuna Farming Zone (TFZ) are poorly known. Observations made throughout 2005/2006 show significant temporal variation in dissolved inorganic nutrient concentrations and phytoplankton biomass, and some spatial variation along a cross-shore transect (e.g. chapter 5). However, to date, we do not know how nutrients derived from tuna farming are cycled through the ecosystem, whether they accumulate in the TFZ or are quickly dispersed, and what their regional scale ecological consequences are. We also do not know what role other sources of nutrients may play in promoting algal blooms in the region, or whether inputs from southern bluefin tuna (SBT) farming are substantial in relation to these other inputs (both natural and anthropogenic). The aim of the current project was to develop an integrated hydrodynamic, biogeochemical and sediment model of the TFZ and surrounds, so that some of these questions could be answered. In this chapter, we present preliminary results from this biogeochemical model. While the model has been developed and simulations have been run with it, it should be noted that the timelines for the project did not allow for a robust validation of the model outputs, and thorough investigation of the models strengths and deficiencies (and hence an understanding of what additional data may be needed to improve its performance), or the running of multiple scenarios to look at the consequences of different management actions. Observations made at offshore sites were used to constrain inputs to the biogeochemical model, which was used to begin to explore the nutrient and phytoplankton dynamics of the region. Scenario simulations provide predictions about the possible ecological effects of SBT fish farm nutrient loads on the biogeochemistry and phytoplankton dynamics of the TFZ.

10.2. Model description

10.2.1. Physical model

A high resolution 3D hydrodynamical model of Boston Bay and the TFZ was implemented and calibrated against observations by Herzfeld et al. (chapter 1). Volume transports from this model were saved at 2 hour intervals over the entire model grid and used to force a more computationally efficient transport model (Herzfeld et al. 2008) over the same model domain. The transport model was coupled to both a sediment model calibrated against observations (chapter 4) and a biogeochemical model to enable the annual simulation of the dynamics of dissolved and particulate substances across the model domain.

Key findings from the hydrodynamical model relevant to the biogeochemistry are the flushing times which vary from 1.5 to 13.9 days for the whole region (Table 1.2 and Figure 10.1); the residual circulation of the region which is ventilated from south to north offshore and by a series of circulation cells inshore (Figure 1.26); and the connectivity of the region which is divided into 3 distinct regions:

1. Landward of Boston Island and Proper Bay with poor connectivity with the rest of the domain;
2. Louth and Peake bays with moderate connectivity with the rest of the domain; and
3. Regions outside these bays and offshore of Boston Island with good connectivity with the remainder of the domain, and subject to greater flushing.

10.2.2. Sediment model

A fully coupled high resolution 3D sediment model was implemented and calibrated against observations by Margvelashvili (chapter 4) to simulate the dynamics of fine sediment particles in the region. Parameters from the fully coupled sediment model were used to constrain the sediment transport model with some adjustments to resuspension parameters due to the coarser temporal resolution of the transport model. The sediment transport model reproduced the essential features of the observed sediment dynamics in Boston Bay and the TFZ.

Figure 10.1. Satellite image (Google Earth™) showing embayments of model domain.

10.2.3. Biogeochemical model

The biogeochemical model applied here is similar to the model used in the Huon Estuary and D'Entrecasteaux Channel to investigate the impact of salmon farms on the coastal marine environment in south-eastern Tasmania (Wild-Allen et al., 2005, Volkman et al., 2008). In Tasmania, the biogeochemical model was fully coupled to the hydrodynamic model, but this necessitated a coarser grid resolution than for the hydrodynamic model alone due to the additional computational burden of 60+ biogeochemical model tracers. In the South Australian study, the biogeochemical model was coupled to a transport model (Herzfeld et al., 2008) for the first time. This is computationally more efficient and enables the biogeochemical model to be integrated on the same high resolution grid as the hydrodynamic model.

Using the transport model, biogeochemical dissolved tracers are advected and diffused in an identical fashion to physical tracers such as temperature and salinity, and ecological particulate tracers sink and are resuspended by the same formulation as sediment particles. At each ecological time step, non-conservative ecological rate processes such as growth, nutrient uptake, grazing and mortality are integrated within the ecological module which returns updated tracer concentrations to the transport model via an interface routine.

10.2.4. Model components

In the biogeochemical model the water column is organised into a pelagic zone with 24 layers of varying thickness, an epibenthic zone which includes additional epibenthic tracers and overlaps with the lowest pelagic layer, and a sediment zone consisting of a thin layer of easily resuspendable material overlying two thicker layers of consolidated sediment.

Ecological processes are organised into the 3 zones with pelagic processes including phytoplankton and zooplankton growth and mortality, detritus remineralisation and fluxes of dissolved oxygen, nitrogen and phosphorus (Figure 10.2). Macroalgae and seagrass growth and mortality are included in the epibenthic zone whilst further phytoplankton mortality, microphytobenthos (benthic diatom) growth, detrital remineralisation and fluxes of dissolved substances are included in the sediment layer (Figure 10.2).

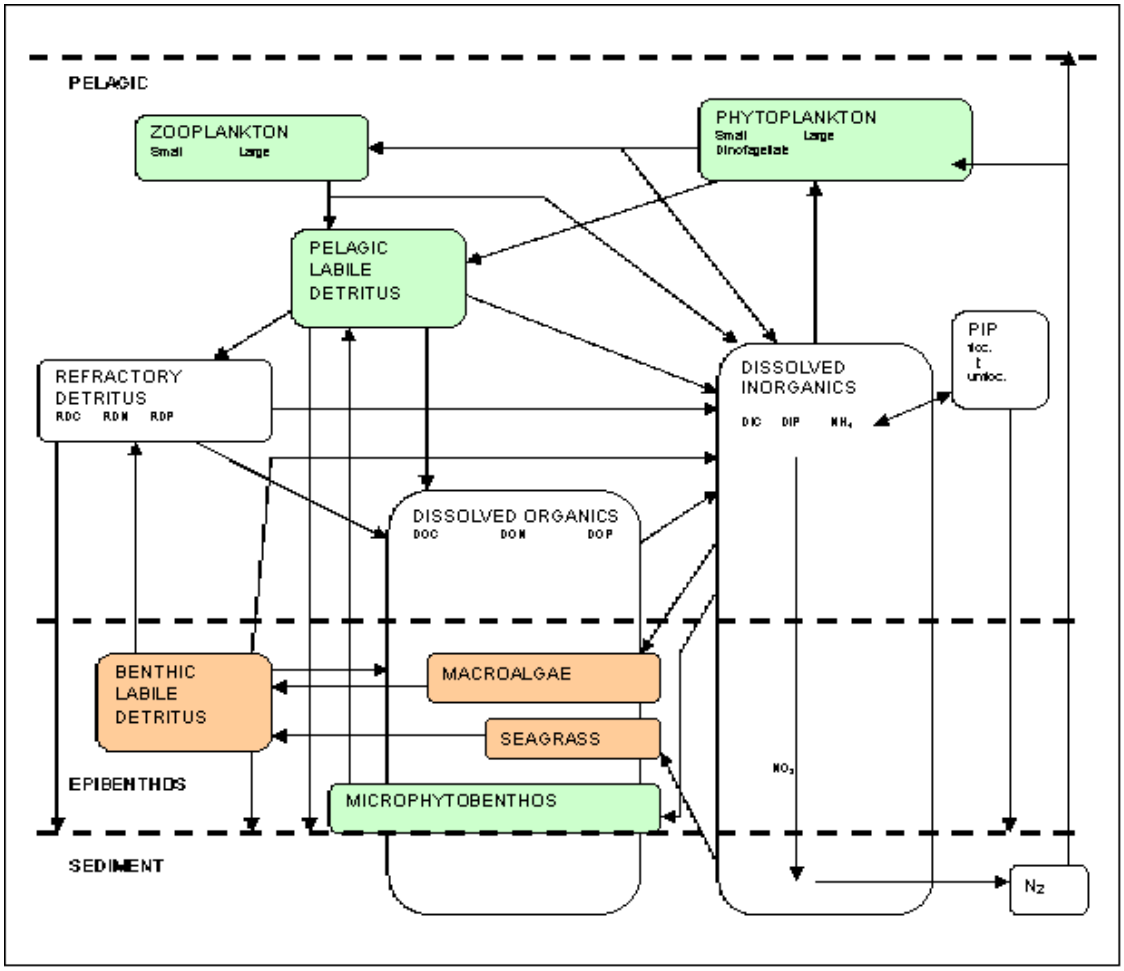

Figure 10.2. Schematic diagram of the biogeochemical model compartments, links and vertical layers. Green compartments have fixed nutrient content at Redfield ratio (106C:16N:1P); brown compartments are fixed at Atkinson ratio (550C:30N:1P).

10.2.5. Primary production

There are 3 groups of microalgae and 2 of macrophytes included in the model (parameters shown in Table 10.1):

- 'Small phytoplankton' representing small flagellates, and photoautotrophic pico- and nano-plankton. These organisms are small, with relatively high growth rates and are typically neutrally buoyant (Table 10.1). Their high surface area to volume ratio enables them to take up nutrients efficiently, even at low concentration, which makes this group of phytoplankton ubiquitous throughout aquatic systems (Fogg 1991). Small phytoplankton are modelled with a fixed nutrient ratio of 106C:16N:1P (Redfield ratio). The biomass of small phytoplankton is heavily constrained by grazing by tightly coupled small zooplankton. Natural mortality occurs when cells drift into the sediment layer.

- 'Large phytoplankton' represents diatoms with opportunistic ecological characteristics. They have a high growth rate which allows them to respond rapidly when nutrients and light are available, despite having lower nutrient uptake efficiency and a tendency to sink out of the euphotic layer (Table 10.1). Modelled large phytoplankton have a fixed nutrient ratio of 106C:16N:1P (Redfield Ratio). Large zooplankton graze on large phytoplankton but their slower growth rate results in a lag in response time allowing bloom events to occur. Large phytoplankton which sink into the sediment layer are assumed to die.

- 'Microphytobenthos' are large cells representative of benthic diatoms (Table 10.1). They have a high sinking rate and grow in the pelagic and sediment layers where there is sufficient light. In the sediment layer they have access to enhanced concentrations of regenerated nutrients. They are modelled with a fixed nutrient ratio of 106C:16N:1P (Redfield ratio) and are grazed by large zooplankton when suspended.

- Seagrass in the model grows in the epibenthic layer where there is sufficient light and sediment nutrients. In the epibenthic layer light from the bottom water column layer is first utilised by macroalgae, which can shade and overgrow seagrass beds given sufficient water column nutrients to support macroalgae growth. Following attenuation by macroalgae biomass the remaining light is available to support seagrass growth. They have a fixed carbon to nutrient ratio of 550C:30N:1P (Atkinson ratio) and utilize nutrients directly from the sediment layer by uptake through their root system. Seagrass mortality occurs when there is insufficient light and/or nutrients to sustain growth in excess of metabolic/respiration requirements.

- Macroalgae in the model represent both benthic macro- and epiphytic- algal groups that might co-exist with seagrass communities. They have a fixed nutrient ratio of 550N:30N:1P (Atkinson ratio) and utilize nutrients from the pelagic water column by absorption across the frond surface. Macroalgal mortality in the model occurs when there is insufficient light and/or nutrients to sustain growth in excess of metabolic/respiration requirements.

All parameters in tables 10.1 – 10.4 were sourced from previous model runs in Australian coastal waters where the model has been calibrated against observations (Wild-Allen, unpublished data). Ideally for a rigorous model application each parameter should be derived from local observations, however as observations of these parameters in Boston Bay are

scarce it was necessary to use parameter values from other regions to implement the pilot biogeochemical model. During model calibration local ranges in parameters such a typical phytoplankton cell size can be explored, however many values vary little between regions.

Table 10.1. Characteristics of primary producers included in the biogeochemical model.

Parameter	Large phyto-plankton	Small phyto-plankton	Microphyto-benthos	Sea-grass	Macro-algae
Cell radius (m)	$1x10^{-5}$	$2.5 x10^{-6}$	$1.0 x10^{-5}$	N/A	N/A
Maximum growth rate (μ) (d^{-1})	2.0	1.25	1.35	0.1	0.02
Respired fraction of μ max (-)	0.025	0.025	0.025	0.025	0.025
Specific absorption cross section (m^2 mg N^{-1})	0.0013	0.0024	0.0013	$1.0 x10^{-5}$	0.001
Stoichiometry coefficient of P (mg P $cell^{-1}$ or m^{-2})	$1.19 x10^{-8}$	$1.75 x10^{-10}$	$1.19 x10^{-8}$	$2.4 x10^{-6}$	$2.4 x10^{-6}$
Mortality term (d^{-1})	0.14	0.14	0.0003	0.00274	0.1
Half saturation constant for N uptake (mgN m^{-3})	N/A	N/A	N/A	5.0	N/A
Half saturation constant for P uptake (mgP m^{-3})	N/A	N/A	N/A	5.0	N/A
Sinking (m s^{-1})	$-5.6 x10^{-6}$	0.0	$-5.79 x10^{-5}$	N/A	N/A

Modelled autotroph growth is determined by access to essential nutrients (nitrogen and phosphate) and photosynthetically active radiation (PAR) using the chemical reaction (CR) model of Baird (1999). Dissolved nitrogen is present as ammonium and nitrate and autotrophs are assumed to take up both equally. Phosphate and dissolved inorganic carbon are also taken up by phytoplankton at Redfield ratio (106C:16N:1P) and by macrophytes at Atkinson ratio (550C:30N:1P). Ambient photosynthetically active radiation (PAR) is calculated from incident surface 24 hour mean PAR attenuated by sea water, coloured dissolved organic substances (CDOM) and organic and inorganic particles. Optical parameters are shown in Table 10.2. Phytoplankton chlorophyll concentration is calculated by assuming a fixed nitrogen to chlorophyll ratio of 7 mg N: 1 mg chlorophyll. All modelled chlorophyll values are for chlorophyll-*a*.

Table 10.2. Optical parameters used in the biogeochemical model.

Parameter	Value
Background attenuation of sea water	0.1
CDOM attenuation coefficient of freshwater (m^{-1})	4.4
Detrital specific attenuation coefficient (m^{-1})	0.0038
TSS specific attenuation coefficient ($m^{-1}(kg\ m^{-3})^{-1}$)	30
Dissolved organic nitrogen specific attenuation coefficient ($m^{-1}(mgN\ m^{-3})^{-1}$	0.0009

10.2.6. Secondary production

There are 2 groups of zooplankton included in the model (parameters shown in Table 10.3):

- 'Small zooplankton' represent microzooplankton less than 200 μm in size such as zooflagellates, tintinnids, ciliates, rotifers, small copepod nauplii and polychaete larvae. They are mobile, feed on small phytoplankton and have rapid turnover rates. They are

modelled with a fixed nutrient ratio of 106C:16N:1P (Redfield ratio) and grow as a function of maximum specific growth rate and grazing rate. Grazing success depends on the food encounter rate which in turn is based on zooplankton swimming speed, food size and density. Inefficient feeding and excretion returns dissolved and particulate material to the water column at the Redfield ratio. A quadratic mortality term is applied to account for both natural mortality and predation – this is the closure term for the model's biogeochemical cycling (explained below).

- 'Large zooplankton' represent mesozooplankton such as copepods and small fish larvae. They are mobile, feed on large phytoplankton, and microphytobenthos. They are modelled with a fixed carbon to nutrient ratio of 106C:16N:1P (Redfield ratio) and have a lower maximum specific growth rate compared to small zooplankton which results in a lag between enhanced primary and secondary production. Grazing success is a function of food encounter rate and inefficient feeding and excretion returns dissolved and particulate material to the water column at the Redfield ratio. The highest trophic level of the food web that is explicitly modelled is that comprising zooplankton. This requires that the rate of zooplankton mortality due to consumption by higher predators be represented by some mathematical function that does not explicitly depend upon the population level of the higher predators, since such predators are not being modelled. This function is called the closure term. Natural mortality and predation of large zooplankton are represented by a quadratic mortality term which is the closure term for the model's biogeochemical cycling.

Table 10.3. Characteristics of secondary producers included in the model.

Parameter	Small zooplankton	Large zooplankton
Radius (m)	12.5×10^{-6}	5.0×10^{-4}
Growth efficiency	0.38	0.38
Maximum growth rate at 15˚C (d^{-1})	3.0	0.1
Swimming velocity (m s^{-1})	2.0×10^{-4}	2.0×10^{-3}
Grazing technique	Rectangular hyperbolic	Rectangular hyperbolic
Fraction of growth inefficiency lost to detritus	0.5	0.5
Mortality (quadratic) rate (d^{-1} (mgN m^{-3})$^{-1}$	0.02	0.0004
Fraction of mortality lost to detritus	0.5	0.5

10.2.7. Detritus and nutrient pools

There are 3 types of particulate detritus and 2 pools of dissolved substances included in the model (parameters are shown in Table 10.4):

- 'Pelagic labile detritus' represents fresh detritus which is rapidly broken down by bacteria, viruses and fungi into refractory detritus, dissolved organic and dissolved inorganic substances on a timescale of about a week. It is modelled with a fixed carbon to nutrient ratio of 106C:16N:1P (Redfield ratio) and generated by inefficient feeding and excretion of large and small zooplankton, and by mortality of phytoplankton and zooplankton. Detrital particles contribute to the attenuation of light, sink and enter the sediment layer where remineralisation processes continue to breakdown labile material

to refractory, dissolved organic and dissolved inorganic substances, as in the water column.

- 'Benthic labile detritus' is similar to pelagic labile detritus but it has a fixed carbon to nutrient ratio of 550N:30N:1P (Atkinson ratio). It is generated by mortality of seagrass and macroalgae. Particles contribute to the attenuation of light, sink and enter the sediment layer where remineralisation processes continue to breakdown labile material to refractory, dissolved organic and dissolved inorganic substances, as in the water column.

- Refractory detritus represents older detrital material with lower nutrient to carbon content and slower remineralisation time scales of about a year. Refractory material is generated by the breakdown of pelagic and benthic labile detritus (with contrasting carbon to nutrient ratios) which necessitates modelling the carbon, nitrogen and phosphorus components independently. Refractory detrital material is remineralised to dissolved organic and inorganic substances. Particles contribute to the attenuation of light, sink and enter the sediment layer where remineralisation processes continue.

- Dissolved organic material (DOM) is considered to be a pool of very refractory nature with very slow remineralisation time scales of about two years. Dissolved organic material is generated by remineralisation of pelagic and benthic labile detritus and refractory detritus and is modelled as independent carbon, nitrogen and phosphorus components. This material is remineralised by bacterial and chemical reaction to dissolved inorganic carbon, nitrogen and phosphorus. Enhanced concentrations of detritus in the sediment give rise to gradients in dissolved organic matter which diffuse into the pelagic layer.

- Dissolved inorganic material is modelled as independent carbon, nitrogen and phosphorus pools. It is generated through inefficient feeding and excretion of zooplankton and by remineralisation of pelagic and benthic labile detritus, refractory detritus and dissolved organic material. These transformations release nitrogen in the form of ammonium which depending on available oxygen, can undergo nitrification to nitrate and denitrification to nitrogen gas, which is then lost to the atmosphere. Dissolved inorganic phosphorus can be adsorbed onto, or desorbed from, suspended sediment particles depending on the concentrations of dissolved and particulate phosphorus and dissolved oxygen. Very small particles can also flocculate into larger particles with different sinking characteristics. Adsorption of phosphorus onto sediment particles limits its availability for algal uptake and growth. Accumulation of labile and refractory detritus in the sediment leads to gradients in dissolved inorganic carbon and nutrient which diffuse back into the pelagic layer at rates enhanced by bio-irrigation. Dissolved inorganic nutrients are the final stage in the recycling process of organic material back into substrate available for algal uptake and growth.

Table 10.4. Modelled detritus parameter values and associated remineralisation rates.

Parameter	Value	Unit
Pelagic labile detritus breakdown rate	0.1	d^{-1}
Refractory detritus breakdown rate	0.0036	d^{-1}
Dissolved organic matter (DOM) breakdown rate	0.00176	d^{-1}
Fraction of labile detritus converted to DOM	0.01	-
Fraction of labile detritus converted to refractory detritus	0.19	-
Fraction of refractory detritus converted to DOM	0.05	-
Maximum water column nitrification rate	0.1	d^{-1}
Maximum sediment nitrification rate	20	d^{-1}
Maximum nitrification efficiency	1.0	-
O_2 half saturation rate for nitrification	500	mg O m^{-3}
Maximum denitrification rate	40	d^{-1}
O_2 content at 50% denitrification rate	1000	mg O m^{-3}
O_2 half saturation rate for aerobic respiration	500	mg O m^{-3}

10.2.8. Dissolved oxygen

The concentration of dissolved oxygen in the model varies with atmospheric exchange at the sea surface, photosynthetic production and respiration of primary producers, respiration of secondary producers and utilization during remineralisation processes. Surface waters are typically oxygen–rich, whilst deeper waters and the sediment layer may become depleted in oxygen depending on vertical mixing and flushing of the sediment.

10.2.9. Initialisation

The model was initialised in September 2005 with spatially uniform pelagic and sediment concentrations of dissolved nutrients, plankton biomass, macrophytes and detritus. State variable concentrations (Table 10.5) were determined where possible from project observations and/or from literature values in for example Fernandes et al. (2007a,b). For substances that were completely unknown the initial conditions were supplied from the final concentration of the substance in repeated simulations of annual cycles. Nevertheless considerable uncertainty remains in the set of initial concentrations supplied to the model due primarily to the paucity of observations in the region in September 2005. This uncertainty was mitigated by allowing a long 'spin up' period so that modelled concentrations evolved to realistic local conditions, and thus results are only presented from January 2006 onwards.

Table 10.5. Initial state variable concentrations.

Substance	Pelagic	Sediment	Unit
Nutrients			
NO_3	1	140	mg N m^{-3}
NH_4	5	140	mg N m^{-3}
DIP	1.5	100	mg P m^{-3}
DON	150	500	mg N m^{-3}
DOP	18	200	mg P m^{-3}
DOC	1500	1500	mg C m^{-3}
DIC	24000	24000	mg C m^{-3}
Phytoplankton Biomass			
Small	3	1	mg N m^{-3}
Large	3	1	mg N m^{-3}
Microphytobenthos	0.3	300	mg N m^{-3}
Zooplankton Biomass			
Small	2	0	mg N m^{-3}
Large	2	0	mg N m^{-3}
Detritus			
Benthic Labile	0.1	200	mg N m^{-3}
Pelagic Labile	2	200	mg N m^{-3}
Refractory N	2	8000	mg N m^{-3}
Refractory P	0.7	1100	mg P m^{-3}
Refractory C	10	80000	mg C m^{-3}
Macrophyte Biomass	**Epibenthos**		
Seagrass	500		mg N m^{-3}
Macroalgae	50		mg N m^{-3}

10.2.10. Boundary forcing

The biogeochemical model is forced with a no-gradient boundary condition for most substances so that concentrations generated within the model domain are neither increased nor diminished at the model boundary. Where data exist, the model can be constrained by an upstream boundary condition to improve resolution of the pelagic biogeochemistry. Upstream boundary conditions force the concentration of in-bound water to observed values whilst allowing locally generated concentrations to leave the model domain.

Data along the boundary of the model were spatially sparse although the mooring deployments provided good temporal resolution. Data were interpolated in space and time to provide an upstream boundary condition along the whole open boundary for nitrate, ammonium, phosphate (Figure 10.3), and large and small phytoplankton biomass (Figure 10.4).

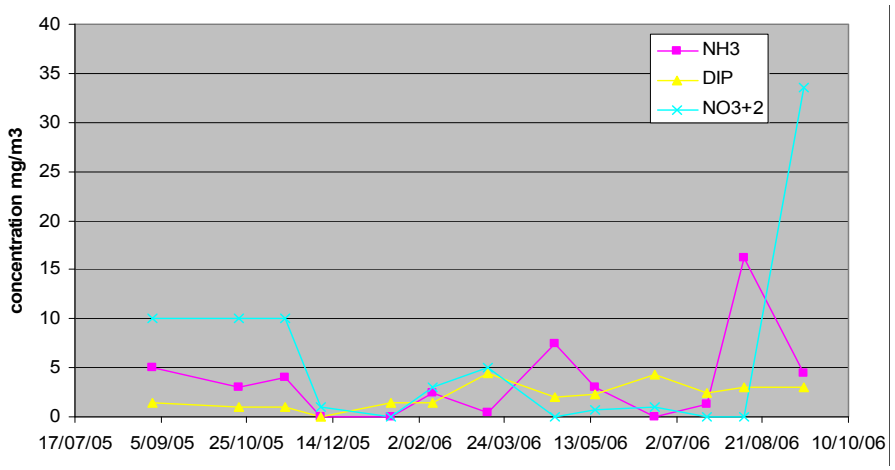

Figure 10.3. Upstream open boundary condition for nutrient concentration.

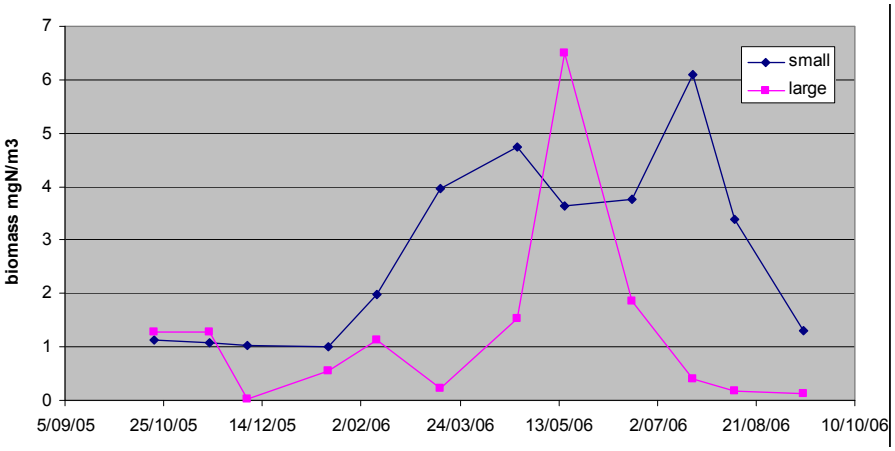

Figure 10.4. Upstream open boundary condition for phytoplankton biomass.

10.2.11. Southern bluefin tuna farm loads

Southern Bluefin Tuna (SBT) fish farms locations for 2006 are shown in Figure 10.5. Feed data for 2006 were received in July 2007 (Figure 10.6). In 2006, SBT farms used only baitfish as feed for the tuna. The two main species of baitfish were local and US sardines. Feed data were converted to environmental dissolved and particulate nutrient loads using the relationships established by Ellis and Rough (2005) and Fernandes et al. (2007a and b). Maximum nutrient loads to the region occurred in autumn (March – Jun). The SBT farming season started in January and ended in September, and from October to the end of year there was zero feed input.

10.2.12. Sewerage treatment plant (STP) loads

Nutrient loads from sewerage discharge along the coast were not included in the model as they were not available when the model was run. In general, such loads are small and diffuse along the relatively sparsely populated coastline. Recent estimates of STP loads into the region (chapter 5), show a seasonal input of nitrogen and phosphorus from the Port Lincoln STP which is small (7-9 tonnes N per annum) compared with nutrient loads from tuna fish farm waste.

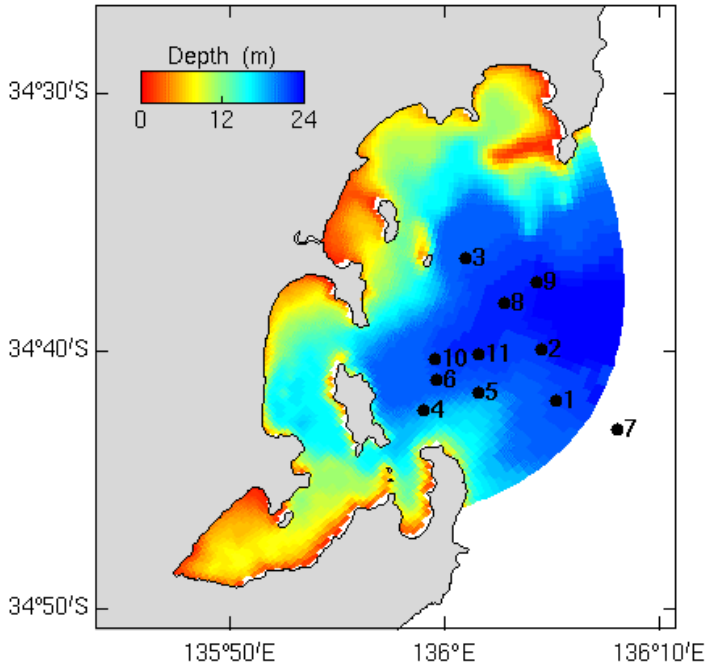

Figure 10.5. Southern Bluefin Tuna farm locations for 2006.

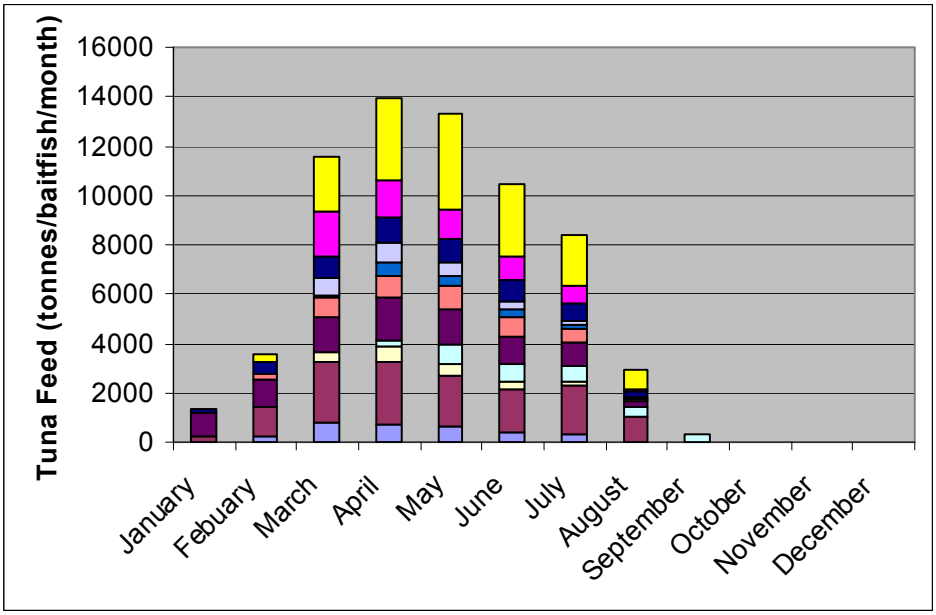

Figure 10.6. Southern bluefin tuna farm cumulative feed input. Different colours reporesent feed inputs to different leases (leases not identified due to confidentiality) Source: TBOASA.

10.3. Results; Model calibration

In-situ observations

Model simulations including phytoplankton and nutrient concentrations along the open boundary and fish farm nutrient loads were compared with independent in-situ observations taken throughout the region (Figure 10.7).

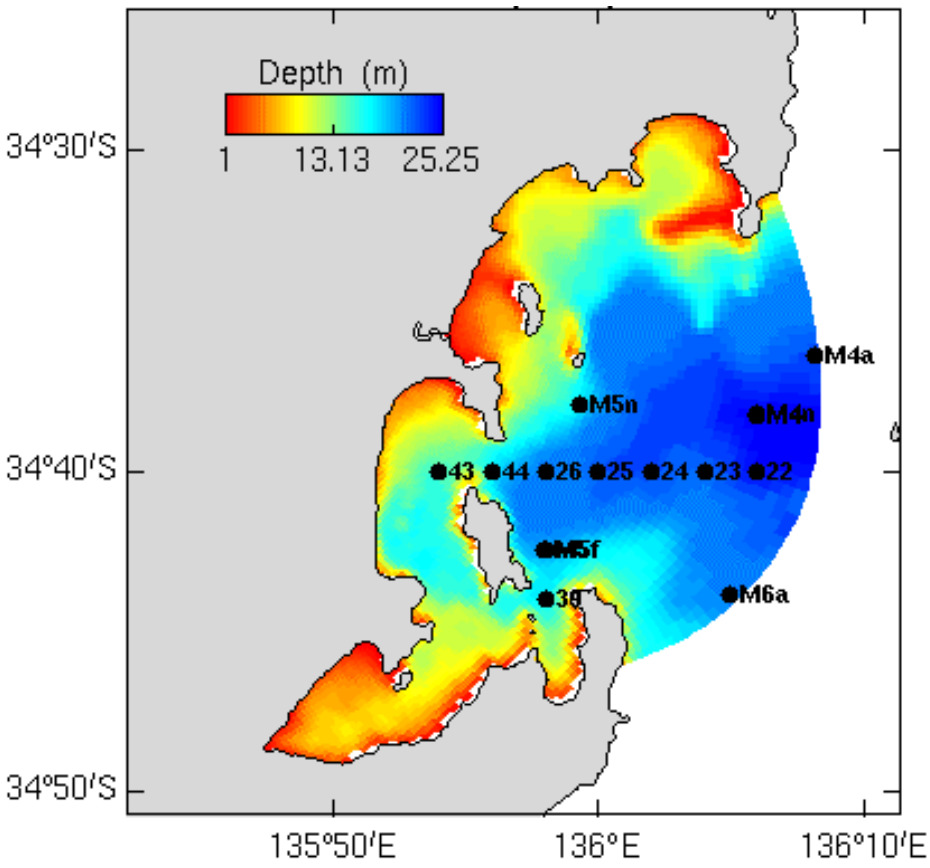

Figure 10.7. CTD and in-situ sampling site locations (22 – 44). Mooring locations shown as M4 – M6, with letters corresponding to n deployment periods (a–f). Monthly sampling procedures and analysis protocols are described in chapter 7.

Bottle Samples: Chlorophyll and Phosphorus

The model was able to reproduce the major features of the observed seasonal cycles of chlorophyll (Figure 10.8) and DIP (Figure 10.9) when compared with observations. However, uncertainty remains in the observed nutrient biogeochemistry of the region. The model did not reproduce a number of 'spikes' in the observed data set possibly because they were associated with sub-grid-scale patchiness or experimental error. Preliminary model results suggest that phytoplankton productivity is seasonally limited by phosphorus during the summer months with elevated chlorophyll concentrations in autumn. At inshore sites the model underestimated the observed concentration of DIP, possibly due to omission of coastal STP loads.

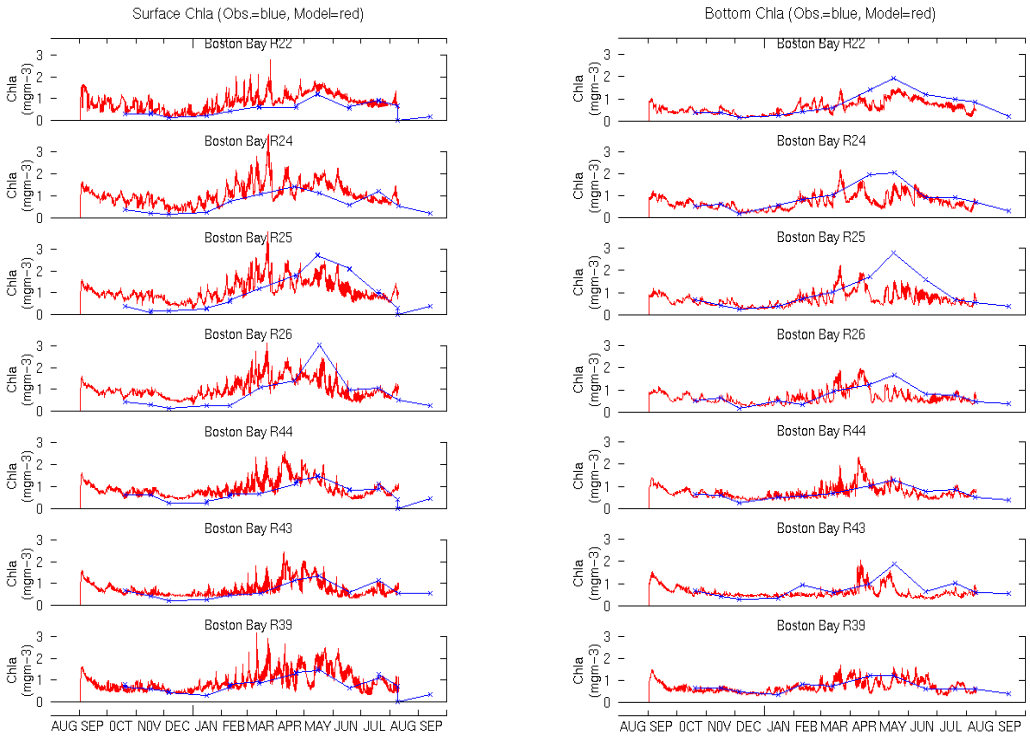

Figure 10.8. Surface (left) and bottom (right) chlorophyll-*a* concentrations from biogeochemical model simulation (red) and in-situ observations (blue) at sites throughout the TFZ.

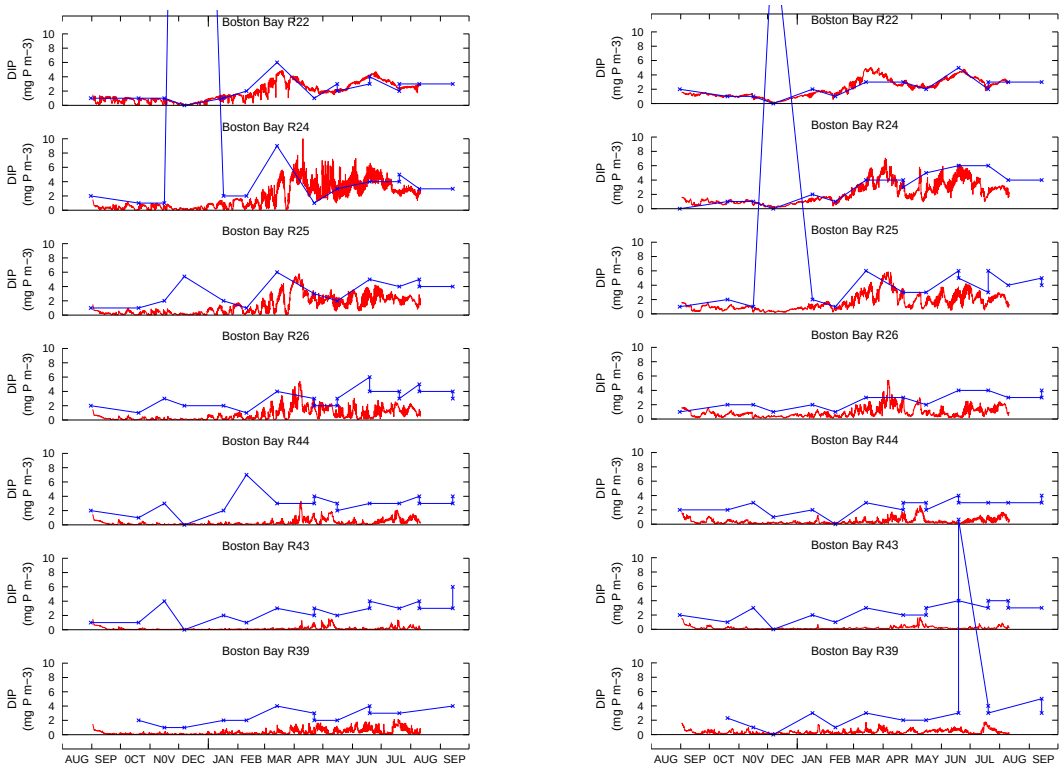

Figure 10.9. Surface (left) and bottom (right) dissolved inorganic phosphate concentrations from biogeochemical model simulation (red) and in-situ observations (blue) at sites throughout the TFZ.

Bottle Samples: Nitrate and Ammonia

The model simulation of observed nitrate (Figure 10.10) and ammonium (Figure 10.11) concentrations throughout the region showed limited skill. Offshore concentrations of nitrate were of similar magnitude, but inshore observations were significantly lower than simulated. Analysis of the nutrient observations shows that primary production is limited by both low nitrogen and low phosphorus concentrations in summer months and silicate may play an important role in the initiation of the autumn phytoplankton peak, which is dominated by diatoms (chapter 7). Whilst the biogeochemical model does not explicitly resolve silicate, the autumn phytoplankton peak simulated by the model is dominated by large phytoplankton analogous to diatoms (Figure 10.4). Excess concentration and high variability in modelled nitrogen concentrations in the TFZ could also result from inappropriate levels of denitrification and/or partitioning of fish farm waste as dissolved rather than particulate bound nutrient.

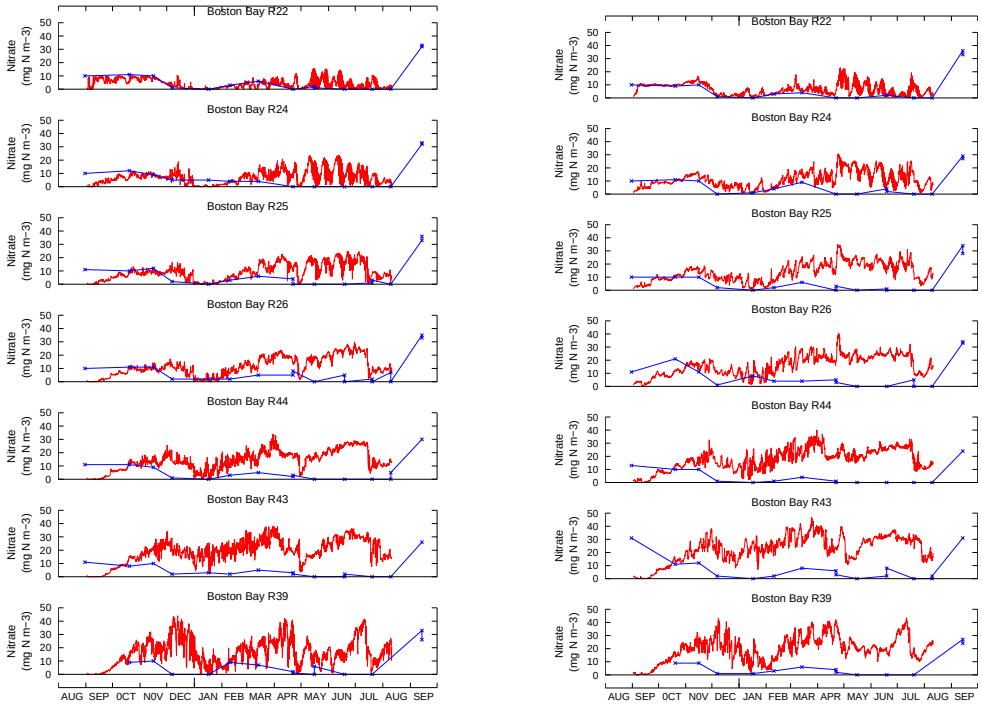

Figure 10.10. Surface (left) and bottom (right) dissolved inorganic nitrate concentrations from biogeochemical model simulation (red) and in-situ observations (blue) at sites throughout the TFZ.

Mooring configuration

There were 8 successful mooring deployments between August 2005 and August 2006 at 5 locations within the model domain (Table 10.6 and Figure 10.12a and b). Moorings were instrumented with an Acoustic Doppler current meter (ADCP), a Seabird multi-sensor which included a CTD, Wetlabs fluorometer, Optode dissolved oxygen sensor and photosynthetically active radiation (PAR) meter, and a transmissometer. Three additional moorings were deployed at the mouth of Spencer Gulf. These were instrumented with CTDs to constrain boundary conditions for the hydrodynamic model but they provided no biogeochemical measurements. Mooring data for temperature, salinity, and current meter observations are described in chapter 1 and for current meter and transmissometer observations in chapter 4.

The moored fluorescence, dissolved oxygen, PAR and turbidity sensors provided 3 time series records with high temporal resolution for comparison with the biogeochemical model. Sparse bottle samples were taken at mooring locations occasionally during the deployment periods but these were insufficient to calibrate the instruments. Moored data can therefore only be considered in relative terms to the model output and uncertainty remains in the quality of the data, for example due to episodic and/or progressive fouling of the instrument packages.

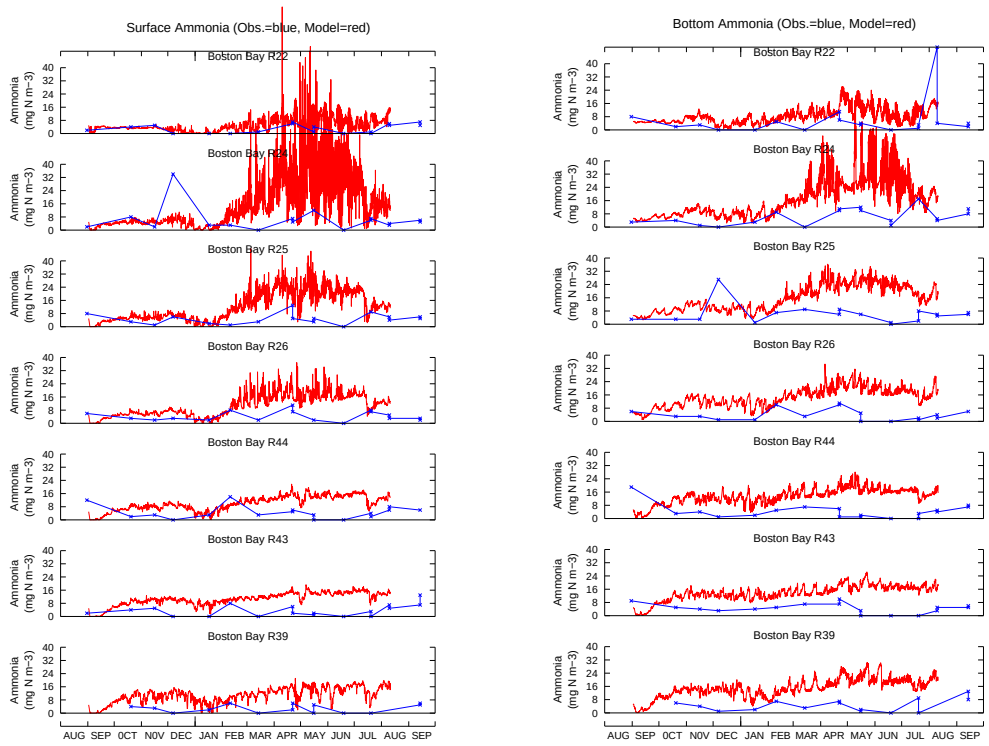

Figure 10.11. Surface (left) and bottom (right) ammonia concentrations from biogeochemical model simulation (red) and in-situ observations (blue) at sites throughout the TFZ.

Table 10.6. Successful mooring deployments within the TFZ.

Deployment	Start	End	Depth	Instrument Depth
Mooring 4a	31 Aug 05	11 Nov 05	24 m	~14 m
Mooring 5a	30 Aug 05	10 Nov 05	19 m	~18 m
Mooring 5b	17 Nov 05	11 Feb 06	20 m	~20 m
Mooring 4c	13 Feb 06	15 May 06	22 m	~10 m
Mooring 5c	13 Feb 06	15 May 06	20 m	~20 m
Mooring 4d	18 May 06	15 Aug 06	22 m	~10 m
Mooring 5d	18 May 06	15 Aug 06	20 m	~20 m
Mooring 6	18 May 06	15 Aug 06	20 m	~10 m

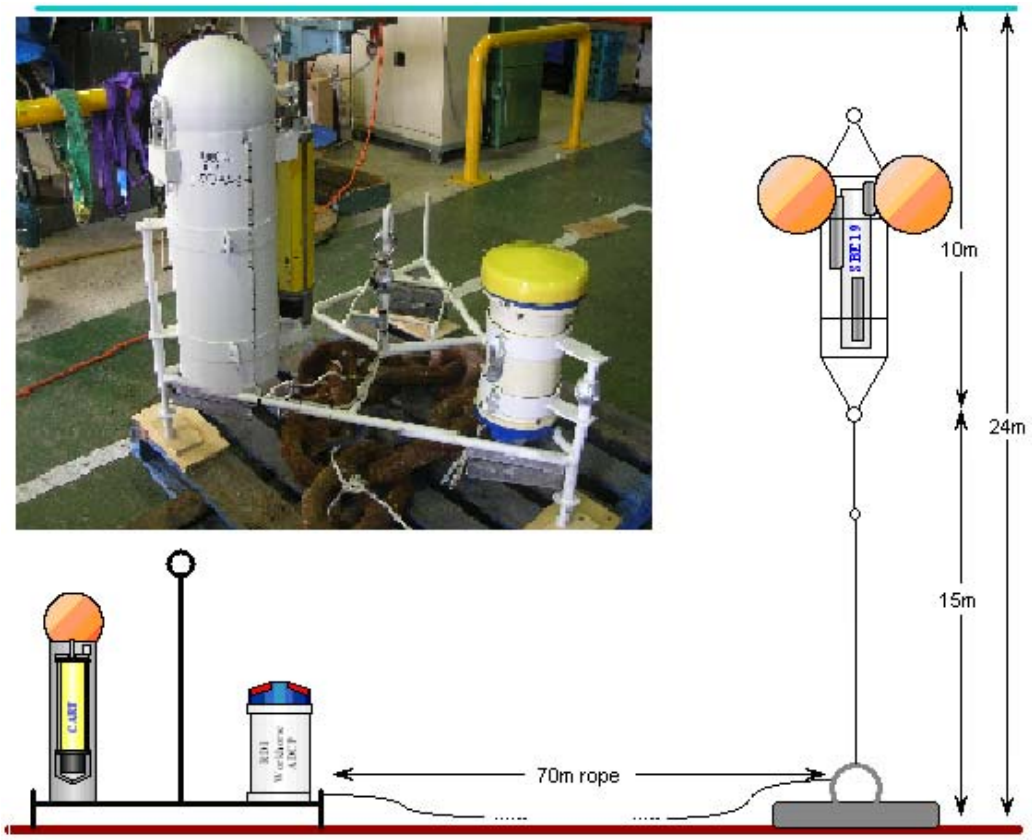

Figure 10.12(a). Moorings 4 and 6 were configured with an acoustic release, a bottom–mounted ADCP, a weight and a mid–water Seabird multi-sensor.

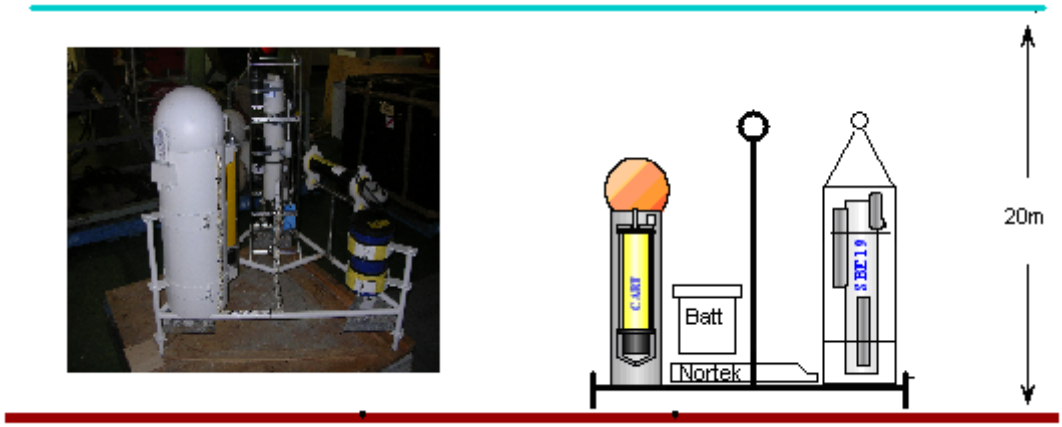

Figure 10.12(b). Mooring 5 was configured with an acoustic release, a bottom–mounted ADCP, a Seabird multi-sensor and transmissometer.

Mooring data: Chlorophyll, fluorescence and oxygen

The high temporal resolution of data from the moored instrumentation shows consistent diurnal variation in chlorophyll fluorescence (Figure 10.13). This may indicate consistent diurnal aggregation of phytoplankton for example by vertical migration of motile cells, but as the reduction of fluorescence was typically synchronised with high PAR intensity it is most

likely due to quenching of fluorescence when photosynthetic cells are subject to intense illumination. In this case, estimation of chlorophyll concentration from fluorescence is most reliable at low PAR intensity, or during night time, and so only these data were considered in the model data comparison.

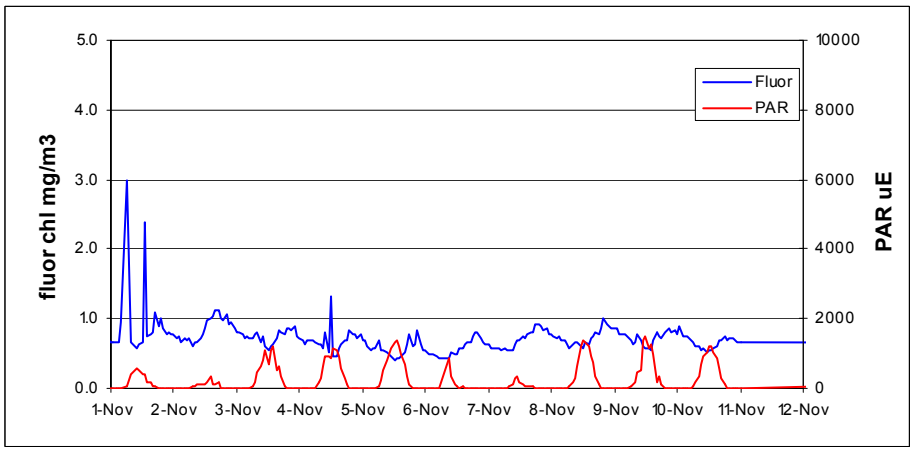

Figure 10.13. Mooring data from M4 showing fluorescence quenching during the daytime.

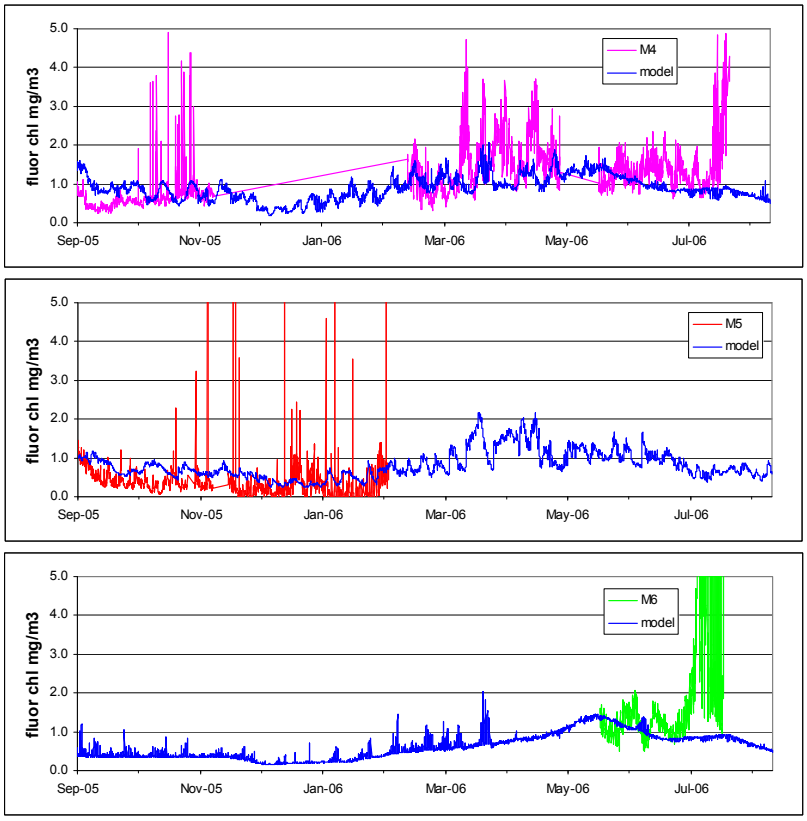

Figure 10.14. Uncalibrated moored fluorometer chlorophyll (with daytime values removed) and modelled chlorophyll for the same locations (M4, M5 & M6) and depths.

Chlorophyll concentrations from the moored fluorometer and the model are of similar magnitude with both showing a seasonal increase in concentration in autumn (Figure 10.14). Whilst the model shows variation in chlorophyll concentration over a tidal cycle of up to 1.5

mg m^{-3} the moored fluorometer shows fluctuations in excess of 3 mg m^{-3}. These fluctuations could result from the advection of small scale horizontal and/or vertical patches of increased chlorophyll concentration past the sensor, which are unresolved by the model grid.

The fluctuations in concentration recorded by the bottom mounted fluorometer at M5 are likely due to episodic resuspension of surface sediment containing microphytobenthos. The transport model advects and diffuses tracers using mean fluid velocities with a time step of 1 hour which makes it inherently difficult to simulate brief high intensity currents and accurately simulate resuspension events.

At M6 there was a significant increase in chlorophyll fluorescence towards the end of the mooring deployment in July 2006 which was also seen at M4. As no analogous increases in bottle chlorophyll concentration were recorded for the same period, this is likely due to fouling of the optical sensor.

Uncalibrated dissolved oxygen concentrations from the moored sensors were consistently lower than modelled concentrations for the same locations and depths (Figure 10.15). This may be due to bias in the sensor calibration and at M5 there may be some drift in the stability of the sensor or cumulative fouling. All records show a decline in concentration in late summer, when seasonal water temperature is maximal and limits dissolution of oxygen in water, and an increase in dissolved oxygen in winter. At M5 spikes of reduced concentration may be due to episodic resuspension of oxygen–depleted sediments, but this is not reproduced by the model.

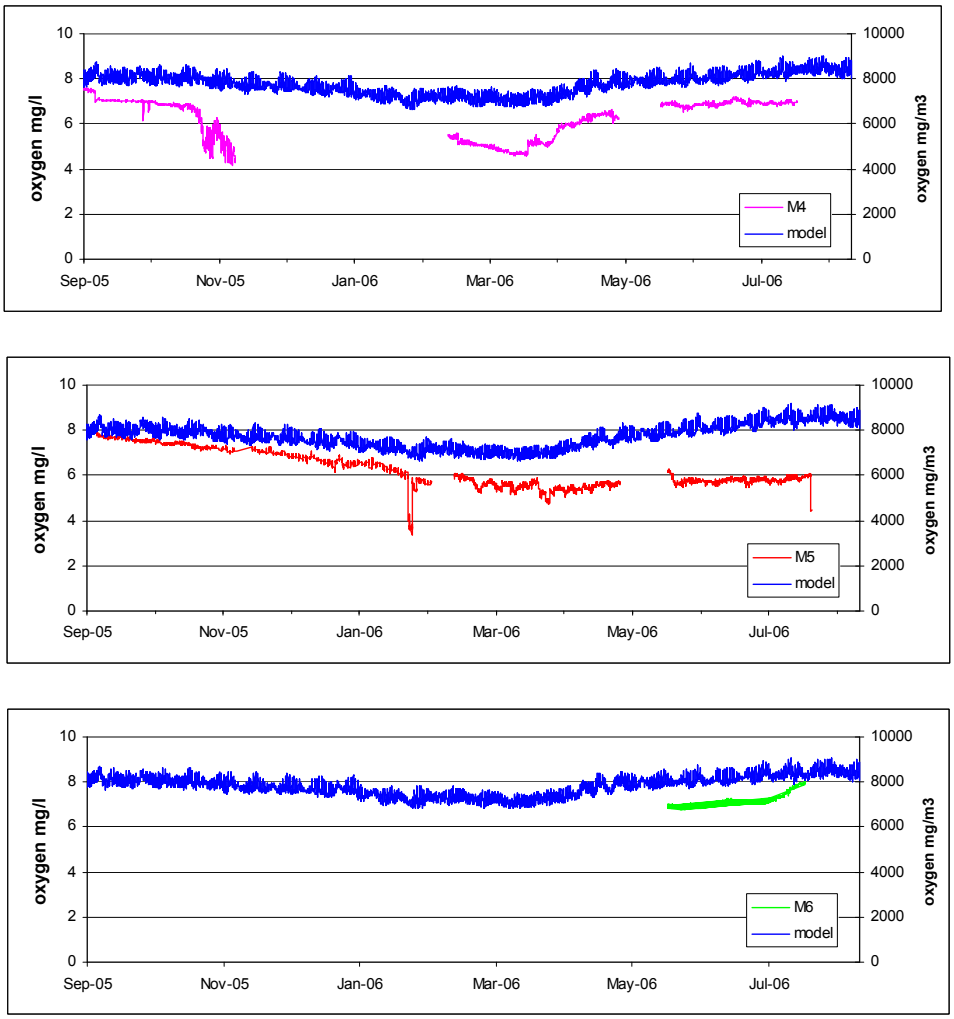

Figure 10.15. Uncalibrated moored dissolved oxygen concentration (mg L^{-1}) and modelled dissolved oxygen concentration for the same locations (M4, M5 & M6) and depths.

In a related Tasmanian study a similar biogeochemical model had a tendency to overestimate dissolved oxygen concentrations likely due to excessive ventilation of bottom waters associated with the relatively coarse resolution of the sea bed bathymetry (Wild-Allen et al., 2005). This is less here, where we use a much finer model resolution and a smoother bathymetry. However, the model skill at reproducing observed dissolved oxygen concentrations has not been fully verified.

Mooring data: PAR and turbidity

The uncalibrated PAR data from the shallow moored sensors at M4 and M6 and modelled data show a seasonal cycle with peak irradiance in summer (Figure 10.16). In deeper water the seasonal cycle is less apparent although modelled winter values are very low. Daily fluctuations in sensor PAR exceed those of modelled PAR which is provided as a 24 hour mean intensity. Gradual drift in the moored PAR data towards the end of each deployment likely reflects fouling of the sensor.

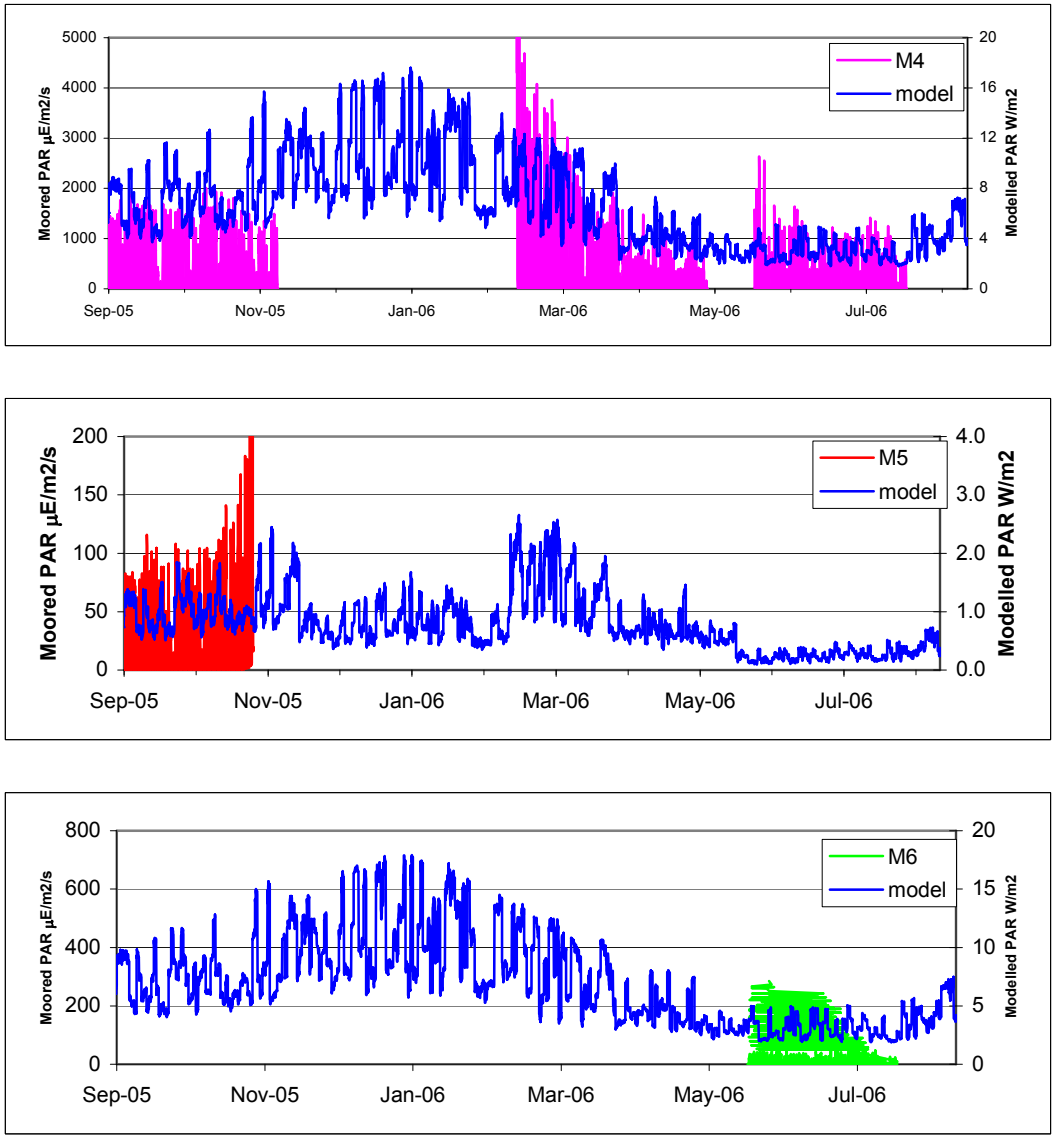

Figure 10.16. Uncalibrated moored PAR data (µE m^{-2} s^{-1}) and modelled PAR (W m^{-2}) for the same locations (M4, M5 & M6) and depths.

Moored turbidity data were bias–corrected for instrument offsets between deployments (Figure 10.17). Data from M6 suggests that the instrument was fouled or buried in July 2006. M4 and M5 mooring data show brief peaks of elevated turbidity throughout the year at both the bottom–mounted and mid–water sensor. This suggests frequent resuspension of bottom sediment throughout the water column followed by rapid settling. These processes are unresolved by the transport model and hence the modelled attenuation coefficient remains virtually constant throughout the year.

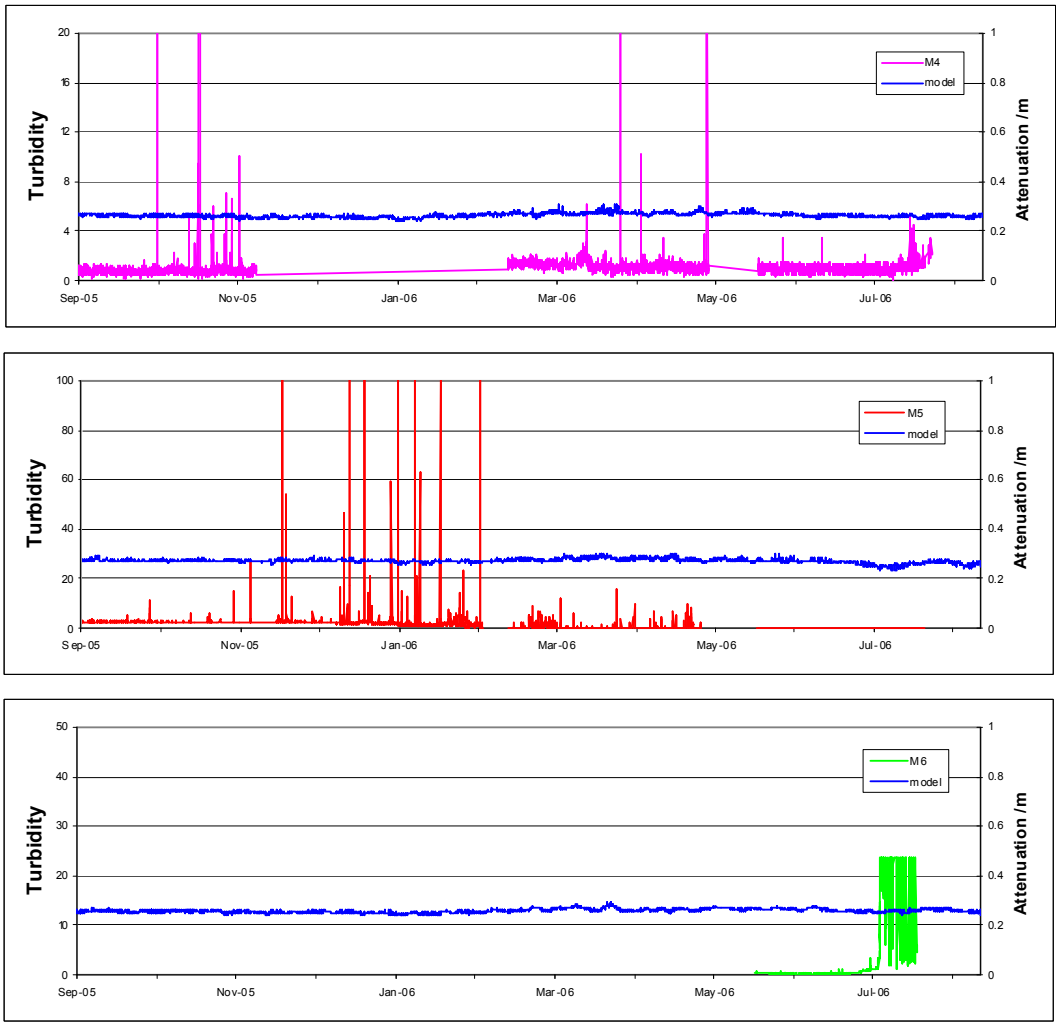

Figure 10.17. Uncalibrated turbidity from the moored transmissometer and modelled attenuation coefficient (m^{-1}) for the same locations (M4, M5 & M6) and depths.

10.3.1. Calibration summary

The model was able to reproduce the seasonal dynamics of observed phytoplankton chlorophyll, and with slightly less accuracey, DIP. However, uncertainty remains in the observed biogeochemistry of the region which appears to experience nutrient limitation by phosphorus, nitrogen and silica at different times of the year. Inshore modelled nitrogen concentrations were generally higher than observed possibly due to inappropriate levels of denitrification and/or partitioning of fish farm waste as dissolved rather than particulate bound nutrient. Simulated dissolved oxygen concentrations were also higher than observed by moored sensors which showed greater seasonal draw-down of oxygen in late summer than captured by the model. Finally the model was unable to reproduce resuspension events recorded by moored sensors in the TFZ, which means that it may underestimate sediment ventilation of pore water and overestimate light propagation and availability for photosynthesis during resuspension events. Whilst the cumulative sum of periods of resuspension is small, such events could have a significant effect on the biogeochemistry of the region.

10.4. Results: Modelled seasonal pelagic biogeochemistry

10.4.1. Pelagic chlorophyll and oxygen dynamics

Throughout summer and late winter the model results showed relatively low concentrations of surface chlorophyll (≤ 1 mg m^{-3}, Figure 10.18). The highest monthly mean surface chlorophyll values occurred in autumn, when chlorophyll concentrations doubled (Figure 10.18). The autumn phytoplankton peak as predicted by the model, was dominated by large phytoplankton. In the model, large phytoplankton are parameterised as fast growing, opportunistic species, able to quickly utilise nutrients which are attributes characteristic of diatom species. The model results therefore agree with the magnitude and timing of the observed diatom peak.

In deep water, modelled chlorophyll concentrations were lower than surface waters as there was insufficient light for in-situ growth (Figure 10.19). Model results showing transect profiles across the SBT farming zone used the CTD transect points (Figure 10.7). The chlorophyll transect (Figure 10.20) demonstrates the progression of the diatom peak to deeper in the water column.

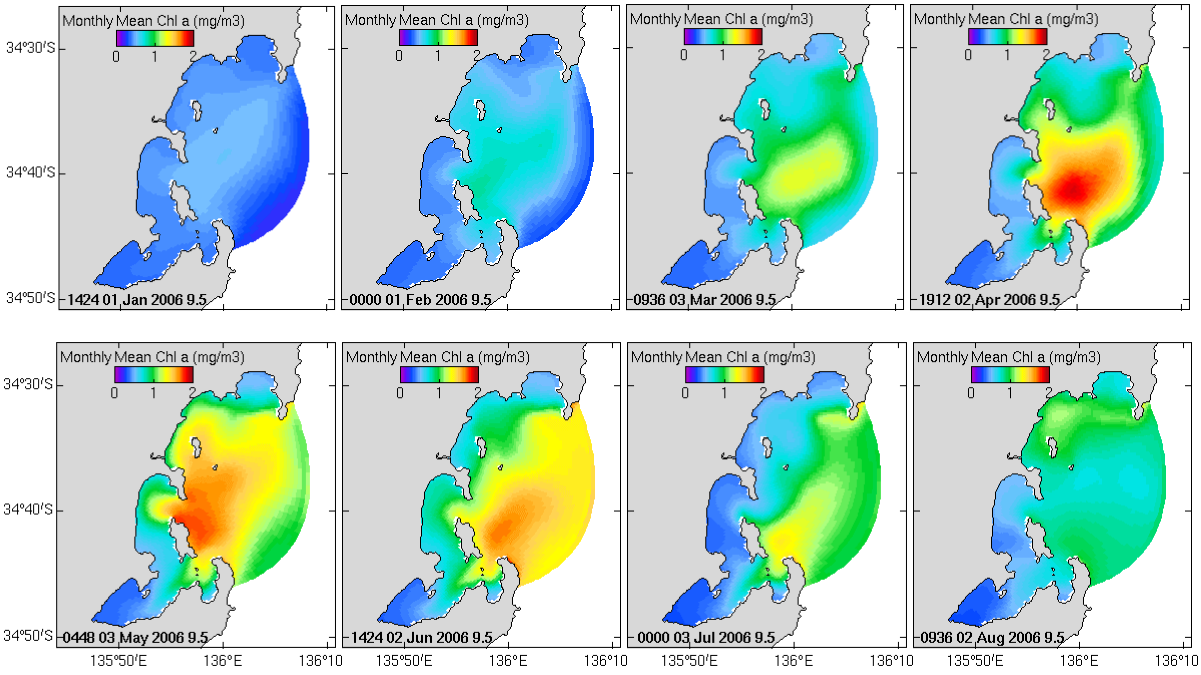

Figure 10.18. Monthly mean surface chlorophyll-*a*

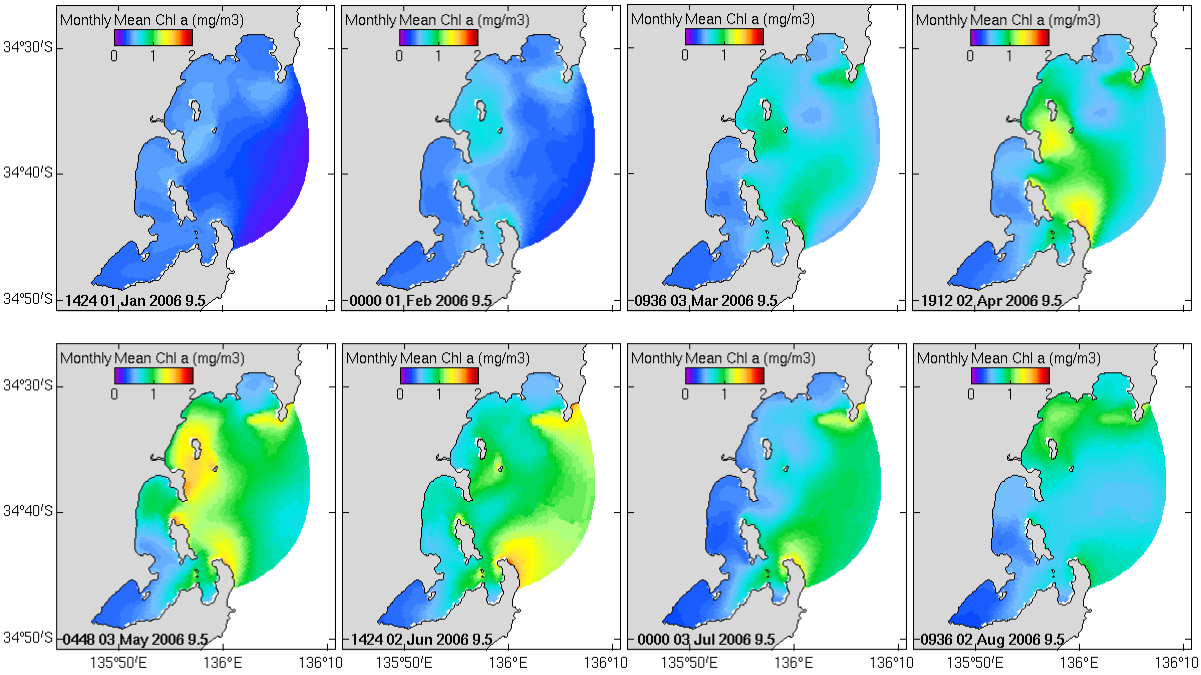

Figure 10.19. Monthly mean bottom water chlorophyll-*a* concentration.

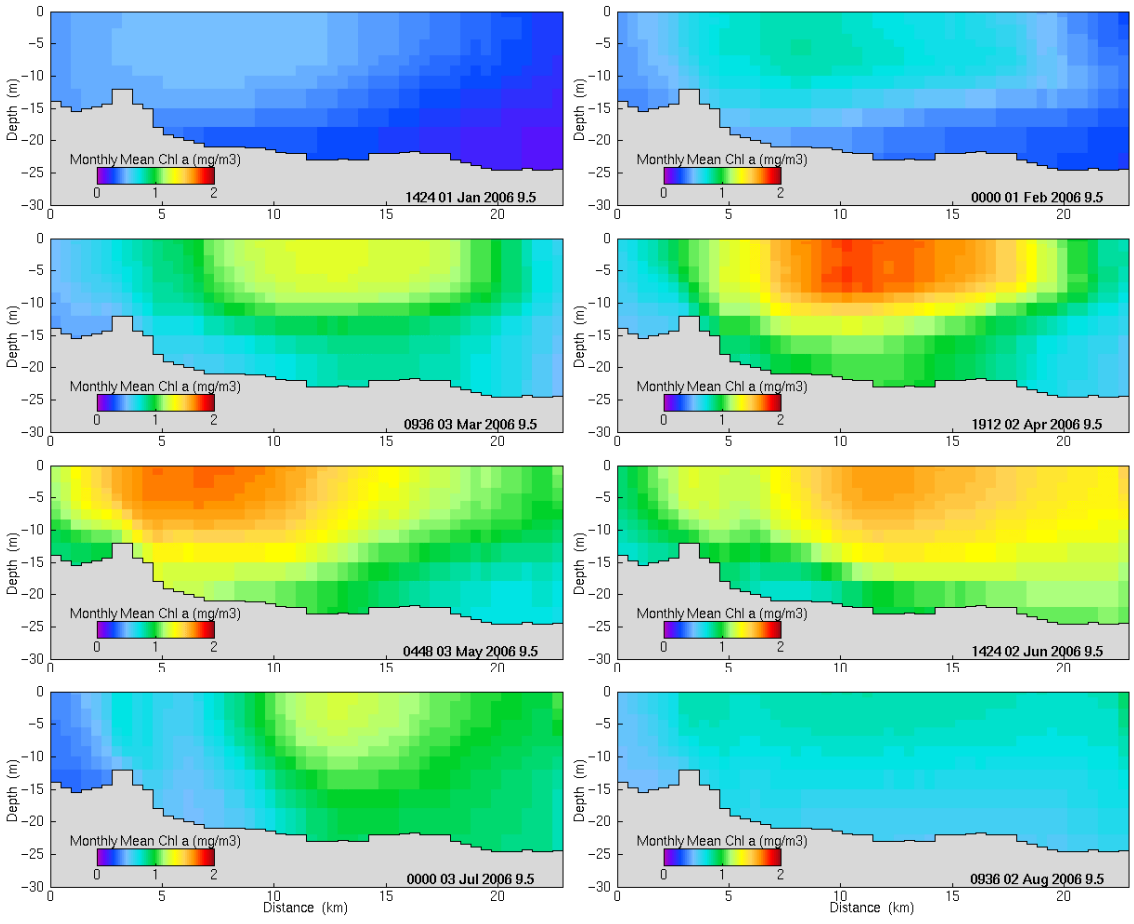

Figure 10.20. Monthly mean chlorophyll-*a* concentration along CTD transect (Figure 10.7) from west (left) to east (right).

Percent oxygen saturation for the model time period was generally high throughout the region as most of the model system is well flushed (Table 1.2). Higher mean oxygen percent saturation for bottom waters at the open boundary was due to hydrodynamic circulation from outer waters into the model domain (Figure 10.21). This is particularly evident around Cape Donnington early in the year, with incoming water having an oxygen satuaration > 100% moving into the TFZ. Modelled oxygen concentrations were higher than observed for the same locations and depths (Figure 10.15). Percent oxygen saturation increased in the surface waters in summer and autumn as surface waters became supersaturated with oxygen produced by phytoplankton photosynthesis (Figure 10.22). Percent oxygen saturation was also lower during winter in the bottom waters near the inshore sites (Figure 10.22). This draw-down of oxygen saturation at depth may be associated with benthic oxygen demand for remineralisation of organic detritus.

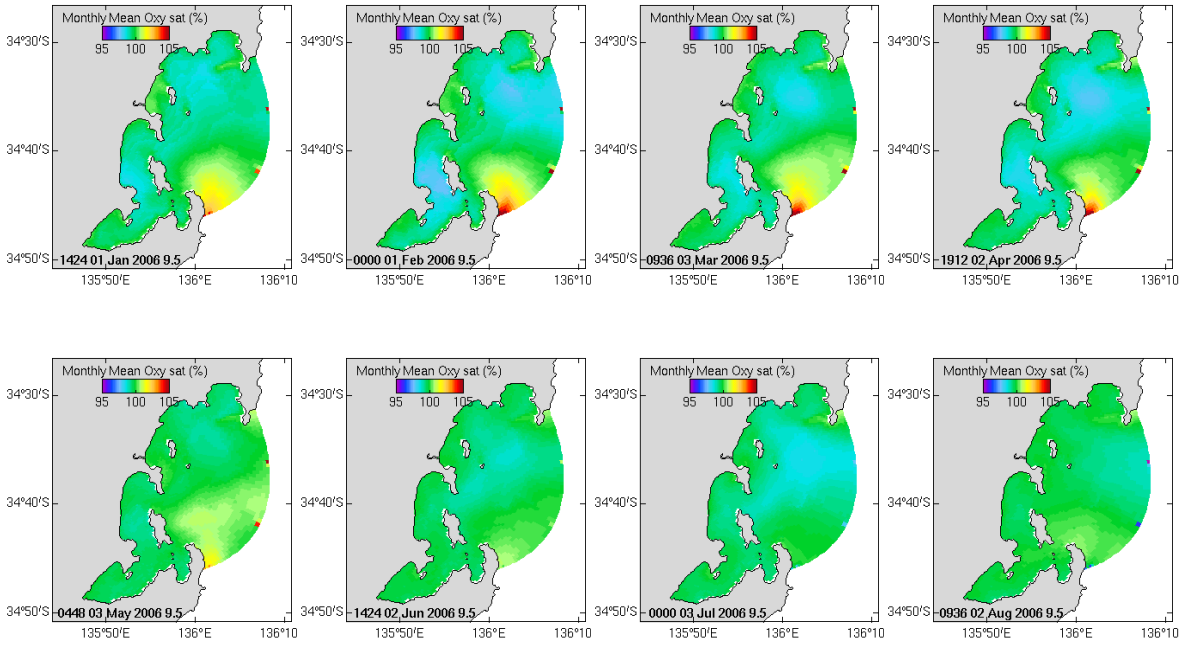

Figure 10.21. Monthly mean bottom water dissolved oxygen (DO) saturation.

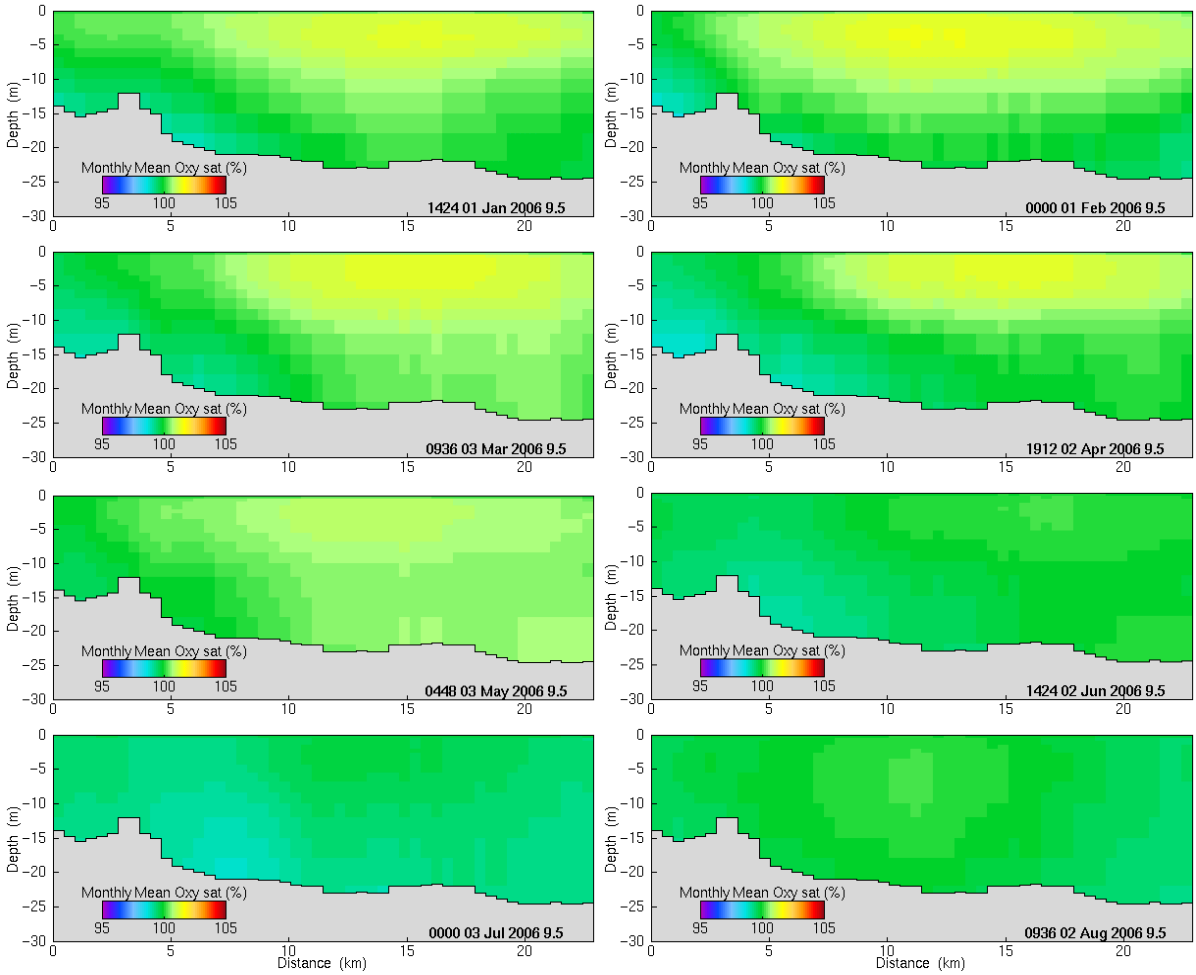

Figure 10.22. Monthly mean dissolved oxygen (DO) saturation along CTD transect (Figure 10.7) from west (left) to east (right).

10.4.2. Pelagic nutrient dynamics

In summer, surface nitrogen and phosphorus concentrations were depleted throughout the offshore region due to phytoplankton assimilation (surface DIN ≤ 25 mg m^{-3} Figure 10.23 and Figure 10.25; surface DIP ≤ 1 mg m^{-3} Figure 10.26 and Figure 10.27). In areas away from the fish farms in autumn there was a slight reduction in dissolved inorganic nitrogen (DIN) in the surface waters compared with bottom waters (bottom DIN ~ 40 mg m^{-3} *cf.* surface ~ 25 mg m^{-3}; Figure 10.25). Waters entering from outside the model domain had low nitrogen levels so DIN was not elevated in offshore regions throughout the model time period.

Dissolved inorganic phosphorus (DIP) was highest in areas surrounding fish farms (surface ≥ 4 mg m^{-3}) and lowest in the embayments and near–shore areas (≤ 1mg m^{-3}; Figure 10.26), although at least some of this seems to be coming in across the open boundary of the model. At inshore sites the model underestimated the observed concentration of DIP possibly due to omission of coastal sewerage treatment plant (STP) or catchment loads.

High NH_x (NH_3 + NH_4) levels (≥ 40 mg m^{-3}) were observable as hotspots near fish farms in the model transect from April through to July (Figure 10.29). Bottom water model results for NH_x also show hotspots in the vicinities of fish farms from May though to July (≥ 30 mg m^{-3},

Figure 10.28). Higher levels are observable in bottom waters of Proper Bay, but these results could not be confirmed, as observations were not taken.

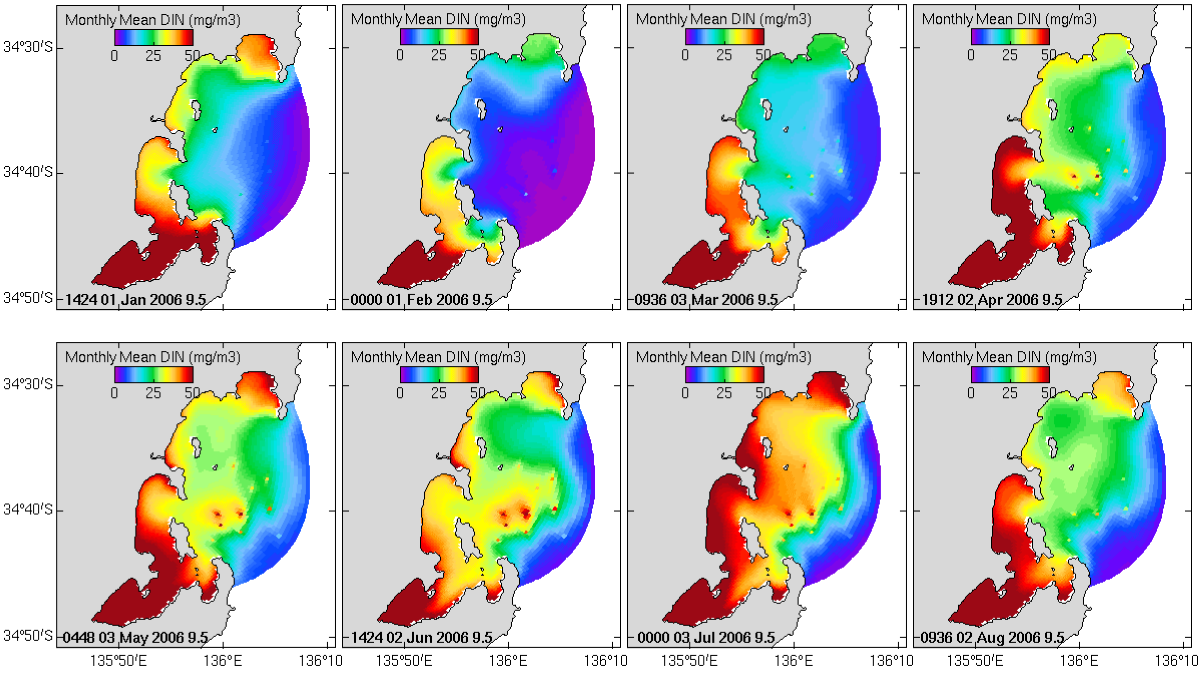

Figure 10.23. Monthly mean surface dissolved inorganic nitrogen (DIN).

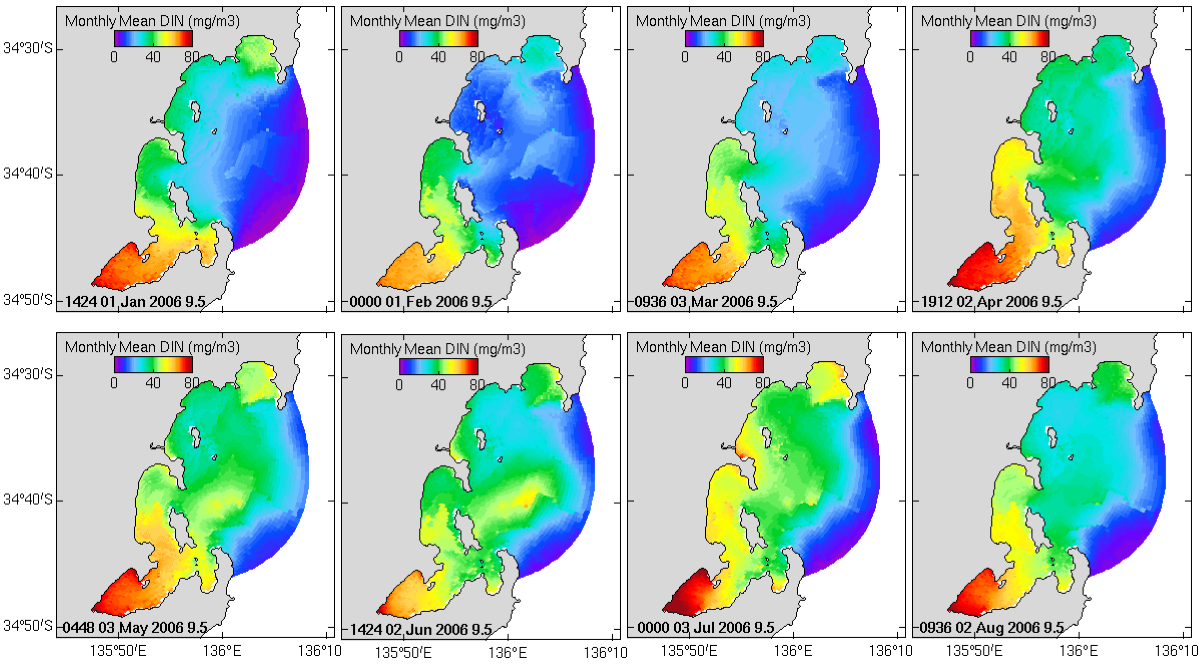

Figure 10.24. Monthly mean bottom water dissolved inorganic nitrogen (DIN).

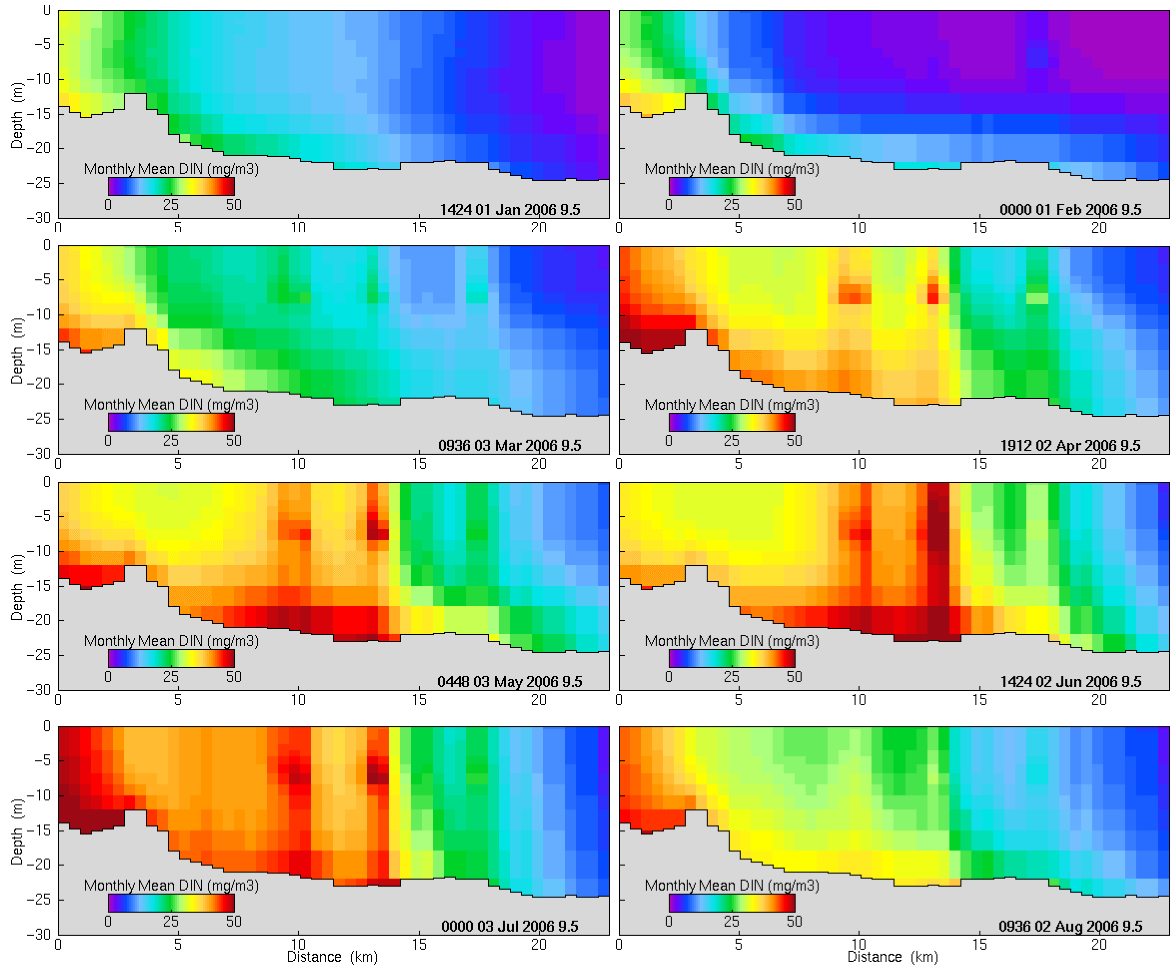

Figure 10.25. Monthly mean dissolved inorganic nitrogen (DIN) concentration along CTD transect (Figure 10.7) from west (left) to east (right).

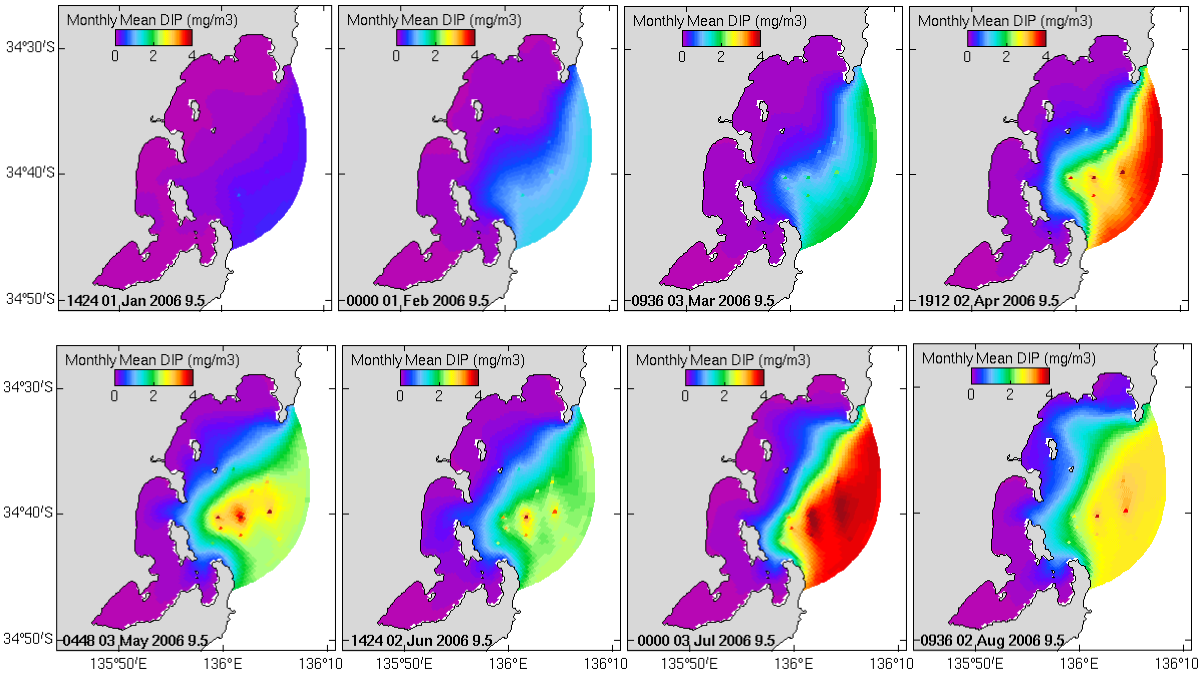

Figure 10.26. Monthly mean surface dissolved inorganic phosphorus (DIP).

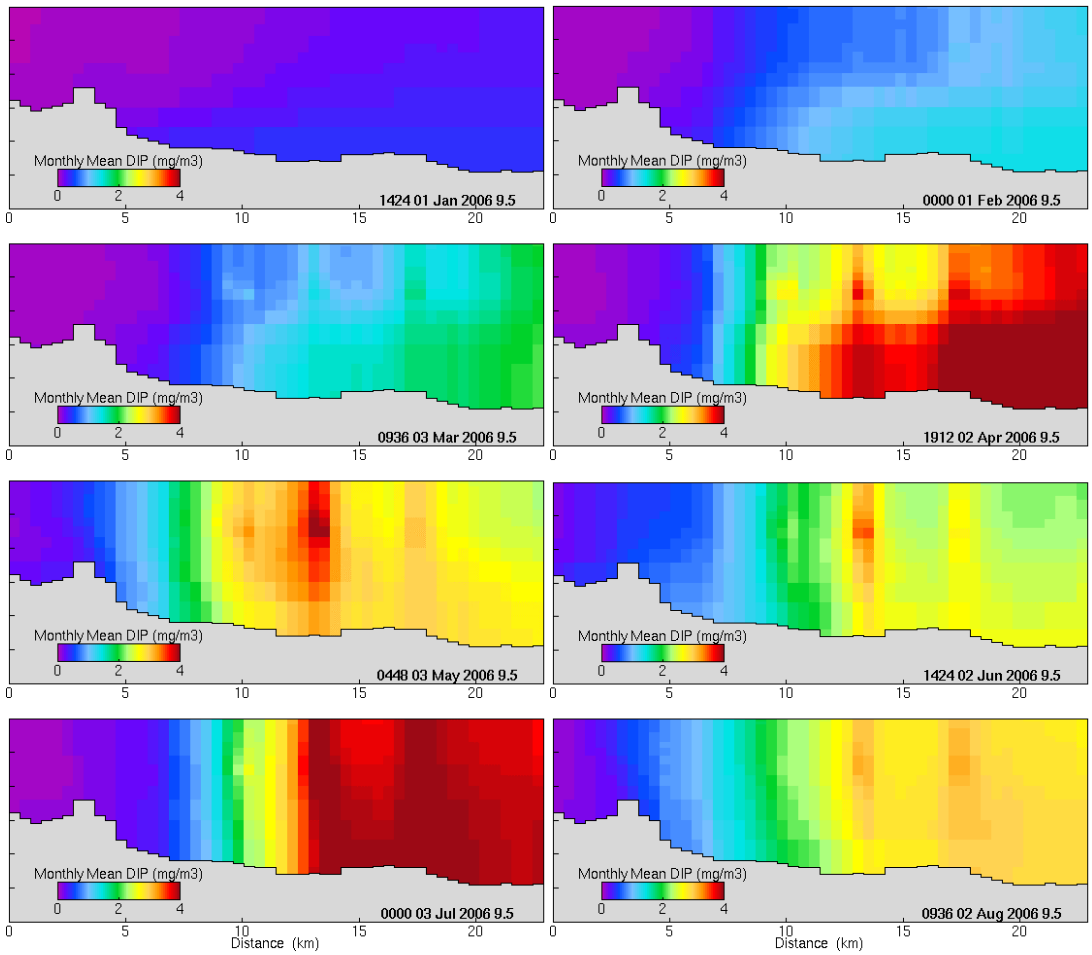

Figure 10.27. Monthly mean dissolved inorganic phosphorus (DIP) concentration along CTD transect (Figure 10.7) from west (left) to east (right).

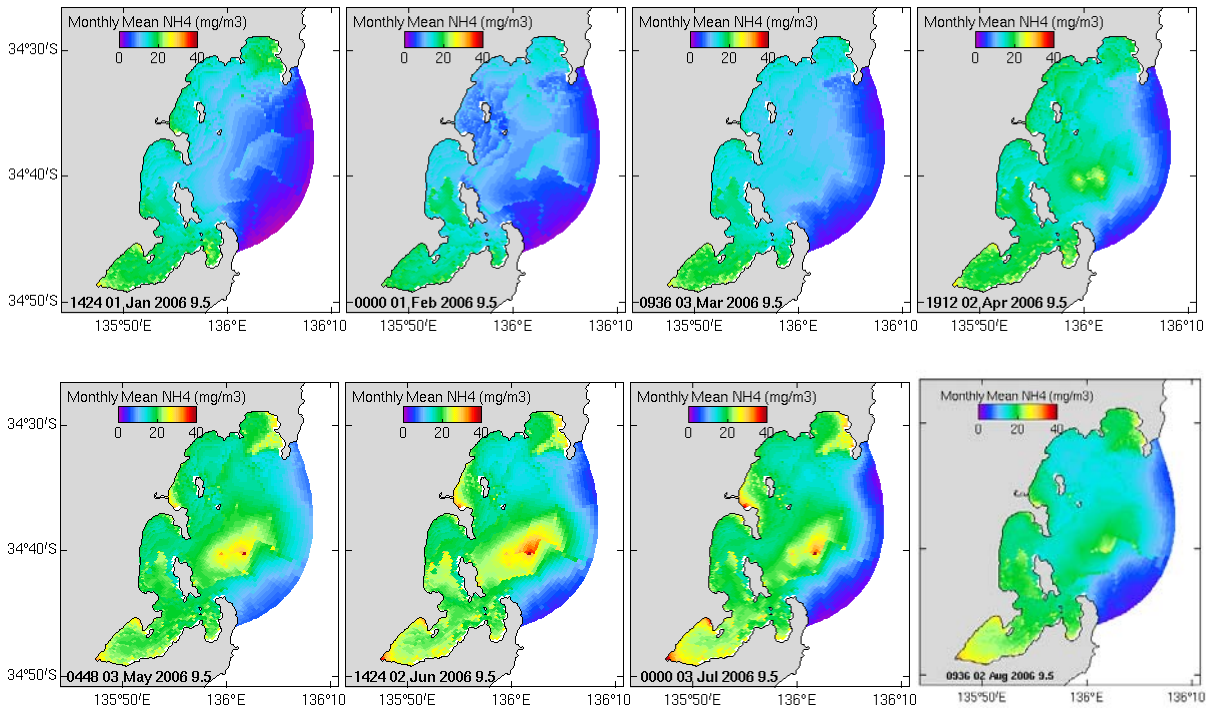

Figure 10.28. Monthly mean bottom water ammonium (NH_x).

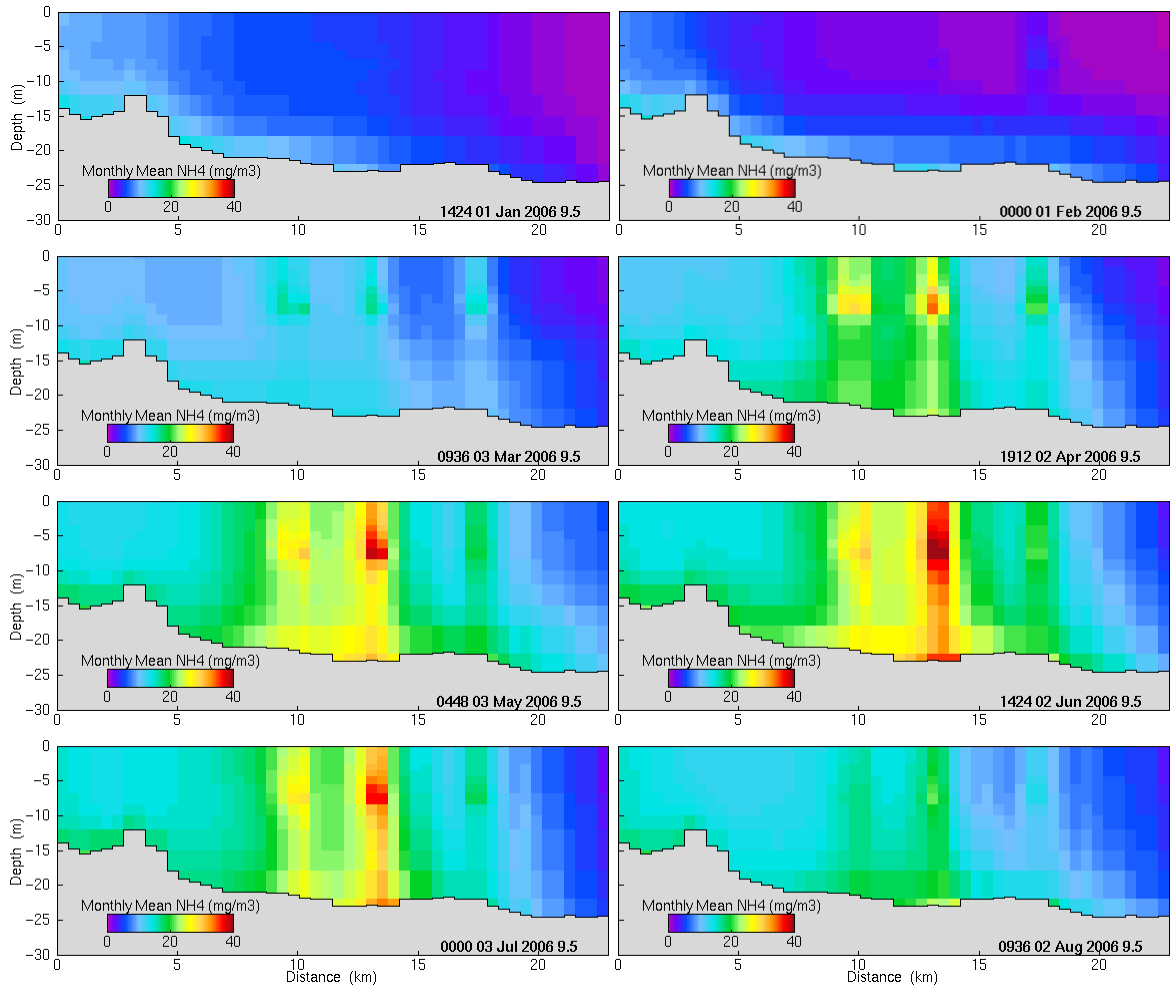

Figure 10.29. Monthly mean ammonium (NH_x) concentration along CTD transect (Figure 10.7) from west (left) to east (right).

10.4.3. Fish farm impacts on pelagic nutrients, chlorophyll and oxygen

The maximum nutrient loads due to feed input from the farms (Figure 10.5) occurred at the time of the autumn diatom peak (Figure 10.18). From April to July, higher levels of DIN (≥ 50 mg m^{-3}; Figure 10.23 and Figure 10.25), NH_x (≥ 40 mg m^{-3}; Figure 10.28 and Figure 10.29) and DIP (≥ 4 mg m^{-3}; Figure 10.26) were observed in the model results as hotspots in the surface and bottom waters and in the transect profile in the areas around the fish farms. The model transect profile also show increased nitrogen moving to depth from surface waters (Figure 10.25), and possibly into near-shore areas and bays. DIP showed a similar shift from the surface waters to depth (Figure 10.27). However, the model was not validated in near–shore areas as there were no observations to calibrate against.

The number of months and percent of region impacted are shown in the charts analysing fish farm impact on pelagic depth integrated DIN, DIP, chlorophyll and bottom water dissolved oxygen (DO) saturation (Figure 10.30). For example, for 1 month of the year 59% of the region had a DIN value 50% above the baseline attributable to fish farm impact and for 6 months of the year 16 % of the region had a DIN value 50% above the baseline attributable to fish farm impact. Likewise the analysis showed that 23% of the region had a chlorophyll value 20% above the baseline for 3 months of the year. The SBT farm impact on bottom water oxygen saturation was negligible according to the model analysis

The regional classification based on annual mean pelagic chlorophyll concentration in the upper 12 m of the water column demonstrates the water column changes from 100 % oligotrophic with no SBT farms to 98 % oligotrophic and 2 % mesotrophic when SBT farms are included (Table 10.7). This is based on the scheme of Smith et al (1998).

Table 10.7. Regional classification based on annual mean pelagic chlorophyll concentration in upper 12 m of the water column after Smith et al. (1998) (SBT: Southern Bluefin Tuna).

	Oligotrophic	Mesotrophic	Eutrophic
No SBT Farms	100 %	0	0
Including SBT Farms	98 %	2 %	0

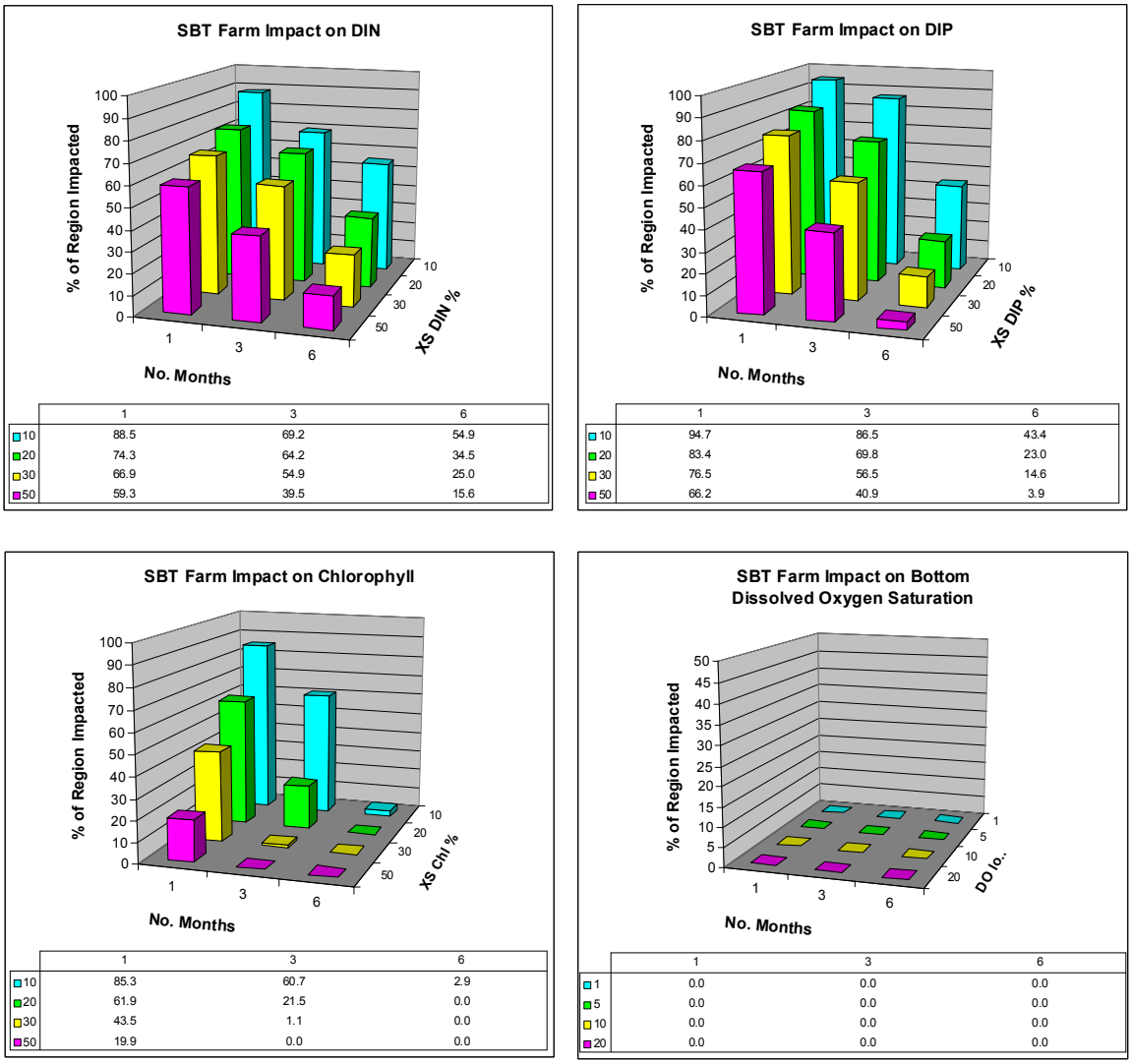

Figure 10.30. Fish farm impact on pelagic depth integrated DIN, DIP and chlorophyll, and bottom water dissolved oxygen saturation. XS – increase in nutrient above what the model predicts without farm inputs. The table at the bottom of each panel indicates the percentage of the year for which levels are at least y % (y = 10, 20, 30, 50 except for DO where y= 1, 5, 10, 20) above ambient for at least x months (x = 1, 3, 6).

10.5. Results: Seasonal epibenthos and sediment

10.5.1. Sediment properties

The model simulated the growth of seagrass in areas where there was sufficient illumination of the surface sediment (Figure 10.31). The microphytobenthos impact includes reduced chlorophyll in some areas due to increased light attenuation (Figure 10.32).

10.5.2. Fish farm impacts on sediment properties

The monthly DO concentrations in the surface sediments were lower in areas surrounding the fish farms (Figure 10.33). NH_x, DIN and DIP in surface sediments were also higher and showed observable hotspots where fish farms were located (Figure 10.34 to Figure 10.36). Figures depicting excess monthly mean depth integrated DIN, DIP and chlorophyll and reduction of DO due to fish farm waste loads also show the influence of farms with observable hotspots near fish farm locations (Figure 10.37 to Figure 10.40).

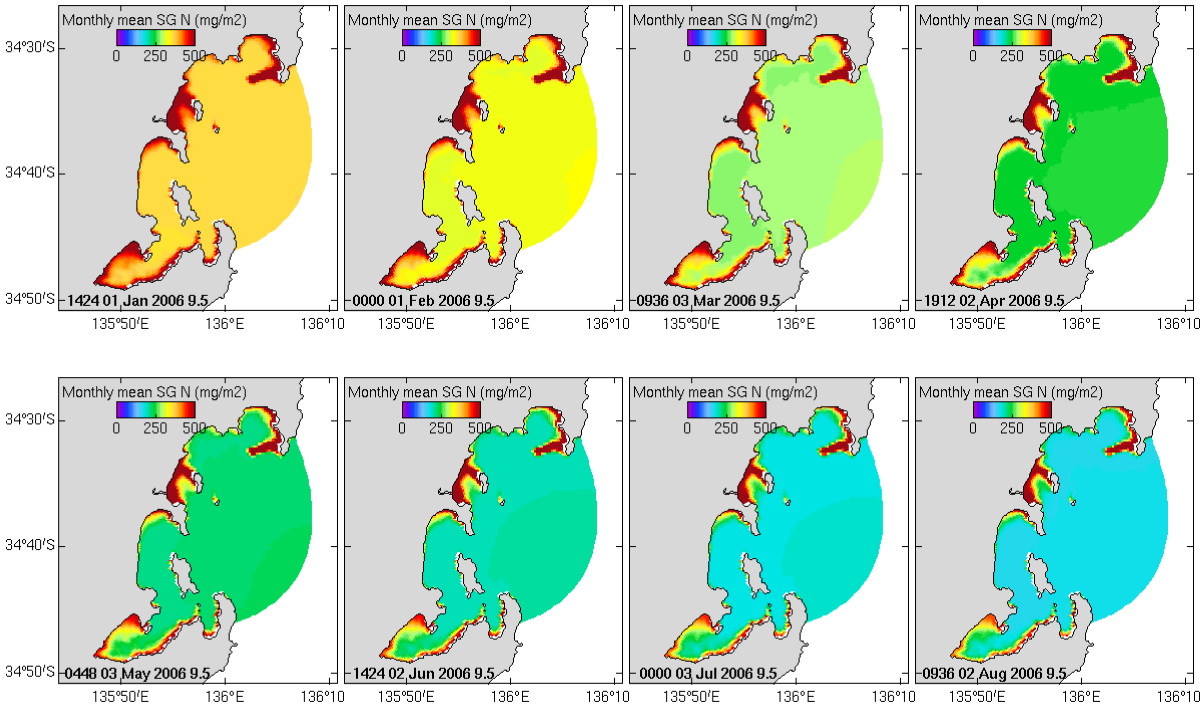

Figure 10.31. Monthly mean seagrass nitrogen.

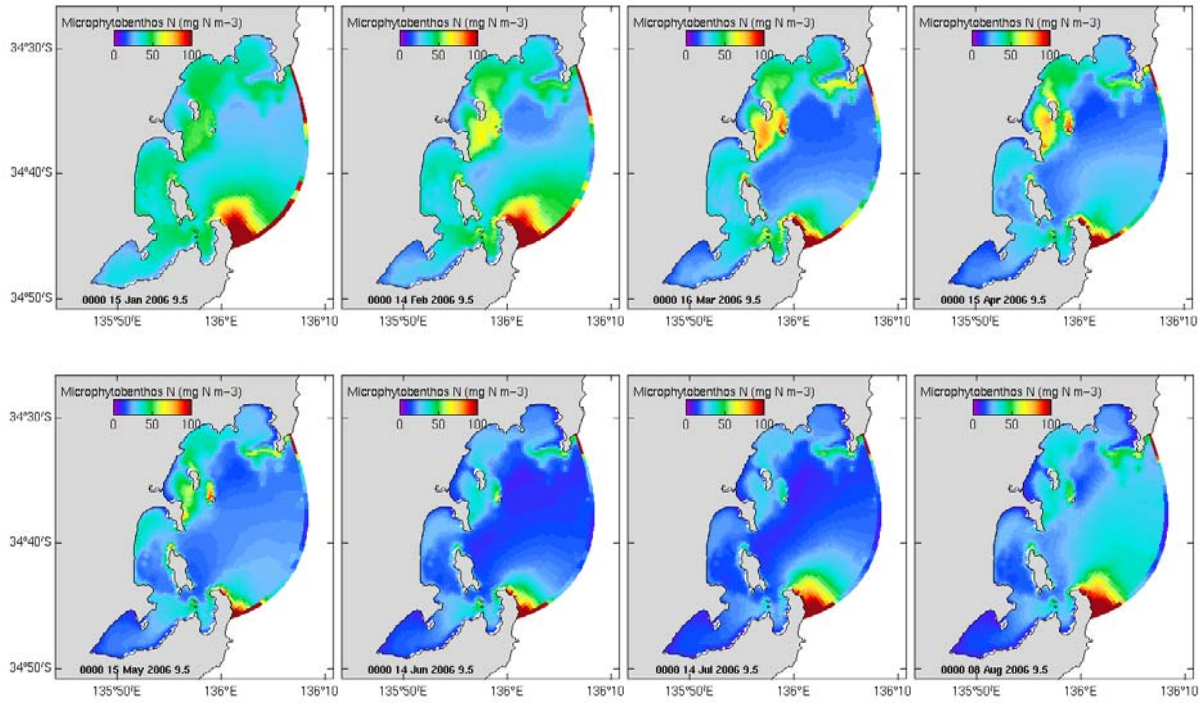

Figure 10.32. Monthly snapshots of microphytobenthos nitrogen in the surface sediment (correct units are mgN m^{-2}).

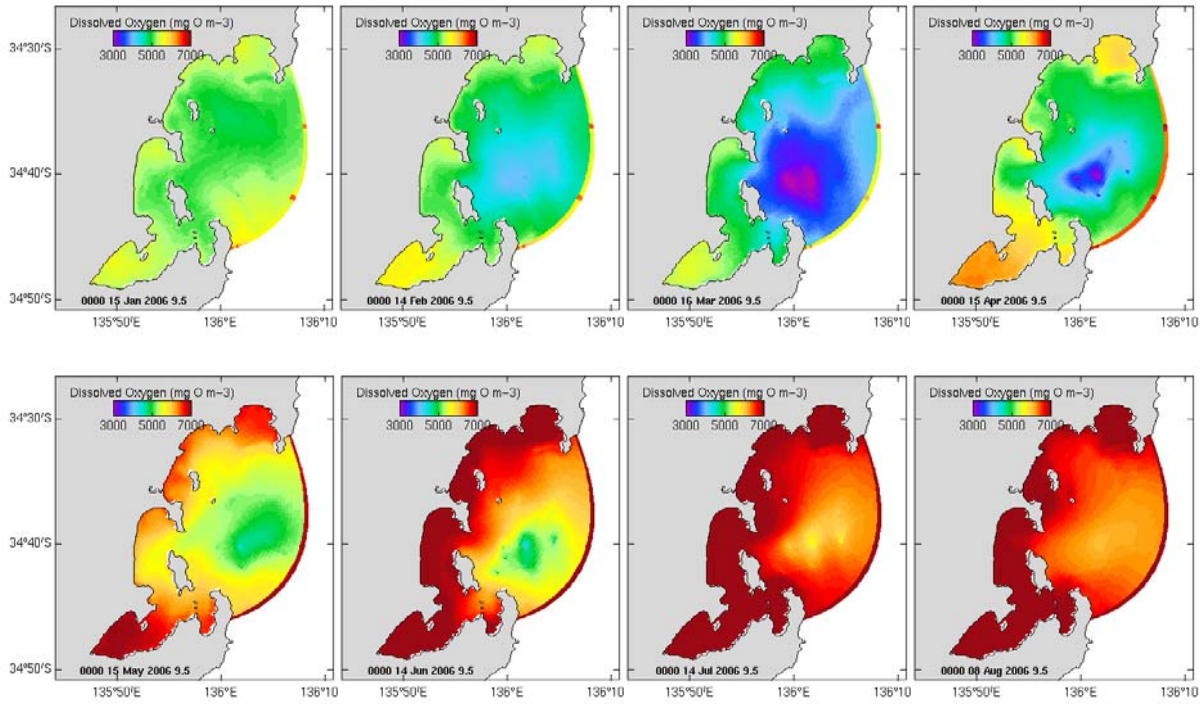

Figure 10.33. Monthly snapshots of dissolved oxygen (DO) concentration in the surface sediment.

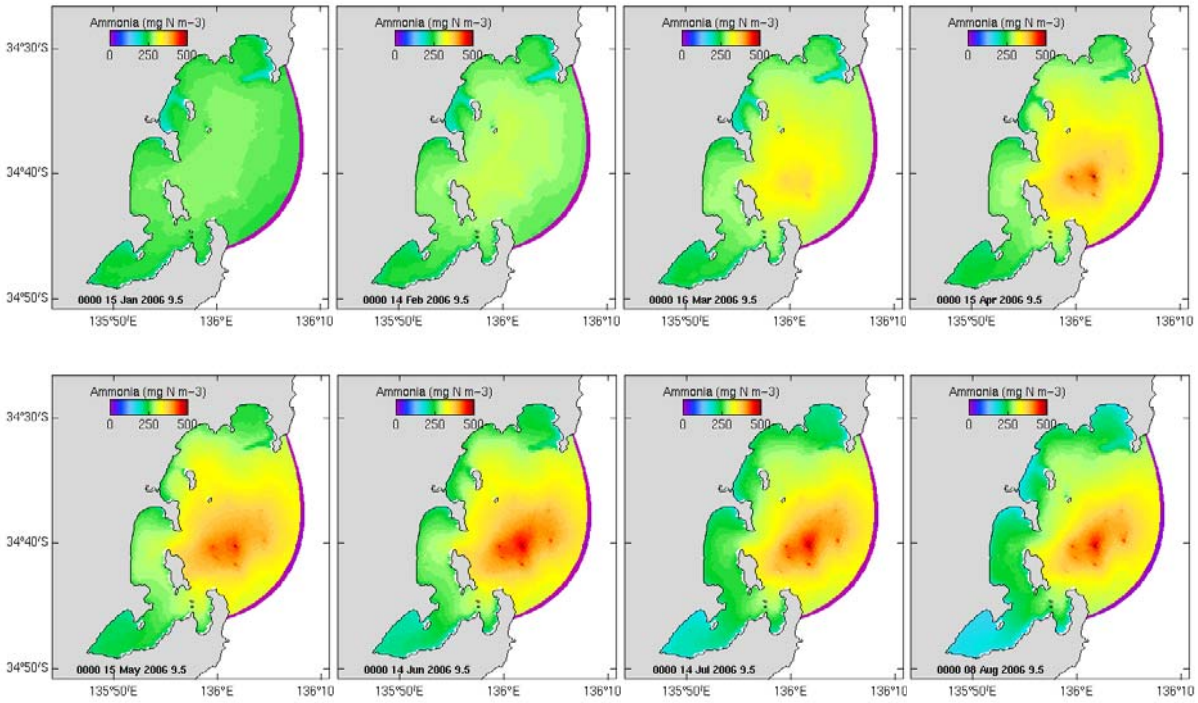

Figure 10.34. Monthly snapshots of ammonia (NHx) in surface sediment.

The excess DIN in surface sediment due to fish farm waste loads showed hotspots around the farms from April through to August (Figure 10.35). To a lesser extent DIP increased around the fish farm areas from March to July (Figure 10.36). In some areas the "excess chlorophyll" in surface sediment due to fish farm waste loads was actually "reduced chlorophyll" (Figure 10.43) due to fish farm waste loads decreasing light attenuation and therefore lowering photosynthesis. Surface sediment chlorophyll was reduced by up to 0.6 mg m^{-3} in April in the outer reaches of the TFZ in the model run with fish farm loads. In other months the reduction in sediment chlorophyll in the model run without farm loads was smaller. Similarly DO was reduced in surface sediments due to fish farm waste loads in areas surrounding the fish farms from March through to June (Figure 10.44).

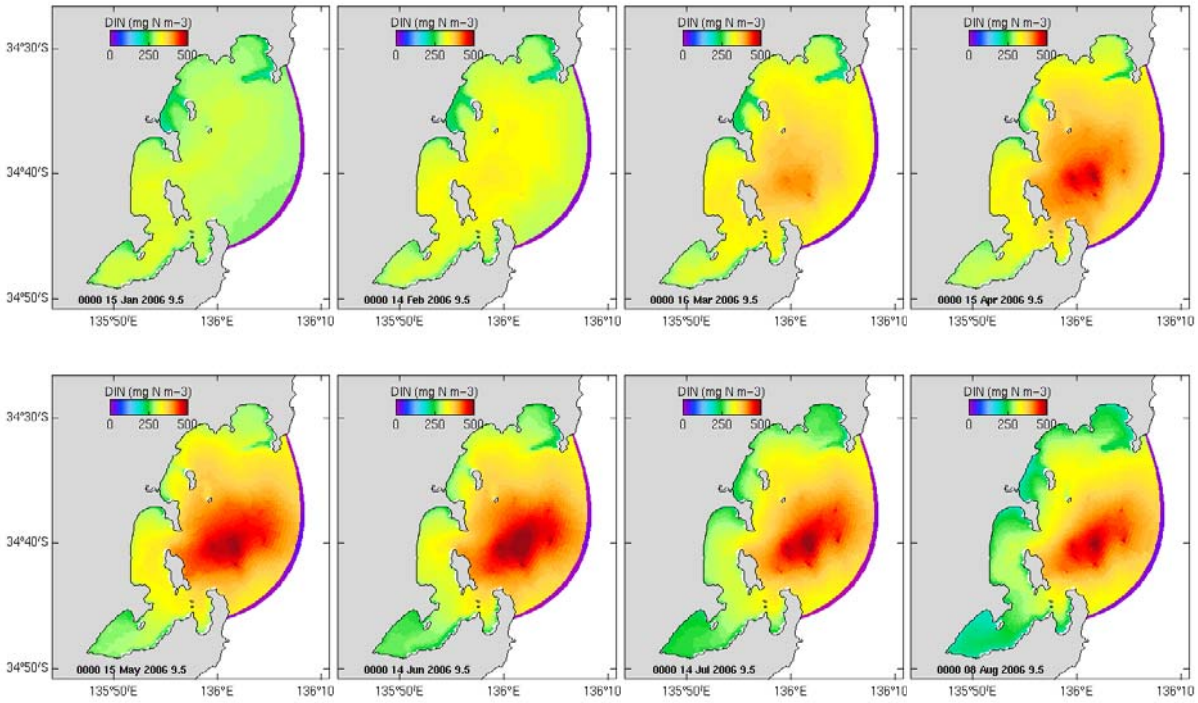

Figure 10.35. Monthly snapshots of dissolved inorganic nitrogen (DIN) in surface sediments.

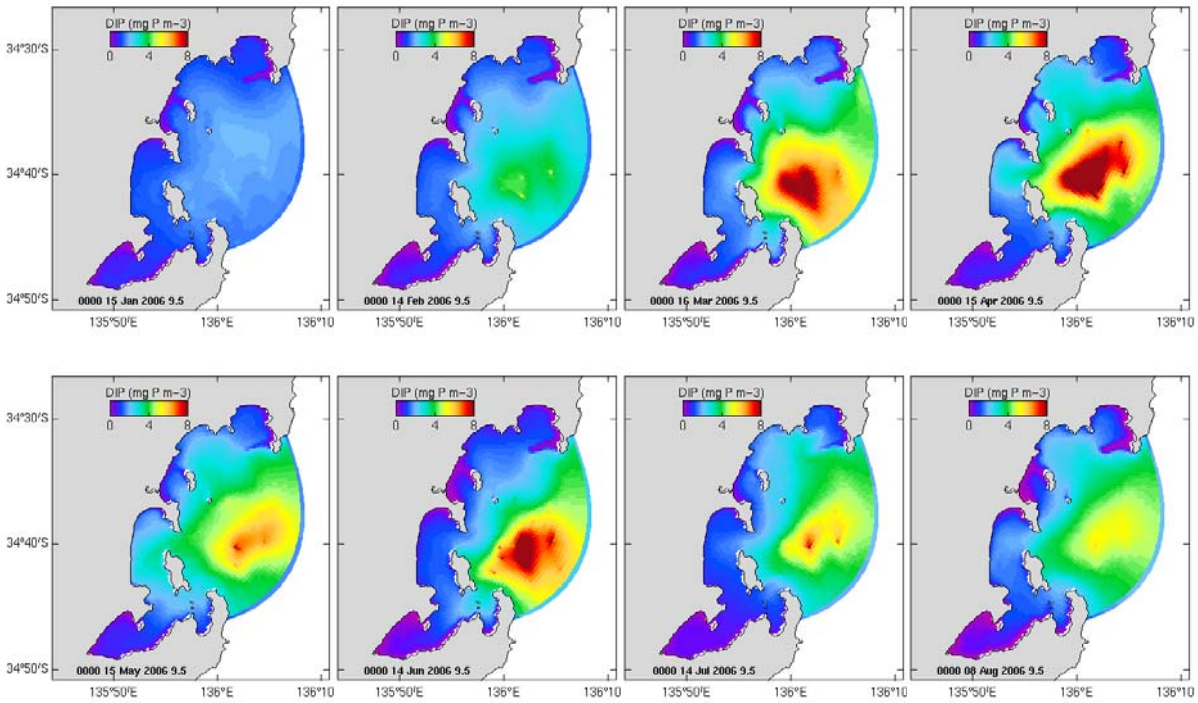

Figure 10.36. Monthly snapshots of dissolved inorganic phosphorus (DIP) in surface sediment.

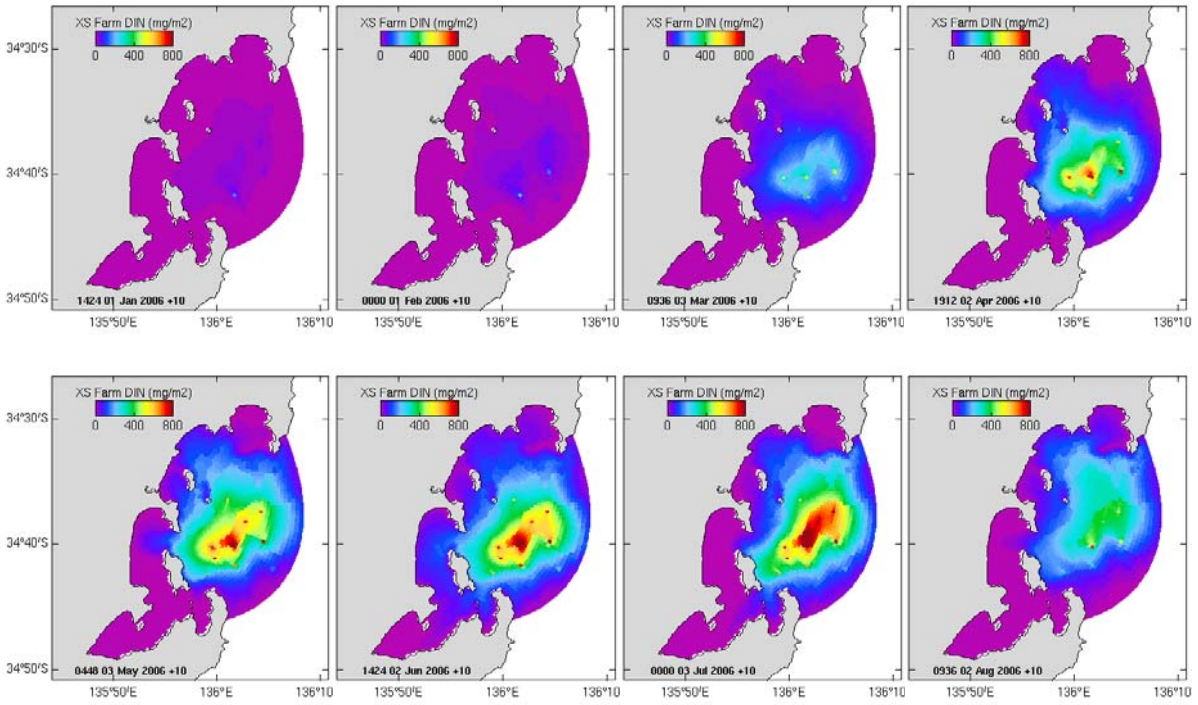

Figure 10.37. Excess monthly mean depth integrated dissolved inorganic nitrogen (DIN) due to fish farm waste loads.

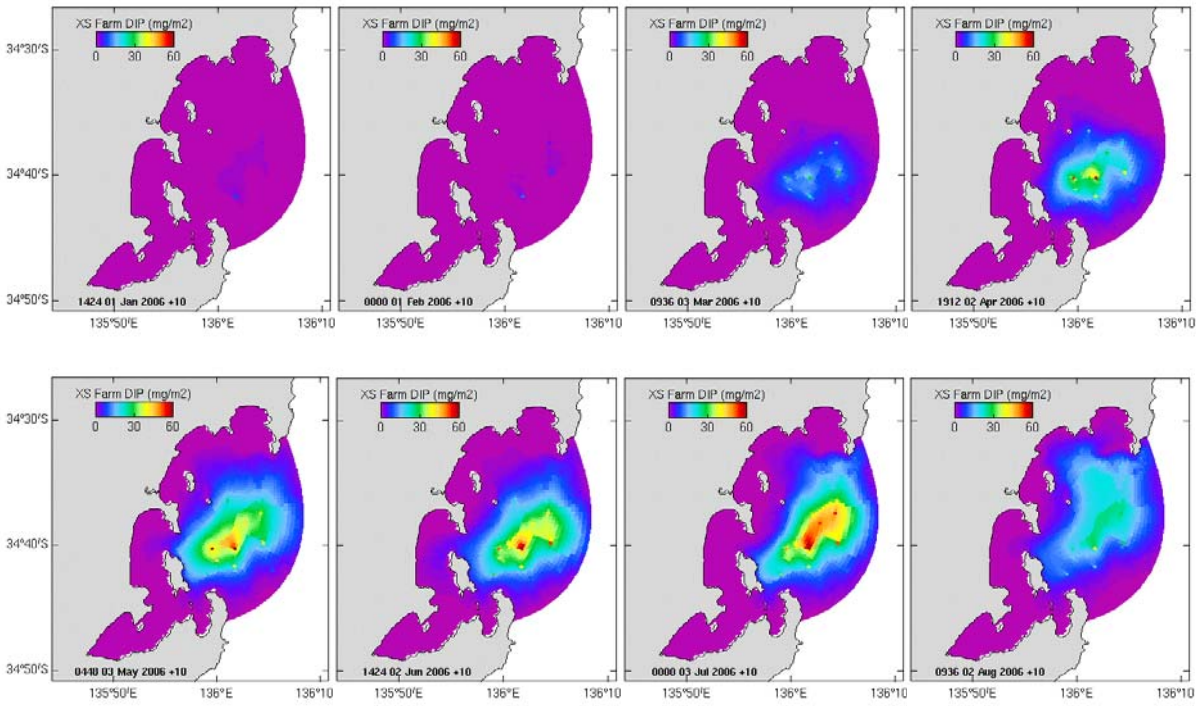

Figure 10.38. Excess monthly mean depth integrated dissolved inorganic phosphorus (DIP) due to fish farm waste loads.

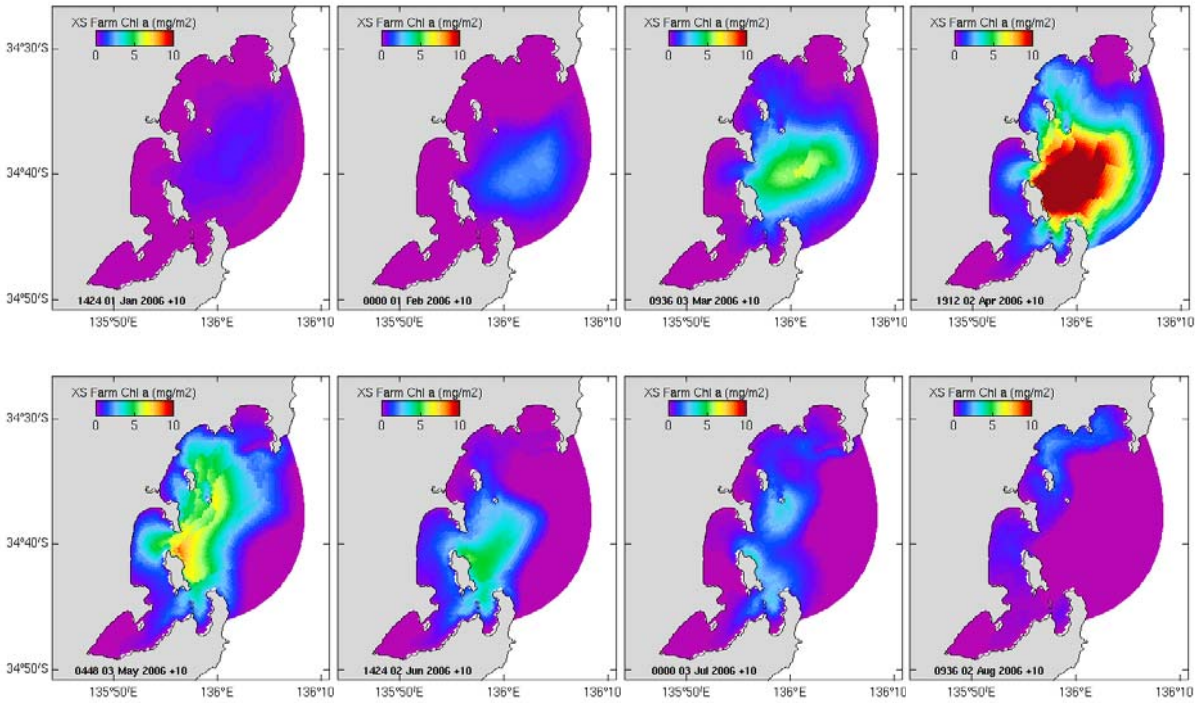

Figure 10.39. Excess monthly mean depth integrated chlorophyll due to fish farm waste loads.

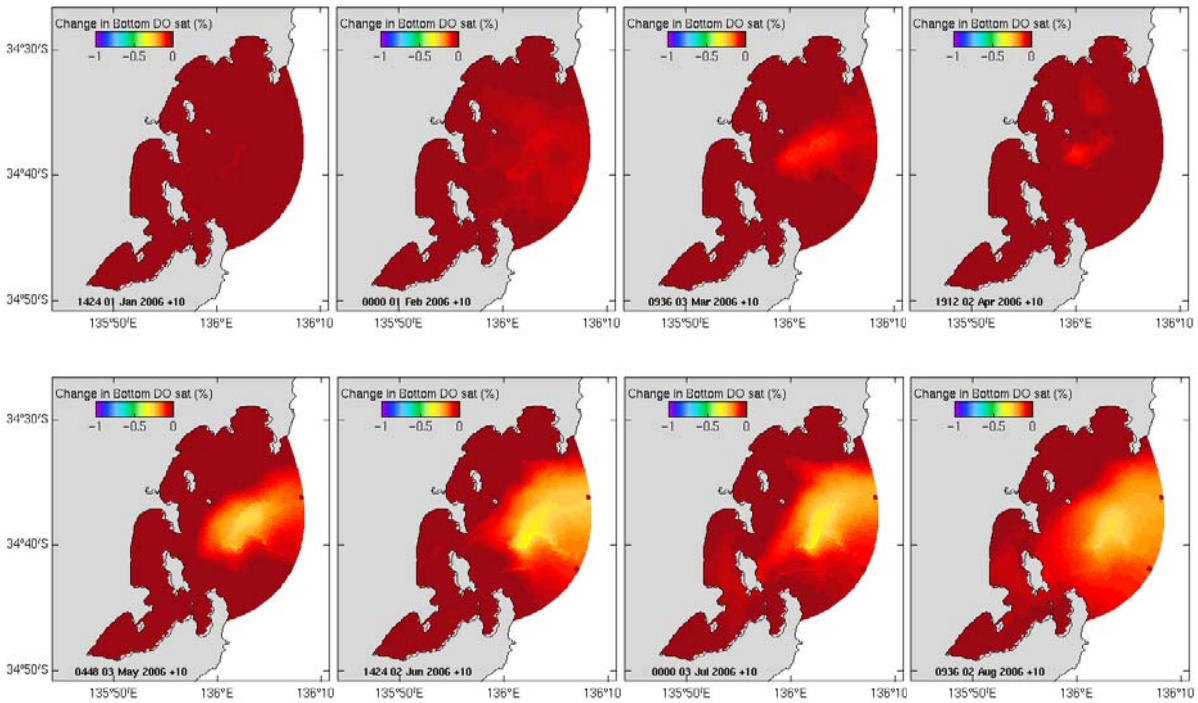

Figure 10.40. Reduction in monthly mean bottom water dissolved oxygen (DO) due to fish farm loads.

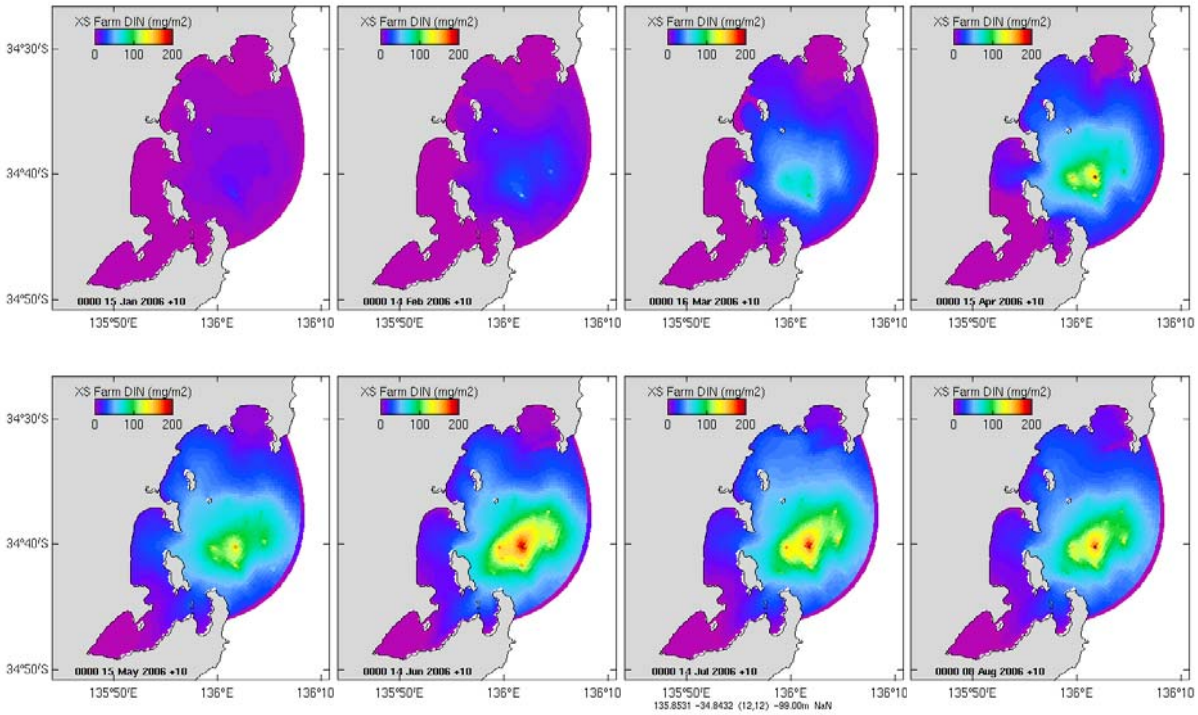

Figure 10.41. Monthly snapshots of excess dissolved inorganic nitrogen (DIN) in surface sediment due to fish farm waste loads.

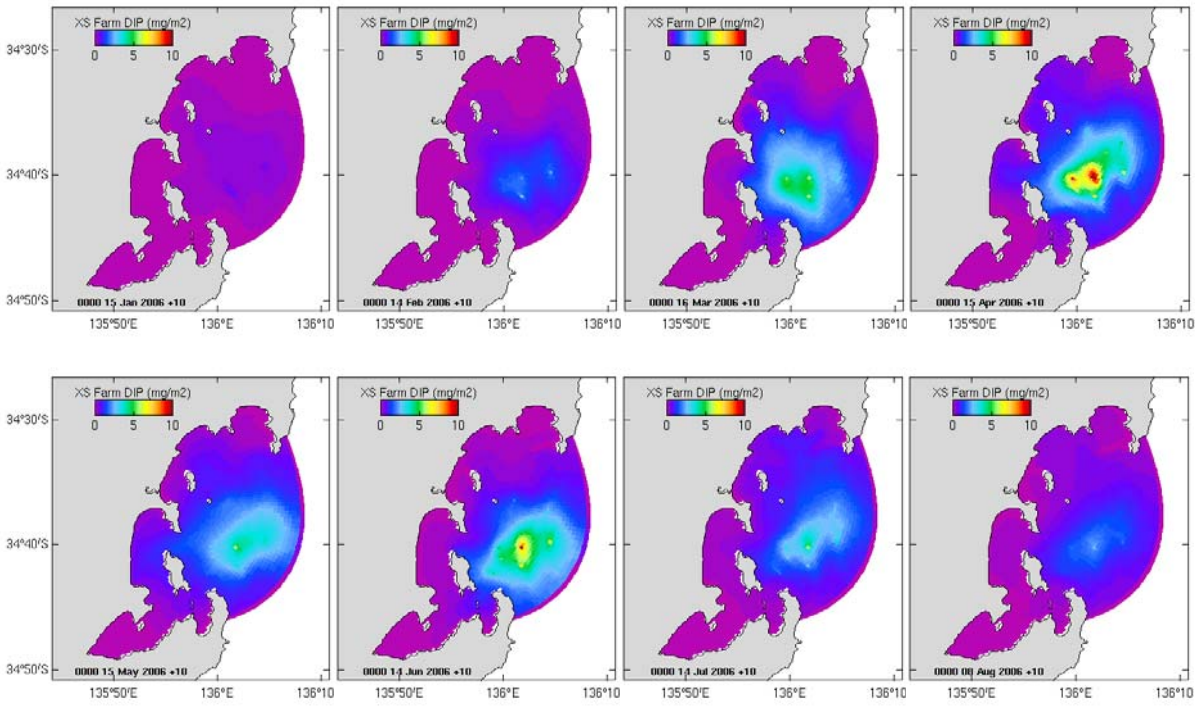

Figure 10.42. Monthly snapshots of excess dissolved inorganic phosphorus (DIP) in surface sediment due to fish farm waste loads.

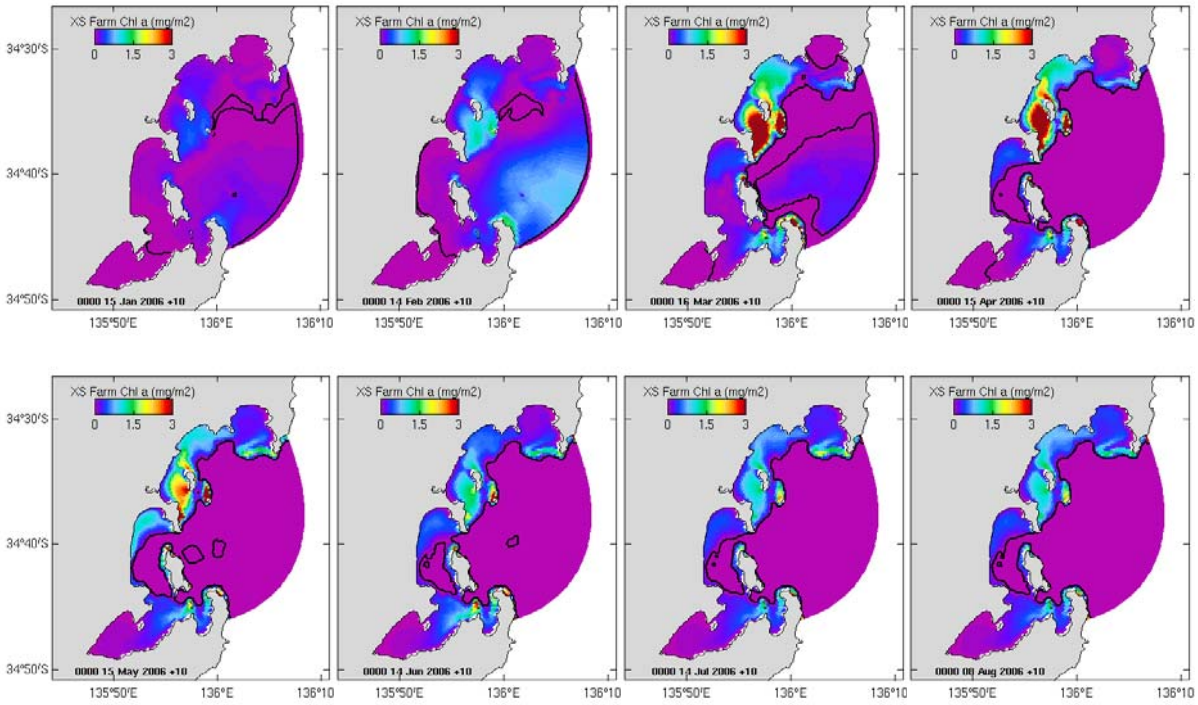

Figure 10.43. Monthly snapshots of excess chlorophyll in surface sediment due to fish farm waste loads. Note contoured areas in purple have reduced chlorophyll due to fish farm waste loads.

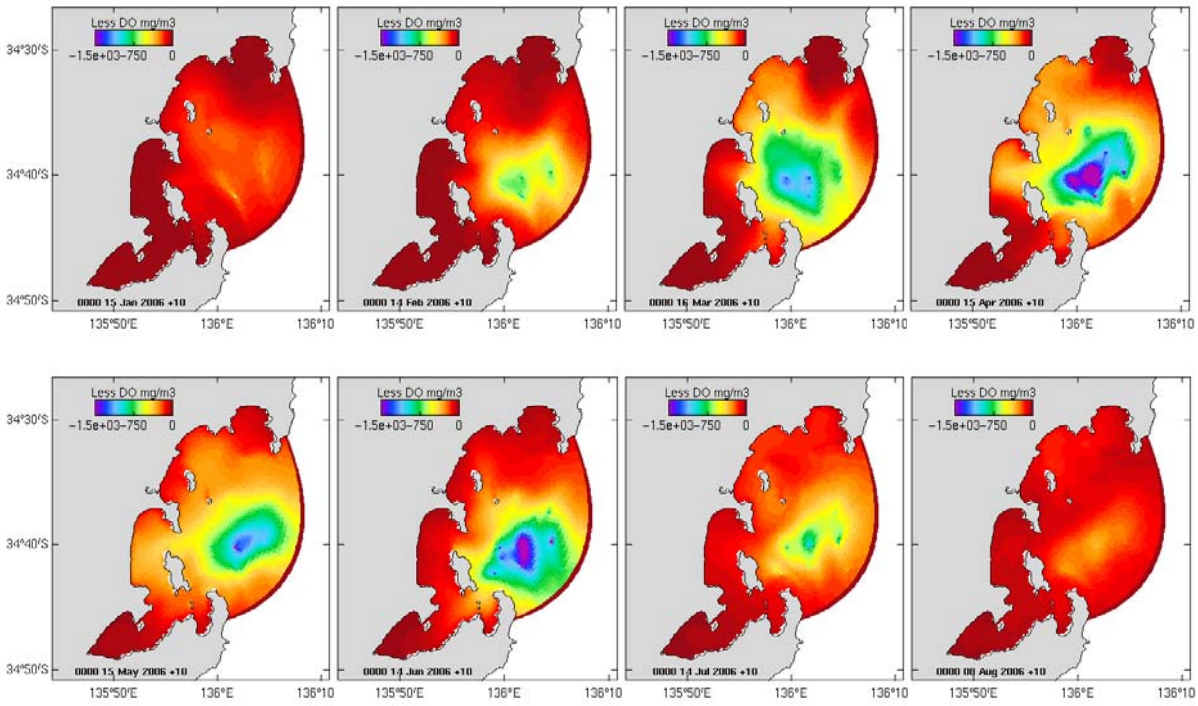

Figure 10.44. Monthly snapshots of reduced dissolved oxygen (DO) in surface sediment due to fish farm waste loads.

10.5.3. Regional fish farm impacts on sediment properties

The analysis of impact on regional surface sediment properties (Figure 10.45) demonstrates that for 3 months of the year in 14% of the region, sediment DIN was 20% above baseline levels due to fish farms. Likewise sediment DIP was more highly affected than the pelagic layer with 50% of the region impacted for 3 months of the year with 30% excess DIP due to fish farms. Fish farm impact on sediment oxygen demonstrated for 3 months of the year a reduction of 10% DO for 14% of the region. These benthic effects may be reduced by the seagrasses and benthic fauna.

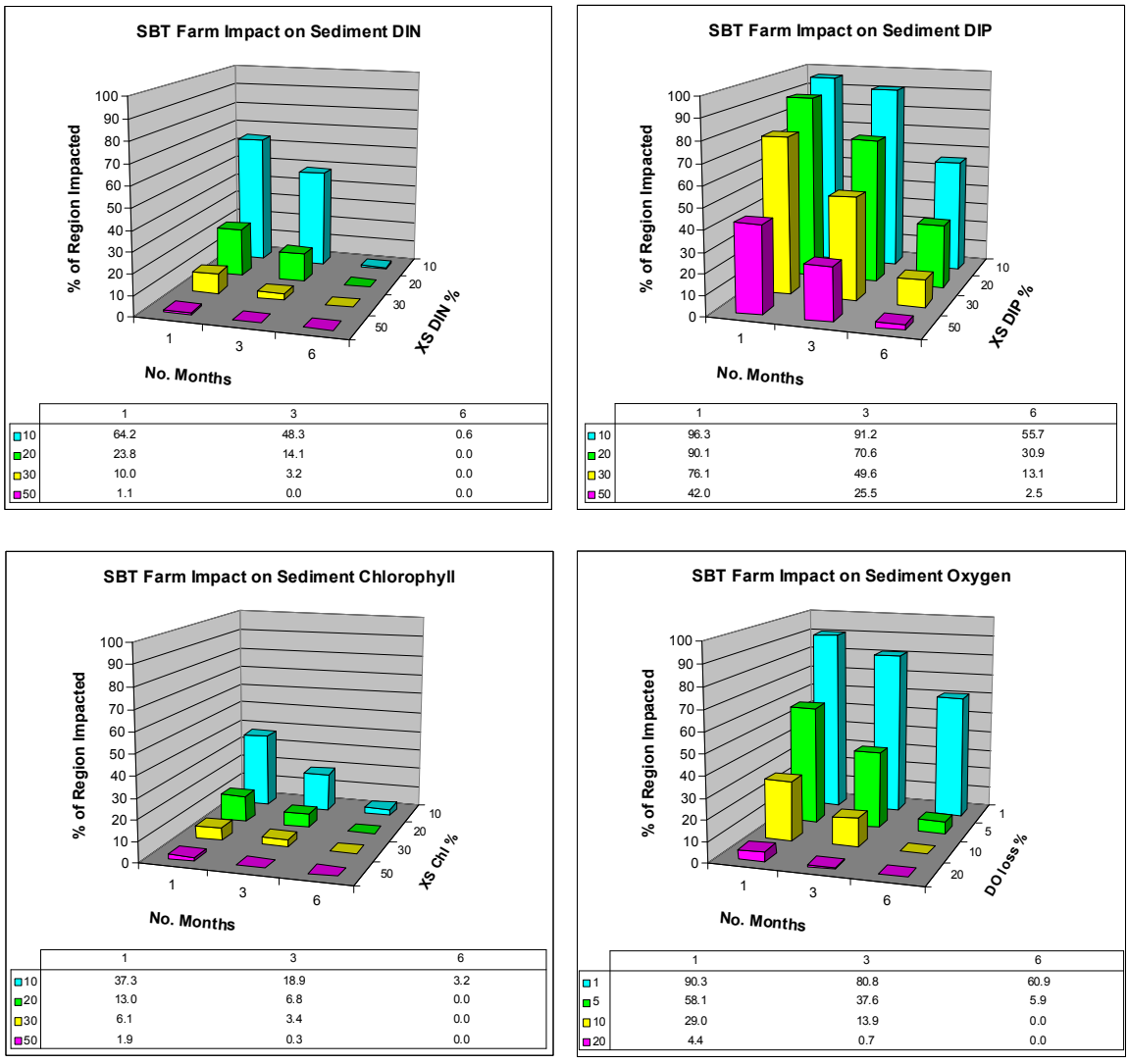

	1	3	6
10	64.2	48.3	0.6
20	23.8	14.1	0.0
30	10.0	3.2	0.0
50	1.1	0.0	0.0

	1	3	6
10	96.3	91.2	55.7
20	90.1	70.6	30.9
30	76.1	49.6	13.1
50	42.0	25.5	2.5

	1	3	6
10	37.3	18.9	3.2
20	13.0	6.8	0.0
30	6.1	3.4	0.0
50	1.9	0.3	0.0

	1	3	6
1	90.3	80.8	60.9
5	58.1	37.6	5.9
10	29.0	13.9	0.0
20	4.4	0.7	0.0

Figure 10.45. Fish farm impact on regional surface sediment properties.

10.6. Conclusions

The model successfully reproduces the seasonal dynamics of observed phytoplankton and chlorophyll and to a lesser extent DIP, in the TFZ. Uncertainty still remains in the observed biogeochemistry of the region. At different times of the year the system appears to experience phosphorus, nitrogen and silica nutrient limitation (chapter 5). The nitrogen and phosphorus limitations for phytoplankton can be observed in the model results. As shown by observations, silicate may also play an important role in the autumn diatom peak (chapter 5). While the biogeochemical model does not explicitly resolve silicate, the model was

successful in its representation of both the timing and nature of the autumn diatom peak. Throughout the region the chlorophyll levels at depth remain below 1 mg m^{-3} for the time period of the model run. There are increases in nutrient levels in the areas close to fish farms and these are discernable as observable hotspots in the model results.

The increase in feed input from SBT farms does correlate with the timing of the autumn/winter diatom peak from both model and observational results, but the timing and magnitude of this co-occurrence may be coincidental rather than cause and effect. Further observations and modelled scenarios are needed to test this relationship.

The model results indicate higher nutrient levels in near–shore areas due to fish farm inputs which could lead to environmental effects distant from the farm. Unfortunately no observations were taken in areas in the shallower regions and embayments to verify this. More observations in these areas would help calibration of the model.

It is important to note that the model is not yet well constrained and these outputs must be viewed as preliminary. The model was unable to reproduce short-term resuspension events and therefore may underestimate sediment ventilation of pore water and overestimate light propagation and availability for photosynthesis during resuspension events. Although small, such events could be significant on the biogeochemistry of some parts of the SBT farming zone. Further modelling calibration exercises proposed in a follow on project are needed to verify and extend these findings.

10.7. References

Aller, R., Blair, N., Xia, Q. and Rude, P. 1996. Remineralization rates, recycling and storage of carbon in Amazon shelf sediments. Continental Shelf Research 16:753-786.

Baird, M. E. and Emsley S. M. 1999. Towards a mechanistic model of plankton population dynamics. Journal of Plankton Research. 21:85-126.

Edyvane, K. 1999. Conserving marine biodiversity in South Australia - Part 2 - Identification of areas of high conservation value in South Australia. SARDI Aquatic Sciences, Adelaide, 281 pp.

Ellis, D. and Rough, K. 2005. Quality and nutritional evaluation of baitfish used for SBT farming (including baitfish profiles). Technical Report, Aquafin CRC Project 1A.2, FRDC Project 2000/221. Aquafin CRC, Adelaide, 39 pp.

Fogg, G. E. 1991. Tansley Review No.30: The phytoplanktonic ways of life. New Phytology. 118:191-232.

Fernandes, M., Lauer, P., Cheshire, A. and Angove, M. 2007a. Preliminary model of nitrogen loads from southern bluefin tuna aquaculture. Marine Pollution Bulletin 54:1321-1332.

Fernandes, M., Angove, M., Sedawie, T. and Cheshire, A. 2007b. Dissolved nutrient release from solid wastes of southern bluefin tuna (*Thunnus maccoyii*, Castelnau) aquaculture. Aquaculture Research. 38:388-397.

Herzfeld, M., Middleton, J.F., Andrewartha, J.R., Luick, J. and Wu, L. (2008) Numerical Hydrodynamic Modelling of the Tuna Farming Zone, Spencer Gulf. Technical report, Aquafin CRC Project 4.6, FRDC Project 2005/059. Aquafin CRC, Fisheries Research & Development Corporation and South Australian Research & Development Institute (Aquatic Sciences), Adelaide. SARDI Publication No F2008/000745-1, SARDI Research Report Series No 342, 100 pp.

Smith, V.H. 1998. Cultural eutrophication of inland, estuarine and coastal waters. In: Successes, Limitation and Frontiers in Ecosystem Science. Pace, M. L. and P. M. Groffman (eds.). Springer-Verlag, New York, pp. 7–49.

Wild-Allen, K., Parslow, J. Herzfeld, M., Sakov, P., Andrewartha, J. and Rosebrock, U. 2005. Biogeochemical modelling of the D'Entrecasteaux Channel and Huon Estuary. Aquafin CRC Technical Report, Hobart, Australia.

Volkman, J.K., Thompson, P., Herzfeld, M., Wild-Allen, K., Blackburn, S., Macleod, C., Swadling, K., Foster, S., Bonham, P., Holdsworth, D., Clementson, L., Skerratt, J., Rosebrock, U., Andrewartha, J. & Revill, A. 2008. A whole-of-ecosystem assessment of environmental issues for salmonid aquaculture. Aquafin CRC Technical Report, Hobart, Australia.

Chapter 11. Conclusions

11.1. Benefits and Adoption

This project provides both the tuna industry and government regulatory agencies a comprehensive assessment of the likely regional environmental impacts of tuna farming, as well as a tool that can be used to examine the consequences of environmental disturbances for the tuna industry. Once properly validated, it will be possible to run model scenarios to answer a variety of what if questions that are of interest to each group. For example, it will be possible to look at the likely environmental consequences of increasing the biomass stocked, of farming year-round, and of moving leases within the model domain. It will also be possible to look at the consequences for the industry of disturbances such as extreme storm events, and phytoplankton blooms that may occur outside the farming zone with the potential to propagate into the farming area.

Another benefit of the project will be the ability to design a comprehensive regional environmental monitoring program once the model is properly validated. This monitoring program would specify what to monitor, where to monitor to pick up the largest impacts, and how often to monitor.

Even without further model validation, this project has provided a good assessment of phytoplankton and benthic microalgal dynamics, including an assessment of the risks of harmful algal blooms forming. It also provides a much better understanding of how well the TFZ is connected to the rest of Spencer Gulf and the Great Australian Bight.

The original application identified the flow of benefits as being 100% to the southern bluefin tuna aquaculture sector. In reality, the work that has been undertaken also benefits other sectors. For example, hydrodynamic data collected as part of this project will be utilised in a new FRDC project (2008/011) to model prawn and blue crab larval dispersal in Spencer Gulf. In addition, a potential extension of the project would take into account other aquaculture industries in the model domain, including yellowtail kingfish, mussels, oysters and abalone, and thus provide information on their regional environmental impacts.

11.2. Further Development

When this project was originally proposed, the intention was to develop an integrated hydrodynamic, sediment and biogeochemical model of the TFZ, and to run a series of scenario analyses that would allow predictions to be made about the response of the environment to different stocking levels, as well as to allow the potential impacts of extreme environmental events on the industry to be predicted. This was always going to be a challenging task and application of the models to a new environment has not been straightforward. As a consequence, while a functional integrated model has been developed that appears to be behaving sensibly, this model has not been fully validated and calibrated within the existing project, and the only scenario analysis that has been done is a comparison between the existing level of tuna farming and no tuna farming.

As a consequence, the biogeochemical model needs to be properly validated and calibrated so that it can provide a better synthesis of the nutrient and phytoplankton dynamics in the TFZ and to enable farmers and managers the possibility of running a variety of scenarios. It will then be possible to recommend a monitoring program for the TFZ, as we will be able to

determine where and when adverse consequences of farming are more likely to arise, and in what component of the environment they are likely to be experienced in.

A number of work elements have been identified:

- The biogeochemical model takes output from a physical transport model. This model requires some further refining and calibration. It presently uses mean fields generated hourly, which may not capture the more extreme events.

- The hydrodynamic model has revealed the presence of at least 3 sub-regions each with different flushing rates and connectivity with each other. Further hydrodynamic, nutrient and phytoplankton data are needed, both to calibrate the models and to determine the spatial domain required for the monitoring program.

- We have very little data from Louth and Proper bays and yet the model suggests that nutrients from fish farming are likely to have ecological effects outside of the actual TFZ. Deployment of moorings for a limited period (January to August) to provide data on hydrodynamics and biogeochemistry in these areas is required. Additional sampling may also be required.

- There are still some uncertainties about the nutrient dynamics of this ecosystem and there seems to be some unique features in the region. The modelling suggests that there may be co-limitation of nutrients with N and P both important at different times of the year. There is an unexplained peak in silicate which may be fuelling a diatom peak. It is unclear whether this is a local phenomenon (e.g. from sediments) or advected from outside the zone. The biogeochemical model does not presently include silicate and we need to assess whether there would be benefits if it was included.

- A better conceptual model of how the ecosystem operates is required which we will achieve from the additional measurements and by using the biogeochemical model to formulate and test hypotheses. The model should be augmented by including point source nutrients, and other aquaculture sectors such as yellowtail kingfish and mussels.

- The phytoplankton peak in the TFZ is co-incident in timing when the feed input at the farms is greatest, but we require better characterisation of the timing and extent of phytoplankton dynamics outside the TFZ to establish the extent to which the farms contribute to these peaks. Questions such as the possible role of the nitrogen-fixing phytoplankter *Trichodesmium* need to be considered.

11.3. Planned Outcomes

1. An understanding of nutrient cycling around tuna farms in the context of natural processes occurring that may influence nutrient levels. This will allow industry, regulators and the public to have increased confidence that current and future nutrient inputs are environmentally acceptable, and won't produce negative feedbacks to industry such as from increased risk of damaging phytoplankton blooms.

The biogeochemical model was run under scenarios with and without tuna farming, allowing the influence of tuna farming on nutrient levels throughout the model domain to be calculated. Figures 10.37 and 10.38, for example, show the increase in water column nitrogen and phosphorus levels as a result of tuna farming, with the major increase being in the middle

of the TFZ. However, this translates into an increase in chlorophyll inshore of the farming zone. Similarly, Figures 10.41 and 10.42 show the effects of farming on sediment nutrient levels, with elevated sediment chlorophyll being concentrated in Louth Bay. In all cases, nutrient and chlorophyll levels appear to decrease substantially in August, which is towards the end of the farming season when feed inputs have decreased substantially. The model predicts that increases in chlorophyll on the order of 50% above background only occur over a relatively small proportion of the model domain (~20%) and for a relatively short time (< 3 months). These results suggest that the tuna industry is not currently causing major phytoplankton blooms in the region, although it is increasing phytoplankton biomass.

2. An assessment of ecosystem carrying capacity and an ability to run modelled scenarios in which stocking amounts or duration are changed.

While ecosystem carrying capacity per se has not been identified as part of the current project, the biogeochemical model does show the ecosystem level consequences of the nutrient additions from tuna farming. These consequences can then be assessed by relevant regulatory agencies to determine if they are acceptable, and if there is room for increasing the stocked biomass. As these decisions are based around social acceptability of particular consequences, it is not possible to rigorously define a carrying capacity. It would be possible, however, to run a series of model scenarios to determine at what stocking rate a pre-defined trigger level for a given environmental impact is met. These scenarios could involve changing both the amount of fish stocked, as well as the duration of stocking, to allow the potential consequences of long-term holding to be assessed. While these scenarios could be run now, the lack of data from inshore areas where the greatest impacts appear to be occurring means that our confidence in the results would be substantially reduced.

3. Enhanced knowledge of sediment resuspension, and the conditions under which it could become problematic. While a rare event, resuspension can be very costly to industry, and this knowledge could help to reduce the cost of a severe resuspension event by allowing the likelihood to be predicted several days in advance based on forecast weather conditions.

Between them, chapters 2, 3 and 4 provide extensive information on sediment resuspension and the conditions under which it can become problematic. In chapter 4, we suggest that sediment resuspension is most likely to occur within the TFZ itself when swell from the Southern Ocean enters Spencer Gulf from the S-SSW, with an open ocean height of > 5m. Locally generated wind waves only resuspend sediments at a depth of 20 m if the wave height is > 1-2 m, which is unusual for this region. While routine (annual periodicity or greater) storms do resuspend some sediments, they tend to remain in the lower 10 m of the water column, and thus do not interact directly with the tuna pens. It is only unusual events that have the potential to trigger sufficiently large waves to resuspend sediments into the upper 10 m of the water column. As much of the TFZ is in a depositional environment, however, there is potential for sediments resuspended in shallower waters to be advected into the area, with negative implications for stock. Extreme wind events do, however, pose a substantial risk of resuspension, and as there are substantial deposits of fine sediments in the area, once their cohesive nature has been broken and they enter the water column, they are likely to remain their for substantial periods of time before settling.

4. Transfer of modelling capability to South Australia through training at CSIRO of the post-doc to be employed at SARDI.

After the project was approved by the Aquafin CRC/FRDC, SARDI employed a senior physical oceanographer, negating the need to transfer hydrodynamic modelling capability from CSIRO. On the basis of this, and the presence of a biological oceanographer at SARDI who had the capability to learn the biogeochemical modelling, a post-doc was not employed. The subsequent departure of the biological oceanographer, and the lack of a replacement until late in the project, meant that the biogeochemical modelling skills were not transferred. It is anticipated that the newly appointed biological oceanographer at SARDI will develop the skills to undertake future biogeochemical modelling. To this end, SARDI, under the MISA (Marine Innovation SA) banner, is funding two oceanographers half-time to develop the model infrastructure necessary to undertake future projects involving integrated hydrodynamic and biogeochemical modelling. While this model infrastructure will use a different platform to the SHOC model used here, it will build upon what we have learnt in the current project. The new model will cover the whole of Spencer Gulf and Gulf St Vincent, allowing interactions between different aquaculture zones to be examined, as well as interactions between aquaculture and other spatially disjunct industries. This is particularly important given the anticipated expansion of aquaculture in SA, which is expected to be focussed within Spencer Gulf.

5. An understanding of the hydrodynamic connections between the tuna farming zone and surrounding areas, particularly the Great Australian Bight and the rest of Spencer Gulf.

The TFZ does not appear to be as well connected to Spencer Gulf as was previously thought. Figures 1.6 and 1.13, for example, show that the major currents in Spencer Gulf bypass the TFZ in both summer and winter. While there is some movement of water into the zone, current speeds are a lot lower than elsewhere in the gulf. In addition, it can be seen from Figure 1.26 and section 1.5, that while the TFZ itself is well flushed, water moves further inshore into Boston and Louth Bays, rather than moving offshore. Thus the nutrients released from the tuna farms are advected into shallow inshore areas where they remain for some time. Particle tracking studies suggest that the average residence time within the model domain of a particle released in the farming zone is on the order of 20 days, although it will only spend 2 days in the zone itself, with most of the rest of the time being in inshore areas.

These conclusions from the hydrodynamic modelling are supported by the results of the phytoplankton studies documented in chapter 7. Here we show that the phytoplankton assemblages in the TFZ are distinct from those found outside the zone, with the possible exception of a site at the very seaward margin of the farming zone. This result indicates that penetration of algae into the zone from outside is limited, and that water stays resident within the zone for long enough for distinct phytoplankton assemblages to develop.

6. The primary outcome of this project will be a system for assessing how a specific event (e.g. phytoplankton bloom, oil spill) will propagate into the TFZ, as well as for assessing suitable response strategies in terms of determining potential areas to relocate pontoons to avoid the event. Response strategies for a range of scenarios considered to be of interest by the tuna industry and managers will be modelled a priori, and risk mitigation strategies developed for these scenarios, while unforeseen situations can be modelled as they arise. This will benefit the entire tuna farming industry by minimizing costs associated with such unpredictable events, and allowing advance planning for events identified as possible a priori.

The model developed here provides a system for assessing how various waterborne disturbances can propagate into the TFZ, and allows for response strategies, in terms of identification of areas that will not be affected greatly by the disturbance, to be developed. However, before any confidence can be placed in the model predictions, further validation work needs to be undertaken. The model currently predicts that nutrients move from the TFZ to inshore areas, where no sampling was carried out. Thus it was not possible to validate this behaviour. In addition, there were insufficient resources made available to properly establish what inputs were being transported across the open model boundary from Spencer Gulf. As a consequence of these issues, and unanticipated logistical problems that caused delays in getting the biogeochemical model running, it was not possible to undertake any scenario analysis, with the exception of a comparison between farming and no farming.

11.4. Conclusions

The project successfully delivered on the first six objectives, although the final objective has not been completed, as the application of the existing modelling suite to a new environment has not always proven to be straightforward.

1. Characterisation of the main oceanographic features of the tuna grow-out region at Port Lincoln through field studies and calibration of the three dimensional hydrodynamic model previously developed for salmonid farming in Tasmania.

Chapter 1, and its accompanying technical report, provide a detailed description of the hydrodynamics of the TFZ, and also detail how the zone is connected to both the areas inshore of it (Boston, Louth & Proper bays) and the rest of Spencer Gulf. This was achieved by deployment of current meters and other oceanographic instrumentation for a period of one year at the start of the study, followed by the development of a hydrodynamic model. The modelling system used was SHOC (Sparse Hydrodynamic Ocean Code), which is the three dimensional model that CSIRO have previously used in the salmon farming region in Tasmania, as well as elsewhere around Australia. For the purposes of this study, two nested models were developed. The larger and coarser scale model was of the whole of Spencer Gulf, and a smaller finer scale model of the TFZ a surrounding waters was nested within this to provide greater detail of that region. The finer scale model included all inshore areas from Cape Donnington in the south to Point Bolingbroke in the north, including Proper, Boston & Louth bays.

2. Identification and description of dynamics of phytoplankton and benthic microalgal species, the factors causing algal blooms and the role, if any, of nutrients released from tuna farming.

The spatial and temporal dynamics of phytoplankton assemblages in the TFZ are described in chapter 7, based not only on an intensive sampling regime throughout the first year of the study, but also on other data sets, including ten years of remote sensing imagery, the data collected by the tuna industry since 1999, data collected by the South Australian Shellfish Quality Assurance Program since 1999, and some recent data from the Great Australian Bight. These data generally show a peak in phytoplankton abundance in autumn (May during the year of intensive sampling), which occurs several months after a peak in dissolved silica levels. However, there is no evidence to suggest that a major bloom with adverse environmental consequences has occurred in the area during the period in which data is available from. Diatoms account for most of the phytoplankton observed, and this group contains few potentially harmful species. However, most of the phytoplankton pigments in

the water column come from organisms < 5 μm in diameter, and hence would not be seen in conventional microscopic analysis of phytoplankton samples. Pigment analysis suggested that diatoms also dominated this small size class.

Diatoms also dominated the benthic microalgal assemblage, as shown in chapter 8. Biomass tended to be lowest during summer and at the inshore sites, and there was evidence of heavy grazing in the form of degradation products of chlorophyll-*a*. There was no indication of the presence of active dinoflagellates, which form the majority of potentially harmful spoecies, although the methods used would be unlikely to have detected the presence of resting stages of this group.

While the peak in phytoplankton abundance coincided with the time of maximum feed inputs, the remote sensing data suggest that phytoplankton abundance increases in autumn over a much larger scale than what nutrient inputs to the TFZ are likely to influence, especially given the shoreward movement of these nutrients. The biogeochemical modelling indicates that 23% of the model domain had a chlorophyll value 20% above the baseline (what would occur if there was no tuna farming) for 3 months of the year. The regional classification based on annual mean pelagic chlorophyll concentration in the upper 12 m of the water column demonstrates the water column changes from 100 % oligotrophic with no SBT farms to 98 % oligotrophic and 2 % mesotrophic when SBT farms are included.

3. Integration of phytoplankton and nutrient data into a 3D biogeochemical model for the Port Lincoln farming area that will allow movement of blooms etc to be predicted.

A three dimensional biogeochemical model has been developed that shows how nutrient levels and chlorophyll-*a* (a measure of phytoplankton abundance) vary both spatially and temporally in the TFZ and its surrounds. This model seems to predict phytoplankton levels fairly well, at least within the TFZ where data were collected to validate it. The model also does well at predicting phosphorus levels in the water column, but performs relatively poorly with respect to dissolved inorganic nitrogen. However, the good predictive ability for phytoplankton suggests that the movement of blooms within the model domain can be predicted, and that is would be possible to force the model with inputs across the open boundary to simulate the ingress of a bloom from outside of the model domain.

4. Refine description of variations in sediment type and assimilative capacity for organic matter including an assessment of the role of microbial and faunal communities in carbon remineralisation and nutrient release.

Sediments were collected from a grid to the east of Boston Island covering the TFZ. These sediments were analysed for the contents of organic C, N, P, porewater nutrients, carbonate, and also for mineral grain size distribution and the stable isotopic signature of organic C and N. Based on these data, maps were produced for the spatial distribution of sediment types at a fine-scale resolution. Sediments in the central TFZ contain significantly more nutrients (organic carbon, total nitrogen and porewater ammonium and phosphate) than those found elsewhere in the study region, although it is not yet clear what, if any, role that tuna farming plays. These nutrient-rich sediments also have a higher percentage of fine silts and a heavier isotopic signature for nitrogen, suggesting increased microbial (and possibly faunal) activity in these locations. The distribution of mineral grain size suggests a link between sediment resuspension and swell events, which can introduce fine sediments to the water column (typically in the lower 10 m) and decrease water quality. So far, no formal assessment has

been made on the role of microbial and faunal communities on organic matter remineralisation in the area. The ongoing PhD project of Emlyn Jones will provide information on the role of microbial populations in recycling nitrogen from bioavailable forms in the sediments (i.e. NO_3^-) to gaseous forms (i.e. N_2 and N_2O) lost to water column and ultimately, the atmosphere.

5. Application of sediment models to identify likelihood of sediments being resuspended and identification of factors affecting this together with an assessment of their role in algal blooms.

The sediment modelling suggests that there is a very low probability of fine consolidated sediments being resuspended throughout the TFZ, although unconsolidated sediment will frequently be resuspended throughout much of the zone (chapter 4). It would generally take several days with no disturbance for fine unconsolidated sediments to compact and become consolidated, and thus sediments are only likely to be unconsolidated after major and unusual storm events. As would be expected, the areas most at risk of having fine sediments resuspended also have the coarsest sediments in the zone, which substantially decreases the risk of resuspension. However, as much of the zone has relatively fine sediments, there is a high risk of resuspension when unusual acute events occur, such as the storm of April 1996.

As sediment resuspension appears to be an unusual event, and studies of the benthic microalgae failed to detect the presence of dinoflagellates, it is unlikely that sediment resuspension will contribute to the formation of a major algal bloom. However, a previous study has found resting stages of harmful dinoflagellate species in inshore areas around Boston Island and Boston Bay (outside the current TFZ), and if these are resuspended by an unusual event, it is possible that they could trigger a bloom in these more sheltered areas. A risk assessment for harmful algal species also indicates that the risk of a bloom forming in the TFZ is relatively low, although there are a number of factors that could change this in the future, including increased nutrient inputs to the area and climate change.

6. Further development of the near real-time telemetered environmental observation system with web access.

The SBT telemetry-based environmental monitoring system developed as part of "2001/104: Development of regional environmental sustainability assessments for tuna sea-cage aquaculture" was re-deployed as part of this project. However, before the re-deployment, the system required upgrades and modifications and Measurement Engineering Australia (MEA), who built the system, was engaged to work in collaboration with SARDI to carry out the upgrades. The changes required included improvements to the power supply, enclosures for the logger and battery and housing for the sensors. In addition, the existing system consisting of temperature, conductivity (EC), dissolved oxygen (DO) and wind speed and direction, was further expanded with the addition of an Eco Fluorometer (Eco FL) to measure chlorophyll-*a*. The chlorophyll sensor had a connector at the sensor end to allow removal of the sensor for cleaning and maintenance and a connector fitted to the logger end of the cable to facilitate connection and installation.

The system was deployed during the 2006 farming season from 30th April to 22nd August 2006, but encountered problems during the season and some of the data recorded were considered unreliable. Development and trial of sensors had been towards a cost-effective system, consequently, some of the sensors trialled could not withstand the extreme weather conditions experienced around Port Lincoln at times, as they were not high quality and more

expensive oceanographic grade instruments. However, the data collected when reliable had been useful for both industry and research.

In addition, a new system with an Acoustic Doppler Current Profiler was successfully deployed in late 2007. This system provided regular data, updated several times a day, on current speed and direction throughout the water column, as well as wave height. Unfortunately, due to the late supply and approval by Telstra of suitable NextG modems, this system was deployed with a CDMA modem. This was done as Telstra were running over a year late with providing suitable NextG modems. With the switching off of the CDMA network in April, this system has had to be removed to be updated with a new modem now that they are available.

7. The above all lead to the primary objective, which is to develop an integrated hydrodynamic and biogeochemical model of the Port Lincoln tuna farming area, that will assist managers and farmers to assess how external and internal disturbances are likely to move through the area, and thus allow them to make informed decisions on how to best mitigate the risks associated with any given disturbance, and to develop pre-prepared emergency management protocols for particular events.

Although the biogeochemical model has yet to be fully validated, and shows poor predictive skill for some model compartments (e.g. dissolved inorganic nitrogen), this project has delivered an integrated hydrodynamic and biogeochemical model of the TFZ and surrounding regions. Importantly, the hydrodynamic model has good predictive skill in the TFZ itself, as does the biogeochemical model for phytoplankton. This suite of models can be used to assess how passive waterborne disturbances are likely to move through the farming zone, although the lack of data to validate the model results for inshore areas means that there is some uncertainty in its predictions.

In addition to meeting the specific project objectives as discussed above, this project has contributed to several of the objectives of the Aquafin CRC.

- An ability to predict the environmental impact of cage aquaculture at the system-wide scale

The integrated hydrodynamic, sediment and biogeochemical model allow the prediction of likely impacts of southern bluefin tuna aquaculture on a system-wide scale. Chapter 10 suggests that the main impacts are likely to be occurring inshore of the TFZ, as nutrients are advected to the north-west into Louth and Peake bays in particular, but also into Boston and Proper bays. The model shows how much nutrient and chlorophyll levels, among other parameters, are elevated in the model domain and how long for, as a result of tuna farming.

- Improved monitoring of the environmental performance of cage aquaculture operations

Once properly validated, the model developed here will allow the major hotspots for environmental impacts of tuna farming to be identified, along with the type of impact to expect (e.g. elevated nutrients, chlorophyll etc). With this information, it will be possible for managers to design a well targeted regional monitoring program that identifies what to monitor, where to monitor it, and how often to monitor.

- Better community understanding of aquaculture and the environment

As this final report is expected to be publicly available, it will provide the community with a resource with which to better understand what the environmental impacts of southern bluefin tuna aquaculture are.

Appendix 1: Intellectual Property.

This report will be made freely available to the public via the Aquafin CRC, FRDC and SARDI.

Appendix 2: Project Staff.

SARDI:	Dr Jason Tanner (PI)
(Aquatic Sciences)	Mr Jeremy Barnett
	Dr Simon Bryars
	Dr Greg Collings
	Ms Yvette Eglinton
	Dr Milena Fernandes
	Ms Jodi Lill
	Dr Maylene Loo
	Dr John Luick
	Mr Leo Mantilla
	Dr Sam McClatchie
	Dr John Middleton
	Mr Bruce Miller-Smith
	Ms Genevieve Mount
	Mr Jason Nichols
	Ms Emma O'loughlin
	Ms Michelle Roberts
	Dr Kate Rodda
	Mr Keith Rowling
	Ms Mandee Theil
	Mr Paul Van Ruth
	Ms Sonja Venema
	Ms Kathryn Wiltshire
RV Ngerin	Mr Neil Chigwidden
(SARDI)	Mr Dave Kerr
	Mr Ralf Putz
	Mr Chris Small
RV Breakwater Bay	Mr Brenton Ebert
(SARDI)	
CSIRO:	Dr John Volkman
(Marine and Atmospheric	Mr Phil Adams
Research)	Mr John Andrewartha
Dr Sue Blackburn	
	Dr Pru Bonham
	Dr Lesley Clementson
	Dr Mike Herzfeld
	Dr Nugzar Margvelishvilli

	Mr Uwe Rosebrock
	Dr Jenny Skerratt
	Dr Peter Thompson
	Dr Karen Wild-Allen
Adelaide University:	Mr Paul Bierman
(Earth & Environmental	Dr Megan Lewis
Sciences)	Dr Bertram Ostendorf
Flinders University:	Mr Emlyn Jones
(School of Chemistry,	Dr Jochen Käempf
Physics & Earth Sciences)	Ms Lee Ying Wu
TBOASA:	Mr David Ellis
	Ms Danielle Foote